

Lipid biomolecules reveal patterns of microbial metabolism in extreme environments

Dissertation
zur Erlangung des Doktorgrades
der Naturwissenschaften
- Dr. rer. nat. -

dem Fachbereich Geowissenschaften
der Universität Bremen

vorgelegt von

Matthias Kellermann

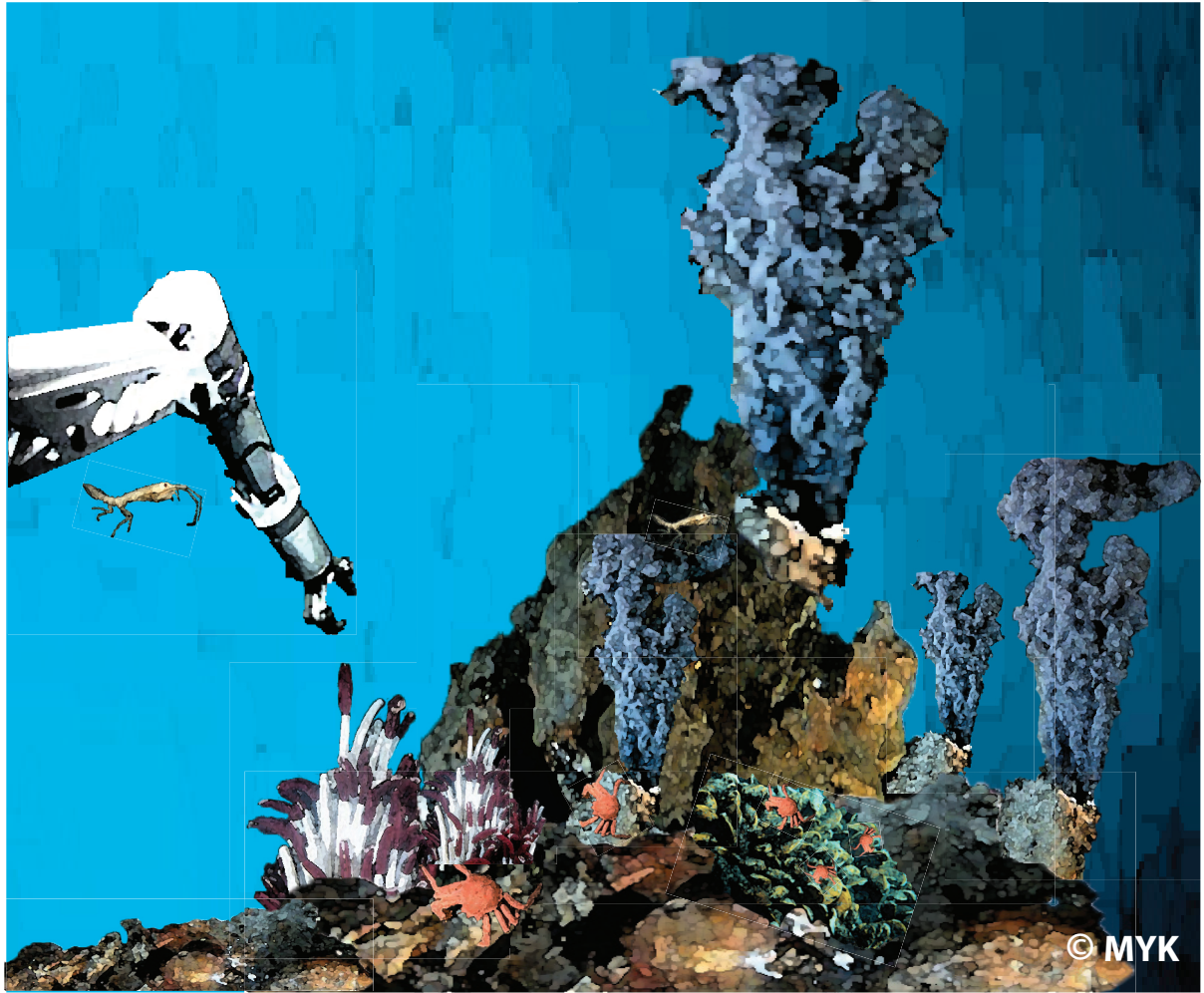
Bremen
February 2012

Die vorliegende Arbeit wurde in der Zeit von Mai 2008 bis Februar 2012 in der Arbeitsgruppe Organische Geochemie am MARUM – Zentrum für Marine Umweltwissenschaften und dem Fachbereich Geowissenschaften der Universität Bremen angefertigt.



1. Gutachter: Prof. Dr. Kai-Uwe Hinrichs
2. Gutachter: Prof. Dr. Stuart G. Wakeham

Tag des Promotionskolloquiums: 23. März 2012



"It's a magical world, Hobbes, ol' buddy...Let's go exploring!"

Bill Watterson, cartoonist, "Calvin and Hobbes"

Table of Contents

ABSTRACT	I
KURZBESCHREIBUNG	III
ACKNOWLEDGEMENTS	V
LIST OF ABBREVIATIONS	VIII
CHAPTER I	1
Introduction and Methods	
CHAPTER II	35
Symbiont–host relationships in chemosynthetic mussels: A comprehensive lipid biomarker study	
CHAPTER III	57
Dominance of autotrophic carbon fixation in hydrothermal sediments inhabited by methanotrophic communities	
CHAPTER IV	77
Systematic fragmentation patterns of archaeal intact polar lipids by high-performance liquid chromatography/electrospray ionization ion-trap mass spectrometry	
CHAPTER V	105
Stable isotope probing of an anaerobic methane–oxidizing enrichment provides clues on archaeal tetraether lipid biosynthesis	
CHAPTER VI	125
Concluding remarks & future perspectives	
REFERENCES	133
APPENDIX	155

ABSTRACT

This dissertation used state-of-the-art organic geochemical techniques to explore the lipid biosignatures of microorganisms inhabiting at cold and hot vents. The association of organisms and their carbon metabolisms were assessed and the current knowledge on the microbially-mediated oxidation of reduced compounds under aerobic and anaerobic conditions, especially at methane-rich environments, was expanded. By using the taxonomic information encoded in intact polar lipid (IPL) molecules, this work confirmed the presence of aerobic chemotrophic bacteria living symbiotically with mussels recovered from seep and vent environments. This was the first application of IPLs in symbiont ecology, providing a semi-quantitative estimation of the importance of methanotrophic and thiotrophic symbionts within the gills of *Bathymodiolus* mussels. In addition, the stable carbon isotopic composition of a suite of lipid biomarkers (e.g., fatty acids, sterols, bacteriohopanepolyols) derived from symbionts and hosts highlighted the importance of a chemosynthetic lifestyle in these extreme settings. The anaerobic oxidation of methane (AOM) performed by naturally enriched anaerobic methanotrophic (ANME) archaea belonging to the ANME-1 subgroup and sulfate-reducing bacteria (SRB) belonging to the HotSeep-1 cluster from the Guaymas Basin (Gulf of California) sediments was studied using a novel dual stable isotope probing (SIP) method. Dual-SIP was applied to bulk microbial lipids (total lipid extract, TLE) and involves the assimilation of deuterated water (D_2O) and $^{13}C_{DIC}$ (DIC = dissolved inorganic carbon), which allows the simultaneous assessment of auto- and heterotrophic carbon fixation. This work was the first to demonstrate autotrophic lipid production for both ANME and SRB, in contrast to previous AOM studies which suggested a significant contribution of direct methane assimilation during microbial growth. These results have a direct implication in the interpretation of natural lipid stable carbon isotopic compositions in AOM systems. To further access the ^{13}C assimilation into individual archaeal IPLs an extensive preparative HPLC separation of lipids was performed. This work demonstrated an increase of up to 35 times in sensitivity on IPLs (IPL-SIP) rather than bulk lipids (TLE-SIP). Moreover, the label assimilation of individual di- and tetraether IPLs uncovered a possible role of a diether phospholipid as precursor in archaeal tetraether biosynthesis. Finally, it was hypothesized that the tetraether membrane, especially the formation of glycosidic (Gly) glycerol dibiphytanyl glycerol tetraether (GDGT), is used to reduce proton-permeability, thereby protecting the integrity of cells at extreme conditions from the Guaymas Basin. Along with this hypothesis, the ubiquity of 2Gly-GDGTs in marine sediments worldwide may likely represent an expression of cell-wall adaptation to cope with energy stress.

Keywords: anaerobic oxidation of methane | intact polar lipids | stable isotope probing | hot and cold vents | chemotrophic microorganisms | Guaymas Basin | Archaea | Bacteria | auto- and heterotrophy | archaeal lipid biosynthesis

KURZBESCHREIBUNG

In der vorliegenden Dissertation wurden mithilfe neuester organisch-geochemischer Methoden Lipid-Biosignaturen von Mikroorganismen in heißen und kalten Quellen analysiert. Die Untersuchung des Kohlenstoffmetabolismus im Zusammenwirken von Organismen insbesondere an methanreichen Standorten hat neue Erkenntnisse im Bereich der mikrobiell initiierten aeroben und anaeroben Oxidation reduzierter Komponenten gebracht. Durch die Entschlüsselung taxonomischer Information von intakten polaren Membranlipiden (IPLs), konnte die Existenz aerober chemotropher Bakterien in einer Symbiose mit Muscheln an kalten und heißen Quellen nachgewiesen werden. Der erstmalige Einsatz von IPLs im Bereich der Symbiontenforschung ermöglichte eine semiquantitative Bestimmung der Bedeutung methanotropher und thiotropher Symbionten in den Kiemen der *Bathymodiolus* Muscheln. Die isotopische Zusammensetzung des Kohlenstoffs verschiedener Lipidbiomarker (z.B. Fettsäuren, Sterole oder BHPs) verdeutlichte die Relevanz chemosynthetischer Prozesse für Muscheln und Symbionten unter extremen Umweltbedingungen. Mithilfe einer neu entwickelten Dual-SIP Methode (duale Isotopenmarkierung von zwei Substraten) wurde die anaerobe Oxidation von Methan (AOM) in Proben aus dem Guaymas Becken (Golf von Kalifornien) untersucht, welche von einem Konsortium von anaeroben methanotrophen Archaeen (ANME) aus der ANME-1 Untergruppe und sulfatreduzierenden Bakterien (SRB) aus dem HotSeep-1 Cluster durchgeführt wird. Um eine Aussage über autotrophen und/oder heterotrophen Einbau des Kohlenstoffs in mikrobielle Biomasse treffen zu können, wurde der gesamte mikrobielle Lipidpool hinsichtlich einer Aufnahme von deuteriertem Wasser (D_2O) und ^{13}C -markiertem anorganischem Kohlenstoff (DIC) geprüft. Die Untersuchungen belegen eindeutig, dass die Lipidproduktion der ANME and SRB ein ausschließlich autotropher Prozess ist. Diese Ergebnisse stehen somit im Gegensatz zu früheren Studien, die einen signifikanten Anteil des mikrobiellen Wachstums der direkten Aufnahme von Methan zuschreiben. Die neu gewonnenen Erkenntnisse haben eine unmittelbare Auswirkung auf die Interpretation der natürlichen Kohlenstoffisotopenzusammensetzung von Lipiden in AOM-beeinflussten Systemen. Zur genaueren Bestimmung der ^{13}C -Aufnahme in einzelne Archaeen-IPLs wurde eine aufwendige präparative Auftrennung von Lipiden durchgeführt. Diese Aufarbeitung hatte zur Folge, dass die Empfindlichkeit der Bestimmung der Aufnahme des ^{13}C markierten Substrats deutlich gesteigert wurde. So zeigten die IPLs verglichen mit dem gesamten Lipidpool (TLE-SIP) eine bis zu 35-fache Signalverstärkung. Darüber hinaus deutet die unterschiedliche Aufnahme von ^{13}C -markiertem Substrat in einzelne Di- und Tetraether-IPLs auf ein Diether-Phospholipid als möglichen Vorläufer in der Tetraether Biosynthese hin. Die Erkenntnisse dieser Arbeit legen die Vermutung nahe, dass eine Lipidmembran bestehend aus Tetraethern, insbesondere Glyceroldibiphytanylglyceroltetraether mit glycosidischen Kopfgruppen, die Protonendurchlässigkeit verringert und dadurch die Integrität der Zellen an extremen Standorten sichert. Es ist daher anzunehmen, dass die Präsenz von diglycosidischen Tetraetherlipiden in weltweit verteilten marinen Sedimenten, eine Art Anpassung der Zellwand darstellt, die ein Überleben auch an Standorten mit geringen Energiequellen ermöglicht.

ACKNOWLEDGEMENTS

The foremost thanks go to my advisor, **Prof. Dr. Kai-Uwe Hinrichs**. Kai's support and assistance are the foundation on which my work is built. Thank you for the opportunity to work and progress as part of your group. Thanks for creating an inspiring and positive working atmosphere which allowed me day-to-day to explore and enjoy science.

Prof. Dr. Stuart Wakeham, thank you for being a member of my thesis committee, thanks for the discussions, your ideas, your input and your time, coming a long way for my defense. I am really honored that you will be part of my defense party and I am looking forward to future projects involving you as an appreciated and valued mentor and colleague.

Thanks to **Prof. Dr. Wolfgang Bach**, **PD Dr. Matthias Zabel**, **Dr. Julius Lipp** and **Nadine Broda** for their help with the thesis defense process.

None of this would have been possible without the commitment and generous support of **Dr. Florence Schubotz**, **Dr. Gunter Wegener** and **Dr. Marcos Y. Yoshinaga**. I hope that someday I can return all the time that you guys spent discussing, commentating and criticizing my work.

I've been fortunate to have a number of outstanding colleagues among the organic geochemistry group who have provided everything from the help of instruments, advice on writing to practical advice in the lab. Especially **Marcus Elvert**, **Julius Lipp**, **Xavier Prieto** and **Birgit Schmincke** who helped me on a daily basis should be mentioned here. Thanks to the organic geochemistry members, all my office and lab buddies – Arne, Julio, Tobi, Pame, Tobias, Florence, Benni, Florian, Lars, Jan, Jan-Lars, Yu-Shih, Travis, Sitan, Gerard, Frauke, Verena, Rong, Jenny, Thomas, Daniel, Jessica, Raika, Guangchao, Evert, Charlie, Xiaolei, Gina, Solveig, Jörn, Bernhard, Eoghan, Marshall, Kevin, Marlene, Felix, Nadine, Nadine, Nadine, Tim und Susanne – for the incredibly positive atmosphere at work. You've all helped me in so many ways and I've gained learned so much by doing science with you.

Thanks also to **Prof. Dr. Andreas Teske** for inviting me to the cruises to the Guaymas Basin hydrothermal vent system and allowing me to explore the mysteries of the dark-ocean in the manned deep-ocean research submersible *Alvin*.

ACKNOWLEDGEMENTS (continued)

Meinen Freunden und meiner Familie ist der letzte Teil meiner Danksagung gewidmet.

Freund und Kollege waren in den letzten Jahren größtenteils eins: Tagsüber eine Privatvorlesung über Fragmentationsmuster von Archeenlipiden und abends von der selbigen Person mit Korn und Bier beim Kickern abgefüllt und vorgeführt zu werden... Marcos, du hast es wirklich geschafft, mir täglich meine Grenzen aufzuzeigen und mich gleichzeitig immer dazu bewegt, mir höhere Ziele zu stecken. Ich danke dir für Alles und hoffe, wir werden es schaffen, uns ein Leben lang gegenseitig herauszufordern. Gunti, mir tut's Leid für die vielen grauen Haare, die ich dir bereitet habe, aber sei gewiss, mir hat's großen Spaß gemacht! Ich hoffe, wir werden uns noch an vielen gemeinsamen Projekten die Haare raufen. Floflo, was würde ich ohne Dich nur machen. Egal wie voll dein Terminplan auch ist, du nimmst Dir Zeit und, viel wichtiger, hast immer positive und aufmunternde Worte parat, die jedes noch so große Problem winzig klein erscheinen lassen.

Während meiner Doktorarbeit habe ich viele meiner Liebsten vernachlässigt. Ich möchte mich hiermit bei denjenigen entschuldigen, denen ich in den letzten Jahren nicht gerecht geworden bin. Janine, danke dafür, dass du stets an mich gedacht und von Zeit zu Zeit deine Gedanken mit mir geteilt hast. Mensch Peter, wie wär's mit einer ausgedehnten Wanderung in Deutschlands Mittelgebirge? Wie ich finde wäre es wieder an der Zeit für einen weiteren Road Trip! Malde, Sonnti, Stinka - schnürt Euch die Schuhe, wir gehen tanzen!

Vielen Dank meinen Mitbewohnern in der Mainstraße (ausschließlich Hochparterre und 1. Obergeschoss) für Unterkunft, Speis, Trank und liebe Worte - wir haben zusammen viel erlebt und ich bin wirklich dankbar, dass wir zur selben Zeit am gleichen Ort waren. Schade Klausens, dass du schon weiter gezogen bist, ich werde dich nicht vergessen.

Finally, **the family**, Mama und Papa. Euch sei gedankt, dass ihr diese Familie gegründet und all die Jahre zusammengehalten habt. Ihr seid der Grund, warum ich mit positiven Gedanken unbeschwert durchs Leben gehen kann. Es ist ein schönes Gefühl zu wissen, dass ihr stets für mich da seid und immer auf mich Acht gebt. Vielen Dank für einen großartigen Ali, meinen Bruder, der mir schon von Klein auf gezeigt hat wie die Dinge wirklich laufen. Ohne dich wär' ich bestimmt nicht ich. Und natürlich Susanne – mit dir bin ich groß geworden, du hast mir die Welt gezeigt und jeden Tag eröffnest du mir neue Wunder, die ansonsten einfach so an mir vorbeikrabbeln würden. Deine verdrehte und unsortierte, kunterbunte Ansicht auf die Welt erhellt mein Leben und lässt so manche Dinge auch im Dunkeln strahlen.

...

LIST OF ABBREVIATIONS

ΔG_0	standard free Gibbs energy
$\mu\text{mol d}^{-1}\text{g}_{\text{dm}}^{-1}$	micromol per day per gram dry mass sediment
16S rRNA	small subunit of ribosomal ribonucleic acid with a sedimentary unit of 16
AEG	acylether glycerol
ANA	aldonitrile acetate
ANME	anaerobic methanotrophic archaea
AOM	anaerobic oxidation of methane
AR	archaeol (C_{20} - C_{20} isoprenoidal chains)
assim_{IC}	assimilation rate of inorganic carbon
ATP	adenosine triphosphate
BBr_3	boron tribromide
BPG	bisphosphatidylglycerol
BHPs	bacteriohopanepolyols
BP	biphytane
BSTFA	bis-(trimethylsilyl) trifluoroacetamide
C_{16} -PAF	1-O-hexadecyl-2-acetyl- <i>sn</i> -glycero-3-phosphocholine
Cer	ceramide
CH_4	methane
CO_2	carbon dioxide
CoA	coenzyme A
CSIA	compound-specific isotope analysis
D	deuterium
D_2O	deuterated water
Da	dalton
DAG	diacylglycerol
DAGE	dialkylglycerolether
DCM	dichloromethane
DEG	dietherglycerol
DFG	Deutsche Forschungsgemeinschaft
DGD	dialkylglyceroldiether
dGly	deoxy-glycosyl
DIC	dissolved inorganic carbon
diOH-AR	dihydroxylated archaeol
DNA	desoxyribonucleic acid
DPG	diphosphatidylglycerol (cardiolipin)
DSS	<i>desulfosarcina/desulfococcus</i> group
ELSD	evaporative light scattering detector
ESI	electrospray ionization

eV	electron volts
Ext-AR	extended archaeol (C ₂₀ -C ₂₅ isoprenoidal chains)
FA	fatty acids
FAME	fatty acid methyl esters
FID	flame ionization detector
FISH	fluorescent <i>in-situ</i> hybridization
G-1P	glycerol-1-phosphate
G-3P	glycerol-3 phosphate
Gal	galactose
GC	gas chromatography
GC-FID	gas chromatography coupled to flame ionization detector
GC-irMS	gas chromatography coupled to isotope ratio mass spectrometer
GC-MS	gas chromatography coupled to mass spectrometer
GDGT	glycerol dibiphytanyl glycerol tetraether (C ₄₀ -C ₄₀ isoprenoidal chains)
g _{dm}	gram dry mass
Glc	glucose
GLOMAR	Global Changes in the Marine Realm
Gly	glycosyl (hexose)
GoM	Gulf of Mexico
H ₂	hydrogen gas
H ₂ S	hydrogen sulfide
H ₃ PO ₄	phosphoric acid
HPLC	high performance liquid chromatography
ID	inner diameter
IPL	intact polar lipid
IS	internal standard
IT-MS	ion-trap mass spectrometer
KOH	potassium hydroxide
Li(C ₂ H ₅) ₃ BH	lithium triethylborohydride solution (super-hydride)
LLE	liquid-liquid extraction
<i>m/z</i>	mass to charge ratio
MAGE	monoalkylglycerolether
MAR	macrocylic archaeol
MARUM	Center for Marine Environmental Sciences
mbsf	meters below seafloor
mbsl	meters below sea level
MeOH	methanol
mL	milliliter
mM	millimolar
MPL	main polar lipid

MS ¹	primary order mass spectrometry stage
MS ²	secondary order daughter ion mass spectra
MSD	mass selective detector
MS ⁿ	higher order daughter ion (multistage) mass spectra
n.a.	not analyzed
n.d.	not detected
n.i.	not identified
NH ₃	ammonia
NMR	nuclear magnetic resonance
NO ₂ ⁻	nitrogen dioxide
NO ₃ ⁻	nitrate
NSF	National Science Foundation
O ₂	dioxygen
OH-AR	monohydroxylated archaeol
OMZ	oxygen minimum zone
PA	phosphatidic acid
PC	phosphatidylcholine
PCR	polymerase chain reaction
PDME	phosphatidyl-(N,N)-dimethylethanolamine
PE	phosphatidylethanolamine
PG	phosphatidylglycerol
PGP	phosphatidylglycerolphosphate
PI	phosphatidylinositol
PLFA	polar lipid-derived fatty acid
PME	phosphatidyl-(N)-methylethanolamine
PnE	phosphonoethanolamine
PO ₄	phosphate
prod _{Lipid}	total lipid production rate
PS	phosphatidylserine
PUFA	polyunsaturated fatty acid
Q-PCR	quantitative polymerase chain reaction
R _{a/p}	assim _{IC} /prod _{lipid} ratio
RNA	ribonucleic acid
ROV	remotely operated vehicle
SIMS	secondary ion mass spectrometry
SIP	stable isotope probing
SMTZ	sulfate-methane transition zone
SO ₄ ²⁻	sulfate
SR	sulfate-reduction
SRB	sulfate-reducing bacteria

TCA	trichloroacetic acid
TFA	trifluoroacetic acid
TIC	total ion chromatogram
TLE	total lipid extract
TMS	trimethylsilyl
TOC	total organic carbon
UK	unknown
Uns-AR	unsaturated archaeol
VFA	volatile fatty acid
VPDB	Vienna Pee Dee Belemnite standard
ZnCl ₂	zinc chloride

[CHAPTER I] - INTRODUCTION AND METHODS

I.1. GENERAL INTRODUCTION

This introduction section provides an overview on the importance and function of hydrothermal vents and cold seeps in the oceanic system. As opposed to other ecosystems, which rely directly or indirectly on photosynthetic activity, complex communities depend on chemosynthetic primary production in these two deep-ocean environments (see Fig. I.1). The geological settings of these unique sites are explained and the major aerobic and anaerobic biological processes at the sediment-water interface and within sediments are described. In addition, a detailed introduction into the hydrothermally active Guaymas Basin, representing the main focus of this thesis, is provided. Finally, an overview of major laboratory methods and the main objectives of this dissertation will be outlined.

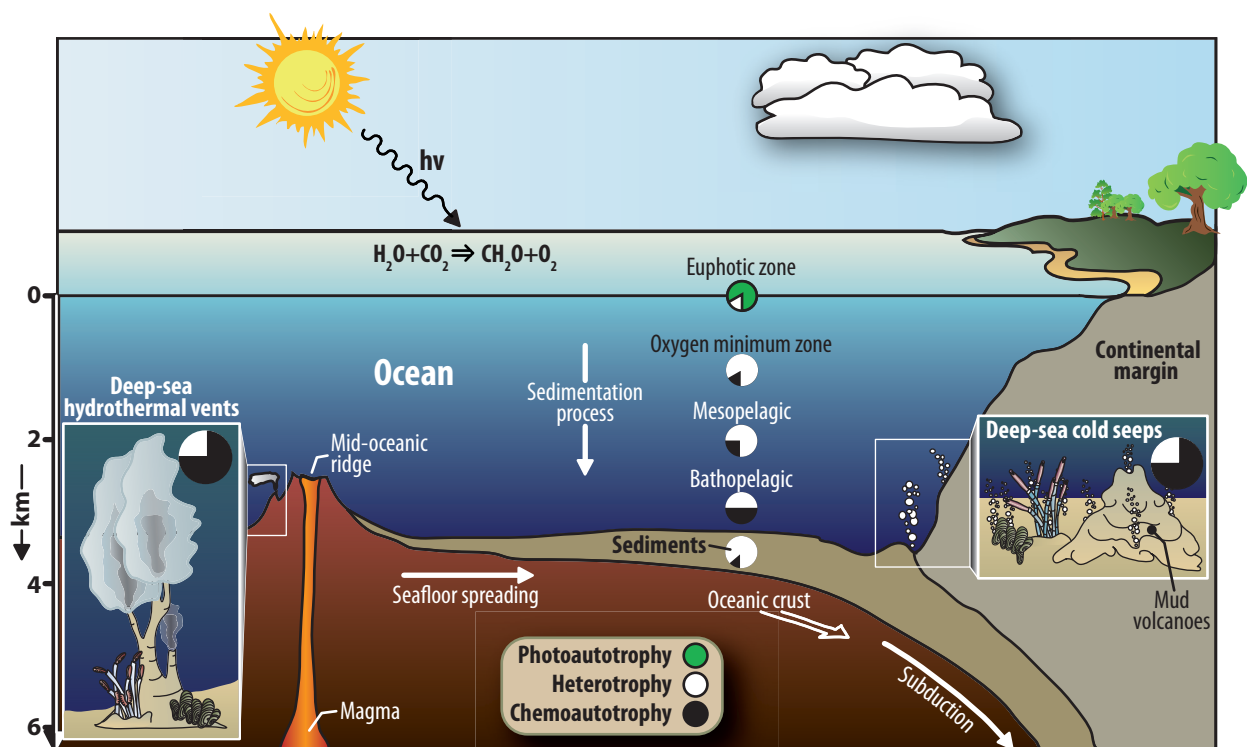


Fig. I.1. Schematic overview of the ocean water body including its major dark oceanic environments with seafloor structures such as hydrothermal vents and cold seeps. Pie charts provide a general overview on the relative importance of microbial processes. Sunlight, the driver of photosynthesis, only reaches the upper water body. Nevertheless, organic matter derived from photosynthesis is the major carbon source for heterotrophic microorganisms in the water column and also in the sediment. With increasing water depth the relative importance of photosynthetic derived organic matter as carbon source decreases and microorganisms that rely solely on inorganic carbon and chemical energy sources (chemoautotrophy) dominate the food chain in dark oceanic habitats. This figure has been modified after Jørgensen and Boetius (2007), Bach et al. (2006) and Dubilier et al. (2008).

I.1.1. Hotspots of life in the dark-ocean: Hot and cold vents

Roughly 70% of the Earth's surface is covered by oceanic waters, averaging 4,000 m in depth and reaching as deep as 11,000 m at the Mariana Trench. However, sunlight, the driver of photosynthesis, penetrates only the upper water body down to a maximum of 100-150 m

depth, leaving the remaining part of the ocean in the dark. Consequently, the dark-ocean represents the largest aqueous habitat for microbial life on Earth (Bach et al., 2006; Jørgensen and Boetius, 2007; Orcutt et al., 2011). In order to inhabit the remote deep sea, microorganisms need alternative energy sources, and have to adapt to the high hydrostatic pressure (up to 1,100 bar at the Mariana Trench) and the low temperatures (−1 to 4°C). Not long ago, the seabed was thought to be like a desert under water: uniform and biologically inert. However, the development and operation of marine technical tools for observing, mapping and sampling the seabed, e.g., remotely operated vehicles (ROVs), autonomous underwater vehicles (AUVs), and manned submersibles, enabled scientists to discover the highly dynamic and populated ecosystems in the dark-ocean, caused by interaction of the geo- and biosphere (e.g. Kelley et al., 2001; 2005; Teske et al., 2002; Haase et al., 2007; Inagaki et al., 2006; Reeves et al., 2011). For example, discoveries such as the rich microbial communities at hydrothermal vents (Corliss et al., 1979) and cold seeps (Paull et al., 1984; Kennicutt et al., 1985) changed the recognition of the ocean seafloor from plain seafloor to a highly diverse and dynamic environment (see Fig. 1.2).

1.1.2. A tight coupling between geo- and biosphere: Hydrothermal vents and cold seeps

1.1.2.1. Hydrothermal vents

Since the discovery of the Galapagos hot springs in 1977 (Corliss et al., 1979) more than 500 vent sites, concentrated at plate boundaries, have been found in the oceans (Godet et al., 2011) (Fig. 1.3). Deep sea hot vents are characterized by massive discharge of hydrothermal fluids into the overlying water column, thereby connecting the deep-ocean water body with the oceanic crust. The replacement of the hydrothermally discharged water masses is regulated by sea water intrusions from exposed outcrops of the oceanic crust. Those hydrothermal fluids can either be discharged in focused fluid flows (e.g., black smokers at the mid ocean ridges), or as diffuse emissions of cooler fluids across larger areas of the seafloor (Elderfield and Schulz, 1996; Hutnak et al., 2008). Hot vent fluids exhibit temperatures up to 400°C. Based on emission temperature and appearances hot vents are either classified as white smokers (temperatures between 100 to 300°C), whereas black smokers expel fluids with temperatures up to 400°C (Haase et al., 2007). The bright appearance of white smokers is caused by precipitation of barium, calcium and silica minerals, whereas black smokers are characterized by precipitation of sulfidic mineral phases (Fig. 1.2). Diffuse venting fluids showed temperature ranges from a few degrees above seawater temperature to about 100°C. Thus, although hot vents display only a smaller fraction of the hydrothermal fluid emissions they account for nearly half of the total heat flux from hydrothermal systems (German and von Damm, 2003).

Intense hydrothermal activities at the seafloor often occur directly at or close to tectonic boundaries (Fig. 1.3). The following four processes summarize the cause of hydrothermal activity:

- i. Formation of new oceanic crust along mid–ocean ridges. Due to tectonic forces two plates move apart from each other and new oceanic crust is formed (e.g., Mid Atlantic Ridge; East Pacific Rise; Guaymas Basin, Kelly et al., 2001;2005; Simoneit and Lonsdale, 1982).
- ii. Midplate volcanic hot spots can lead to a new crust formation in a form of islands such as the Hawaiian and Cape Verde islands and archipelago, Iceland or the Canary islands (e.g., Karl et al., 1988; Carracedo et al., 1998).
- iii. Compressional subduction processes occur where two platonic plates collide and one plate is subducted beneath the other (e.g., Marianas Trench reaching a water depth of almost 11 km below sea level; Seno and Maruyama, 1984; Schrenk et al., 2010).
- iv. Back arc basins which are derived from a combination of seafloor spreading and subduction processes (e.g., Manus Basin, Mariana Trough; Karig et al., 1970; Dunn and Martinez, 2011).

At hydrothermal vents a huge range of different thermally charged fluids (also called geofuels) are produced at high pressure and temperature, resulting in a transformation to hydrothermally altered fluids, which are reduced relative to the seawater. Thereby, the chemical composition of these hydrothermal fluids are largely dependent on the nature of the heat source, composition of the source rock, the temperature and the duration of the water rock interaction (Tivey, 2007). In general, hydrothermal fluids are particularly depleted in Mg, SO_4^{2-} and O_2 , whereas other chemical species, e.g., CH_4 , reduced sulfides, H_2 , reduced metals and silica have been added to the vent fluids (Allen and Seyfried et al., 2003; Tivey, 2007). However, depending on the tectonic setting and the underlying geology, the chemistry of vents can vary significantly depending on the site and also over time. Three different types of hydrothermal methane seeps have been described:

- i. Abiogenically produced methane from serpentinization reactions – e.g., at the Lost City Hydrothermal Field (Kelly et al., 2001; 2005).
- ii. Thermogenically produced methane from water–rock reactions at high temperatures – e.g., on the Juan de Fuca Ridge (Baross et al., 1982; De Angelis et al., 1993).
- iii. Thermogenic alteration of buried sedimentary organic matter – e.g., the Guaymas Basin in the Gulf of California (Simoneit and Lonsdale, 1982; Welhan et al., 1988; Bazylnski et al., 1988; see section 1.2).

The importance of hydrothermally driven convection for the global element cycles has been shown in different studies. For instance, geochemical model simulations hypothesized that the entire volume of the ocean–water body circulates through the crust within 4,000 to 70,000 years (Elderfield and Schulz, 1996; Wheat et al., 2003). This crustal fluid flow of seawater interacts with the seafloor basalt, leading to a fluid–rock interaction, which greatly impacts

the global ocean chemistry. For example, Sander and Koschinsky (2011) estimated that the hydrothermal fluids could account 9 and 14% of the total deep-ocean dissolved iron and copper budgets, respectively.

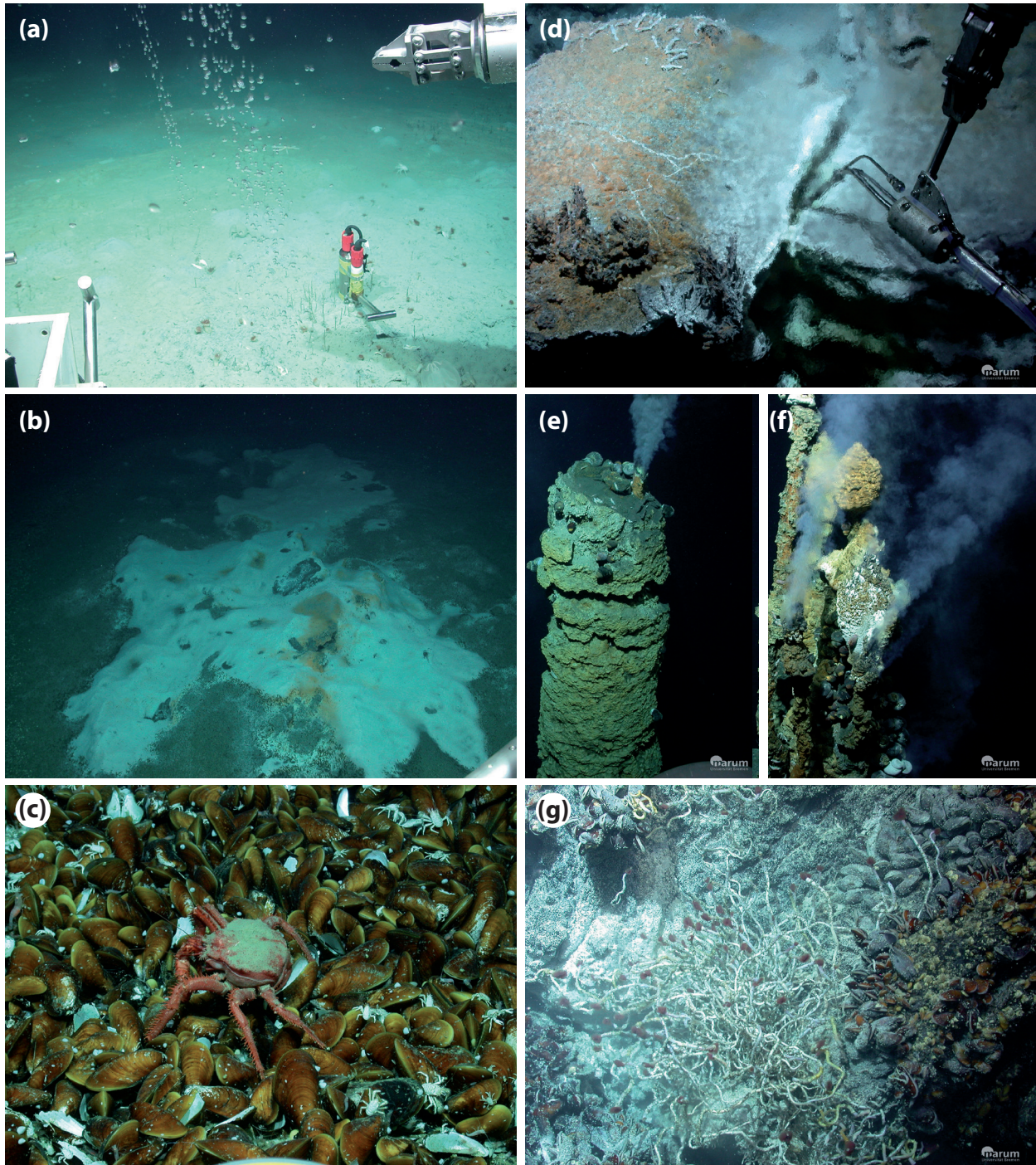


Fig. 1.2. Typical pictures presenting biological oases in the dark-ocean: (a–c) Cold seep habitats from the continental margin off Pakistan (Meteor Expedition M74/3). (d–g) Typical hydrothermal vent features found in the Manus Basin, Papua New Guinea (Sonne Expedition SO216). All images were taken by the remotely operated vehicle Quest (courtesy of MARUM, University of Bremen).

1.1.2.2. Cold seeps

Shortly after the discovery of hydrothermal vents, a second type of chemosynthetic seafloor environment was detected: cold seeps. Unlike hydrothermal vents, cold seeps are characterized by the advection of fluids with temperatures only slightly above ambient seawater (~4°C). The first cold seep system has been identified in the northern Gulf of Mexico continental slope (Florida Escarpment; Paull et al., 1984). Nowadays, cold seeps are recognized as a globally widespread feature, which can be found in either active continental margins such as the Peruvian Margin (close proximity to plate boundaries; Kulm et al., 1986; Lallemand et al., 1992) or passive continental margins such as the Gulf of Mexico (Paull et al., 1984; Hovland, 1992; Fig. 1.3). Cold seeps have been found in shallow waters such as the coastal zones of the Eckernförde Bay (Anderson et al., 1998) or at Cape Lookout Bay (Martens and Val Klump, 1980) but also in deep sea trenches in several thousand meters depth (Japan Trench; Kobayashi et al., 1992). Their surface expression can range from centimeter to kilometers scale in diameter (Kopf et al., 2002) and the type of cold seep surface feature (e.g., gas seeps, mud volcano, pockmarks and brine/oil pools) may depend on the geological settings, the intensity of the fluid flow and nature of the discharge (e.g., gas, fluid, mud).

Depending on the fluid source, the seep discharge can be loaded with hydrocarbons, CO₂ and H₂S. However, the most important fluid constituent is CH₄, exceeding 90% of the total dissolved gases (Dimitrov, 2002; Kopf, 2002). In the following potential CH₄ sources are described:

- i. Microbial methane production: biological methane production is performed by microorganisms known as methanogens. Methanogenesis is the last step in the anaerobic degradation of organic matter (cf. [BOX I]), where single-celled methanogenic archaea utilize fermentative end products such as acetate and CO₂/H₂ to produce methane (e.g., Whiticar et al., 1986).
- ii. Thermogenic methane production (deep thermogenic reservoirs): organic material which escaped microbial degradation is subsequently converted by heat-induced processes to heavy gaseous and liquid hydrocarbons at temperatures between 80-120°C (early thermogenic gas formation) which ultimately are converted to CH₄ at temperatures between 150-200°C (late thermogenic gas formation; Claypool and Kvenvolden, 1983).
- iii. Abiogenic methane production: abiogenic methane formation is independent of organic matter and also from microbial activity. Abiotic methane is predominantly produced by diagenesis of fresh oceanic rocks, such as found in the Lost City Hydrothermal vent fields from the Mid Atlantic Ridge (Rona et al., 1992; Kelley et al., 2001; 2005). In these places, the heating of rock material to temperatures above 300°C releases, by serpentinization, hydrogen which can react with CO₂ resulting in abiogenic methane (Foustoukos and Seyfried, 2004). Production of abiogenic CH₄

is suggested to play a minor role in the global methane budget (Sherwood Lollar et al., 2002).

- iv. From the dissociation of gas hydrates: gas hydrates are ice-like solids, formed by water crystals encaging large volumes of natural gas (Kvenvolden, 1993). They represent the greatest CH_4 reservoir on Earth, and are extremely abundant in oceanic sediments (e.g., Kvenvolden, 1993; Bohrmann and Torres, 2006). The stability of gas hydrates is mainly controlled by temperature, pressure and the concentration of gases, so that slight changes in in situ conditions (e.g., increase in temperature or decrease in pressure) may abruptly release a vast quantity of CH_4 (cf., Bohrmann and Torres, 2006).

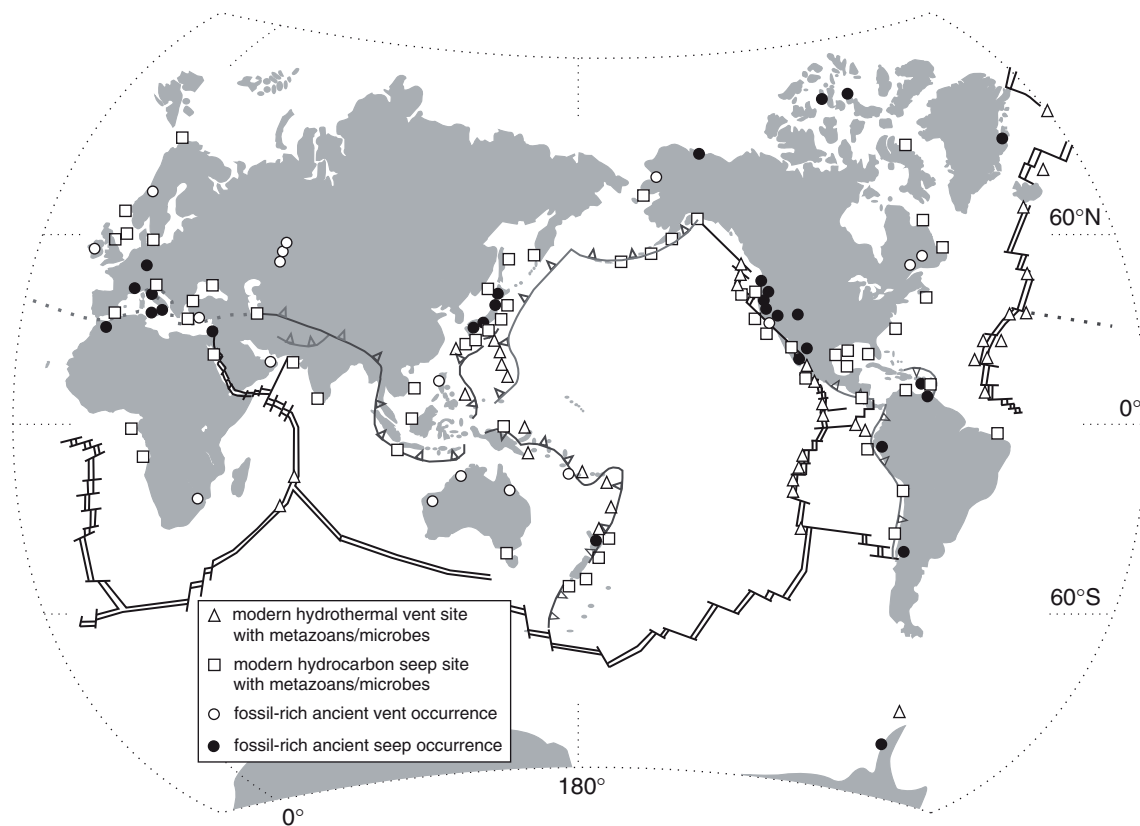


Fig. I.3. Global distribution of modern and fossil chemosynthesis-based hydrothermal vents and cold seeps. Hydrothermal vents at the seafloor often occur directly at or close to tectonic boundaries. Figure has been adapted from Campbell (2006).

Due to tectonic activities, fissures and faults in the sediments, hydrocarbon-rich gases and fluids migrate upward through cracks and channels from deeply buried sediments towards the surface sediments (Fig. I.2; Brocks et al., 1984; Sassen et al., 1999). A vast fraction of discharged methane is consumed by aerobic and anaerobic methane oxidizing microorganisms in the near surface sediments (see section I.1.4), however, when the potential for methane utilization is exceeded, CH_4 is released into the hydrosphere (Fig. I.2). Thus, methane plumes can reach several hundred meters into the water column (Greinert et al., 2006; Sauter et al., 2006), reaching in some cases, the atmosphere if the seeps are located in shallow waters. Methane in the atmosphere acts as greenhouse gas with 25 times higher potential than CO_2 (Lelieveld

et al., 1993) and has a major impact on Earth's climate. However, the quantification of upward-migrating methane from cold seeps into the atmosphere is difficult and thus up to date poorly constrained (Solomon et al., 2009).

1.1.3. Chemosynthetic biomass production as driver of dark-ocean benthic habitats

In 1977, the discovery of the hydrothermal vent ecosystems (Galapagos Rift, Pacific Ocean) based entirely on chemosynthesis communities changed the understanding of the limits of life on Earth (Corliss et al., 1979; Jannasch and Mottl, 1985; Deming and Baross, 1993; Van Dover et al., 2002; Bach et al., 2006). The first cold seep faunal assemblages were described in the northern Gulf of Mexico (Kennicutt et al., 1985) and at subduction zones in the northwestern Pacific (Suess et al., 1985). The metabolic strategies of microorganisms in the dark ocean differ from the sunlight-dependent photosynthetic world (0–300 m depth), where metabolic energy is gained from the coupling of redox reactions (see [BOX I]).

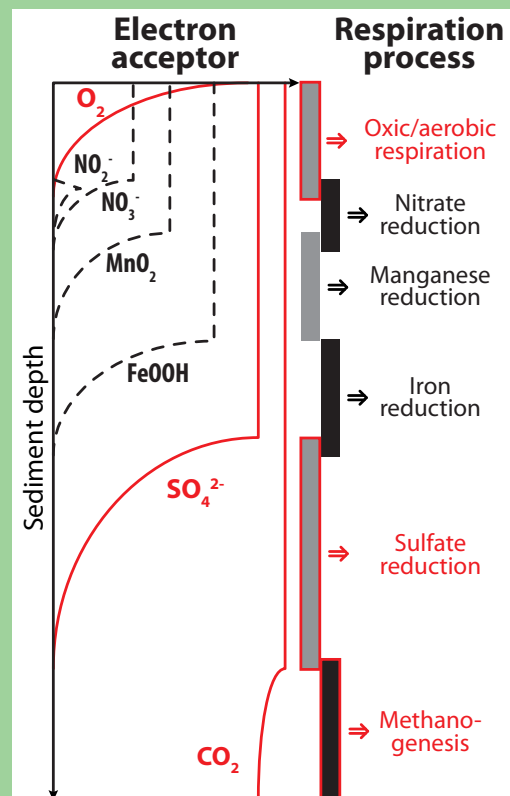
BOX I Electron donors and acceptors in the marine & dark oceanic environments

In contrast to photoautotrophic carbon fixation where the energy comes from sunlight, chemosynthesis is the process by which microorganisms harness the energy in chemical bonds to convert one-carbon molecules (e.g., CO_2 and or CH_4) into biomass. Chemosynthesis is carried out exclusively by Bacteria and Archaea.

The activity of microorganisms in the sunlight-independent dark ocean depends on the availability of electron donors (oxidizable compounds) and acceptors (reducible compounds). Within typical marine sediments, a well-known cascade of preferred electron donors and acceptors is observed (Froehlich et al., 1979). The major electron donors in the dark oceans are organic matter, hydrogen (H_2), methane (CH_4), reduced sulfur, iron and manganese compounds. These electron sources differ in significance for microbial metabolism, since they have differences in abundance and energy potential. On the other hand, the major electron acceptors can be characterized by the order of highest electron accepting potential, starting with O_2 , NO_2^- , NO_3^- , Mn and Fe oxides, oxidized sulfur compounds (e.g., SO_4^{2-}), and finally CO_2 (Fig. I.4; Froehlich et al., 1979).

In marine sediments the majority of the organic matter degradation is coupled to sulfate reduction. Since SO_4^{2-} exists in almost unlimited quantities in seawater and oxygen is quickly consumed by aerobic respiration, SO_4^{2-} is consequently the most important electron acceptor in marine sediments (Jørgensen, 1982).

Fig. I.4. Schematic representation of the broad range of redox-active compounds in marine environments and the names describing the respiration process. The order of electron acceptors utilization is based on the thermodynamic potential of the process and the energy available to the organisms. The most important electron acceptors/respiration processes dealt with in this dissertation are highlighted in red. Figure has been modified from Canfield and Thamdrup (2009).



The primary producers living in these extreme environments are microorganisms that live either as chemolithoautotrophs using inorganic chemicals as electron donor and CO_2 as carbon source, or chemoorganoheterotrophs consuming CH_4 as both electron donor and carbon source. However, microorganisms can only gain the chemical energy if the reaction is thermodynamically favorable. This is the case when the electron-donor rich fluids encounter cold seawater, rich in electron-acceptors. Hereby, chemotrophic organisms gain their energy by oxidizing reduced elements of the vent/seep fluids such as H_2 , CH_4 , H_2S , NH_3 , Fe(II) , Mn^{2+} , with available oxidants supplied by the seawater such as CO_2 , SO_4^{2-} , S , Fe(III) , NO_3^- or O_2 (see [BOX I]). The presence of chemosynthetic communities at the seafloor is thus indicative of near-surface methane and/or sulfide discharge (Fig. I.2). However, the redox processes at these extreme environments depend indirectly also on sunlight. For example, the vast fraction of CH_4 discharged at cold and hot seeps is most often derived from the decay of organic matter, which was originally derived from photosynthesis. In addition, the electron-acceptors for primary production (e.g., O_2 , SO_4^{2-} and NO_3^-) derived from seawater have been ultimately oxidized by photosynthesis.

The simultaneous appearance of electron-donor and electron-acceptor rich fluids at the seafloor of both hot and cold seeps is the cause of a massive accumulation of symbiotic and free living microfauna (Fig. I.2). In fact, CH_4 -fuelled microbial communities have been shown to harbor the largest amounts of biomass of all marine ecosystems (up to 10^{12} cells per cm^3 ; Michaelis et al., 2002; Treude et al., 2007). A symbiotic association of chemotrophic microorganisms with invertebrates is probably one of the most characteristic features occurring at cold seeps and hydrothermal vents. For example, bivalves and clams are known to host symbionts in their gills (see [BOX II]; e.g., Fisher et al., 1993; Distel et al., 1995) and tubeworms rely on endosymbionts in their trophosome (Cordes et al., 2005; Lösekann et al., 2008). However, methanotrophic and thiotrophic symbionts have also been observed as free living microorganisms, without a symbiotic partner such as the widespread and giant sulfur-oxidizing Gammaproteobacteria *Beggiatoa*, *Thiomargarita*, and *Thioploca* (e.g., Jannasch et al., 1989; Sassen et al., 1993).

Due to elevated temperatures at hydrothermal vents, many record-holding extreme microorganisms have been isolated from such environments. Those extremophiles are able to tolerate extreme conditions such as high temperatures, hydrostatic pressure, toxic chemistry, extreme pH, and permanent fluctuations of environmental conditions (Takai et al., 2006). For example, a newly isolated, hyperthermophilic methanogen *Methanopyrus kandleri* strain has been shown, to survive under laboratory conditions at high hydrostatic pressure (20 MPa) and temperatures of up to 122°C (Takai et al., 2008). This temperature is the current upper temperature limit of life under laboratory conditions; but further evidence suggests that this limit of life might actually be closer to 150°C (Schrenk et al., 2003; Hoehler et al., 2007).

BOX II Symbiotic chemosynthesis at cold seeps and hot vents

The term “symbiosis” has Greek roots; “sym” means with and “bio” means living. Symbiosis can be defined as a close association between two different organisms. Up to now, at least seven animal phyla (e.g., mussels, snails, worms, sponges and single-celled ciliates) are known to host chemosynthetic symbiotic microorganisms. Chemosynthetic symbioses have been found at different habitats including hydrothermal vents and cold seeps. Hereby, the symbionts provide the eukaryotic host nutrition, while the host supplies the symbiotic bacteria with fluids, enriched in electron donors such as CH_4 or H_2S and electron acceptors such as O_2 , by positioning themselves at the interface between reduced and oxidized fluids (Petersen and Dubilier, 2010).

In general, *Bathymodiolus spp.* are known to dominate the biomass production at hydrothermal vents and cold seeps (Fig. I.5a; Van Dover, 2000). These mussels have been found in association with sulfur-oxidizing (Cavanaugh, 1983; Distel et al., 1988) and methane-oxidizing bacteria (Childress et al., 1986) and specimens hosting both groups of these Gammaprotobacteria (Fisher et al., 1993; Distel et al., 1995). Just recently, Petersen et al. (2011) found that the symbionts of the hydrothermal vent mussel *Bathymodiolus puteoserpentis* recovered from the Mid-Atlantic Ridge can also use H_2 as electron donor, extending the number of substrates for chemosynthetic bacteria (Fig. I.5b). The symbionts can either be housed as endosymbionts within specialized gill bacteriocytes (intra- or extracellularly) or ectosymbionts, which are found to be attached to the outside surface of the host (Dubilier et al., 2008; Duperron et al., 2009). Many host organisms known to harbor endosymbionts have shown reduced digestive systems and/or none functional guts, highlighting the evolutionary adaption of a food web solely based on their symbionts (Page et al., 1990; Colaço et al., 2006; Cavanaugh et al., 2006).

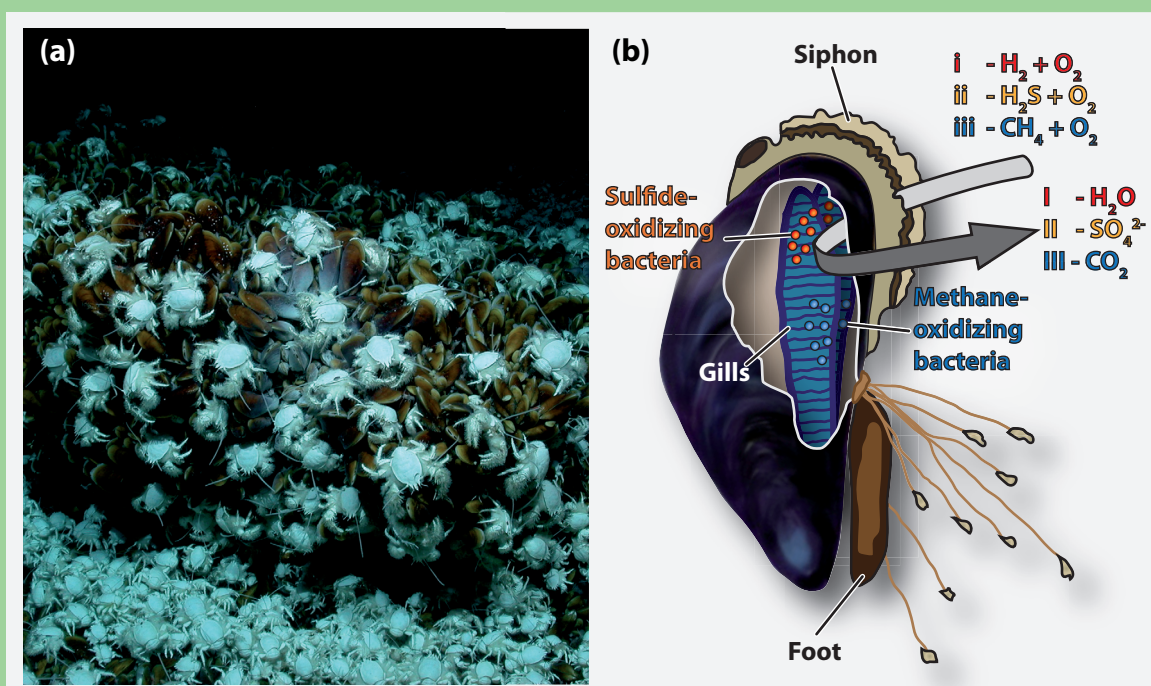


Fig. I.5. Symbiotic chemosynthesis in extreme environments. (a) Picture shows a mussel vent field from a cold seep located off Pakistan taken by the remotely operated vehicle Quest (MARUM, University of Bremen). (b) Schematic drawing of the function of symbionts within a *Bathymodiolus spp.* mussel. The gray arrow indicates the three possible metabolic reactions performed by bacteria to harness energy (i) oxidation of H_2 to H_2O and (ii) oxidation of H_2S to SO_4^{2-} both performed by sulfide oxidizing bacteria; (iii) oxidizing CH_4 to CO_2 performed by methane oxidizing bacteria. Figure has been modified after Orphan and Hoehler (2011).

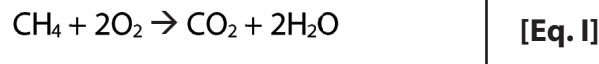
Cross Reference: [Chapter II] examined symbiont–host interactions within *Bathymodiolus* mussels using a comprehensive lipid biomarker approach. This study targets IPLs (see section I.3.1.2) as a lipid class capable of distinguish bacterial from host derived biomass.

1.1.4. Methane oxidation: A globally important biogeochemical process

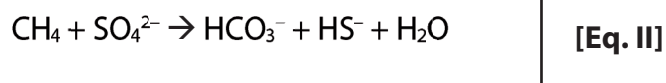
Methane, the simplest and most abundant hydrocarbon in the atmosphere, plays an important role in Earth's greenhouse problem. Its ability to trap heat via absorption and re-emission of infrared radiation has been shown to be roughly 25 times stronger than CO₂ (Lelieveld et al., 1993). Therefore, its concentration in the atmosphere significantly influences the energy budget of the Earth. However, marine environments, considering the high production rates and large reservoirs of CH₄ in marine sediments, contribute only little to the atmospheric budget (Judd et al., 2002; Reeburgh, 2007), due to aerobic and anaerobic microbial methane oxidization.

1.1.4.1. Aerobic oxidation of CH₄

At the sediment–water interface at cold seep and hot vent environments high fluxes of upward-advecting CH₄ gas can be oxidized aerobically. Aerobic methanotrophy can be described by the reaction equation [Eq. I]:



Compared to the anaerobic oxidation (see section 1.1.4.2), the efficiency of the aerobic methane oxidation is more than one order of magnitude higher (Nauhaus et al., 2007), therefore the aerobic oxidation of the seep and vent community represents an efficient sink for CH₄ (Sommer et al., 2009). However, at cold and hot vents, the aerobic oxidation of methane is limited by the rapid consumption of oxygen (Suess et al., 1999). Sulfate, on the other hand, exists in exhaustless concentration in seawater (29mM; Jørgensen, 1982; Reeburgh, 2007), enabling the sulfate–dependent anoxic methane oxidation (Reeburgh et al., 1969). Thus, the main biological sink for CH₄ consumption in marine sediments, including seep and vent environments, is the anaerobic oxidation of methane (AOM; [Eq. II]) with sulfate as oxidant.



1.1.4.2. The history of AOM: A globally important process regulating ocean's CH₄ emission

The oceans contribute about 7–25% to the total global methane production (Hinrichs and Boetius, 2002; Reeburgh, 2007). However, more than 90% of the total oceanic methane production is consumed by the anaerobic oxidation of methane (AOM), thereby reducing the oceans contribution to the atmosphere methane budget to less than 2% (Valentine and Reeburgh, 2000; Reeburgh, 2007). The main niches for AOM-performing microorganisms in the marine realm are sulfate methane transition zones (SMTZ; [BOX III]), where both methane (transported from below) and sulfate (transported from above) are simultaneously consumed. In marine sediments, first evidence for AOM came from *in situ* pore water gradients, showing the mutual depletion of methane and sulfate in methane-rich anoxic sediments (e.g., Reeburgh,

1969; Martens and Berner, 1974; Barnes and Goldberg, 1976; Reeburgh, 1976, 1980; Iversen and Blackburn, 1981; see [BOX III]). The stoichiometric relationship of methane oxidation and sulfate reduction was first published by Reeburgh (1976; [Eq. II]). Later, Iversen and Jørgensen (1985) showed that rates of maximal methane oxidation coincide with a maximum in sulfate reduction at the SMTZ [BOX III], indicating that CH_4 consumption is directly linked to sulfate reduction. The consumption of methane and the formation of sulfide from sulfate are coupled at a molar ratio of approximately 1:1 (e.g., Nauhaus et al., 2002, Holler et al., 2009; 2011b), confirming the stoichiometric equation of AOM (cf. [Eq. II]).

BOX III Sulfate methane transition zones and the appearance of AOM

The sulfate methane transition zone (SMTZ) is present in all anoxic marine systems where CH_4 is transported upwards from the zone of production (methanogenic zone) and SO_4^{2-} derived from the overlying water column diffuses downwards (Reeburgh et al., 2007). In this centimeter-scale sediment horizon microbial activity is enhanced by the anaerobic oxidation of methane (AOM; see section I.1.4.2) coupled to autotrophic sulfate reduction (e.g., Hinrichs and Boetius 2002; Parkes et al., 2005).

For example, in typical marine sediments the relatively slow upward movement of CH_4 allows AOM-mediating organisms to remove CH_4 at the SMTZ efficiently (Iversen and Blackburn, 1981; Iversen and Jørgensen, 1985; Fossing et al., 2000). Considering the enormous aerial extent of marine sediments (Whitman et al., 1998), the SMTZ plays a key role in the global CH_4 cycle (Hinrichs and Boetius, 2002; Reeburgh, 2007). Carbon cycling within the SMTZ, in general under cm scale, shapes geochemical gradients (e.g., CH_4 , SO_4^{2-} , DIC/alkalinity) and also stable carbon isotopic profiles of CH_4 and DIC at the scale of meters both above and below this biogeochemically active horizon. The intersection of both CH_4 and SO_4^{2-} concentration (see Fig. I.6a), as well as depleted stable carbon isotopic compositions of both CH_4 and DIC (see Fig. I.6b) enables to identify the hotspot of active AOM (e.g., Valentine and Reeburgh, 2000). Further evidence for AOM is provided by radiolabeling experiments, where methane oxidation rates ($^{14}\text{CH}_4$) and sulfate reduction rates ($^{35}\text{SO}_4^{2-}$) peak within the SMTZ (see Fig. I.6c).

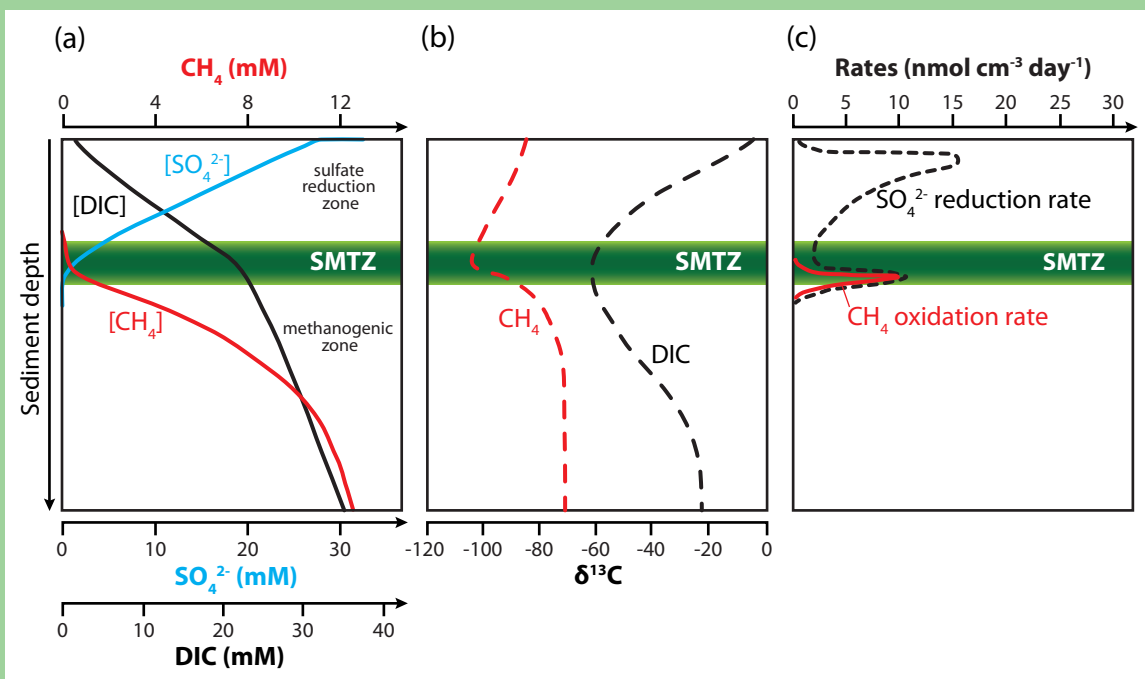


Fig. I.6. General geochemical profiles in marine sediment where the anaerobic oxidation of methane (AOM) takes place. (a) Concentration profiles of SO_4^{2-} , DIC, CH_4 (modified after Reeburgh, 2007); (b) stable isotope data ($\delta^{13}\text{C}$) for DIC and CH_4 (redrawn from Pohlman et al., 2008); (c) rates of SO_4^{2-} reduction and CH_4 oxidation (redrawn from Iversen and Jørgensen, 1985).

In 1994, Hoehler and colleagues postulated that AOM is performed most likely in a syntrophic reaction by methanogenic archaea and sulfate-reducing bacteria: a reversely acting methanogen consumes methane and produces hydrogen (via a reversal of CO_2 reduction) which in turn is metabolized by a sulfate-reducing partner. Although thermodynamic calculations for this reaction [Eq. II] resulted in extremely low energy yields ($\Delta G^\circ = -20$ to -40 kJ mol^{-1} ; Hoehler et al., 1994; Knab et al., 2008; Alperin and Hoehler, 2009a), their hypothesis for the functioning of AOM is still accepted. Nevertheless, the poor energy yield of this redox reaction, which furthermore needs to be split between both partners, contradicts the traditional view of the minimum free energy threshold of -20 kJ mol^{-1} determined for bacteria (i.e., the amount of energy needed to generate ATP/mole H^+ ; Schink, 1997). Therefore the understanding of the physiology and biochemistry of AOM remains incomplete.

The involvement of Archaea in AOM was indicated by strong ^{13}C depletion of characteristic archaeal biomarkers ($\delta^{13}\text{C}$ of archaeol = -100‰ ; $\delta^{13}\text{C}$ of hydroxyarchaeol = -110‰) identified in seep sediments, leading to the conclusion that AOM microbial communities directly assimilate ^{13}C -depleted methane (Hinrichs et al., 1999). Later, numerous other studies presented $\delta^{13}\text{C}$ biomarker data showing additional isotopically depleted lipids for the methane oxidizing archaea, such as isoprenoidal hydrocarbons like tetramethylhexadecane (crocetane) and pentamethyleicosane (PMI), as well as diagnostic fatty acids (FAs) and non-isoprenoidal glycerol ethers for the sulfate-reducing bacterial partner (SRBs). Those archaeal and bacterial biomarkers showed $\delta^{13}\text{C}$ values ranging from -70‰ to -130‰ and -60‰ to -100‰ , respectively (e.g., Elvert et al., 1999, 2003, 2005; Hinrichs et al., 1999, 2000; Pancost et al., 2000; Blumenberg et al., 2004; Niemann and Elvert, 2008).

Cross Reference: Previous studies interpreted extremely ^{13}C -depleted archaeal and bacterial lipid biomarkers as clear indicator for methane-driven lipid biosynthesis. However, just recently, Alperin and Hoehler (2009b) questioned the exclusive methanotrophic carbon fixation by the Archaea and hypothesized a possible autotrophic CO_2 fixation pathway for both Bacteria and Archaea. Their hypothesis has been fueled by observations of Wegener and colleagues (2008) amending cold seep AOM communities with either $^{13}\text{CH}_4$ or $\text{H}^{13}\text{CO}_3^-$ and detecting a mixed carbon assimilation of CH_4 and CO_2 within the Archaea and a pure autotrophic lipid production within the Bacteria. [Chapter III] has used a similar approach as Wegener et al. (2008) in which the dominant carbon source of both the Archaea and the Bacteria has been investigated by applying an improved SIP approach (Dual-SIP; see section I.3.2.4).

Boetius and colleagues (2000) were the first to visualize the consortium of ANME and the SRBs via microscopy of cells hybridized with fluorochrome-labeled specific oligonucleotide probes. These aggregates of ANME and SRB have been shown to be the dominant microbial population in various cold seep environments, representing more than 90% of the total microbial community in this habitat (Boetius et al., 2000; Michaelis et al., 2002; Orphan et al., 2002). Gene-based studies (16S rRNA, *mcrA*) revealed that AOM in marine environments is mediated by three distinct clusters of Euryarchaeota (ANME-1, ANME-2, and ANME-3). These three phylogenetic clusters of archaea are related to the orders of *Methanosarcinales* and

Methanomicrobiales, however, the phylogenetic distance between all three clusters is large. Thus, ANME-1, ANME-2, and ANME-3 belong to independent families, which may enable AOM in a wide range of environmental settings (Knittel et al., 2005; Knittel and Boetius, 2009). The associated sulfate-reducing partners of the ANMEs have been shown to be mainly relatives of the *Desulfosarcina/Desulfococcus* or *Desulfobulbus* branch of Deltaproteobacteria (Boetius et al., 2000, Michaelis et al., 2002; Knittel et al., 2003, 2005; Niemann et al., 2006). However, ANME are not restricted to the physical co-occurrence with a bacterial partner. Particularly ANME-1 appears frequently as single cells or as monospecific aggregates and filaments (Orphan et al., 2002; Reitner et al., 2005).

1.2. The Guaymas Basin vent site – A rare example of hydrothermal alteration of buried sedimentary organic matter

Most hydrothermal vents are situated in the open ocean, which is characterized by low sedimentation, and thus newly formed oceanic crusts are not covered by sediments. However, the Guaymas Basin hydrothermal vent site in the Gulf of California represents an exception. Due to its proximity to land the actively spreading ocean basin is covered by a thick (>400 m) organic-rich sediment layer (Simoneit and Lonsdale, 1982). Thus, magma intrudes into fresh mud, heating the surrounding sediments, which leads to thermogenic decay of the organic matter and drives the formation of closely spaced and mountain-forming seafloor vents (Calvert, 1966; Einsele et al., 1980; Lonsdale and Lawver, 1980; Lonsdale and Becker, 1985). This unique setting results in the hydrothermal formation of petroleum by organic matter alteration, which typically only occurs at great depth and over long timescales (Didyk and Simoneit, 1989). At Guaymas, hydrothermal fluids are enriched in thermogenic isotopically depleted hydrocarbons (mainly CH₄; Welhan, 1988; Bazylinski et al., 1988; Whelan et al., 1988) and low molecular weight organic acids (Martens, 1990), which are transported towards the sediment–water interface, where they feed dense benthic microbial communities (Edgcomb et al., 2002; Goetz and Jannasch, 1993; Guezennec et al., 1996; Teske et al., 2002; 2003; Pearson et al., 2005). The range of methane δ¹³C carbon isotopic compositions of –43 to –51‰ (Welhan, 1988) has been recognized to be dominantly biogenic- and only partly thermogenic-derived (Pearson et al., 2005).

The upward flux of reduced substrates in combination with a steep temperature gradient near the sediment surface (Fig. 1.7) causes a compressed centimeter-scale sequence of aerobic and anaerobic microbial processes, including sulfide oxidation (Jannasch et al., 1989; Nelson et al., 1989; Gundersen et al., 1992), sulfate reduction (Jørgensen et al., 1990, 1992; Elsgaard et al., 1994; Weber and Jørgensen, 2002; Kallmeyer et al., 2003), methane oxidation (Teske et al., 2002; Kallmeyer and Boetius, 2004), and methanogenesis (Welhan et al., 1988), which in other marine sediments would spread out over tens to hundreds of meters below the seafloor (e.g., D'Hondt et al., 2002, 2004). However, recent and ongoing research has shown that CH₄ is the key biogeochemical driver for microorganisms in Guaymas Basin sediments (Holler et al.,

2011a, Biddle et al., in press). These authors indicated that AOM and the responsible archaeal communities exist over a wide range of temperatures (between 5 and 70°C), indicating the biogeochemical relevance of AOM and ANME archaea in not only cold but also hot marine habitats.

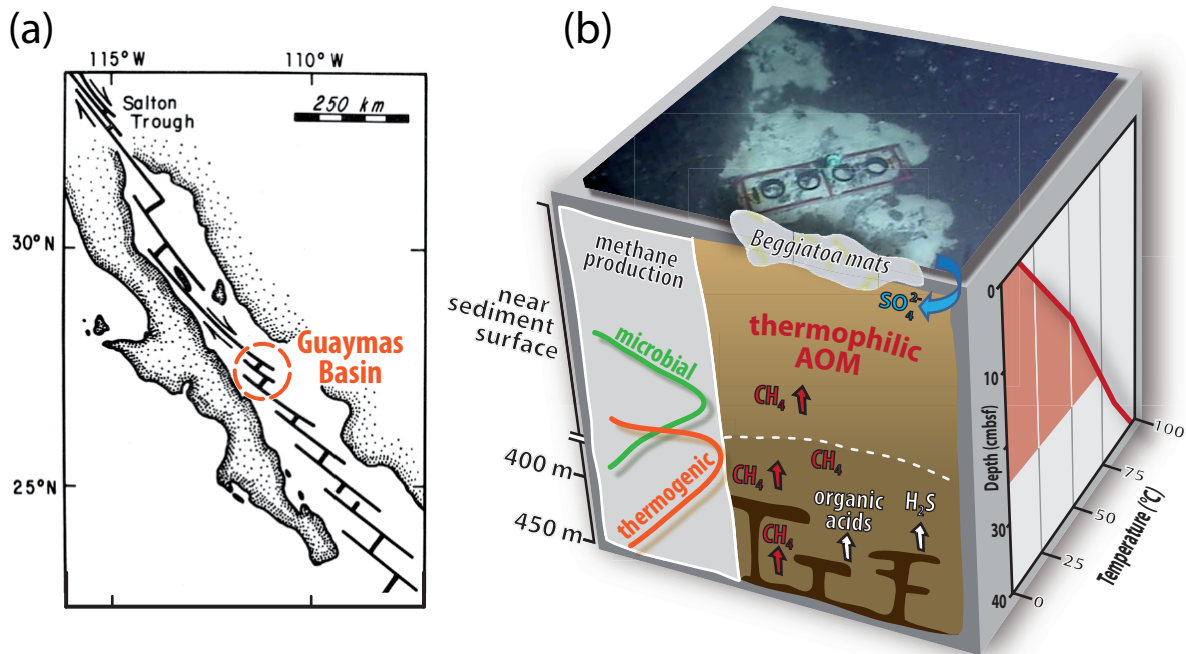


Fig. 1.7. (a) Schematic map showing the location of the hydrothermal vent site in the Guaymas Basin (adapted from Lonsdale, 1980). (b) Cube illustration merging a typical hydrothermally-influenced Guaymas Basin surface sediment photography (top panel) with a schematic view of the Guaymas Basin hydrothermal setting (left panel), and the measured temperature profiles (research cruise AT 15–56 push core 4569-8; right panel). Extensive and unusually thick mats of autotrophic, sulfur-oxidizing *Beggiatoa* at the surface are a characteristic feature of Guaymas Basin sediments, which are powered by the metabolic AOM byproducts H₂S and CO₂ (Jannasch et al., 1989; Nelson et al., 1989). The picture (top panel) is courtesy of the Woods Hole Oceanographic Institution and the schema (left panel) has been modified from Amend and Teske (2005).

1.2.1. Possible thermophilic AOM in hydrothermal environments

Hydrothermal vent systems are in general not optimal habitats for AOM communities, since most hydrothermal areas lack any sediment cover and rapid changes of environmental conditions such as temperature may inhibit the propagation of slow-growing organisms. Furthermore, hydrothermal fluids are mostly sulfate-free and the ambient sulfate-rich seawater contains oxygen, which is toxic to ANME organisms. However, first hints for a broader temperature range of anaerobic methanotrophs were given by identification of 16S rRNA genes of ANME-1 (Teske et al., 2002; Schrenk et al., 2004; Roussel et al., 2008) and ANME-specific core tetraether lipids (Schouten et al., 2003) in hydrothermally influenced marine sediments. Also the detection of trace AOM in such sediments, using ¹⁴CH₄, indicated possible AOM at temperatures of up to 80°C (Kallmeyer and Boetius, 2004). Most recently, a subgroup of thermophilic ANME and their novel partner bacteria were isolated from Guaymas Basin sediments (Holler et al., 2011). These authors performed laboratory experiments providing evidence for active methane oxidation

with a thermophilic temperature optimum between 45°C and 60°C (cf. Fig. I.8) and an upper limit of AOM up to 70°C. These results finally extend the known growth range of ANME organisms, which was before defined as a moderately psychrophilic or mesophilic process widespread in marine sediments and cold seep environments (e.g., Orphan et al., 2002; Knittel et al., 2005; Nauhaus et al., 2007; Holler et al., 2009; Knittel and Boetius, 2009).

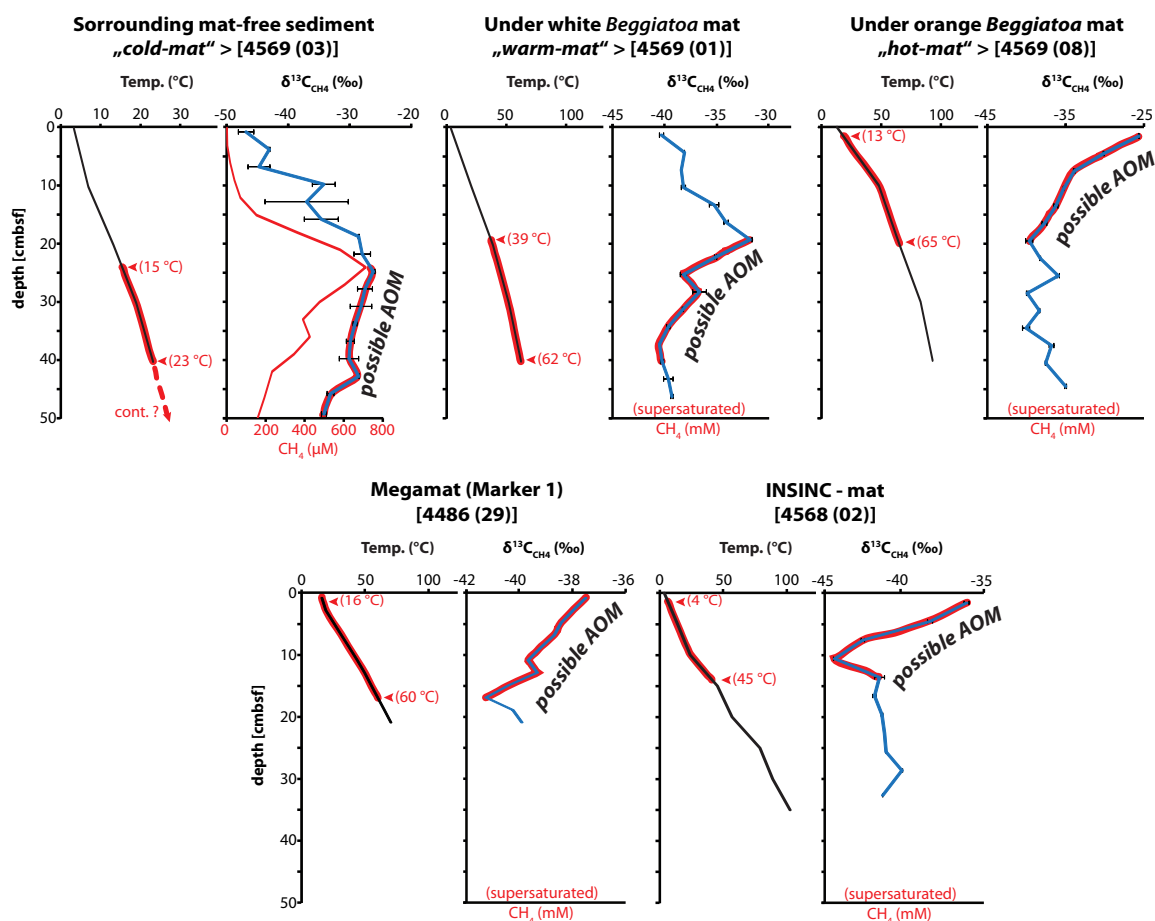


Fig. I.8. Geochemistry of CH_4 for different push core stations analyzed during two Guaymas Basin research cruises (AT 15–40; AT 15–56). Selected profiles of temperature, concentration and carbon isotopic composition of CH_4 from different locations are shown. Here, $\delta^{13}\text{C}$ -isotopic signatures of CH_4 provided consistent evidence of ongoing AOM at elevated temperatures (Kellermann et al., unpublished results; cf. Biddle et al., in press). Zones of possible AOM (here indicated in red), coincides with a thermophilic temperature optimum between 45°C and 60°C observed by Holler and coworkers (2011a).

Since AOM operates close to the thermodynamic equilibrium (Hoehler et al., 1994; Knab et al., 2008; Alperin and Hoehler, 2009a), the growth yield of the organisms is extremely low (around 1% relative to CH_4 oxidation; Nauhaus et al., 2007; Treude et al., 2007; Wegener et al., 2008; Holler et al., 2011a). For example, AOM consortia from cold methane-rich environments with a temperature optimum between 5 to 20°C have been shown to grow with doubling times of three to seven months (Nauhaus et al., 2005; 2007; Holler et al., 2009). However, the recently obtained thermophilic AOM enrichment showed a shortened doubling time of 68 days (Holler et al., 2011a). The feasibility of sulfate-dependent thermophilic AOM up to temperatures of 100°C has been demonstrated by La Rowe et al. (2008) who conducted thermodynamic calculations of the Gibbs free energy yield.

1.3. Methods

1.3.1. *The lipid biomarker approach*

Molecular biosignatures or biomarkers are metabolites or biochemicals that encode for particular kinds of living organisms (Eglinton et al., 1964; Eglinton and Calvin 1967). Potential biomolecules such as amino acids, nucleic acids, proteins, carbohydrates and lipids are all essential components of living cells. However, in contrast to the aforementioned biomolecules, lipid biomarkers can be used for both: as proxy for modern organisms (White et al., 1979; Harvey et al., 1986; Moodley et al., 2000) as well as molecular fossils originated from formerly living organisms (Brocks and Summons, 2003). This method section will emphasize on the application of intact polar membrane lipids (IPLs) as tool to examine microbial communities thriving at marine hydrothermal and cold seep settings.

1.3.1.1. *The function and structure of membrane lipids*

In microorganisms lipids can represent up to 7% of the cell dry weight and are essential components of cellular membranes (Langworthy et al., 1983). The hydrophilic (greek: *water-loving*) polar headgroup and hydrophobic (greek: *water-fearing*) tail of membrane lipids build up the physical basis for the lipid bilayer that segregates the internal part of the cell from the external environment (Fig. 1.9a). In addition to that barrier function, lipids execute indispensable functions. For example, lipids enable membranes to divide, reproduce and allow intercellular membrane trafficking. They are used for energy storage (e.g., caloric reserve in the form of triacylglycerols and steryl esters), transport of nutrients into the cell, provide a stabilizing matrix for proteins, and are responsible for the maintenance of the proton-motive force (Dowhan and Bogdanov, 2002; Eyster, 2007; Haucke and Di Paolo, 2007; van der Meer et al., 2008). Furthermore, lipids are also able to regulate membrane fluidity by modifying their polar headgroup or hydrophilic tail in response to external conditions such as pressure, temperature and pH (see section 1.3.1.4; Hazel and Williams, 1990; Hazel, 1995; Russel et al., 1995).

The majority of membrane lipids are glycerol-based, with two hydrophobic chains connected to the glycerol backbone through ester and/or ether bonds (Fig. 1.9b,c). The headgroups of lipids are typically phosphate-based, but membranes with glycosidic-, amino- or sulfate-based headgroups are also commonly found (Dembitsky, 1996; Hölzl and Dörmann, 2007). An example of the most dominant headgroups in nature is provided in Fig. 1.9d.

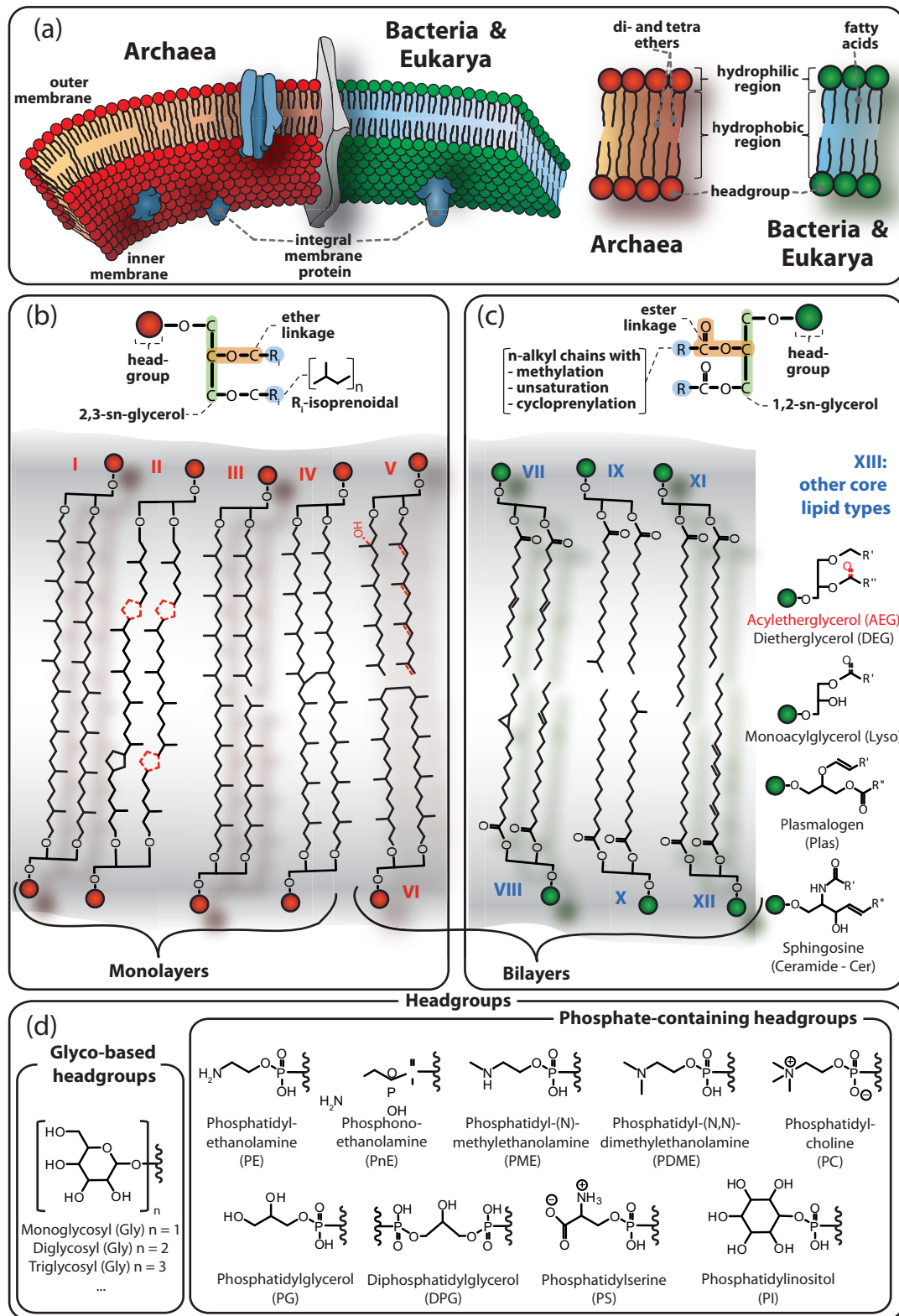


Fig. 1.9. Intact polar membrane lipid structures from Archaea, Bacteria and Eukarya. (a) Cytoplasmic membrane showing the lipid molecules and the integral membrane proteins. The schematic structures of an archaeal and bacterial/eukaryal membrane lipids are shown in red and green, respectively. The different chemical structures of (b) Archaea and (c) Bacteria/Eukarya are presented together with the most prominent core lipids found in these organisms. Typical core lipids for Archaea: I- GDGT without cyclopentane rings, II- GDGT with cyclopentane rings; III-GTGT; IV- H-shaped GDGT; V- AR with possible hydroxylation or unsaturation; VI-macrocylic-AR. Core lipids for Bacteria: DAG containing FA combinations VII- $C_{16:1\omega7}/C_{16:1\omega7}'$; VIII-cy $C_{17:0\omega5,6}/C_{16:1\omega5}'$; IX- $C_{15:0}/iC_{15:0}'$; X- $C_{15:0}/aiC_{15:0}'$. Typical core lipids for Eukarya: DAG containing FA combinations XI- $C_{14:0}/C_{18:0}'$; XII- $C_{14:0}/C_{18:3}'$. (d) Major polar headgroups of Archaea, Bacteria and Eukarya. For compound acronyms the reader is referred to the List of Abbreviations.

1.3.1.2. IPLs representing all three domains of life

The membrane constituents of the three domains of life (Archaea, Bacteria and Eukarya) have fundamental differences (Kates et al., 1978; Langworthy, 1982; Koga et al., 1993). Archaeal IPLs are comprised of isoprenoidal side chains (C_{15} , C_{20} , C_{25} , C_{40} : farnesyl, phytanyl, sesterterpanyl and biphytanyl, respectively) bound at the *sn*-2 and *sn*-3 position via di- or tetraether linkage to the glycerol backbone, while the headgroup is attached at the *sn*-1 position (Fig. I.9b; e.g., Koga et al., 1993; Koga and Morii, 2007). Thus, archaeal membranes can occur both as bilayer (diether lipids) or monolayer (tetraether lipids). By contrast, bacterial and eukaryotic membranes, build up membrane lipids containing headgroups attached to the glycerol backbone at the *sn*-3 position. In general, two fatty acid chains are linked to the glycerol backbone via ester bonds in the *sn*-1 and *sn*-2 position (Fig. I.9c). Bacterial and eukaryal IPLs differ in the length of carbon chains and the degree of unsaturation of the core lipids. Typically, eukaryotic FAs have predominantly even-numbered carbon atoms (Lechevalier and Lechevalier, 1988), and are often polyunsaturated (Brett and Müller-Navarra, 1997). Bacteria produce FAs with chain lengths of 14 to 24 carbon atoms, monounsaturated fatty acids and/or penultimate (iso) or ante-penultimate (anteiso) methyl-branched compounds (Zhang and Rock, 2008). In addition, Bacteria and Eukarya differ in the production of cyclic isoprenoids: Whereas Bacteria produce preferentially hopanoids, eukaryotes synthesize sterols in their membranes (see [BOX IV]; Ourisson et al., 1987).

BOX IV Hopanoids and sterols as membrane rigidifiers

Bacteriohopanepolyols (BHP) are a class of lipid which is known more generally as hopanoid. Hopanoids are pentacyclic isoprenoids, which are found in many Bacteria, and particularly in cyanobacteria (Rohmer et al., 1984; Rohmer et al., 1993; Summons et al., 1999). Sterols, on the other hand, are generally absent in Archaea and Bacteria (Bouvier, 1976), but represent a conspicuous feature in lipid membranes of eukaryotes (Fig. I.10; Ourisson et al., 1987). As an exception, 4-methyl sterols have been detected in some aerobic methanotrophic bacteria, making them an ideal marker for this group of bacteria (Fig. I.10; Bouvier et al., 1976; Ourisson et al., 1987; Elvert and Niemann, 2008). Due to structural similarity (e.g., molecular dimensions, semi-planar polycyclic ring structure and amphiphilic character) both hopanoids and sterols are believed to serve as membrane stabilizers within the bacterial and eukaryotic membrane, respectively (Ourisson et al., 1987).

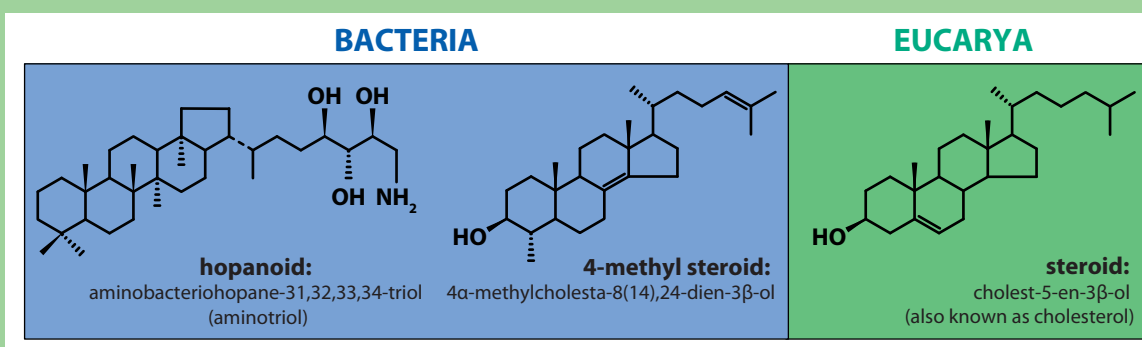


Fig. I.10. Chemical structure of characteristic triterpenoids.

Cross Reference: In [Chapter II] the taxonomic information encoded in the intact polar lipid (IPL) molecules enabled us, in a quantitative manner, to distinguish endosymbiotic bacteria from their eukaryotic host, which were recovered from cold- and hot seep environments.

1.3.1.3. IPLs as taxonomic marker for the active microbial biomass

The specialization of microorganisms to a wide range of biological processes has led to the formation of a variety of membrane lipids with differential functional roles. The vast abundance of IPL membrane compositions can be assigned to: (1) responses with respect to environmental parameters (see section 1.3.1.4), or (2) from different membrane characteristics of organism groups that are either phylogenetically related or have similar metabolisms (Langworthy, 1982; Goldfine, 1984; Langworthy and Pond, 1986; Kaneda et al., 1991; Itoh et al., 2001).

Based on recent developments in analytical chemistry, membrane lipids are now accessible to be analyzed in their intact form using liquid chromatography coupled to mass spectrometry (LC-MS; see section 1.3.1.5). Before this direct measurement of IPLs using the LC-MS technique, indirect measurements of IPLs have been performed using mostly silicagel column in order to separate lipid extracts into fossil, glyco- and phospholipid fractions (Guckert et al., 1985; Oba et al., 2006; Pitcher et al., 2009), which subsequently were hydrolyzed and/or ether-cleaved in order to release their core lipids. Such conventional biomarker analyses focused mainly on the polar lipid-derived fatty acids (PLFAs) or other IPL derivatives such as isoprenoidal hydrocarbon chains (e.g., Parkes and Calder, 1985; Boschker et al., 1998; Orcutt et al., 2005; Wakeham et al., 2007). The advantage of direct IPL analysis compared to traditional membrane lipid analysis is a better taxonomic differentiation in environmental samples, since additional structural information, such as headgroup and core lipid composition can be determined simultaneously (Fang et al., 2000b; Rütters et al., 2002b; Sturt et al., 2004; Biddle et al., 2006; Zink et al., 2008; Schubotz et al., 2011b; Yoshinaga et al., 2011). However, most importantly, IPLs are thought to be labile compounds which tend to (bio) degrade (hydrolysis of the polar headgroup) soon after cell death (White et al., 1979; Harvey et al., 1986; Moodley et al., 2000). Hence, in comparison to their more stable and recalcitrant core lipids, the presence of IPLs in sediments is thought to reflect viable microbial cells (e.g., Sturt et al., 2004; Biddle et al., 2006; Schubotz et al., 2011b). However, the stability of IPLs, especially for glycosidic archaeal IPLs, is an intensively discussed topic in the field of organic geochemistry (e.g., Lipp and Hinrichs et al., 2009; Schouten et al., 2010).

The increasing numbers of publications related to IPL research reflect their reputation. For example, a vast number of recent publications applied IPLs as chemosynthetic markers extracted either from cultures (e.g., Koga et al., 1998; Koga and Morii, 2005; Koga and Nakano, 2008) or various natural environments in the marine and terrestrial sediments (e.g. Rütters et al., 2001, 2002a, 2002b; Zink et al., 2003; Biddle et al., 2006; Lipp et al., 2008; Schubotz et al., 2009; Liu et al., 2010; 2011), surface waters of the oceans (e.g. Van Mooy et al., 2006; Schubotz et al., 2009; Van Mooy and Fredericks, 2010; Pendorf et al., 2011) and cold seeps and hydrothermal

vents (e.g., Rossel et al., 2008, 2011; Schubotz et al., 2011b; Yoshinaga et al., 2011).

Cross Reference: [Chapter III and V] investigated the lipid composition of a natural enrichment of thermophilic AOM consortia, originally retrieved from the hydrothermally-influenced sediments of the Guaymas Basin. In [Chapter III] we analyzed the ether-cleaved and hydrolyzed core lipids from the AOM community, which were dominated by thermophilic ANME-1 and partner bacteria from the HotSeep-1 cluster (Holler et al., 2011). [Chapter V], on the other hand, focused on individual archaeal IPLs (IPL-SIP) extracted from the same ANME-1 community analyzed in [Chapter III].

1.3.1.4. Membrane adaptation strategies of Archaea and Bacteria to cope with extreme environmental conditions

In general, archaeal ether lipids are considered to be more resistant to stress factors such as high temperature, pH, salinity, and pressure than lipids from Bacteria, containing mostly ester bonds (Valentine, 2007). Therefore, Archaea were assumed to be the dominant group of microorganisms that are able to thrive at extreme environments (e.g., van de Vossenberg et al., 1998; Rothschild and Mancinelli, 2001; Cavicchioli, 2011). In this context, it is interesting to mention that Archaea root very deeply in the phylogenetic tree, pointing to a close relationship with a thermophilic ancestor (Woese et al., 1990; Stetter, 1996). Nevertheless, both Archaea and Bacteria have developed different strategies to protect themselves from changing external environmental conditions by modifying their membrane lipids.

Bacteria have the ability to react to changing external conditions (e.g., increase in temperature, pH, pressure or salinity) by modifying both their apolar fatty acid chain composition (e.g., variations in chain length, unsaturation, cyclopropanisation, and methyl branches; Cronan and Gelmann, 1975; Langworthy, 1982; DeLong and Yayanos, 1986; Nichols et al., 1997; Männistö and Puhakka, 2001; Valentine and Valentine, 2004; Zhang et al., 2008) as well as their polar headgroup composition (e.g., increase in temperature caused thermophilic bacteria to shift from the synthesis of PE to PG, Hasegawa et al., 1980). Compared to the bacterial membranes, the archaeal membranes are much less permeable towards passive diffusion of ions. This enables Archaea to survive under extreme conditions (e.g., Elferink et al., 1994; van de Vossenberg et al., 1995; 1998; Valentine, 2007). For example, compared to diether-based membranes, the presence of membrane-spanning GDGTs and/or macrocyclic archaeol in Archaea has been observed as strategy to tighten their membranes (Mathai et al., 2001). Furthermore, by increasing cyclization of the tetraether isoprenoidal chains (e.g., Gliozzi et al., 1983; Langworthy and Pond, 1986; De Rosa and Gambacorta 1988; Schouten et al., 2003; Macalady et al., 2004) and substituting phospho-based by glycosidic headgroups (e.g., Shimada et al., 2008) archaea reduce proton permeability, withstanding extreme environmental conditions.

Cross Reference: In [Chapter V] we hypothesize that the tetraether membrane, especially the formation of 2Gly–GDGT, is used to reduce proton-permeability, thereby protecting the integrity of cells at extreme conditions.

1.3.1.5. *Sample handling: From extraction to IPL analysis to inter- and intramolecular isotope analysis*

In this dissertation IPLs have been extracted from sediments, microbial enrichments and pure biomass using a modified Bligh and Dyer method (White and Ringelberg, 1998; Sturt et al., 2004). Hereby samples were extracted using a mixture of methanol (MeOH), dichloromethane (DCM) and an aqueous buffer in order to prepare the total lipid extract (TLE). In brief, target sediments were extracted using MeOH:DCM:aq. phosphate buffer (50 mM, pH 7.4) (2:1:0.8, v:v:v) and MeOH:DCM:trichloroacetic acid (50 mM, pH 2) (2:1:0.8, v:v:v). The combined supernatants were washed with water, evaporated to dryness and stored at -20°C . Subsequently, an aliquot of the TLE was analyzed by high performance liquid chromatography coupled to electrospray ionization ion trap multistage mass spectrometry (HPLC/ESI–ITMSⁿ). This analytical technique is particularly appropriate for the analysis of polar molecules such as IPLs. HPLC/ESI–ITMSⁿ allows detailed structural characterization of IPLs by combining information gained in positive and negative ionization modes not only in MS² but also in MS³ (Fig. I.11; e.g., Rütters et al., 2002a; Sturt et al., 2004; Zink and Mangelsdorf, 2004; Yoshinaga et al., 2011).

Intermolecular analysis

Preparative–HPLC is a new methodological advancement to the aforementioned conventional lipid separation enabling to separate for example IPLs from the free/core lipids. Recently, new purification protocols emerged, targeting the isotopic analysis of the apolar side chains of individual IPLs extracted from environmental samples (e.g., Biddle et al., 2006; Schubotz et al., 2011b). However, these protocols used only one dimensional normal–phase preparative HPLC, thus IPLs with similar structural components were not completely separated. In [Chapter V], further purification schemes are presented, involving the combination of normal– and reverse–phase preparative HPLC in order to separate co–eluting archaeal di– and tetraethers into individual fractions.

Intramolecular analysis

After lipid purification of individual IPLs, several cleavage reactions are necessary to obtain GC–amenable compounds for intramolecular isotopic analysis. Recently, protocols have been developed which allow analyzing polar lipid moieties, such as glycosidic headgroups (Lin et al., 2010) and the glycerol backbone (Lin et al., in preparation) together with their apolar side chains (e.g., biphytanes from GDGTs, PLFAs from phospholipids). A schematic diagram illustrating the analytical routes starting from sample extraction until separation of individual lipid moieties is provided in Fig. I.12

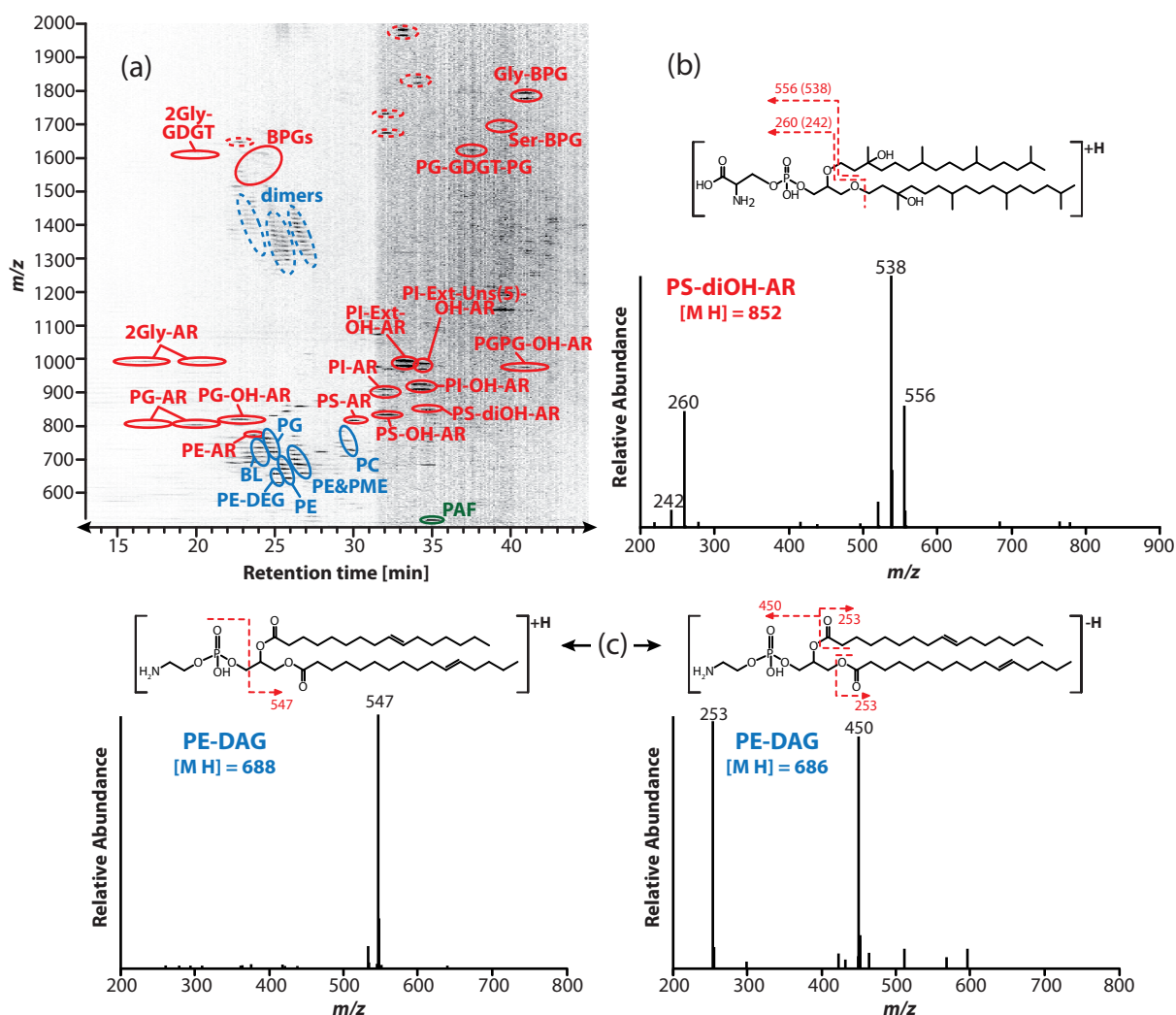


Fig. I.11. (a) Density map showing archaeal (red) and bacterial (blue) lipids analyzed in positive ionization mode by HPLC/ESI-ITMSⁿ. The high diversity of microbial IPLs became apparent after visualization of the chromatogram by way of 3D density maps (x – time, y – m/z , z – intensity). The intensity of the color black is correlated to the concentration of the IPLs. Density maps provide a “fingerprint” of the IPL composition in environmental samples. This sample was originally extracted from a cold seep environment from the continental margin off Pakistan (M74/3, GeoB 12315, water depth 1000 m). Exemplarily, two fragmentation pattern of (b) the archaeal IPL PS–diOH–AR in positive ionization mode and (c) the bacterial IPL PE–DAG in both positive (left) and negative (right) ionization modes. In general, bacterial lipids typically lose its polar headgroup upon fragmentation in positive ion mode in the mass spectrometer from which a headgroup-diagnostic neutral mass loss can be calculated (e.g., PE→loss of 141 Da). In negative ion mode, the bacterial IPL parent ion tends to lose primarily their fatty acid chains (e.g., $C_{16:1}$ → m/z 253 Da). The fragmentation patterns of a wide variety of archaeal IPLs are summarized in more detail in [Chapter IV]. For compound acronyms the reader is referred to the List of Abbreviations.

Cross Reference: [Chapter IV] focused exclusively on the diversity of archaeal IPLs extracted from environmental samples. This chapter revealed a systematic fragmentation pattern during high performance liquid chromatography electrospray ionization mass spectrometry, providing a guide for organic geochemists analyzing archaeal IPLs in natural samples.

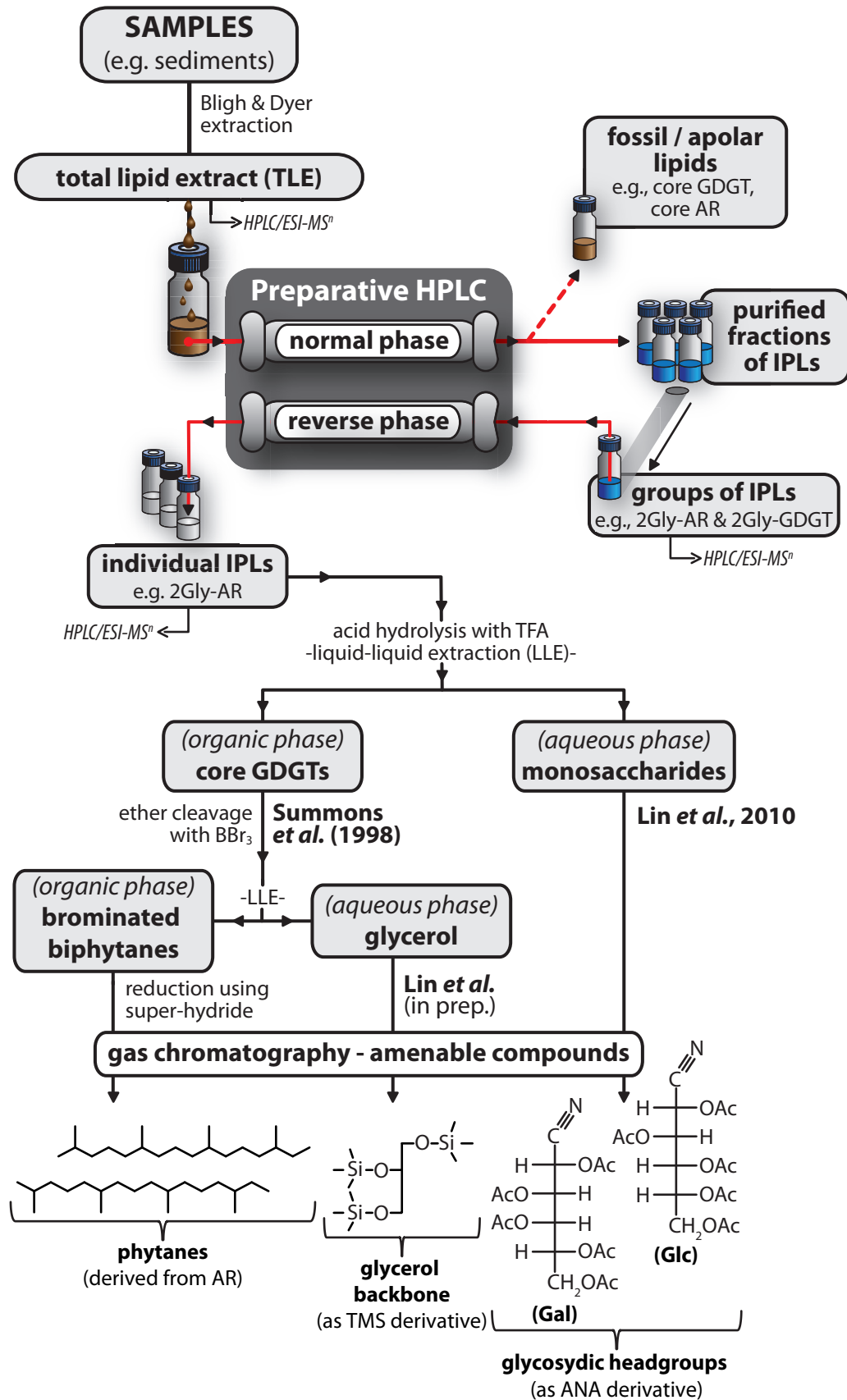


Fig. I.12. Flow chart showing all major steps starting from sample extraction to purification (normal- and reverse- phase prep) towards intramolecular stable carbon isotopic analysis of individual IPLs. Hydrolysis of glycosydic headgroups, glycerol backbone, and isoprenoidal chains (intramolecular analysis) are shown for 2Gly-AR. For compound acronyms the reader is referred to the List of Abbreviations.

1.3.2. Stable carbon and hydrogen isotope analysis as tool in biogeochemistry

Carbon and hydrogen atoms contain variable numbers of neutrons in their nucleus, leading to different isotopes of the same element. The term “isotope” is originated from the greek language, where “iso” means equal and “topos” means location.

Carbon has two stable isotopes: ^{12}C and ^{13}C . The ratio of ^{13}C to ^{12}C can be expressed as $\delta^{13}\text{C}$ as deviation in permill from a reference material [Eq. III] (typically, Vienna Pee dee Belemnite; VPDB). The VPDB standard had a $^{13}\text{C}:^{12}\text{C}$ ratio (0.0112372), which by definition has a $\delta^{13}\text{C}_{\text{VPDB}}$ value of zero.

$$\delta^{13}\text{C} = \left(\frac{\left(\frac{^{13}\text{C}}{^{12}\text{C}} \right)_{\text{sample}}}{\left(\frac{^{13}\text{C}}{^{12}\text{C}} \right)_{\text{standard}}} - 1 \right) \times 1000\text{‰} \quad \text{[Eq. III]}$$

Like carbon, hydrogen has two stable isotopes: ^1H and ^2H . ^1H , consisting only of one proton, is the most common hydrogen isotope. The ^2H isotope is also called deuterium (D) and water enriched in D is called heavy water. The degree of hydrogen deviation ($\delta^2\text{H}$) has been quantified versus an established reference material (Vienna Standard Mean Ocean Water (VSMOW); [Eq. IV]). The isotopic ratios of $^1\text{H}:^2\text{H}$ of the VSMOW standard is defined as 155.76 ± 0.1 ppm (0.00015576). Both, the $\delta^{13}\text{C}$ and the $\delta^2\text{H}$ values are reported in the permill (‰) notation.

$$\delta^2\text{H} = \left(\frac{\left(\frac{^2\text{H}}{^1\text{H}} \right)_{\text{sample}}}{\left(\frac{^2\text{H}}{^1\text{H}} \right)_{\text{standard}}} - 1 \right) \times 1000\text{‰} \quad \text{[Eq. IV]}$$

Typically, biological reactions discriminate against the heavier stable isotope (^2H and ^{13}C) and select for ^1H and ^{12}C , resulting in products which are depleted in ^1H and ^{12}C relative to ^2H and ^{13}C , respectively. Naturally-derived microbial lipids depleted in ^{13}C and ^2H relative to their standard show in general negative $\delta^2\text{H}$ and $\delta^{13}\text{C}$ values, respectively.

1.3.2.1. Analysis of natural abundance stable carbon isotope

In the past, most isotopic analysis on organic matter focused primarily on the ratio of ^{13}C to ^{12}C . The distribution of these naturally occurring isotopes in lipid biomarkers can provide information on the carbon substrate, and/or the carbon fixation pathway of the source organisms. For example, in settings such as marine hydrothermal or cold seep environments, where life is largely supported by chemosynthesis [BOX I], the isotopic composition of carbon is a powerful tool. For instance, the isotopic analysis of cell wall membrane lipids and whole cells of microbes involved in AOM (see section 1.1.4.2) and their potential organic carbon substrates have been used as a tool to reveal metabolic pathways of carbon assimilation (e.g., Elvert et

al., 1999; Hinrichs et al., 1999; Hinrichs and Boetius, 2002; Orphan et al., 2002; Blumenberg et al., 2004). These authors hypothesized that the carbon assimilation during AOM yields carbon isotopic values of the methane oxidizing ANMEs (e.g., archaeol and hydroxyarchaeol) which are 15–50‰ depleted relative to methane as the proposed carbon substrate (Fig. I.13).

Cross Reference: During the process of AOM, the formation of biomass from anaerobic methanotrophic archaea is generally thought to be related to methane as their dominant carbon source. This assumption will be discussed and also questioned in [Chapter III].

The distribution of ^{13}C in natural systems is affected by thermodynamic reactions and kinetic fractionation processes. Thermodynamic fractionation, on the one hand, is an important process between reservoirs where the carbon exchange is slow enough to approach isotopic equilibrium. Typically the associated isotope effects of these pure physical reactions are small. For example, the exchange between CO_2 in the air and the dissolved inorganic carbon ($\text{DIC} = \text{CO}_3^{2-} + \text{HCO}_3^- + \text{H}_2\text{CO}_3 + \text{CO}_{2\text{aq}}$) in seawater causes an unequal isotope distribution between the dissolved species (Pearson, 2010). On the other hand, the kinetic fractionation, during biologically-mediated carbon transfers, has a stronger control on the ^{13}C distribution. Thus, biochemical reactions that convert one carbon molecule (e.g., CO_2 and or CH_4) into organic matter show large fractionation effects, whereas heterotrophic reactions, using complex organic matter as substrates, have small fractionation effects. This biological turnover leads to ^{12}C enrichment in the products and a ^{13}C enrichment in the residue of the substrates. The extent of the preferential incorporation of the isotopically light ^{12}C into the biomass within Bacteria and Archaea (biological fractionation) has been associated with different carbon-fixation pathways (metabolic mode of the organism; cf. Hayes et al., 2001; House et al., 2003; Holler et al., 2009; Pearson, 2010).

To effectively track the carbon fixation pathway of microorganisms the isotopic composition of the potential substrate has to be known (You are what you eat!; De Niro and Epstein, 1976). Therefore, to characterize the food web of microorganisms, the isotopic composition of total organic carbon (TOC), dissolved inorganic carbon (DIC) and hydrocarbon gases such as methane are important parameters in geochemical studies. Fig. I.13 provides an overview of common $\delta^{13}\text{C}$ ranges of various carbon reservoirs and organisms found in nature.

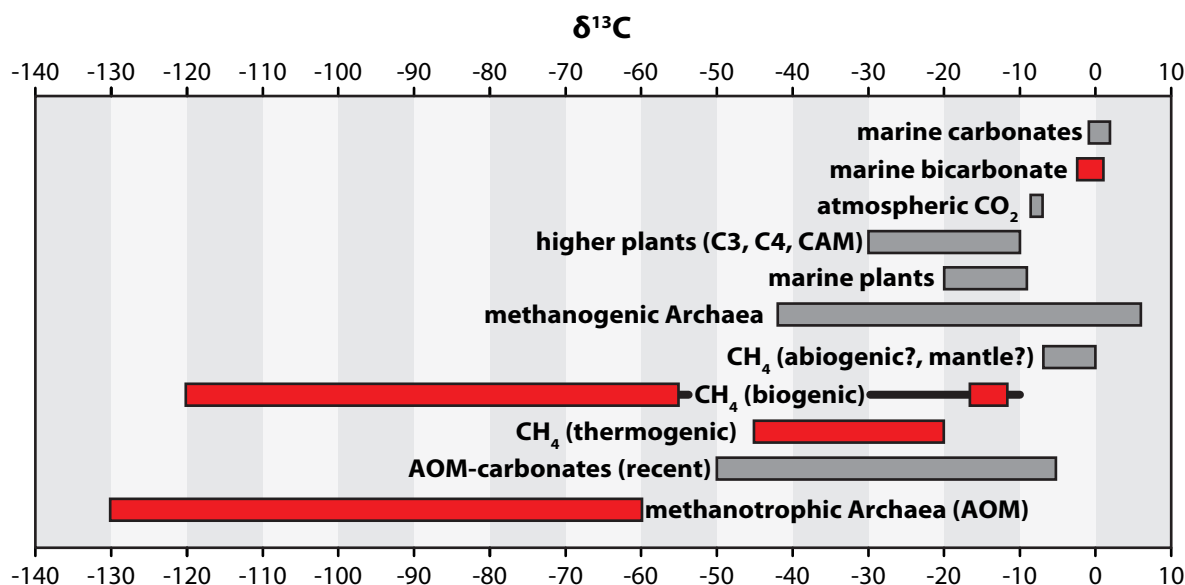


Fig. 1.13. Summary of $\delta^{13}\text{C}$ ranges of mostly marine carbon reservoirs and organisms. The most important carbon reservoirs dealt with in this dissertation are highlighted in red. Figure has been modified after Blumenberg et al. (2010).

1.3.2.2. Natural abundance and stable hydrogen isotope analysis

Besides carbon, stable hydrogen isotope compositions of lipid compounds can also be analyzed by GC-IRMS. As already shown for carbon, variability in lipid $\delta^2\text{H}$ values can also be a useful tracer for biogeochemical processes (Hoering, 1974). The hydrogen content of the organic matter is originally derived from the ambient water (Estep and Hoering, 1980). In contrast to terrestrial waters, marine waters only show little variations in $\delta^2\text{H}$ on a spatial and temporal scale (Schmidt et al., 1999), making hydrogen in the marine realm a potential marker to track biogeochemical processes. Up to now, only little is known about the usefulness of measurements of microbial lipids from marine systems. However, a few studies have investigated the D/H ratios of lipids derived from marine organisms, resulting for example in large, systematic differences within one compound class (e.g., fatty acids; Jones et al., 2008), among different compound classes (e.g., n-alkyl and isoprenoid species, Sessions et al., 1999) but also showed alterations in $\delta^2\text{H}$ within alkenones associated to changes in temperature, salinity or growth rate (Schouten et al., 2006; van der Meer et al., 2007, 2008). Just recently, an extensive survey of lipid $\delta^2\text{H}$ values, ranging from -32 to -348‰ , from marine sources including short- and long-chain n-alkanes, n-alcohols, and n-acids, steroids and hopanoids and also archaeal isoprenoids emphasized strong fractionations associated with particular metabolic capabilities of its producing organism (Li et al., 2009).

Cross Reference: The large and systematic differences among isoprenoidal chains (-150 to -290‰) and different FAs (-86 to -230‰) have also been observed in [Chapter III]. This chapter extracted a natural enrichment dominated by thermophilic ANME-1 and their partner bacteria from the HotSeep-1 cluster (Holler et al., 2011).

1.3.2.3. Stable isotope probing experiments of lipid biomarkers

Stable isotope probing (SIP) is a cultivation-independent approach which attempts to identify microorganisms responsible for specific metabolic processes. SIP experiments rely on the incorporation of a substrate, usually enriched in its heavier stable isotope (e.g., ^{13}C or ^2H), which in turn will result in biomolecules (e.g., lipids, carbohydrates, DNA, RNA, protein) with positive isotopic values when the substrate is used as source during biosynthesis. First SIP studies combined ^{13}C labeling (^{13}C -acetate and $^{13}\text{CH}_4$) with isotopic analysis of lipid biomarkers such as phospholipid derived fatty acids (PLFAs) by isotope-ratio mass spectrometry (IRMS) (Boschker et al., 1998). Up to date, lipid biomarker SIP is a popular approach since this biomolecule class is extremely sensitive to GC-IRMS analysis and requires only low amounts of label assimilation (Hayes et al., 1990; Brenna et al., 1997).

Until now, lipid-based SIP experiments focused mainly on the apolar, hydrophobic moieties such as bacterial PLFAs (Boschker et al., 1998; Webster et al., 2006; Bühring et al., 2006) or archaeal di- and tetraether lipids (Blumenberg et al., 2005; Wegener et al., 2008; [Chapter III]). However, some of these SIP studies combined free and intact lipid pools, thereby mixing signals from dead and living microbial biomass. Particularly the pool size of archaeal lipids such as fossil/core GDGTs in marine sediments, have been shown to greatly outnumber membrane lipids derived from living biomass (intact GDGTs), by up to one order of magnitude (Lipp and Hinrichs, 2009; Liu et al., 2010, 2011), thus leading to a substantial isotope dilution, minimizing the sensitivity of lipid-SIP.

Cross Reference: [Chapter III and V] are two SIP studies tracking the assimilation of ^{13}C labeled into bulk and intact derived microbial lipids, respectively.

1.3.2.4. Dual SIP experiments

Just recently, Wegener and coworkers (in revision) introduced the concept of dual labeling, using ^{13}C -labeled bicarbonate ($^{13}\text{C}_{\text{DIC}}$) and deuterated water (D_2O) as tracers. They reported that the sulfate-reducer *Desulfosarcina variabilis* incorporates H_2 from water protons to build up the majority of its lipids, independent of the carbon fixation pathway. Hence assimilation of D_2O can be used as sensitive tool to measure total lipid production (via assimilation of deuterated protons from water), whereas the assimilation of inorganic carbon (determined via $^{13}\text{C}_{\text{DIC}}$ uptake in lipids) indicates autotrophy. In addition, the ratio of inorganic carbon assimilation to total lipid production yields an estimation of auto- and heterotrophic carbon fixation, without addition of further labeled carbon sources.

Cross Reference: In [Chapter III] we performed a dual labeling study using ^{13}C -labeled bicarbonate ($^{13}\text{C}_{\text{DIC}}$) and deuterated water (D_2O) and identify the AOM performing archaea and their sulfate-reducing bacterial partner as mainly autotrophs.

1.3.2.5. IPL-SIP: Intramolecular isotopic analysis on individual IPLs

To overcome the problems of a mixed signal derived from fossil and intact lipids normal phase liquid chromatography has been shown to be sufficient for excluding the apolar sample matrix from different groups of IPLs (e.g., Biddle et al., 2006; Schubotz et al., 2011b). However, in order to purify individual IPLs, new purification protocols using a set of orthogonal columns of normal- and reversed-phases have been applied (Lin et al., in preparation). The advantage of IPL-SIP has been shown, for the first time, by Pependorf and coworkers (2011), who combined SIP (using ^{13}C -bicarbonate and ^{13}C -glucose) and preparative HPLC (to separate individual IPLs), in order to reveal bacteria-specific photoautotrophic and heterotrophic lipid production in surface ocean waters.

Furthermore, recent and ongoing developments in sample purification together with improved protocols for the chemical hydrolysis of individual IPLs (Lin et al., 2010; Lin et al., in preparation) established the possibility to study the carbon assimilation not only within the hydrophobic moieties (e.g., FAs and isoprenoidal chains) but also the polar components of individual IPLs (i.e. glycerol and their headgroup; Fig. I.12).

Cross Reference: [Chapter V] unambiguously presents the advantage of IPL-SIP over TLE-SIP.

I.4. Structure and main objectives of this thesis

In this thesis, lipid biomolecules and carbon metabolism of aerobic and anaerobic chemosynthetic microorganisms at cold seeps and hot vents were examined by using and improving state-of-the-art geochemical techniques.

[**Chapter II**] focused on the aerobic oxidation of reduced compounds (e.g., CH₄ and H₂S) by chemosynthetic microorganisms living in symbiosis inside mussels from the genus *Bathymodiolus*. We analyzed a suite of lipids in muscle and gill tissues from *Bathymodiolus*, collected from methane seeps and sulfide-rich hydrothermal vents. This chapter examined symbiont–host interactions using a holistic lipid biomarker approach by investigating IPLs, BHPs, FAs and sterols.

Research question:

- What are the advantages of IPL analysis over the traditional biomarker approach regarding the characterization of bacterial and eukaryotic biomass?
- Can methane– and sulfur–oxidizing symbionts be differentiated by their biomarker signatures and their stable carbon isotopic composition?
- Does the semi-quantitative IPL analysis allow an estimation of the abundance of symbionts living in the gills of the host?

[**Chapter III**] of this thesis investigated carbon fixation during thermophilic anaerobic oxidation of methane (AOM). Natural enrichments from the Guaymas Basin, which were dominated by ANME-1 and sulfate-reducing bacteria from the HotSeep–1 cluster (Holler et al., 2011) were examined using a combined multiple (¹³CH₄ and ¹³C_{DIC}) and dual (D₂O and ¹³C_{DIC}) stable isotope probing approach. Microbial biomass production was assessed as ¹³C and D labeled lipid biomarkers recovered at different time points (0, 10, 17 and 24 days) and treatments (with and without methane at 37 or 50°C).

Research question:

- Which lipids are produced by the organisms performing AOM at elevated temperatures?
- What are the roles of methane and inorganic carbon as carbon sources for microorganisms involved in the thermophilic AOM?
- What are the patterns of microbial lipid production in presence and absence of methane?
- What is the relative importance of heterotrophic and autotrophic carbon fixation at different temperatures?

[**Chapter IV**] reveals a systematic fragmentation pattern from archaeal IPLs during high performance liquid chromatography electrospray ionization mass spectrometry. Analyzed IPLs were exclusively retrieved from environmental samples; thereby this work is particularly useful for a rapid and straightforward characterization of intact archaeal membrane lipids.

In [**Chapter V**] we studied the assimilation of inorganic carbon during thermophilic AOM into individual archaeal IPLs. This chapter merges the recent advances in preparative HPLC together with newly developed protocols for chemical hydrolysis of IPLs. The assimilation of ^{13}C -labeled bicarbonate was evaluated as follows: (1) archaeal IPLs vs. bulk lipids (TLE); (2) among individual IPLs (di- and tetraethers); (3) intramolecular analysis (isoprenoids, sugar moieties and glycerol backbone).

Research question:

- How strong does the large pool of fossil archaeal lipids influence the actual ^{13}C uptake of the living archaeal community?
- Can adaptations of archaea to thermophilic environments be identified by the IPL distribution?
- What are the patterns of label assimilation into isoprenoidal side chains, sugar headgroups and glycerol moieties of individual lipids?
- What can be told from IPL-SIP: Towards *de novo* synthesis of biomass in Archaea.

I.5. Contribution to publications

This PhD thesis enfolds three first-author and one second-author manuscripts prepared for publication in international journals [Chapters II–V]. [Chapter II] and [Chapter IV] are published and [Chapter III] and [Chapter V] are ready for submission. All other co-author contributions are summarized in the [Appendix] containing manuscript abstracts in combination with their most significant figure.

[Chapter II]

Symbiont–host relationships in chemosynthetic mussels: A comprehensive lipid biomarker study.

Matthias Y. Kellermann, Florence Schubotz, Marcus Elvert, Julius S. Lipp, Daniel Birgel, Xavier Prieto Mollar, Nicole Dubilier, Kai–Uwe Hinrichs

N.D. and K.–U.H. designed the project; N.D. provided the samples; M.Y.K. extracted, analyzed and evaluated lipid data with help from F.S., M.E., J.S.L., D.B., X.P.M.; M.Y.K. and F.S. wrote the paper with input of all co–authors.

Published in *Organic Geochemistry* 43, 112–124.

doi:10.1016/j.orggeochem.2011.10.005

[Chapter III]

Dual isotopic probing reveals dominant autotrophic carbon fixation in methane–rich sediments from the Guaymas Basin.

Matthias Y. Kellermann, Gunter Wegener, Marcus Elvert, Marcos Y. Yoshinaga, Yu–Shih Lin, Thomas Holler, Xavier Prieto Mollar, Kai–Uwe Hinrichs

M.Y.K., G.W. and Y.S.L. designed the project; G.W. and T.H. provided the samples; M.Y.K. extracted, analyzed and evaluated lipid data with help from M.E., M.Y.Y., X.P.M.; M.Y.K., G.W. and M.Y.Y. wrote the manuscript with input of all co–authors.

In preparation for *Geochimica et Cosmochimica Acta*.

[Chapter IV]

Systematic fragmentation patterns of archaeal intact polar lipids by HPLC/ESI/ITMS.

Marcos Y. Yoshinaga, Matthias Y. Kellermann, Pamela E. Rossel, Florence Schubotz, Julius S. Lipp, and Kai-Uwe Hinrichs.

M.Y.Y. and M.Y.K. designed the project; M.Y.Y., M.Y.K. and P.E.R. provided the samples; M.Y.Y., M.Y.K. and P.E.R. extracted, analyzed and evaluated lipid data and M.Y.Y. wrote the manuscript with input of all co-authors.

Published in *Rapid Communication in Mass Spectrometry* 25, 3563–3574.

doi: 10.1002/rcm.5251

[Chapter V]

Stable isotope probing of an anaerobic methane-oxidizing enrichment provides clues on archaeal tetraether lipid biosynthesis.

Matthias Y. Kellermann, Marcos Y. Yoshinaga, Gunter Wegener, Yu-Shih Lin, Thomas Holler, and Kai-Uwe Hinrichs

M.Y.K., M.Y.Y. and G.W. designed the project; G.W. and T.H. provided the samples; M.Y.K. extracted, analyzed and evaluated lipid data with help from M.Y.Y., G.W. and Y.S.L.; M.Y.K., M.Y.Y. and G.W. wrote the manuscript with input of all co-authors.

In preparation for *Geochimica et Cosmochimica Acta*.

[CHAPTER II] - BACTERIAL SYMBIOSIS IN MUSSELS**Symbiont–host relationships in chemosynthetic mussels: A comprehensive lipid biomarker study**

Matthias Y. Kellermann ^{a*}, Florence Schubotz ^{a1}, Marcus Elvert ^a, Julius S. Lipp ^a, Daniel Birgel ^{a,c}, Xavier Prieto-Mollar ^a, Nicole Dubilier ^b, Kai-Uwe Hinrichs ^a

Published in Organic Geochemistry

Vol: 43 (2012), page: 112–124, doi:10.1016/j.orggeochem.2011.10.005

© 2011 Elsevier Ltd. All rights reserved.

^a Organic Geochemistry Group, MARUM Center for Marine Environmental Sciences & Department of Geosciences, University of Bremen, Leobener Strasse, D-28359 Bremen, Germany

^b Max Planck Institute for Marine Microbiology, Celsiusstr. 1, D-28359 Bremen, Germany

^c Department of Geodynamics and Sedimentology, University of Vienna, Althanstrasse 14, A-1090 Vienna, Austria

¹ Present address: Department of Earth, Atmospheric and Planetary Sciences, Massachusetts Institute of Technology, Cambridge, MA 02139, USA.

* Corresponding author.

Tel.: +49 421 218 65742; Fax: + 49 421 218 65715

E-mail address: kellermann.matthias@gmail.com

Keywords:

symbionts | *Bathymodiolus* mussels | methane oxidizers | sulfur oxidizers | lipid biomarker | intact polar lipids | bacteriohopanepolyols | fatty acids | sterols | stable carbon isotopes

II.1. Abstract

Symbiosis with chemosynthetic microorganisms allows invertebrates from hydrothermal vents and cold seeps, such as mussels, snails and tubeworms, to gain nutrition independently of organic input from photosynthetic communities. Lipid biomarkers and their compound specific stable carbon isotopes ($\delta^{13}\text{C}$) have greatly aided the elucidation of chemosynthetic symbiosis. Due to recent methodological advances in liquid chromatography it is now possible to obtain a more holistic view of lipid biomarkers, including the analysis of intact polar membrane lipids (IPLs) and bacteriohopanepolyols (BHPs). This study provides an extensive examination of polar and apolar lipids in combination with stable carbon isotope analysis of three *Bathymodiolus* mussels (*Bathymodiolus childressi*, *Bathymodiolus cf. thermophilus*, *Bathymodiolus brooksi*) hosting different types of bacterial symbiont (methane-oxidizing, sulfur-oxidizing and a dual symbiosis with methane- and sulfur-oxidizing symbionts, respectively). We propose that IPLs with $\text{C}_{16:1}$ acyl side chains, and phosphatidylglycerol (PG), diphosphatidylglycerol (DPG) and phosphatidylethanolamine (PE) head groups, which were only detected in the gill tissue, can be used as symbiont-characteristic biomarkers. These putative symbiont-specific IPLs provide the opportunity to detect and quantify the methanotrophic and thiotrophic symbionts within the gill tissue. Additional characteristic markers for methanotrophic symbionts were found in *B. childressi* and *B. brooksi*, including the BHP derivatives aminotriol and aminotetrol, 4-methyl sterols and diagnostic fatty acids (FAs), such as $\text{C}_{16:1\omega 9}$, $\text{C}_{16:1\omega 8}$ and $\text{C}_{18:1\omega 8}$. In general, the $\delta^{13}\text{C}$ values of FAs, alcohols and BHP-derived hopanols were in accordance with carbon assimilation pathways of the respective methanotrophic or thiotrophic symbionts in all three *Bathymodiolus* mussels. Differences in BHP distribution as well as $\delta^{13}\text{C}$ values in the two mussels hosting a methanotrophic symbiont may indicate the presence of different methanotrophic symbionts and/or changes in the nutritional status. In all three mussel species the $\delta^{13}\text{C}$ values of lipid biomarkers assigned to the symbionts were similar to those of the hosts, indicating the importance of the bacterial symbionts as the main carbon source for the mussel tissue.

II.2. Introduction

Cold seeps and hydrothermal vents are highly productive, chemosynthetic ecosystems in the deep ocean, fueled by microbial oxidation of compounds supplied by fluids such as H_2 , H_2S , CH_4 and reduced metals (Lonsdale, 1977). Chemosynthetic bacteria, representing the smallest members of the food chain, can either be free living or hosted by invertebrates such as mussels, snails, tubeworms or sponges (Petersen and Dubilier, 2010). The first discovery of invertebrates gaining most of their energy through the oxidation of H_2S was reported in the late 1970s (Rau and Hedges, 1979). The presence and function of these endosymbiotic bacteria has been the subject of many studies (references detailed below). The symbiont provides the eukaryotic host with nutrition, while the host supplies the symbiotic bacteria with fluids, enriched in electron donors such as CH_4 or H_2S and electron acceptors such as O_2 , by positioning itself at

the interface between reduced fluid and oxidized fluid (Petersen and Dubilier, 2010).

Bathymodiolus mussels have been found in association with sulfur-oxidizing (Cavanaugh, 1983; Distel et al., 1988) or methane-oxidizing bacteria (Childress et al., 1986); specimens hosting both groups of these Gammaprotobacteria have also been described (Fisher et al., 1993). Bacterial symbiosis in *Bathymodiolus* mussels has been identified via transmission electron microscopy (Childress et al., 1986; Fisher et al., 1987), molecular methods such as comparative 16S rRNA sequence analysis (Eisen et al., 1992), fluorescence *in situ* hybridization (Duperron et al., 2005, 2007; Riou et al., 2008) and carbon incorporation experiments using isotopically labelled CH_4 or HCO_3^- for identification of methanotrophic or thiotrophic symbiont uptake pathways (Fisher et al., 1987; Scott and Cavanaugh, 2007; Riou et al., 2010). A distinct lipid fingerprint of an endosymbiotic microorganism was first described by Gillan and coworkers (1988) and was further specified with regard to the function of the symbiont by way of analysis of compound specific stable carbon isotopic compositions (e.g. Fang et al., 1993; Abrajano et al., 1994; Jahnke et al., 1995; Pond et al., 1998).

The biomass and lipid biomarkers of seep and vent communities become strongly depleted in ^{13}C when the chemosynthetic bacteria incorporate ^{13}C depleted methane (Summons et al., 1994) or metabolites derived from autotrophic carbon fixation (Ruby et al., 1987). Specifically, diagnostic biomarkers of aerobic methanotrophic bacteria in cultures (Makula, 1978; Nichols et al., 1985; Bowman et al., 1991) and the environment (e.g. Pond et al., 1998; Niemann et al., 2006) are monounsaturated C_{16} fatty acids (FAs) with double bonds at positions $\omega 7$, $\omega 8$ and $\omega 9$, methyl steroids (e.g. Bouvier et al., 1976; Conway and McDowell-Capuzzo, 1991; Fang et al., 1992; Elvert and Niemann, 2008; Birgel and Peckmann, 2008) and hopanoids (e.g. Rohmer et al., 1984; Summons et al., 1994; Elvert and Niemann, 2008; Birgel et al., 2011). Many groups of bacteria also contain bacteriohopanepolyols (BHPs) which have been suggested to act as membrane stabilizers (Ourisson and Rohmer, 1982; Ourisson et al., 1987). BHPs are useful microbial markers because of organism-specific functionalization of the hopanoid side chain, e.g. BHPs with a terminal NH_2 group (aminopentol and aminotetrol) are indicative of methanotrophic bacteria (Talbot et al., 2001).

Intact polar membrane lipids (IPLs) are thought to reflect the presence of intact cells and thus viable biomass (White et al., 1979; Rütters et al., 2002; Sturt et al., 2004). In combination with conventional biomarkers [e.g. polar lipid-derived FAs (PLFAs)], IPLs provide additional taxonomic information encoded in their head group. Therefore, a quantitative overview of the major IPLs together with PLFA analysis provides a more holistic characterization of the active microbial community (cf. Fang et al., 2000; Rütters et al., 2002). Phospholipids are crucial membrane components of all living cells and comprise the most common IPLs in the bacterial and eukaryotic domain (Goldfine, 1984; Dowhan, 1997; Zhang and Rock, 2008). Bacteria can often be distinguished from Eukarya on the basis of their combined head group and core lipid composition. In general, Bacteria typically contain glycerol-based phospholipids, with two FA chains in the range C_{14} to C_{20} (Zhang and Rock, 2008). For example, methanotrophic bacteria have been described to produce phospholipids with phosphatidylglycerol

(PG), phosphatidylethanolamine (PE), phosphatidylmethylethanolamine (PME) and phosphatidyl dimethylethanolamine (PDME) head groups, containing predominantly C_{16:1} and C_{18:1} FAs (Fang et al., 2000). Information on sulfide oxidizers is scarcer, but DPG, PE and PG were shown to be the dominant IPL classes in thiotrophic bacteria isolated from thyasirid bivalves (Fullarton et al., 1995). For comparison, different species of marine and freshwater eukaryotic molluscs are dominated mainly by two types of phospholipids: (i) glycerol- and plasmalogen-based lipids with phosphatidylcholine (PC) and PE head groups and (ii) sphingolipids with phosphono-based head groups, e.g. ceramide phosphonoethylamine (PnE-Cer; Matsubara et al., 1990; Kostetsky and Velansky, 2009; Colaço et al., 2009). The core lipids of PnE-Cer in marine molluscs typically comprise C_{16:0} FA (Matsubara et al., 1990).

This study aimed to examine symbiont–host interactions using a comprehensive lipid biomarker approach. It targets IPLs as a lipid class that captures the overall distribution of bacterial and eukaryotic biomass between the symbiont and the host. IPLs were specifically utilized for the detection of different symbiont types and to assess their distribution within three *Bathymodiolus* mussel species from both vent and seep environments. In addition, FAs, BHPs and selected methyl sterols were chosen as target compounds because they encode specific information about various bacteria and enable, along with their compound-specific stable carbon isotopic composition, the determination of the dominant symbiotic lifestyle of the mussels. Three different types of symbiotic associations were chosen: one host species containing methanotrophic symbionts [*B. childressi* from the Gulf of Mexico (GoM; Duperron et al., 2007)], a second containing thiotrophic symbionts [*B. cf. thermophilus* from the Pacific Antarctic Ridge (PAR; Petersen and Dubilier, unpublished data)] and a third with both methanotrophic and thiotrophic symbionts [*B. brooksi* from the GoM (Duperron et al., 2007)]. Lipid biomarkers were extracted from the symbiont containing gill tissue and the symbiont-free foot tissue, with the latter serving as a reference for the host's lipid signature.

II.3. Material and methods

II.3.1. Sample collection and storage

B. brooksi and *B. childressi* were collected in October 2003 using the deep sea submersible Alvin during the Deep Sea Cruise 11 Leg I at a cold seep in the GoM near the Alaminos Canyon (26°21.320N, 94°30.120W, 2226 m water depth). *B. cf. thermophilus* was recovered in June 2001 using a TV controlled grab during the RV Sonne cruise SO 157 on the PAR near the Foundation Chain (from station 30 GTV at 37°47.4430S, 110°54.8340W, 2212 m water depth). Mussels were dissected on board into gill and foot tissue, except for *B. childressi*, for which only gill tissue was collected. Samples were stored at -20°C until analysis.

II.3.2. Lipid extraction

Mussel tissue (between 70 and 250 mg dry mass) from one individual per species was

mixed with ca. 5 g combusted quartz sand to enhance mechanical lysis during ultrasonic extraction. Samples were extracted (6x) using a modified Bligh and Dyer method described by Sturt et al. (2004). In brief, cell material was extracted (3x) using MeOH:CH₂Cl₂: aq. phosphate buffer (50 mM, pH 7.4) (2:1:0.8, v:v:v) and MeOH:CH₂Cl₂:CCl₃CO₂H (50 mM, pH 2) (2:1:0.8, v:v:v). The combined supernatants were washed with water, evaporated to dryness and stored at -20°C until analysis.

II.3.3. FAs and neutral lipids

For analysis of FAs, sterols and *sn*-1-mono-*O*-alkyl glycerol ethers (MAGEs), an aliquot of the total lipid extract (TLE) was saponified with 6% KOH in MeOH following the protocol of Elvert et al. (2003). Subsequently, the neutral lipids were extracted (4x) with *n*-hexane from the basic solution, which was acidified to pH 1 by addition of concentrated HCl; the FAs were then extracted (4x) with *n*-hexane. FAs were converted to methyl esters (FAMES) using 14% BF₃ in MeOH. Sterols and other alcohols, such as MAGEs, were converted to trimethylsilyl (TMS) ethers using bis(trimethylsilyl)trifluoroacetamide (BSTFA) in pyridine. Concentrations were derived from normalization to cholestane as injection standard. To determine double bond positions of FAs, an aliquot of the FA fraction was treated with 100 µL dimethyl disulfide (DMDS) and 20 µL iodine solution (6% w/v in Et₂O) under an O₂-free atmosphere at 50°C for 48 h. Samples were purified from the remaining iodine solution by sodium thiosulfate addition and extraction with *n*-hexane (Nichols et al., 1986).

Identification and quantification of FAMES and neutral lipids was performed with a gas chromatography–mass spectrometry (GC–MS) system (Thermo Electron Trace MS) equipped with a 30 m RTX-5MS fused silica column (0.25 mm i.d., 0.25 µm film thickness). The system was operated in electron impact (EI) mode at 70 eV with a scan range of *m/z* 40–900 at 1.5 scan s⁻¹. The interface temperature was 300°C and He was used as carrier gas at a constant flow of 1.4 mL min⁻¹. The temperature programme for FAMES and neutral lipids was: 60°C (1 min) to 150°C at 15°C min⁻¹, then to 320°C (held 27.5 min) at 4°C min⁻¹. The carbon isotopic composition of compounds was determined using a GC-isotope ratio-MS (Hewlett Packard 5890 series II gas chromatograph, Thermo Finnigan Combustion Interface-II, Finnigan MAT 252 mass spectrometer) equipped with a 30 m RTX-5MS fused silica column (0.25 mm i.d., 0.25 µm film thickness) with He as carrier gas. Stable carbon isotopic composition is expressed as δ¹³C values in the ‰ notation relative to Vienna Peedee Belemnite (VPDB). Precision of the isotopic analysis was controlled using cholestane as injection standard. The analytical error was <1.0‰. The δ¹³C values were corrected for additional carbon introduced during derivatization.

II.3.4. Bacteriohopanepolyols

An aliquot of the TLE was separated over a tightly packed glass wool Pasteur pipette into a *n*-hexane soluble (maltenes) and a CH₂Cl₂/MeOH soluble (asphaltene) fraction. An aliquot of the asphaltene fraction was acetylated using Ac₂O in pyridine and heated to 50°C for 1 h. The

reaction mixture was left to stand overnight. BHPs were analyzed via atmospheric pressure chemical ionization liquid chromatography/multi-stage ion trap mass spectrometry (APCI-LC/MSⁿ) according to Talbot et al. (2001). The high performance liquid chromatography (HPLC) instrument was equipped with a reversed phase column (Alltech Prevail C₁₈, 150 x 2.1 mm, 3 μm, Alltech, München, Germany) and a guard column of the same packing material (7.5 x 2.1 mm). The APCI source was operated in positive ionization mode. Prior to injection, the acetylated fraction of the extract was dissolved in MeOH/propan-2-ol (60:40 v/v). Separation was achieved using three different eluents (A, MeOH; B, deionized water; C, propan-2-ol) with the following linear gradient: 90% A and 10% B (0–5 min); 59% A, 1% B and 40% C (at 45 min) and hold for 25 min. The flow rate was 0.2 mL min⁻¹. APCI vaporizer temperature was 400°C, discharge current was 5 μA and sheath gas flow was 40 (arbitrary units).

To determine δ¹³C values of BHPs, we converted BHPs to hopanols (Rohmer et al., 1984; Innes et al., 1997), which were analyzed by way of GC-isotope ratio (IR)-MS. In brief, an aliquot of the asphaltene fraction was stirred for 1 h at room temperature with periodic acid (H₅IO₆; 300 mg in 3 mL tetrahydrofuran/water (8:1 v/v)). After addition of water, the resulting aldehydes were extracted with petroleum ether and the extract was evaporated. Subsequently, the aldehydes were reduced to primary alcohols by stirring for 1 h at room temperature with NaBH₄ in EtOH. After addition of KH₂PO₄ the mixture was extracted with petroleum ether, evaporated and the resulting hopanols were derivatized with BSTFA in pyridine prior to GC-IR-MS analysis.

II.3.5. Intact polar lipids

The TLE was dissolved in 5:1 CH₂Cl₂/MeOH and an aliquot directly analyzed using HPLC without further treatment (Thermo- Finnigan Surveyor HPLC equipped with a 150 x 2.1 mm, 5 μm LiChrospher Diol-100 column fitted with a 7.5 x 2.1 mm guard column of the same packing material; Alltech GmbH, Munich, Germany) coupled to an ion-trap mass spectrometer (ThermoFinnigan LCQ Deca XP Plus) equipped with an electrospray ion source in positive and negative ionization mode. HPLC analysis was conducted with gradients described by Sturt et al. (2004) [eluent A: *n*-hexane, 2- propanol, formic acid and NH₃ (79:20:0.12:0.04, v:v:v); eluent B: propan-2-ol, water, formic acid and NH₃ (90:10:0.12:0.04) at 0.2 mL min⁻¹]. Identification of the phospholipids was performed largely in positive mode according to published MS data, whereas the negative mode provided information about the molecular mass of the acyl moieties (Matsubara et al., 1990; Fang and Barcelona, 1998; Rütters et al., 2002; Sturt et al., 2004; Zemski Berry and Murphy, 2004; Schubotz et al., 2009).

II.3.6. Quantification of symbiont- and host -derived IPLs

Absolute IPL concentration was estimated from peak areas of molecular ions in extracted ion mass chromatograms relative to an internal standard (1-O-hexadecyl-2-acetyl-*sn*-glycero-3- phosphocholine; PAF). Relative response factors of individual IPL head group classes were not accounted for. Since previous studies have shown that the response factor

can vary significantly for IPLs with different head groups (e.g. Schubotz et al., 2009; Van Mooy and Fredricks, 2010), reported IPL concentration values are semiquantitative. Response factors of various commercially available authentic standards compared with PAF ranged from 0.5 to 2 (cf. Schubotz et al., 2009). This work consequently focuses on the relative distribution of IPLs among different mussel species and tissues.

The distinction of symbiont- and host-derived IPLs was based on complementary MS information obtained in positive and negative ionization mode during HPLC–ESI–MS analysis. Symbiont specific FAs (largely C_{16:1} FAs; see section II.3.2) were identified in the negative ionization mode and their corresponding IPL molecular ions (m/z 688 for PE-di-C_{16:1} and m/z 736 for PG-di-C_{16:1}) were extracted and quantified in the positive ion mode, resulting in an approximation of symbiont- and host-derived IPLs.

II.3.7. Identification of plasmalogens

In contrast to PE–plasmalogens (1-O-alk-10-enyl-2-acyl glycerophospholipids), which are clearly identifiable using HPLC–MS (Fig. II.3a; Zemski Berry and Murphy, 2004), PC–plasmalogens are not unambiguously recognized since their MS² fragment (m/z 184) is the same as for PC–diacylglycerol (DAG). The presence of two PC containing IPL classes became apparent after visualization of the chromatogram by way of 3D density maps (x – time, y – m/z , z – intensity; Fig. II.1a). To test for the presence of PC plasmalogens, we used preparative HPLC to obtain a fraction concentrated with IPLs with PC head groups. Preparation of fractions of distinct IPL classes was achieved according to a protocol described by Biddle et al. (2006), but with slight modification. We used a preparative LiChrospher Diol-100 column (250 x 10 mm, 5 μ m, Alltech, Germany) connected to a ThermoFinnigan Surveyor HPLC instrument equipped with a Gilson FC204 fraction collector. Flow rate was 1.5 mL min⁻¹ and the eluent gradient was: 100% A (n-hexane/propan-2-ol; 79:20, v:v) to 100% B (propan-2-ol/water; 90:10, v:v) in 120 min, then held at 100% B for 30 min, with 30 min column re-equilibration with 100% A. In total, 14 fractions were collected. Fraction 7 contained the fractions of IPLs with PC head groups and we therefore used this fraction to convert potential PC plasmalogens to dimethyl acetals by way of acid hydrolysis (Fig. II.1b and c; Rao et al., 1967). Thereby, an aliquot of fraction 7 was blown down to dryness and treated with methanolic HCl [6 M HCl/MeOH (1:9, v/v)] at 50°C overnight. Finally, MilliQ water was added and the solution extracted (4x) with n-hexane. The organic phase was evaporated under a gentle stream of N₂ and directly analyzed via GC–MS as described above. Characteristic fragmentation patterns confirmed the presence of plasmalogen-derived dimethyl acetals during GC–MS analysis (Fig. II.1c).

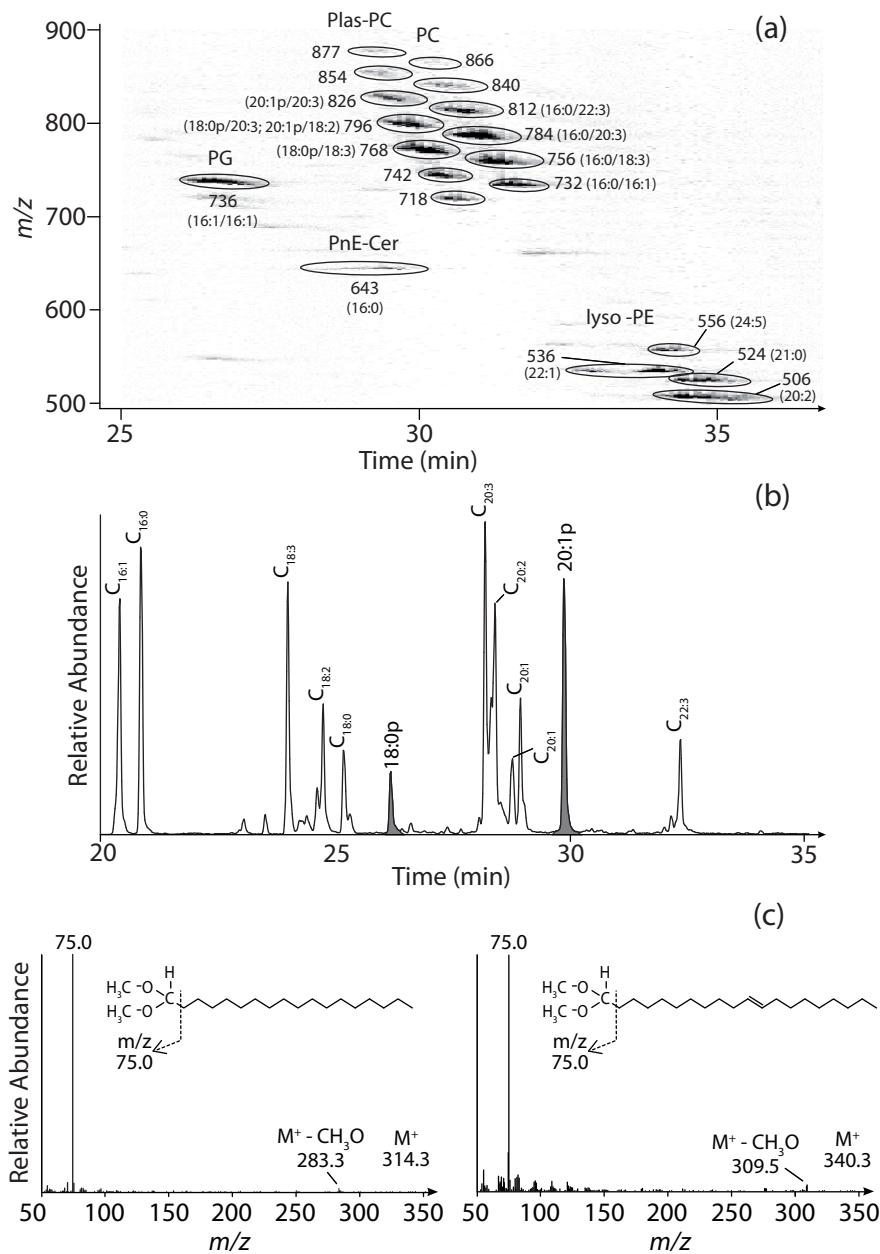


Fig. II.1. (a) Partial density map showing distribution of intact polar lipid in preparative HPLC fraction 7 (F7) of *B. brooksi* (gill tissue). Numbers in bold refer to the molecular mass (Da), numbers in brackets give information about the FA side chains (p indicates chain length of plasmalogen side chain). For abbreviations of lipid names refer to the text or see Appendix II.1. (b) Gas chromatogram of FAMES from acidic transesterification of F7 (*B. brooksi*). Plasmalogens are converted to dimethyl acetals (highlighted in grey). FA abbreviations characterize carbon chain length and number of double bonds. (c) Electron impact mass spectra of the dimethyl acetals (left: $C_{18:0p}$, right: $C_{20:1p}$). Mass spectra of dimethyl acetals are characterized by a typical base peak at m/z 75 [$C_3H_7O_2$] $^+$ and a fragment ion [$M-CH_3O$] $^+$.

II.4. Results and discussion

II.4.1. IPL abundance and distribution in *Bathymodiolus* mussels

The IPLs in both gill and foot tissue of all three species were dominated by PE and PC (Fig. II.2). The most abundant core lipid types were diacylglycerols (DAGs) and plasmalogens (Plas; Fig. II.3a), followed by ceramides (Cers) and lyso-lipids. Total IPL concentration ranged from 2

to $6 \text{ mg g}_{\text{dm}}^{-1}$ (per g dry mass) in the gills and was slightly lower in the foot tissue, ranging from 1.4 to $2.5 \text{ mg g}_{\text{dm}}^{-1}$ (Table II.1).

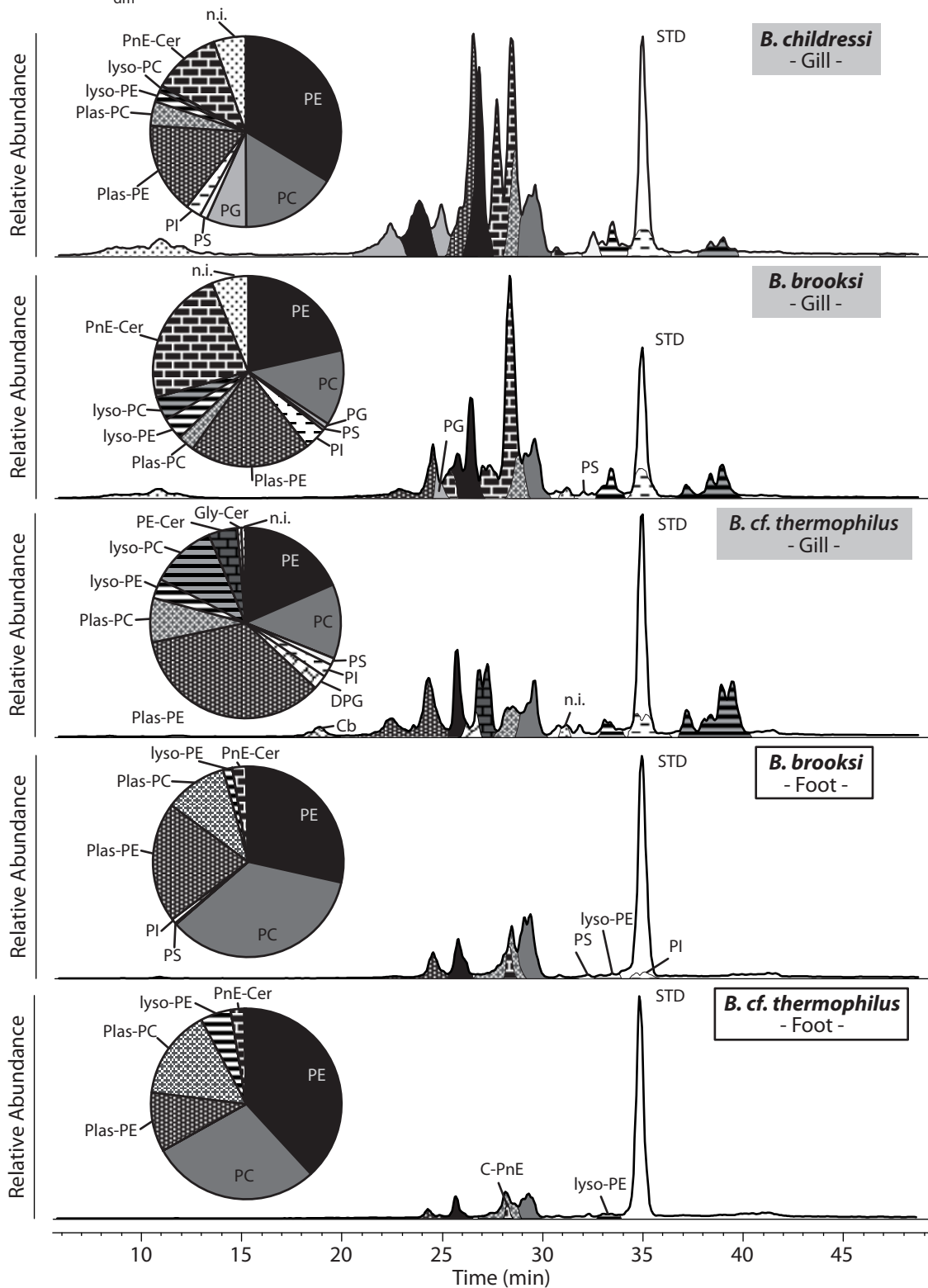


Fig. II.2. HPLC-ESI-MSⁿ data for all mussel tissue samples. The chromatogram shows the base peak plot for the TLE in positive ion mode. The following IPLs (see Appendix II.1 for structures) were detected: PC (phosphatidylcholine); PE (phosphatidylethanolamine); PG (phosphatidylglycerol); PI (phosphatidylinositol); PS (phosphatidylserine); PnE-Cer (ceramide-phosphonoethanolamine); Gly-Cer (cerebroside); PE-Cer (ceramide- phosphatidylethanolamine); lyso membrane lipids (lyso-PE, lyso-PC) containing a single acyl chain. Abbreviations: STD, injection standard (C₁₆-PAF); n.i., not identified. Relative IPL composition is shown as pie charts.

The IPL composition of the foot tissue for *B. brooksi* and *B. cf. thermophilus* was quite similar, comprising ca. 60% PE- and PC-DAGs, ca. 30% PE- and PC-Plass and minor amounts of lyso-PEs and PnE-Cers (Fig. II.2). The only difference was the presence of PI and PS-DAGs in *B. brooksi* (ca. 4% of total IPLs). This similarity suggests that primarily taxonomic affiliation and not environmental factors determine the IPL composition in the foot tissue of the mussels. By comparison, the gill tissues of all three species displayed more diverse IPL distributions. PEs, PCs and PG-DAGs comprised between 30% and 60% of total IPLs, while PEs and PC-Plass ranged from 20% to 40%, and lyso-PCs and PEs and phospho-ceramides varied between 15% and 30%. In particular, the presence or absence of specific IPLs distinguished gill and foot tissue of individual species and gill tissue between different mussel species: PGs with DAG core structures was exclusively found in the gill tissue of *B. childressi* (7% of total IPLs) and *B. brooksi* (<1%). PG-DAGs were absent from *B. cf. thermophilus*, while DPGs were present in the gill tissue of *B. cf. thermophilus* (Fig. II.2, Table II.1). Another distinctive feature of the IPL distribution in the gill tissue was the presence of phosphonoethanolamine ceramide (PnE-Cer; Fig. II.2, Fig. II.3b; Table II.1) in both species recovered from the GoM, whereas *B. cf. thermophilus* lacked it but instead contained small amounts of PE-Cer (5%). These small scale differences in IPL composition between gill and foot tissue within a mussel as well as differences across species could result either from the presence of symbiotic bacteria, their functional properties (Kostetsky and Velansky, 2009), or the nutritional status of the mussel, as discussed below.

II.4.2. FA abundance and distribution in Bathymodiolus mussels

The FA distributions differed between gill and foot tissue of the same species, as well as between the gill tissue of different species. The foot tissue of both *B. brooksi* and *B. cf. thermophilus* was dominated by polyunsaturated C₁₈ and C₂₀ FAs (PUFAs; ca. 40% of total FAs), while monounsaturated C₁₆ and C₁₈ FAs were only a minor component (together ca. 15%). By comparison, C_{16:1ω7} was the most abundant FA in the gill tissues of all three species, comprising between 30% and 40% and C₁₈ and C₂₀ PUFAs covering ca. 20% (Fig. II.4; Table II.2). PUFAs are a common feature in vent and seep mussels (Fang et al., 1993; Pranal et al., 1996; Pond et al., 1998; Allen et al., 2001; Colaço et al., 2006) and are synthesized through chain elongation and unsaturation of the symbiont-derived FAs, mainly C_{16:1ω7} or C_{18:1ω7} (cf. Fang et al., 1993; Pond et al., 1998). Although C_{16:1ω7} is considered a generic FA and is produced by both Eukarya and Bacteria (Guezennec and Fiala-Medioni, 1996; Pond et al., 1998), a high abundance in symbiont-hosting gill tissue has been used as a marker for the presence of symbiotic bacteria (McCaffrey et al., 1989; Guezennec and Fiala-Medioni, 1996; Pranal et al., 1996, 1997; Colaço et al., 2006). This is in accordance with observations by Abrajano et al. (1994), who demonstrated that shallow water mussels without symbionts contained mainly saturated C₁₆ FAs, whereas the proportion of C_{16:1} was elevated in cold seep mussels with symbionts. A similarly elevated concentration of C_{18:1ω7} and C_{20:1ω7} in gill tissue has been assigned to the presence of Bacteria in symbiotic mussels (McCaffrey et al., 1989; Guezennec and Fiala-Medioni, 1996; Pranal et al., 1996, 1997;

Colaço et al., 2006). For *B. cf. thermophilus* no other symbiont specific FAs could be identified. The presence of $C_{16:1\omega8}$ (14%) and $C_{18:1\omega8}$ (3%) in *B. childressi* and $C_{16:1\omega9}$ (9%) and $C_{18:1\omega8}$ (1%) in *B. brooksi* was unequivocally assigned to methanotrophic symbionts (e.g. Makula, 1978; Nichols et al., 1985; Bowman et al., 1991) and is discussed in more detail below (section II.3.5).

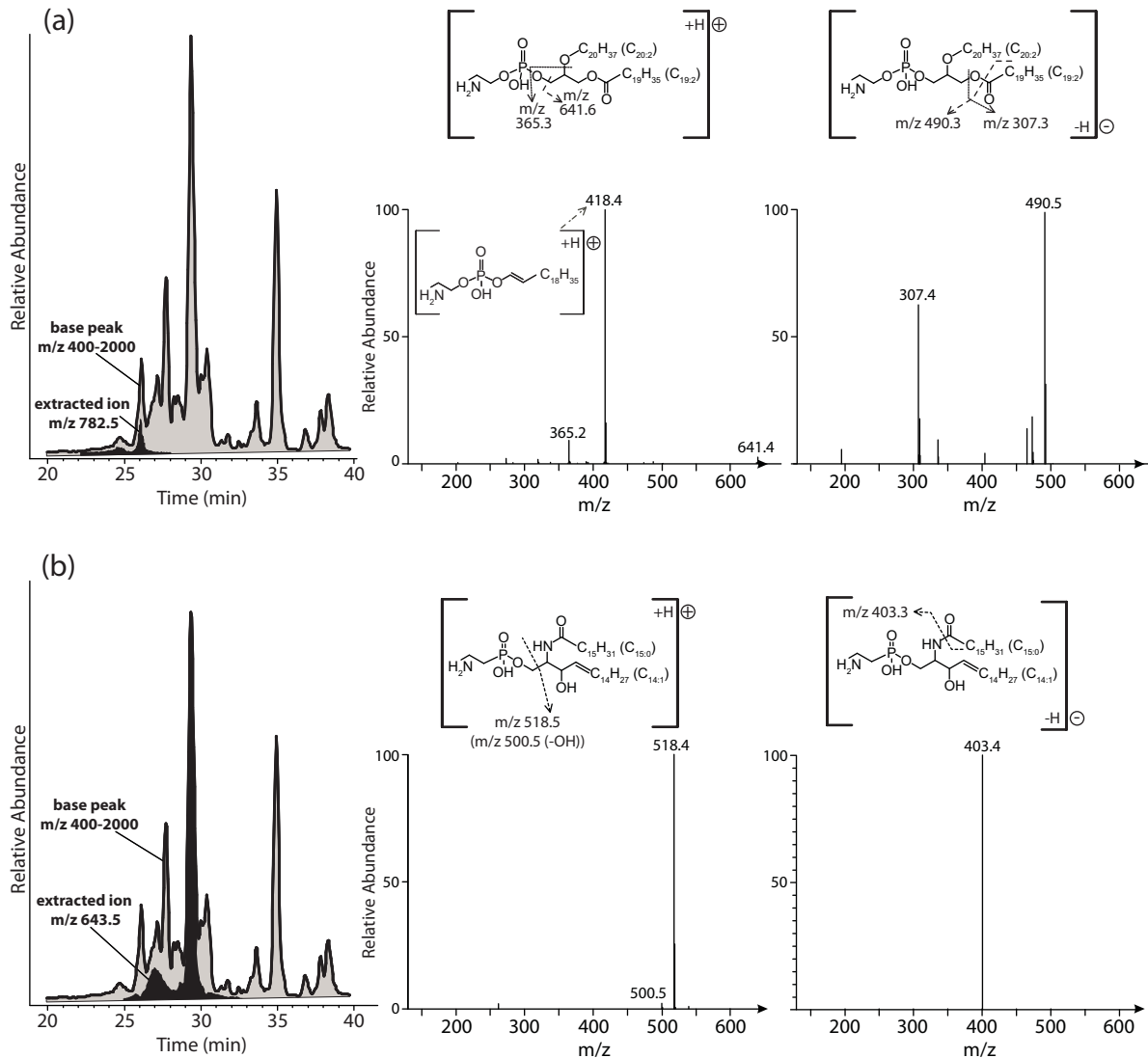


Fig. II.3. HPLC-ESI-MSⁿ data for (a) plasmalogen-phosphatidylethanolamine (PE-Plas) and (b) ceramide-phosphonoethanolamine (PnE-Cer) for the gill tissue of *B. brooksi* as an example. (a) The chromatogram shows the base-peak plot of the TLE in positive ion mode overlain by the m/z 782.5 chromatogram (black area) derived from PE-Plas. (b) The chromatogram shows the base peak plot of the TLE in positive ion mode overlain by the m/z 643.5 chromatogram (black area) derived from PnE-Cer. For both lipids, the fragmentation pattern during MS/MS experiments is schematically illustrated in positive (upper and lower left) and negative ionization (upper and lower right) mode.

Total FA concentration ranged from 22 to 54 mg g_{dm}⁻¹ (Table II.2) in the gill tissue and 1–2 mg g_{dm}⁻¹ in the foot tissue. The apparent discrepancy between IPL and FA dry weight biomass of gill tissue (10x more FAs than IPLs) and foot tissue (0.4–1.4x more FAs than IPLs) can be best explained by abundant triglycerides in symbiont hosting gill tissues as an additional source of FAs. Triglycerides can comprise up to 60% in symbiont-hosting gill tissue of *Bathymodiolus*

brevior and *B. elongatus* (Pranal et al., 1997). Similarly, Allen et al. (2001) observed that the symbiont-hosting gill tissue of the hydrothermal vent clam *Calyptogena pacifica* comprised maximal 50% triglycerides of the total lipid composition (IPLs 50%), but only 4% in the foot tissue (IPLs 80%). Additionally, the presence of free FAs could also be responsible for higher absolute amounts of FAs than IPLs. However, free FAs were shown to comprise only ca. 10% in both gill and foot tissue (Allen et al., 2001). Response factors of IPLs could minimize uncertainty in the estimation of absolute abundances for IPLs.

Table II.1. Major core structures and relative abundance of IPLs in mussel tissue (absolute concentration in $\text{mg g}_{\text{dm}}^{-1}$; n.d., not detected; n.i., not identified).

	<i>B. childressi</i>		<i>B. brooksi</i>				<i>B. cf. thermophilus</i>			
	Gill		Gill		Foot		Gill		Foot	
	Major core	Relative abundance (%)	Major core	Relative abundance (%)	Major core	Relative abundance (%)	Major core structure	Relative abundance (%)	Major core	Relative abundance (%)
PE-DAG	16:1/16:1; 16:1/16:2; 16:0/16:1	34	16:1/16:1; 18:0/18:3; 16:0/16:1	21	18:0/18:3; 16:0/18:3	29	18:0/18:3; 16:1/16:2	18	18:0/18:3	38
PC-DAG	18:0/18:3; 16:0/18:3; 16:1/16:0; 16:1/20:2	16	16:0/16:1; 16:0/20:3; 16:0/18:3	13	16:0/18:3; 18:0/18:3; 16:0/20:3	35	16:0/16:1; 16:0/18:3; 16:0/20:2	13	16:0/20:3; 16:0/18:3; 16:0/16:1	29
PG-DAG	16:1/16:1	7	16:1/16:1	1	n.d.	–	n.d.	–	n.d.	–
PS-DAG	n.i.	1	n.i.	1	n.i.	<1	n.i.	1	n.d.	–
PI-DAG	n.i.	3	n.i.	4	n.i.	1	n.i.	2	n.d.	–
DPG	n.i.	–	n.d.	–	n.d.	–	4x 16:1	3	n.d.	–
Plas-PE	20:1p/20:1; 18:0p/18:3; 22:2	15	20:1p/20:2; 20:1, 20:0; 18:0p/18:2; 22:2	21	20:1p/20:2; 20:1	20	18:0p/18:2; 20:2, 20:1; 20:1p/20:3; 20:1	35	20:1p/20:1	10
Plas-PC	18:0p/18:3	4	n.i.	3	n.i.	11	n.i.	8	n.i.	15
Lyso-PE	20:2; 20:3	2	20:2	4	20:2; 20:3; 22:2	2	20:1; 20:2	3	20:1; 20:2	5
Lyso-PC	15:1	1	15:1; 15:0	4	n.d.	–	16:0; 15:1	11	n.d.	–
Lyso-PS	22:2	<1	n.d.	–	n.d.	–	n.d.	–	n.d.	–
PE-Cer	n.d.	–	n.d.	–	n.d.	–	d20:0/16:1	5	n.d.	–
PnE-Cer	d18:1/16:0; d22:1/16:0	12	d18:1/16:0	23	d18:1/16:0	2	n.d.	–	d18:1/16:0	2
Gly-Cer	n.d.	–	n.d.	–	n.d.	–	n.i.	1	n.d.	–
n.i.	n.i.	5	n.i.	6	n.i.	<1	n.i.	1	n.i.	<1
Σ conc.										

II.4.3. Symbiont-derived IPLs

The different combinations of acyl chain distributions of IPLs were used to differentiate between eukaryotic and bacterial sources (cf. section II.3.6). As reported in section II.4.2, $C_{16:1}$ FAs were most abundant in the gill tissue of the mussels and indicate the presence of the bacterial symbiont. IPLs with head groups common for methanotrophic and thiotrophic bacteria, such as PE-, DPG-, and PG-DAGs with a core lipid composition of di- $C_{16:1}$ acyl chains were only present in the gill tissues of the mussels (cf. Fig. II.2, Table II.2). Fang et al. (2000) identified PGs and PEs with predominantly $C_{16:1}$ FA as major IPLs in type I methanotrophs, supporting the presence of this group of methanotrophs in the gills of both species from the GoM (cf. Duperron et al., 2007). In *B. cf. thermophilus* $C_{16:1}$ FAs were mainly present as DPGs, and some PE-DAGs. Accordingly, DPGs and PEs with exclusively $C_{16:1}$ FAs are interpreted as a marker for the associated thiotrophic bacteria since this mussel has only one symbiont (Table II.1; Petersen and Dubilier, unpublished data). This is in agreement with DPG, PG and PE being the dominant IPL classes in thiotrophic bacteria isolated from thyasirid bivalves (Fullarton et al., 1995). The only other IPL containing

$C_{16:1}$ acyl chains in all three mussel species was PC-DAG. PC-DAG has been observed in some type I methanotrophs (Makula, 1978), but since PC with $C_{16:1}$ acyl chains was also present in foot tissue, it cannot be unambiguously assigned to a bacterial source.

Consequently, the IPL inventory provides clues on the symbiont relative contribution within host gill tissue (Fig. II.5). Comparing the relative abundance of designated symbiont-derived IPLs within the three mussels, they were highest in the predominantly methanotrophic symbiont-hosting *B. childressi* (25% of all IPLs), followed by the thiotrophic and methanotrophic symbiont-hosting *B. brooksi* (11%) and finally by the purely thiotrophic symbiont-hosting *B. cf. thermophilus* (3%). The foot tissue of *B. brooksi* and *B. cf. thermophilus* did not contain any of the putatively assigned symbiont derived IPLs.

II.4.4. Host-derived IPLs

DAG-based IPLs that are mainly derived from the eukaryotic host contain PUFAs such as $C_{18:3}$, $C_{20:2}$ and $C_{20:3}$ which are common in hydrothermal vent mussels but rarely detected in Bacteria (Table II.1; Fang et al., 1993; Pranal et al., 1996; Pond et al., 1998; Allen et al., 2001; Colaço et al., 2006). Likewise, plasmalogen IPLs (e.g. PE-Plas and PC-Plas) contain predominantly long chain PUFAs and the ceramides (PE-Cers and PnE-Cers) comprised $C_{18:1}$ and $C_{20:1}$ or C_{22} sphingolipid backbones with saturated or monounsaturated C_{16} FAs (Table II.1; Fig. II.3b). Plasmalogens are a widely distributed group of IPLs in the animal kingdom (Nagan and Zoeller, 2001). Marine invertebrates are well known to contain plasmalogens, most commonly associated with PEs and PCs (Kraffe et al., 2004), as described here. Similarly, the phosphosphingolipids (PnE-Cers) in *B. childressi* and *B. brooksi* are common in marine animals, e.g. bivalve molluscs (Matsubara et al., 1990; Mukhamedova and Glushenkova, 2000; Kostetsky and Velansky, 2009). The PE-Cer in *B. cf. thermophilus* has to our knowledge not been reported from marine molluscs. However, because of the long chain sphingosine backbone (d20:0; "d" for the two (di-) hydroxyls of sphingosine), we suggest that PE-Cer is, like PnE-Cer, most probably a marker for the host mussel. The biological function of these compounds is under debate, but ceramides are generally known to play an important role in signaling processes (Lahiri and Futerman, 2007).

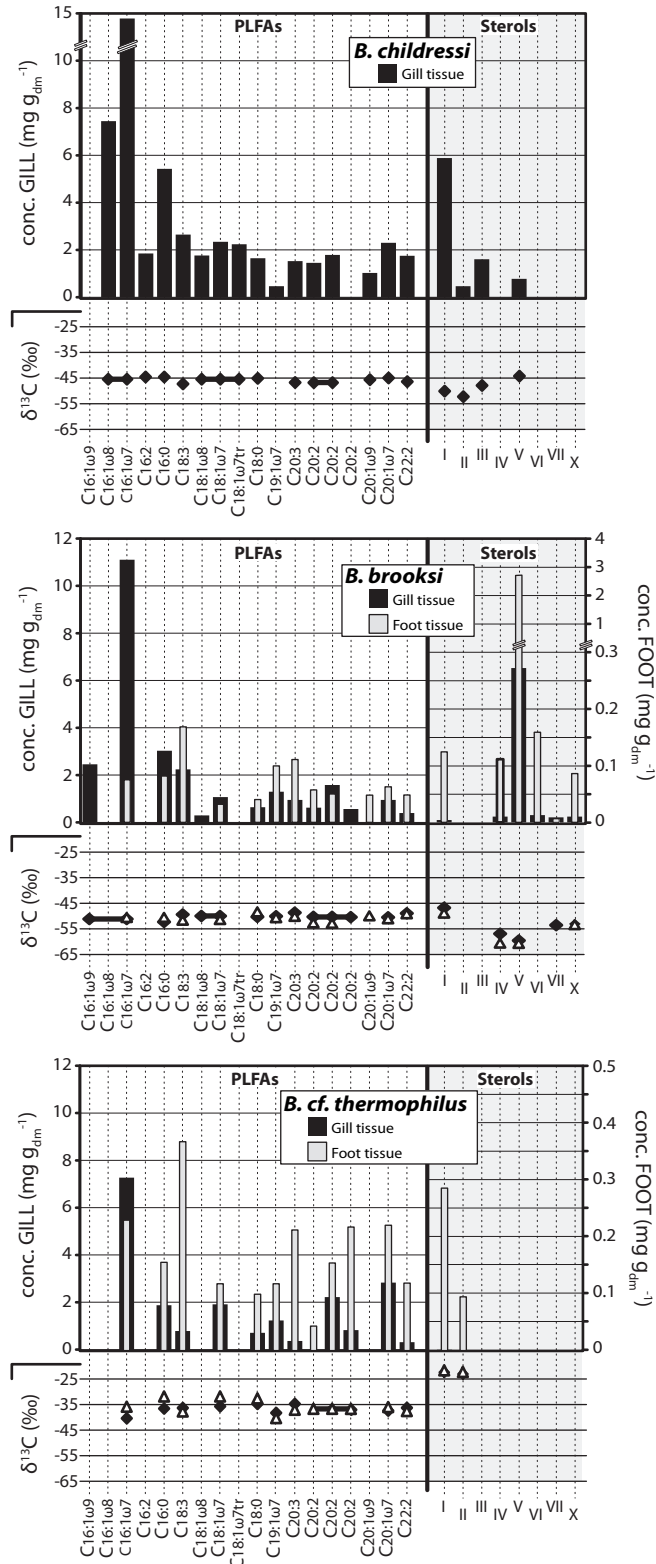


Fig. II.4. Concentrations of FAs and sterols (black bars, gill tissue; light gray bars, foot tissue) and carbon isotopic composition (black diamonds: gill tissue, open triangle, foot tissue) of major FAs and sterols for *B. childressi*, *B. brooksi* and *B. cf. thermophilus*. Co-eluting peaks are indicated with a thick black horizontal line. MAGEs were excluded due to comparatively low abundance. Major sterols (see Appendix II.1 for structures): cholesterol (I); cholestanol (II); cholesta-5,24-dien-3 β -ol (III); 4 α -methylcholesta-8(14)-en-3 β -ol (IV); 4 α -methylcholesta-8(14),24-dien-3 β -ol (V); 4 α -methylcholesta-(14),22,24-trien-3 β -ol (VI); lanosterol (VII); 4,4-dimethylcholesta-8(14),24-dien-3 β -ol (X). The $\delta^{13}\text{C}$ values of the CH_4 at the Alaminos Canyon in the GoM shows a primarily thermogenic origin (-42‰ to -48‰; Lanoil et al., 2001; Becker et al., 2010); carbon isotopic values for CO_2 as carbon source in the PAR have not been described.

II.4.5. *B. childressi* and *B. brooksi* host different methanotrophic symbiont type markers

Diagnostic biomarkers such as BHP, 4-methyl sterols and certain characteristic FAs together with their $\delta^{13}\text{C}$ values confirm the presence of methanotrophic symbionts in *B. childressi* and *B. brooksi*. Both, aminotriol and aminotetrol in the gills of *B. childressi* and only aminotriol in *B. brooksi* is an unambiguous signal for bacterial symbionts (Fig. II.6). The higher abundance of aminotetrol than aminotriol within *B. childressi* potentially points to the presence of type II methanotrophic bacteria (Talbot et al., 2001). The $\delta^{13}\text{C}$ values of BHP-derived hopanols are in the range for methanotrophic hopanoids in sedimentary records (Collister et al., 1992; Hinrichs et al., 2003) and consistent with isotopic fractionation determined for methanotrophic cultures (Summons et al., 1994; Jahnke et al., 1999): -55.5‰ for the aminotriol derivative C_{32} bishomohopanol in *B. brooksi* and -51.1‰ for the aminotetrol derivative C_{31} homohopanol in *B. childressi*. Because of the low concentration, the isotopic composition of aminotriol derived C_{32} bishomohopanol in *B. childressi* was not determined (Fig. II.6). The presence of $\text{C}_{16:1\omega 8}$ FA (-46‰) in *B. childressi* and of $\text{C}_{16:1\omega 9}$ FA (-51‰) in *B. brooksi* is an indicator for type I methanotrophic bacteria (Makula, 1978; Nichols et al., 1985; Bowman et al., 1991; Niemann et al., 2006; Riou et al., 2010), whereas abundant $\text{C}_{18:1\omega 8}$ FA (-45‰) in *B. childressi* points to the additional presence of type II methanotrophic bacteria (Fig. II.4, Table II.2; Nichols et al., 1985; Bowman et al., 1991). The inferred presence of a second type II methanotrophic symbiont in the gills contradicts IPL data, which lack the type II IPLs phosphatidylmethylethanolamine (PME) and phosphatidyl dimethylethanolamine (PDME) with predominantly $\text{C}_{18:1}$ FA and therefore appear indicative of type I methanotrophs. A conclusion based solely on the BHP and FA evidence also contradicts the results from Duperron et al. (2007), who described the mussel symbionts from *B. childressi* as being solely type I methanotrophs. Differences in the methanotrophic biomarker composition also become apparent when comparing the sterol composition of *B. childressi* and *B. brooksi*. While the gill tissue of *B. childressi* was dominated by cholesterol, *B. brooksi* contained predominantly 4-methyl sterols (Fig. II.4, Table II.2). *B. childressi* contained only small quantities of 4 α -methylcholesta-8(14),24-dien-3 β -ol, while *B. brooksi* had a suite of five methyl sterols thought to be biosynthesized via demethylation and hydrogenation of lanosterol (Bouvier et al., 1976; Summons et al., 1994; Elvert and Niemann, 2008). Within the methyl sterols in *B. brooksi*, 4 α -methylcholesta-8(14),24-dien-3 β -ol was by far the most abundant (Fig. 4). Since methyl sterols are known to occur in methanotrophic symbionts (Conway and McDowell-Capuzzo, 1991; Fang et al., 1993; Jahnke et al., 1995; Schouten et al., 2000) and were not reported to appear in symbiont-free mytilid mussels, their presence is an indicator of methanotrophic bacteria in the mussels. This is in line with the absence of 4-methyl sterols from *B. cf. thermophilus*, known to host only thiotrophic symbionts (Petersen and Dubilier, unpublished data; Fig. II.4; Table II.2). Instead, *B. cf. thermophilus* contained small amounts of cholesterol and cholestanol, mainly in the foot. The ^{13}C depletion in the 4-methyl sterols, with δ values of -44‰ in *B. childressi* and as low as -60‰ in *B. brooksi*, further underlines their origin in methanotrophic bacteria (cf. Summons et al., 1994).

Table II.2. Concentration and isotopic composition of major FAs, MAGEs and sterols in mussel tissue (n.d., not detected).

	<i>B. childressi</i>		<i>B. brooksi</i>				<i>B. cf. thermophilus</i>			
	Gill		Gill		Foot		Gill		Foot	
	$\delta^{13}\text{C}$	Conc. ($\text{mg g}_{\text{dm}}^{-1}$)	$\delta^{13}\text{C}$	Conc. ($\text{mg g}_{\text{dm}}^{-1}$)	$\delta^{13}\text{C}$	Conc. ($\text{mg g}_{\text{dm}}^{-1}$)	$\delta^{13}\text{C}$	Conc. ($\text{mg g}_{\text{dm}}^{-1}$)	$\delta^{13}\text{C}$	Conc. ($\text{mg g}_{\text{dm}}^{-1}$)
FAs										
C _{16:1o9}	n.d.	n.d.	-51.1	2.5	n.d.	n.d.	n.d.	n.d.	n.d.	n.d.
C _{16:1o8}	-45.5	7.4	n.d.	n.d.	n.d.	n.d.	n.d.	n.d.	n.d.	n.d.
C _{16:1o7}	-45.5	15	-51.1	11	-50.6	0.075	-40.4	7.3	-35.8	0.23
C _{16:0}	-44.6	5.4	-52.3	3.0	-50.5	0.082	-36.6	1.9	-31.9	0.15
C _{18:3}	-47.3	2.7	-49.4	2.2	-51.6	0.17	-36.3	0.82	-37.7	0.37
C _{18:1o8}	-44.7	1.8	-50.7	0.29	n.d.	n.d.	n.d.	n.d.	n.d.	n.d.
C _{18:1o7}	-44.7	2.3	-50.7	1.1	-51.3	0.032	-35.7	1.95	-31.8	0.12
C _{18:0}	-45.2	1.7	-50.3	0.64	-48.4	0.040	-34.8	0.75	-32.6	0.10
C _{20:3}	-46.8	1.5	-48.7	0.95	-50.1	0.11	-34.8	0.41	-37.0	0.21
C _{20:1o7}	-45.0	2.3	-50.5	0.95	-51.1	0.063	-37.4	2.86	-36.0	0.22
Weighted mean total FAs	-45.5		-50.8		-50.8		-37.8		-35.7	
Total conc. ^a		54		28		0.91		22		2.1
MAGEs										
C _{16:1}	-41.6	0.12	-50.1	1.4	-47.9	0.021	-38.4	0.096	-33.4	0.10
C _{16:0}	-40.6	0.17	-48.4	0.29	-47.9	0.044	-34.1	0.044	-33.4	0.014
C _{18:0}	-40.0	0.24	-48.7	0.14	-48.5	<0.01	-34.9	0.021	-30.7	<0.01
C _{20:1}	-42.0	0.19	-47.2	0.35	-48.5	<0.01	-36.9	0.072	-38.3	0.014
Weighted mean total MAGEs	-40.8		-49.2		-48.0		-36.6		-33.7	
Total conc. ^a		0.95		2.4		0.065		0.20		0.10
Sterols										
Cholesterol	-50.1	5.9	-46.8	0.10	-48.9	0.12	-22.4	0.041	-21.6	0.28
4 α -methylcholesta-8(14),24-dien-3 β -ol	-44.3	0.78	-59.5	6.5	-60.7	2.8	n.d.	n.d.	n.d.	n.d.
Weighted mean total sterols	-49.1		-58.9		-60.0		-23.3		-22.2	
Total conc. ^a		10		7.3		3.1		0.068		0.44

^a Including compounds with no isotopic information.

II.4.6. *B. cf. thermophilus*: Indications for changing environmental conditions

The comparably low proportion of symbiont lipids in *B. cf. thermophilus* gill tissue is notable (Fig. II.5) and may indicate the relative importance of the symbiont within this tissue. Indeed, according to observations by Stecher et al. (2002), the PAR mussel field was on the verge of changing from a symbiosis-dominated to a more filter-feeding assemblage as a result of a decreasing flow of vent fluids at the time of sampling. The concomitant decrease in H₂S concentration could have caused a decrease in the abundance of thiotrophic symbionts in *B. cf. thermophilus* gill tissue. Such a response has been observed in studies in which transfer of *Bathymodiolus* mussels to an environment lacking sulfide led to reduction or loss of their gill symbionts (Raulfs et al., 2004; Kádár et al., 2005). A change in nutritional status from a symbiont-dependent to a filter-feeding mollusc is also reflected in the detection of small amounts of comparably ¹³C-enriched cholesterol (22‰) in both gill and foot tissue of *B. cf. thermophilus* (Fig. II.4 and Table II.2). This δ value is suggestive of a planktonic source; e.g. marine mytilids feeding on phytoplankton had $\delta^{13}\text{C}$ values of ca. -24‰ (Abrajano et al., 1994). This environmental adaptation could also explain the increased levels of plasmalogen IPLs (PE-Plas, PC-Plas) in *B. cf. thermophilus* because it has been suggested that the vinyl ether bond at the sn-1 position makes plasmalogens susceptible to oxidation, while protecting other membrane components (Morand et al., 1988; Brites et al., 2004). Furthermore, the degradation of plasmalogens leads to a buildup of lysolipids (Morand et al., 1988), which were observed in higher amount in *B. cf. thermophilus* than the other two species (Fig. II.2; Table II.2).

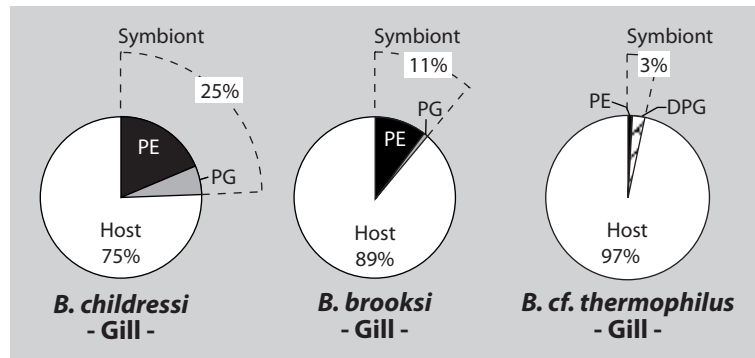


Fig. II.5. Pie charts showing contribution of symbionts within host gill tissue (for details see section II.4.3).

II.4.7. Stable carbon isotopic compositions trace carbon sources

Compound-specific $\delta^{13}\text{C}$ analysis of sterols, FAs and other lipid components such as MAGEs, which are likely derived from a bacterial source (Liefkens et al., 1979), offers valuable information for tracing the carbon source of the mussels and on symbiont activity. Variation in $\delta^{13}\text{C}$ of symbiont-specific FAs and other specific markers has been used to estimate the contribution of bacterial symbionts to host nutrition (Conway and McDowell-Capuzzo, 1991). In our study, all three mussel species had very similar $\delta^{13}\text{C}$ values for both symbiont- and host-derived lipids in both gill and foot tissue (Fig. II.4; Table II.2). This can be best explained by the direct transfer of carbon from the symbionts to host tissue, as proposed previously (Fisher and Childress, 1992; Fang et al., 1993; Riou et al., 2008). Riou et al. (2008) observed a rapid incorporation of ^{13}C labelled substrates in gill tissue hosting symbiotic bacteria, whereas muscle tissue was less responsive to recently digested food. The isotopic homogeneity in the two tissue types suggests that the mussel specimens were dependent on a symbiont-derived carbon source over a long period of time.

The different $\delta^{13}\text{C}$ values for FAs, sterols and MAGEs in mussels from the GoM and the PAR directly reflect the utilization of different carbon substrates (i.e. CH_4 vs. CO_2) by the respective methanotrophic or thiotrophic symbionts. Low average $\delta^{13}\text{C}$ values of FAs in the seep mussels *B. brooksi* and *B. childressi* (-51‰ and -46‰, respectively), MAGEs (-49‰ and -41‰, respectively), and sterols (-59‰ and -49‰, respectively) indicate the important role of methanotrophs for the carbon supply of these hosts (Table II.2; cf. Summons et al., 1994). Relative to *B. brooksi* and *B. childressi*, the FAs in *B. cf. thermophilus* are enriched in ^{13}C (-48‰ vs. -38‰, respectively). As discussed above, a high concentration of $\omega 7$ FAs (e.g. $\text{C}_{16:1\omega 7}$, $\text{C}_{18:1\omega 7}$ and $\text{C}_{20:1\omega 7}$) in *B. cf. thermophilus* suggests the presence of sulfur-oxidizing bacteria (McCaffrey et al., 1989; Pond et al., 1998; Guezennec and Fiala-Medioni, 1996; Riou et al., 2010). Likewise, their $\delta^{13}\text{C}$ values are in accord with an autotrophic lifestyle of the thiotrophic symbionts (cf. Ruby et al., 1987). This demonstrates the importance of carbon supplied by autotrophic carbon fixation of the thiotrophic symbiont.

Even though *B. brooksi* and *B. childressi* were collected from the same sampling site, we note that lipids in *B. childressi* were on average 5–10‰ more enriched in $\delta^{13}\text{C}$ (FAs, sterols,

MAGEs) relative to those in *B. brooksi* (Fig. 4; Table 2). Assuming that both mussels utilize the same local thermogenic CH₄ source, this is a significant difference. A possible explanation involves the co-occurring thiotrophic symbiont within *B. brooksi*. This second symbiont assimilates the already ¹³C-depleted carbon initially produced by the dominant methanotrophic symbiont, resulting in additional carbon isotopic fractionation (cf. Fisher, 1990). Alternatively, a greater dependence on water column derived heterotrophic substrates by *B. childressi* may have resulted in more ¹³C-enriched lipids. *Bathymodiolus* species have filter feeding capability and a functional digestive tract and are therefore capable of operating as heterotrophs, while symbionts provide only a fraction of the diet (Page et al., 1990; Colaço et al., 2006). A third possible explanation for the carbon isotopic difference between *B. brooksi* and *B. childressi* could be the presence of two types of methanotrophic bacteria utilizing carbon assimilation pathways with different isotopic fractionation (type I, ribulosemonophosphate pathway (RuMP) vs. type II, the serine pathway; Summons et al., 1994; Hanson and Hanson, 1996). Evidence for the presence of a second but undetected type II, methanotroph comes from the higher abundance of aminotetrol than aminotriol within *B. childressi* (Fig. II.6) as well as the presence of C_{18:1ω8} as discussed above (section II.4.5). However, as only one individual per mussel was analyzed, the observed discrepancies cannot be further resolved.

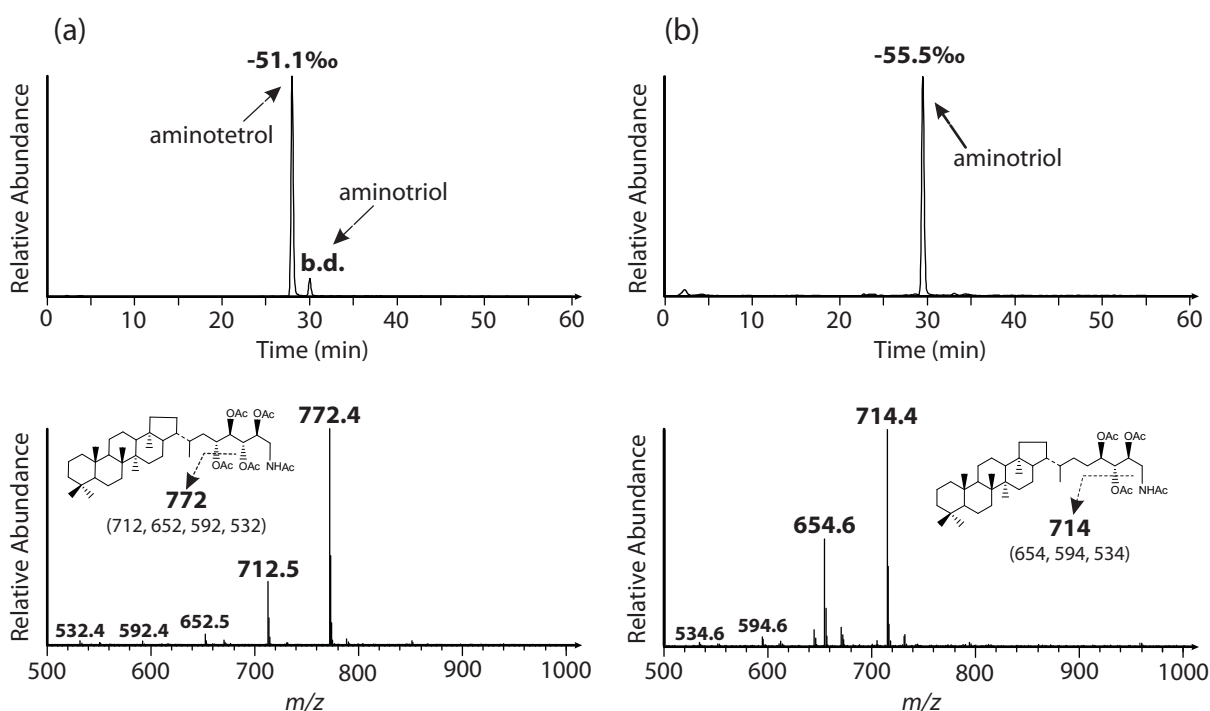


Fig. II.6. HPLC-APCI-MS base peak chromatogram (upper panel) and MS² (lower panel) indicating presence of amino BHPs (see Appendix II.1 for structures) in gill tissue of (a) *B. childressi* and (b) *B. brooksi*. *B. childressi* contains mainly *m/z* 772 = aminobacteriohopane-31,32,33,34-tetrol (aminotetrol) and *m/z* 714 = aminobacteriohopane-32,33,34-triol (aminotriol). *B. brooksi* only possesses *m/z* 714 = aminobacteriohopane-32,33,34-triol (aminotriol). Carbon isotopic composition of the BHPs was determined after side chain cleavage, giving the corresponding terminal hopanols.

II.5. Conclusions

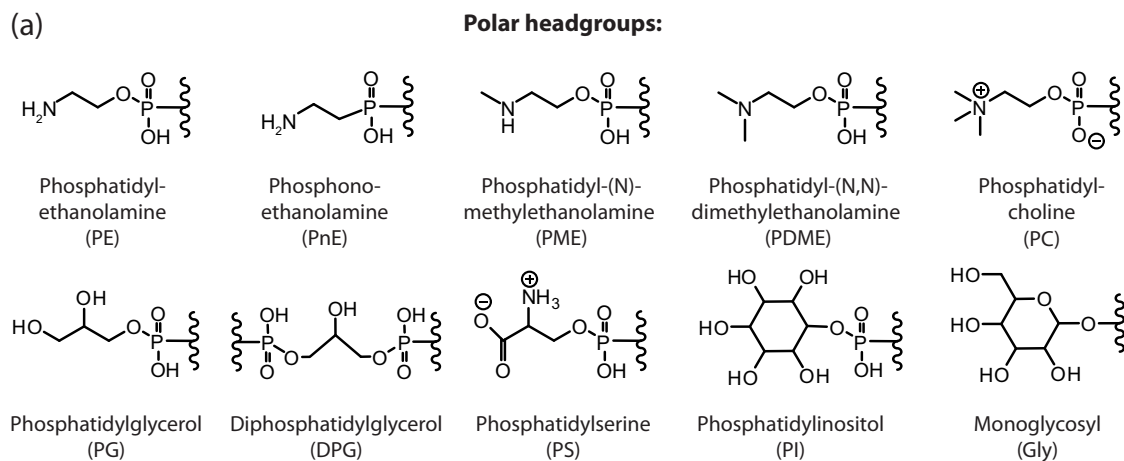
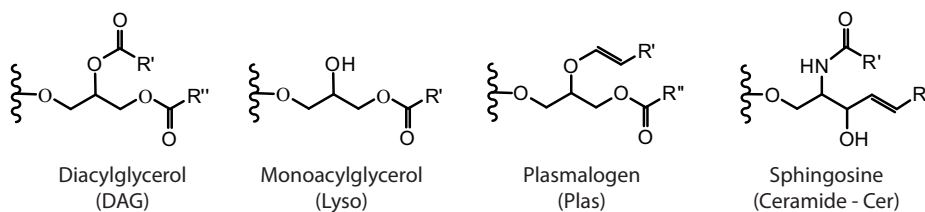
This molecular isotopic study provides a comprehensive, lipid based view of chemosynthetic symbiosis in three mussel species from hydrothermal vents and cold seeps. We detected PE, PG and DPG substituted with two C_{16:1} FA that were only present in the gill tissue of the mussels, suggesting that these compounds can be used for an estimate of the abundance of symbionts. Future studies should be conducted, preferably in tandem with cell-specific quantification protocols, to validate the robustness of IPL-based symbiont quantification.

The $\delta^{13}\text{C}$ values of individual FAs, 4-methyl sterols, MAGEs and BHPs were related to the presence of methanotrophic or thiotrophic symbionts in the host mussels. While the carbon isotopic values of both host and symbiont-specific lipids highlight the importance of chemosynthetic carbon supply for all three bivalves, we suggest that observed compound-specific isotopic variation between mussel species reflects distinct nutritional preferences and/or distinct carbon metabolism of the respective symbiont.

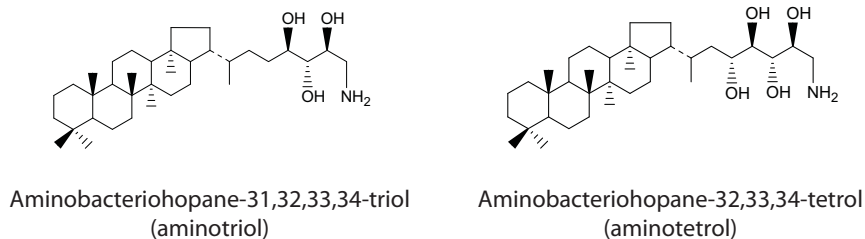
II.6. Acknowledgements

We thank the shipboard and scientific crew of the RV Sonne (SO 157) and the RV Atlantis II (Deep Sea Cruise 11 Leg I) equipped with the DSV Alvin for help with collecting the animal samples in the Gulf of Mexico and the Pacific-Antarctic Ridge. G. Wegener and M.Y. Yoshinaga are acknowledged for advice and critical reading of the manuscript. We would also like to thank two anonymous reviewers for constructive comments. The work was funded and supported by the Deutsche Forschungsgemeinschaft (through the Research Center/ Excellence Cluster MARUM - Center for Marine Environmental Sciences) and the GLOMAR graduate school (to M.Y.K).

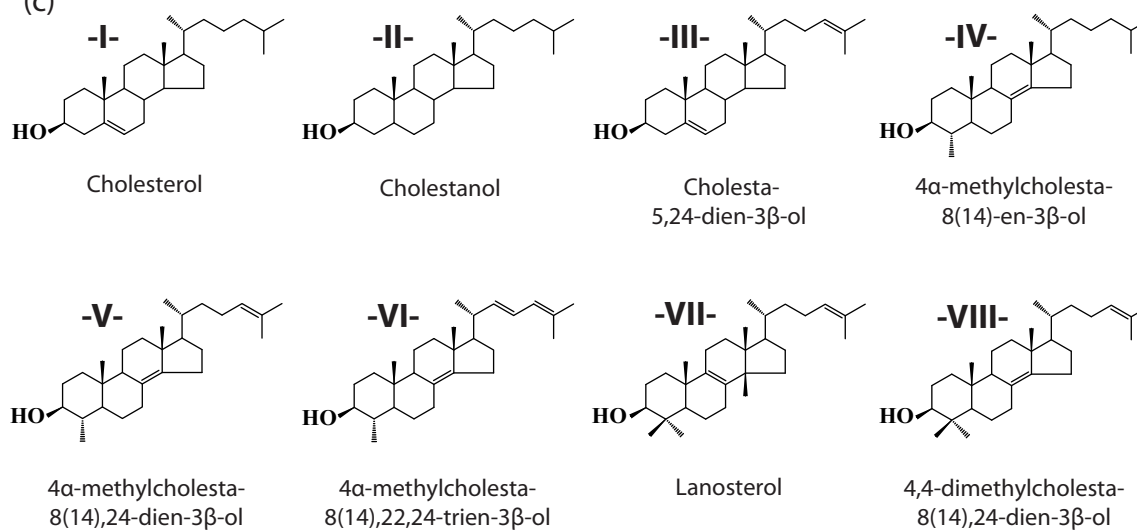
II.7. Supporting information

**Core lipid structures:**

(b)



(c)

**Fig. II.S1.** Structures of (a) head group and core lipids of identified IPLs, (b) BHPs and (c) sterols.

[CHAPTER III] - DUAL-SIP APPROACH**Dominance of autotrophic carbon fixation in hydrothermal sediments inhabited by methanotrophic communities**

Matthias Y. Kellermann^{a*}, Gunter Wegener^b, Marcus Elvert^a, Marcos Y. Yoshinaga^a, Yu-Shih Lin^a, Thomas Holler^b, Xavier Prieto Mollar^a, Kai-Uwe Hinrichs^a

For submission to:

Geochimica et Cosmochimica Acta

^a Organic Geochemistry Group, MARUM Center for Marine Environmental Sciences & Department of Geosciences, University of Bremen, Leobener Strasse, D-28359 Bremen, Germany

^b Max Planck Institute for Marine Microbiology, Celsiusstr. 1, D-28359 Bremen, Germany

* Corresponding author.
Tel.: +49 421 218 65742; Fax: + 49 421 218 65715
E-mail address: kellermann.matthias@gmail.com

Keywords:

methanotrophy | autotrophy | heterotrophy | AOM | Bacteria | HotSeep-1 | Archaea | ANME-1 | Guaymas Basin | lipid biomarkers | fatty acids | phytanes | biphytanes | stable isotope probing | D₂O | ¹³C_{DIC} | ¹³CH₄

III.1. Abstract

The gas-rich, hydrothermally influenced sediments of the Guaymas Basin are inhabited by thermophilic microorganisms, including anaerobic methanotrophic archaea (ANME-1) and sulfate reducing bacteria of the HotSeep-1 cluster. Natural enrichments of these groups have been used to study microbial carbon fixation in thermophilic seep communities by applying multiple carbon sources ($^{13}\text{C}_{\text{DIC}}$ and $^{13}\text{CH}_4$) and dual stable isotope probing (SIP) of ^{13}C and D ($^{13}\text{C}_{\text{DIC}}$ in combination with D_2O) in the presence and absence of methane. The dual SIP allowed to distinguish between hetero- and autotrophically produced lipids by determining the ratio ($R_{a/p}$) of the rate of $^{13}\text{C}_{\text{DIC}}$ assimilation (assim_{IC}) to the rate of D_2O ($\text{prod}_{\text{lipid}}$) incorporation in newly synthesized lipids. In the presence of unlabeled methane, $^{13}\text{C}_{\text{DIC}}$ assimilation was highest in archaeal phytanes and bacterial $\text{C}_{18:1\omega7}$, $\text{iC}_{16:1\omega6}$ and $\text{iC}_{18:1\omega6}$ fatty acids, indicating autotrophic carbon fixation. Incubations with $^{13}\text{CH}_4$ yielded significantly lower ^{13}C incorporation into lipids relative to $^{13}\text{C}_{\text{DIC}}$ incubations, suggesting that direct methane assimilation is not the major carbon source for the microbial community. In the absence of methane, archaeal lipid production stopped and bacterial lipid production dropped by 90%. Under these conditions, the remaining metabolically active microorganisms performed largely heterotrophic carbon fixation. This dual stable isotope probing study reveals novel information on the carbon flow in complex AOM microbial communities.

III.2. Introduction

Methane, an important greenhouse gas, is the most abundant hydrocarbon in anoxic marine sediments. Its upward flux to the sediment-water interface is strongly reduced by the anaerobic oxidation of methane (AOM) coupled to sulfate reduction ([Eq. II]; Reeburgh, 1976; 2007). AOM is presumably performed by a syntrophic association of anaerobic methanotrophic archaea (ANMEs; Hinrichs et al., 1999; Orphan et al., 2002) and sulfate-reducing bacteria (SRB, mainly relatives of *Desulfosarcina* or *Desulfobulbus*, Boetius et al., 2000; Knittel et al., 2005; Niemann et al., 2006; Schreiber et al., 2010). The free energy yield of the net reaction is one of the lowest known for catabolic reactions under environmental conditions (-20 to -40 kJ per mol methane oxidized, e.g., Hoehler et al., 1994; Knab et al., 2008; Alperin and Hoehler, 2009a). Consequently, doubling times range from 2 to 7 months and growth yields are extremely low (around 1% relative to oxidized methane; Nauhaus et al., 2007; Treude et al., 2007; Wegener et al., 2008; Holler et al., 2011).

The biomass of ANMEs and SRBs involved in AOM is usually strongly depleted in ^{13}C . For instance, at methane seep locations, the $\delta^{13}\text{C}$ values of specific bacterial fatty acids and archaeal ether lipids range from -60 to -100‰ and -70 to -130‰, respectively (e.g., Elvert et al., 1999; Hinrichs et al., 2000; Pancost et al., 2000; Elvert et al., 2005; Niemann and Elvert, 2008). Such values were interpreted as evidence for methane incorporation into biomass (e.g. Hinrichs et al., 1999; Bian et al., 2001; Orphan et al., 2002). One way to establish a direct linkage

between carbon sources and biomass formation is to perform stable isotope probing (SIP; Boschker et al., 1998), followed by analysis of biomolecules such as membrane lipids (lipid-SIP hereafter). Previous application of lipid-SIP to cold seep sediments and mats suggested that ANMEs incorporate both methane and inorganic carbon into their lipid biomass, whereas their partner bacteria use only inorganic carbon to produce their lipids and are thus complete autotrophs (Blumenberg et al., 2005; Wegener et al., 2008). This is in line with the modeling work of Alperin and Hoehler (2009b), whose isotope mass balance calculation suggests that the assimilation of methane-derived, already ^{13}C -depleted CO_2 can explain the highly ^{13}C -depleted lipids of anaerobic methanotrophic consortia detected in seep environments and laboratory experiments.

One central question that has not been targeted in these earlier SIP studies is whether and to which extent AOM communities assimilate organic carbon that can explain ^{13}C -depletion (e.g., acetate; Heuer et al., 2009). However, using organic substrates such as ^{13}C -labeled acetate potentially stimulate a change in community structure but also cross-feeding of ^{13}C from the primary consumer to the rest of the microbial community might introduce biases in those AOM-SIP experiments (Dumont and Murrell, 2005). Just recently, Wegener et al. (in revision) introduced a dual D_2O and $^{13}\text{C}_{\text{DIC}}$ labeling method which allows the simultaneous assessment of auto- and heterotrophic carbon fixation in natural environments. This approach uses the ratio of inorganic carbon assimilation (determined via $^{13}\text{C}_{\text{DIC}}$ uptake in lipids) to total lipid production (determined via assimilation of deuterated protons from water) without addition of organic carbon substrates.

In this study we investigated carbon fixation in hydrothermally influenced sediments from the Guaymas Basin, which expressed strong methane-dependent sulfate reduction (Teske et al., 2002; Biddle et al., 2011). Its microbial community was dominated by thermophilic ANME-1 and partner bacteria from the HotSeep-1 cluster (Holler et al., 2011). The dual D_2O and $^{13}\text{C}_{\text{DIC}}$ labeling, our main lipid-SIP strategy, was performed both in the presence and absence of methane. In parallel, incubations with only $^{13}\text{CH}_4$ were used to determine the contribution of methane carbon incorporation into lipid biomass. With these experiments, we aimed to evaluate:

- (I) The role of methane and inorganic carbon as carbon sources for microorganisms involved in thermophilic methanotrophy (37 and 50°C).
- (II) The patterns of microbial lipid production and their potential ecological significance.
- (III) The relative importance of heterotrophic vs. autotrophic carbon fixation.

III.3. Material and Methods

III.3.1. Sample collection and stable isotope labeling experiments

Sediments samples from a gas-rich, *Beggiatoa*-covered hydrothermal site in the Guaymas Basin (27°00.437 N, 111°24.548 W) were retrieved by push-coring during the R/V Atlantis cruise

AT 15–56 (Alvin dive 4570). Samples were immediately transferred into Duran bottles, diluted with artificial seawater medium (Widdel and Bak, 1992), and stored with a methane headspace (100 kPa). A sediment batch of the same material incubated at 50°C for 90 days exhibited 16S rRNA gene libraries enriched in ANME–1 and HotSeep–1 cluster, representing 82% and 66% of total archaeal and bacterial sequences, respectively (Holler et al., 2011). After 90 days of pre-incubation at 37°C, sediment enrichments were equally distributed into 256 mL culture vials (~4 g dry mass (g_{dm}) per vial), amended with labeled substrates at different combinations (D_2O , $^{13}C_{DIC}$, $^{13}CH_4$) and incubated at 37 or 50°C for 0, 10, 17 and 24 days ($t(0)$, $t(10)$, $t(17)$, $t(24)$) with either CH_4 or N_2 atmosphere (w/o- CH_4 incubations hereafter) at 200 kPa (detailed information in Table III.1). Samples amended with D_2O and $^{13}C_{DIC}$ had δD_{H_2O} values of ~ +200,000‰ vs. VSMOW (Vienna Standard Mean Ocean Water) and $\delta^{13}C_{DIC}$ values of ~ +8,400‰ vs. VPDB (Vienna PeeDee Belemnite). Incubations with only $^{13}CH_4$ yielded final $\delta^{13}CH_4$ values of ~ +16,000‰ vs. VPDB. Sediment samples were inactivated with $ZnCl_2$ (2% final concentration) prior to label addition. Samples were incubated at the indicated temperatures on rotary shakers at low speed (40 rpm) and the sulfide production was constantly monitored using a spectrophotometrical method firstly described by Cord–Ruwisch (1985). Sulfide production rates are expressed in micromol per day per gram dry mass sediment ($\mu mol d^{-1} g_{dm}^{-1}$). Finally, pore water samples were taken and the sediment immediately frozen (–20°C) until lipid extraction.

III.3.2. Hydrogen and carbon isotopic composition of the incubation medium

Deuterium isotope values of the medium were determined by cavity ring–down laser spectroscopy (Liquid Water Isotope Analyzer DLT–100, Los Gatos Research, Mountain View, CA, USA) of pre–filtered (0.2 μm nylon filters; Rotilabo®, Karlsruhe, Germany) samples after dilution with pure water (1:100). The stable carbon isotope composition of DIC and CH_4 were measured from the headspace of acidified medium by gas chromatography coupled to an isotope ratio mass spectrometer. In brief, pre–filtered water samples (0.2 μm nylon filters; Rotilabo®, Karlsruhe, Germany) were transferred in a headspace–free 6 mL Exetainer® vials (Labco, Buckinghamshire, UK), 3 mL of that medium replaced with He and the remaining solution acidified with 100 μL of H_3PO_4 (4N). Subsequently, target compounds were transferred into the gas phase and the isotopic composition of the DIC measured using a gas chromatograph coupled to a continuous flow isotope ratio mass spectrometer (VG Optima). Methane carbon isotopic composition was analyzed by gas chromatography (Trace GC ultra, ThermoFinnigan) equipped with a Supelco Carboxen™ 1006 Plot fused–silica capillary column (30 m, 0.32 mm ID) coupled to a Combustion III interface (ThermoFinnigan) and a DeltaPlus XP isotope ratio mass spectrometer (ThermoFinnigan).

III.3.3. Lipid extraction and sample treatment

Lipids were extracted (~4 g_{dm}) using a modified Bligh and Dyer protocol (Sturt et al., 2004) with a mixture of DCM:methanol:aquatic buffer (1:2:0.8), twice buffered at pH 7 (phosphate

buffer) and twice buffered at pH 2 (trichloroacetic acid). Finally, all organic phases were combined and washed by adding DCM and water, respectively.

Bacterial membrane-derived fatty acids (FAs) were released from the intact polar lipids (IPLs) by saponifying a total lipid extract (TLE) aliquot with methanolic KOH solution (6%). After removal of neutral lipids with hexane, the reaction mixture was acidified to pH 1 and FAs were collected by hexane extraction. For gas chromatography, FAs were converted to methyl esters (FAMES) using 14% BF_3 in methanol. To determine possible double bond positions of specific methyl-branched monoenoic FAs, FAMES aliquots were reacted with pyrrolidine in the presence of glacial acetic acid to yield pyrrolidides (Andersson and Holman, 1974). Afterwards, the position of methyl branches in specific lipids was determined by identifying the absence or lowest abundance of characteristic mass fragments. Double bond positions were indicated by spotting a mass fragment interval of 12 instead of 14 atomic mass units, respectively (Fig. III.S2).

Archaeal isoprenoidal moieties were released from ether lipid precursors in the TLE by boron tribromide treatment (Summons et al., 1998) and subsequent reduction of resulting bromides using super-hydride solution (1.0M lithium triethylborohydrate; Aldrich, St. Louis, MO, USA). Ether cleavage products were purified by passing through a short silica gel column (0.2 g of pre-activated silica, 0.06–0.2 mm) eluted with hexane. FAs and isoprenoidal hydrocarbons were quantified by gas chromatography coupled to a flame ionization detector (GC-FID; ThermoFinnigan) using squalane as injection standard.

III.3.4. Preparative HPLC – purification of intact GDGT for isotopic analysis

Archaeal isoprenoidal lipids are known to have long persistence time in natural samples (Lipp and Hinrichs, 2009; Liu et al., 2011), leading to an isotope dilution effect to lipid-SIP work. To circumvent this problem, we used preparative high performance liquid chromatography (HPLC) to purify intact polar glycerol biphytanyl glycerol tetraethers (GDGTs) for subsequent stable isotopic analysis. In brief, we applied IPL purification using orthogonal preparative high performance liquid chromatography (HPLC) involving both normal-phase (LiChrosphere Diol-100 column; 250x10 mm, 5 μm particle size; Alltech, Deerfield, IL, USA)– and reverse-phase (Eclipse XDB- C_{18} column; 250 x 9.4 mm, 5 μm particle size; Agilent, Böblingen, Germany) columns. Subsequently, the intact polar tetraether fractions were subjected to ether cleavage and subsequent reduction (see section III.3.3) to obtain the intact derived archaeal biphytanes (cf. Kellermann et al., in preparation).

III.3.5. GC-FID, -MS, -irMS – instrumentation

Compound quantification was performed on a GC-FID equipped with an Rxi-5ms capillary column (Restek GmbH, Bad Homburg, Germany; L = 30 m; ID = 0.25 mm; 0.25 μm film thickness) with He as carrier gas and a flow rate of 1 mL min^{-1} . All samples were injected at 300°C in splitless mode. The GC was programmed from 60°C (hold for 1 min), followed by heating at 10°C min^{-1} to 150 °C, then at 4°C min^{-1} to 320°C and hold for 27.5 min. All GC analyses described below were

performed using the same method and conditions as for the GC–FID. Pyrrolidine derivatives were analyzed on a GC (Agilent 6890) coupled to mass spectrometer (MS; Agilent 5973 MSD). Carbon and hydrogen isotopic compositions of FAs and isoprenoids were determined at least in duplicates using a GC–isotope ratio–MS (Trace GC Ultra coupled to a GC–IsoLink/ConFlow IV interface and a Delta V Plus isotope ratio mass spectrometer, all from Thermo Scientific GmbH, Bremen, Germany). Carbon compounds were oxidized in a combustion reactor at 940°C, and molecular hydrogen was produced in a pyrolysis reactor at 1420°C. The analytical error was <0.5‰ and <10‰ for non-labeled $\delta^{13}\text{C}$ and δD values, respectively. $\delta^{13}\text{C}$ and δD values were corrected for additional carbon introduced during derivatization.

III.3.6. Calculations of total lipid production rate ($prod_{lipid}$), assimilation rate of inorganic carbon ($assim_{IC}$), and the $assim_{IC}/prod_{lipid}$ ratio ($R_{a/p}$)

The stable hydrogen and carbon isotope values are expressed in the δ -notation in per mill (‰) as deviation of the isotope ratio to a reference standard of known isotopic compositions ([Eq. IV] and [Eq. III]). Stable isotope probing experiments with cultures of sulfate-reducing bacteria showed that the majority of microbial lipid hydrogen derives from water protons, independent of whether the microbe grows hetero- or autotrophically (Wegener et al., in revision). Hence incorporation of D from amended D_2O serves as a sensitive assay to determine the rate of total lipid production ($prod_{lipid}$). The assimilation rate of ^{13}C from labeled inorganic carbon into lipids ($assim_{IC}$) is highest during autotrophic growth.

$Prod_{lipid}$ and $assim_{IC}$ are calculated by multiplying lipid concentration ($conc_{lipid}$) with the increase of the fraction of either D (ΔF_{Lipid}^D) or ^{13}C (ΔF_{Lipid}^{13C}) relative to the fraction of non-labeled samples, divided by the fraction of D (F_{Medium}^D) and ^{13}C (F_{Medium}^{13C}) in the incubated medium ([Eq. V] and [Eq. VI]).

$$prod_{lipid} = conc_{lipid} \times \frac{\Delta F_{lipid}^D}{F_{medium}^D \times t} \quad \text{[Eq. V]}$$

$$assim_{IC} = conc_{lipid} \times \frac{\Delta F_{lipid}^{13C}}{F_{medium}^{13C} \times t} \quad \text{[Eq. VI]}$$

The fractions of F^D and F^{13C} in individual lipids and incubation medium are calculated from the isotope ratios $F^D = R^{D/H}/(R^{D/H}+1)$; $F^{13C} = R^{13C/12C}/(R^{13C/12C} + 1)$, where R derives from the delta notations ([Eq. III] and [Eq. IV]). Both, $prod_{lipid}$ and $assim_{IC}$ are expressed in $\mu\text{g lipid g}_{dm}^{-1} \text{yr}^{-1}$.

Based on the $assim_{IC}/prod_{lipid}$ ratio ($R_{a/p}$), we can distinguish whether a lipid extracted from a mixed community is largely derived from autotrophic or heterotrophic organisms. $R_{a/p}$ values of 0.3 indicate fully heterotrophic and $R_{a/p}$ values close to 1 completely autotrophic

lipid production. $R_{a/p}$ values in between 0.3 and 1 represent a mixed signal (Wegener et al., in revision).

Table III.1. Duration of the incubation, substrate combinations (D_{H_2O} and $^{13}C_{DIC}$; $^{13}CH_4$), labeling strength ($\delta^{13}C_{DIC}$ and $\delta^{13}C_{CH_4}$ of the headspace; δD_{H_2O} of the aqueous media), and the sulfide production rate of all analyzed samples incubated at 37 and 50°C. DEAD = $ZnCl_2$ (final conc. 2%); CO_2 – 50kPa; CH_4 – 200kPa; N_2 – 200kPa.

	time of incubation	substrate combination	$\delta^{13}C_{DIC}$ [‰]	δD_{H_2O} [‰]	sulfide production rate ($\mu mol d^{-1} g_{dm}^{-1}$)
control	37°C; t(0); no label	$CO_2; CH_4$	n.a.	n.a.	n.a.
	37°C; t(0); + CH_4	$CO_2; CH_4; D_2O; Na-H^{13}CO_3$	n.a.	244,000	n.a.
	37°C; t(0); + $^{13}CH_4$	$CO_2; ^{13}CH_4$ (~16,000‰)	n.a.	n.a.	n.a.
	37°C; t(24); dead	$CO_2; CH_4; D_2O; Na-H^{13}CO_3; ZnCl_2$	8,500	199,000	0.4
	50°C; t(17); dead	$CO_2; CH_4; D_2O; Na-H^{13}CO_3; ZnCl_2$	8,700	199,000	1.1
+ CH_4 incubation	37°C; t(10); + CH_4		8,400	196,000	} 6.0±0.4
	37°C; t(17); + CH_4	$CO_2; CH_4; D_2O; Na-H^{13}CO_3$	8,200	206,000	
	37°C; t(24); + CH_4		8,000	206,000	
	50°C; t(17); + CH_4	$CO_2; CH_4; D_2O; Na-H^{13}CO_3$	7,900	204,000	9.0
	37°C; t(24); + $^{13}CH_4$	$CO_2; ^{13}CH_4$	950	n.a.	4.0
w/o- CH_4 incubation	37°C; t(24); w/o- CH_4	$CO_2; N_2; D_2O; Na-H^{13}CO_3$	8,700	210,000	0.7
	50°C; t(17); w/o- CH_4	$CO_2; N_2; D_2O; Na-H^{13}CO_3$	8,600	207,000	1.4

n.a., not analyzed; w/o, without

III.4. Results and discussion

III.4.1. Activity of the thermophilic microbial community

Sediment slurries were incubated at two temperatures, 37°C and 50°C, with and without methane. To estimate microbial activities sulfide concentrations were tracked (see [Eq. II]). The incubations with methane showed the highest increase of sulfide, corresponding to sulfate reduction rates of $6.0 \pm 0.4 \mu mol d^{-1} g_{dm}^{-1}$ at 37°C and of $9.0 \mu mol d^{-1} g_{dm}^{-1}$ at 50°C. Without methane, sulfide production was reduced to 0.7 and $1.4 \mu mol d^{-1} g_{dm}^{-1}$ at 37°C and 50°C, respectively. In AOM, methane oxidation is coupled to sulfide production in a 1:1 stoichiometry ([Eq. II]; Nauhaus et al., 2002; Holler et al., 2009; 2011). Methane consumption was not directly measured but was calculated from the isotopic change of the DIC pool (30 mM). During 24 day incubation at 37°C with ^{13}C -labeled methane ($\delta^{13}C_{CH_4}$ at $T_0 \sim +16,000$ ‰), $\delta^{13}C_{DIC}$ increased by +950‰ (Table III.1). Via mass balance calculations, we obtained methane oxidation rates of $3.4 \mu mol d^{-1} g_{dm}^{-1}$ [Eq. VII].

$$CH_4 \text{ oxidation-rate} = \left(\frac{\Delta F_{DIC}^{13C}}{\text{Excess} \Delta F_{CH_4}^{13C}} \times \text{conc}_{DIC} \right) / \text{time}$$

This is roughly 80% of the sulfate reduction rate measured from the same batch of incubation ($4.0 \mu\text{mol d}^{-1} \text{g}_{\text{dm}}^{-1}$; Table III.1). The slightly higher sulfate reduction rates can be attributed to organic matter oxidation (see discussion below). Our results on thermophilic AOM in Guaymas sediments are similar to other studies showing a tight coupling between sulfate reduction and methane oxidation (Biddle et al., 2011; Holler et al., 2011).

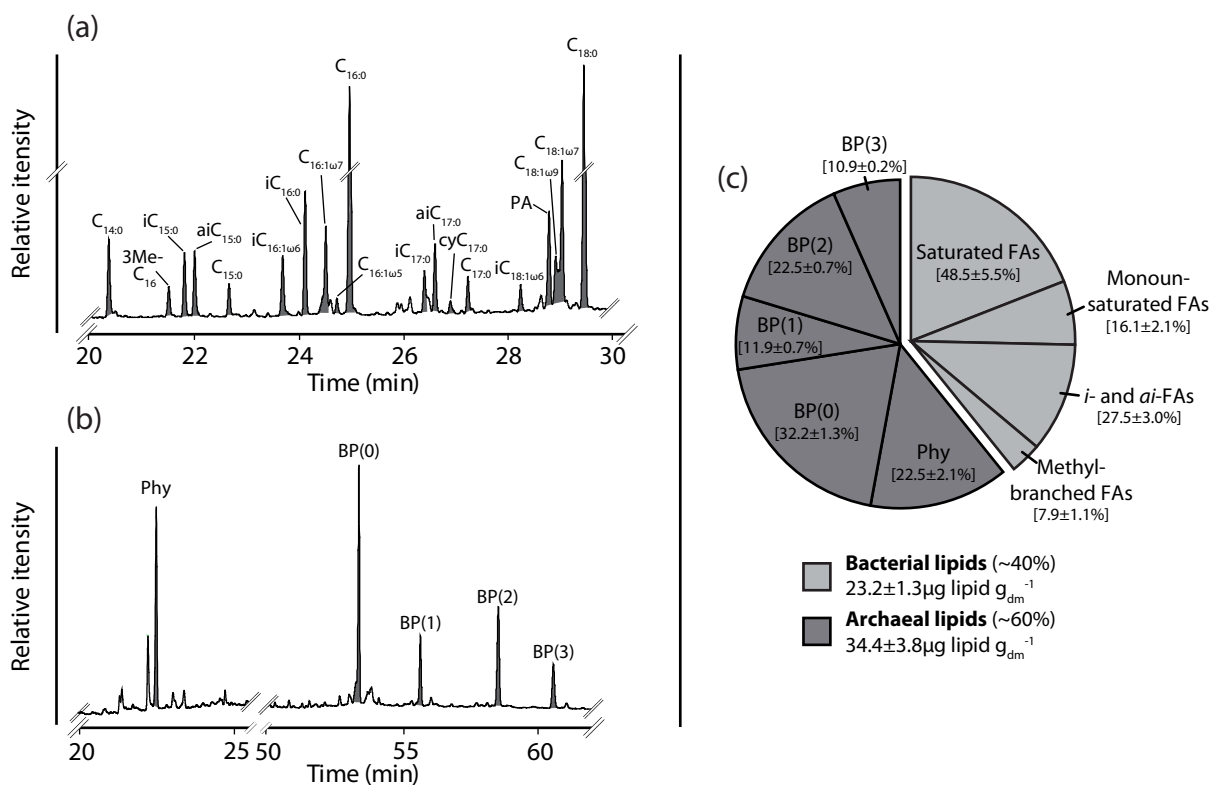


Fig. III.1. Gas chromatogram of (a) fatty acids after saponification and (b) archaeal phytane and biphitynes (0–3) after ether cleavage of the TLE. (c) Pie chart shows the relative abundance of bacterial and archaeal lipids, averaged over all experiments. Absolute concentrations (calculated relative to the injection standard squalane) are normalized to gram extracted dry sediment.

III.4.2. Microbial lipid concentration and natural isotopic compositions

After the incubation, a total lipid extract (TLE) was prepared and aliquots of the TLE were hydrolyzed to yield the total bacterial FAs and archaeal isoprenoids. There was no significant change in concentrations and relative abundances of the detected lipids over the course of incubation (e.g. concentrations of archaeal isoprenoids were $34.4 \pm 3.8 \mu\text{g g}_{\text{dm}}^{-1}$ and bacterial FAs were $23.2 \pm 1.3 \mu\text{g lipid g}_{\text{dm}}^{-1}$; Fig. III.1c), an observation that is consistent with the low growth rates reported for the microbial community (doubling time of 77 days at 37°C; Holler et al., 2011). The major archaeal lipid products from ether cleavage were acyclic biphityane

(BP(0); $32.2 \pm 1.3\%$), phytane ($22.5 \pm 2.1\%$) and bicyclic biphytane (BP(2); $22.5 \pm 0.7\%$), whereas monocyclic biphytane (BP(1); $11.9 \pm 0.7\%$) and tricyclic biphytane (BP(3); $10.9 \pm 0.2\%$) were minor components (Fig. III.1c). High amounts of biphytanes are derived from glycerol–dibiphytanyl–glycerol–tetraethers (GDGTs) which have been routinely found in methane rich sediments and cold seeps dominated by ANME–1 (Blumenberg et al., 2004; Niemann et al., 2005; Niemann and Elvert, 2008). Phytanes, derived from the cleavage of archaeols, are considered to be produced by all ANMEs (e.g. Blumenberg et al., 2004; Elvert et al., 2005; Niemann and Elvert, 2008). However, since archaeal 16S rRNA gene libraries of this enrichment are dominated by sequences of ANME–1 (Holler et al., 2011), we suggest that this specific group is the main source organism for both, phytanes and biphytanes.

The FA fraction is comprised of saturated even numbered ($C_{16:0} > C_{18:0} > C_{14:0}$; $48.5 \pm 5.5\%$), saturated and unsaturated *i*– and *ai*–FAs ($iC_{16:0} > aiC_{17:0} > iC_{15:0} > aiC_{15:0} > iC_{16:1\omega6} > iC_{17:0} > iC_{18:1\omega6}$; $27.5 \pm 3.0\%$), monounsaturated C_{16} and C_{18} FAs ($C_{18:1\omega7c} > C_{16:1\omega7c} > C_{18:1\omega9c} > C_{16:1\omega5c}$; $16.1 \pm 2.1\%$), and isoprenoidal FAs (phytanoic acid (PA) $>$ 4,8,12–trimethyltridecanoic acid (3Me– C_{16} ; $7.9 \pm 1.1\%$; Fig. III.1, Table III.S1). This FA pattern differs significantly from previously described lipid patterns of cold seep sediments, in which $aiC_{15:0}$, $C_{16:1\omega5c}$, $C_{16:1\omega7c}$, $C_{16:0}$, $cyC_{17:0\omega5,6}$, $C_{18:1\omega7c}$ are the major FAs (Hinrichs et al., 2000; Elvert et al., 2003; Blumenberg et al., 2004; Niemann and Elvert, 2008). The AOM communities in these cold seep systems were usually dominated by partner bacteria of the SEEP–SRB–1a group (Schreiber et al., 2010). The methyl branched and unsaturated FAs $iC_{16:1\omega6}$ and $iC_{18:1\omega6}$ which we found in the thermophilic enrichments (Fig. III. S2), have to our knowledge never been described at other seeps, but have been detected in some sulfate–reducing bacteria (mostly in *Desulfovibrios* species; Kohring et al., 1994; Suzuki et al., 2009). Phylogenetic analysis of the thermophilic enrichment indicated that the dominant sulfate reducers belong to the HotSeep–1 cluster (Holler et al., 2011), suggesting that the production of these lipids is widespread within the *Deltaproteobacteria*.

Both, archaeal isoprenoids and bacterial FAs had relatively low $\delta^{13}C$ values at the beginning of the experiment; phytanes and biphytanes ranged from -18 to -47‰ and bacterial FAs from -21 to -50‰ (Table III.S1). δD values ranged from -147 to -286‰ for archaeal isoprenoids and from -86 to -232‰ for FAs (Table III.S1), which is in accordance with the results of Li et al. (2009), who demonstrated a remarkably large range in hydrogen isotopic compositions in anoxic marine sediments.

III.4.3. Assimilation of D_2O , $^{13}C_{DIC}$ and $^{13}CH_4$ into microbial lipids

Although lipid concentrations were relatively constant during incubation, the shift in lipid isotopic compositions toward more positive values indicated lipid production via incorporation of D and ^{13}C label added to the incubation medium (Table III.2; Fig. III.2). For better clarity, we define that an isotopic shift ($\Delta\delta$) is the change in isotopic values of individual lipids in incubated samples relative to the time–zero values, and by weight–averaging of $\Delta\delta$ values of individual lipids based on their relative concentrations we obtained a mean isotopic shift (denoted as $\emptyset\Delta\delta$)

for a given lipid pool (i.e. archaeal vs. bacterial or phytanes vs. biphytanes vs. FAs). The change in isotopic compositions of microbial lipids was strongest for incubations using D_2O and $^{13}C_{DIC}$ in presence of methane, and the enrichment of heavy isotopes in lipids increased with time. The extent of label uptake differed between individual compounds, with a highest change in $\Delta\delta D$ and $\Delta\delta^{13}C$ found for archaeol-derived phytane and bacterial lipids such as $iC_{18:1\omega 6}$, $iC_{16:1\omega 6}$ and $C_{18:1\omega 7}$ FAs (Table III.2). For instance, in the 24-day long incubation at $37^\circ C$ under a methane atmosphere, changes in phytane isotopes ($\Delta\delta D = \sim +12,000\text{‰}$ and $\Delta\delta^{13}C = \sim +530\text{‰}$) were remarkably higher than the weighted average isotopic shift of biphytanes ($\emptyset\Delta\delta D = \sim +300\text{‰}$ and $\emptyset\Delta\delta^{13}C = \sim +10\text{‰}$) (Table III.2; Fig. III.2). The D enrichment of bacterial FAs in the range from C_{14} – C_{18} ($\emptyset\Delta\delta D = \sim +12,000\text{‰}$) was comparable to that of phytane, but ^{13}C enrichment was significantly lower ($\emptyset\Delta\delta^{13}C = \sim +380\text{‰}$; (Table III.2; Fig. III.2). In the dead-control, no significant enrichment of D and ^{13}C in lipids was detected (Table III.S1).

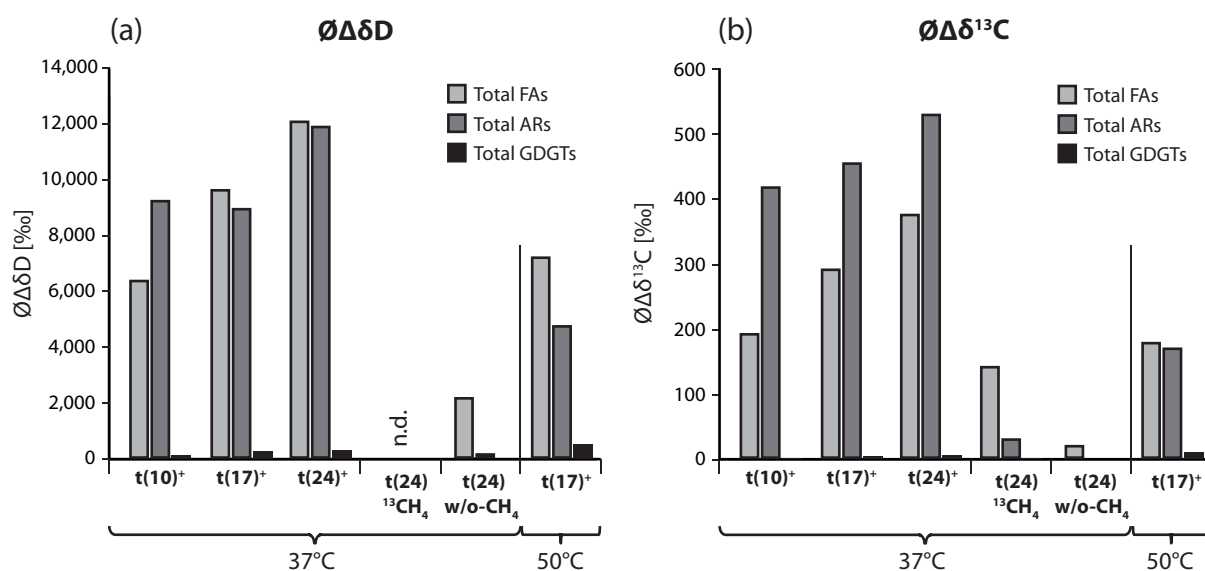


Fig. III.2. Weighted-average isotopic shifts of (a) hydrogen and (b) carbon expressed as $\emptyset\Delta\delta$ of total fatty acids, archaeols and GDGTs in the incubations. (+) indicates incubations with unlabeled methane.

In the 24-day long incubations without CH_4 at $37^\circ C$, archaeal lipids showed only traces of D label assimilation and no uptake of ^{13}C ($\emptyset\Delta\delta D = \sim +50\text{‰}$; $\emptyset\Delta\delta^{13}C = \pm 0\text{‰}$); likewise the uptake into bacterial lipids was strongly reduced compared to the incubations with methane ($\emptyset\Delta\delta D = \sim +2,200\text{‰}$ and $\emptyset\Delta\delta^{13}C = \sim +20\text{‰}$; Table III.2; Fig. III.2). This observation confirms the central role of methane as an energy substrate in the examined thermophilic AOM system, analogous to findings in cold seep sediments (e.g. Nauhaus et al., 2007; Wegener et al., 2008).

Incubation with $^{13}CH_4$ ($37^\circ C$; 24 days) caused a relatively low increase of ^{13}C in lipids. The $\emptyset\Delta\delta^{13}C$ values are around 30‰ for both bacterial and archaeal lipids (Table III.2; Fig. III.2), corresponding to about 1/12 and 1/4 of the $\emptyset\Delta\delta^{13}C$ values for the respective lipid pools in the parallel experiment with addition of $^{13}C_{DIC}$ and unlabeled methane. We address the slight positive shift in $\delta^{13}C$ values of lipids in the course of this experiment not to direct biosynthetic utilization of $^{13}CH_4$ but rather to indirect uptake via assimilation of the increasingly ^{13}C -

enriched DIC pool resulting from continuous methane oxidation (after 24 days $\delta^{13}\text{C}_{\text{DIC}}$ was approximately 950‰; Table III.1). This implies that not only SRBs, but also ANME-1 archaea assimilate predominantly inorganic carbon. Our findings are in agreement with the result from Treude and coworkers (2007), who detected a predominance of $^{14}\text{CO}_2$ over $^{14}\text{CH}_4$ incorporation within a microbial mat known to be dominated by ANME-1/SRB consortia. However, this result differs from a previous labeling study with cold seep sediments by Wegener et al. (2008), in which methane contribution of up to 50% were found in the archaeal lipid carbon pool of mixed ANME-1/ANME-2 and ANME-2 dominated communities.

Table III.2. Isotopic shifts ($\Delta\delta$) of individual lipids relative to time-zero values and the weighted average isotopic shifts ($\emptyset\Delta\delta$) of specific lipid pools.

name microbial lipids	t(10) + CH ₄		t(17) + CH ₄		t(24) + CH ₄		t(24) + ¹³ CH ₄		t(24) w/o-CH ₄		t(17) + CH ₄ (50°C)	
	$\Delta\delta^{13}\text{C}$ [‰]	$\Delta\delta\text{D}$ [‰]	$\Delta\delta^{13}\text{C}$ [‰]	$\Delta\delta\text{D}$ [‰]	$\Delta\delta^{13}\text{C}$ [‰]	$\Delta\delta\text{D}$ [‰]	$\Delta\delta^{13}\text{C}$ [‰]	$\Delta\delta\text{D}$ [‰]	$\Delta\delta^{13}\text{C}$ [‰]	$\Delta\delta\text{D}$ [‰]	$\Delta\delta^{13}\text{C}$ [‰]	$\Delta\delta\text{D}$ [‰]
$\emptyset\Delta\delta$ bacterial lipids	200	6,400	290	9,600	380	12,000	32	n.a.	22	2,200	180	7,200
C _{14:0}	64	1,800	100	3,200	135	4,000	26		7	1,200	13	1,200
3Me-C ₁₅	1	400	0	660	0	580	0		0	480	0	710
i-C _{15:0}	41	3,800	57	6,500	86	7,600	13		33	4,500	71	6,900
ai-C _{15:0}	200	8,600	270	12,000	370	16,000	74		110	7,900	260	9,800
C _{15:0}	50	2,000	64	2,700	96	3,800	9		21	1,700	21	2,800
i-C _{16:1ω6}	830	20,000	1,200	32,000	1,600	40,000	120		0.31	630	1,100	31,000
i-C _{16:0}	340	12,000	500	19,000	700	25,000	73		18	4,700	700	28,000
C _{16:1ω7}	170	5,800	260	7,500	350	10,000	27		0	1,500	91	6,400
C _{16:1ω5}	160	3,100	200	4,500	240	6,100	19		46	1,900	40	6,500
C _{16:0}	63	3,300	100	4,100	150	6,600	12		8	1,500	38	2,900
i-C _{17:0}	44	3,100	75	5,400	100	5,600	6		12	2,500	78	7,700
ai-C _{17:0}	160	5,500	200	8,200	280	10,000	30		16	2,500	290	11,000
C _{17:0}	38	1,500	52	1,800	113	2,100	1		9	830	33	2,200
i-C _{18:1ω6}	1,300	31,000	1,600	56,000	2,300	49,000	180		0.41	700	1,800	41,000
PA	93	6,900	200	11,000	200	11,000	8		55	2,600	64	2,300
C _{18:1ω9}	370	14,000	680	24,000	690	23,000	48		170	7,000	180	8,300
C _{18:1ω7}	830	20,000	1,300	28,000	1,500	32,000	100		20	2,000	300	8,900
C _{18:0}	31	1,200	52	2,700	72	5,200	7		3	560	3	1,200
$\emptyset\Delta\delta$ archaeal lipids	95	2,100	110	2,200	120	2,900	34	n.a.	0.41	46	48	1,500
Phytane	420	9,200	450	8,900	530	12,000	140		2	170	170	4,700
Bp(0)	4	180	13	430	12	420	3		0	20	12	510
Bp(1)	0	130	5	400	15	510	6		0	10	24	850
Bp(2)	0	27	0	93	2	190	2		0	0	13	550
Bp(3)	0	6	0	5	0	16	0		0	0	0	150

III.4.4. Rates of total lipid production ($\text{prod}_{\text{lipid}}$) and inorganic carbon assimilation (assim_{IC}) and implications for microbial carbon fixation

By conversion of the bacterial and archaeal lipid incorporation of D₂O and $^{13}\text{C}_{\text{DIC}}$ into total lipid production rates ($\text{prod}_{\text{lipid}}$) and assimilation rates of inorganic carbon (assim_{IC}), respectively, we are able to evaluate the relative importance of heterotrophic ($R_{\text{a/p}} \sim 0.3$) and autotrophic ($R_{\text{a/p}} \sim 1$) microbial carbon metabolism (Wegener et al., in revision).

Table III.3. $\text{assim}_{\text{IC}}/\text{prod}_{\text{lipid}}$ ratios ($R_{\text{a/p}}$) of individual fatty acids and isoprenoidal hydrocarbons.

name microbial lipids	t(10) + CH ₄			t(17) + CH ₄			t(24) + CH ₄			t(24) w/o-CH ₄			t(17) + CH ₄ (50°C)		
	assim_{IC} (ng lipid g _{dm} ⁻¹ yr ⁻¹)	$\text{prod}_{\text{lipid}}$	$R_{\text{a/p}}$	assim_{IC} (ng lipid g _{dm} ⁻¹ yr ⁻¹)	$\text{prod}_{\text{lipid}}$	$R_{\text{a/p}}$	assim_{IC} (ng lipid g _{dm} ⁻¹ yr ⁻¹)	$\text{prod}_{\text{lipid}}$	$R_{\text{a/p}}$	assim_{IC} (ng lipid g _{dm} ⁻¹ yr ⁻¹)	$\text{prod}_{\text{lipid}}$	$R_{\text{a/p}}$	assim_{IC} (ng lipid g _{dm} ⁻¹ yr ⁻¹)	$\text{prod}_{\text{lipid}}$	$R_{\text{a/p}}$
Σ - bacterial lipids	18,700	27,098	0.7	16,592	24,100	0.7	15,100	21,400	0.7	873	3,830	0.2	10,200	18,000	0.6
C _{14:0}	291	358	0.8	274	372	0.7	256	333	0.8	12	102	0.1	34	140	0.2
3Me-C ₁₅	1	31	b.d.	0	30	b.d.	0	18	b.d.	0	15	b.d.	0	32	b.d.
i-C _{15:0}	149	610	0.2	123	616	0.2	131	510	0.3	50	303	0.2	153	651	0.2
ai-C _{15:0}	709	1,340	0.5	564	1,070	0.5	543	1,040	0.5	165	518	0.3	542	908	0.6
C _{15:0}	96	171	0.6	73	133	0.5	77	135	0.6	17	60	0.3	24	138	0.2
i-C _{16:1ω6}	2,670	2,850	0.9	2,180	2,650	0.8	2,070	2,380	0.9	0	37	0.0	2,080	2,550	0.8
i-C _{16:0}	2,260	3,460	0.7	1,960	3,180	0.6	1,930	3,000	0.6	51	570	0.1	2,730	4,810	0.6
C _{16:1ω7}	757	110	0.7	657	847	0.8	633	837	0.8	0	116	0.0	236	724	0.3
C _{16:1ω5}	127	110	1.1	94	95	1.0	82	91	0.9	16	29	0.5	19	138	0.1
C _{16:0}	1,380	3,190	0.4	1,490	2,310	0.6	1,390	2,640	0.5	74	583	0.1	488	1,650	0.3
i-C _{17:0}	153	470	0.3	153	482	0.3	144	356	0.4	17	155	0.1	159	684	0.2
ai-C _{17:0}	592	915	0.6	461	798	0.6	437	685	0.6	24	171	0.1	630	1,050	0.6
C _{17:0}	75	129	0.6	61	90	0.7	93	77	1.2	7	30	0.2	39	112	0.3
i-C _{18:1ω6}	1,640	1,710	1.0	1,150	1,800	0.6	1,200	1,120	1.1	0	16	b.d.	1,300	1,320	1.0
PA	529	1,730	0.3	668	1,570	0.4	470	1,160	0.4	130	273	0.5	213	331	0.6
C _{18:1ω9}	1,190	2,010	0.6	1,290	1,980	0.7	921	1,340	0.7	232	413	0.6	349	695	0.5
C _{18:1ω7}	5,500	5,870	0.9	4,820	4,740	1.0	4,160	3,890	1.1	54	237	0.2	1,180	1,530	0.8
C _{18:0}	589	1,000	0.6	582	1,310	0.4	564	1,800	0.3	22	196	0.1	37	565	0.1
Σ - archaeal lipids	13,700	13,600	1.0	9,020	8,220	1.1	7,470	7,650	1.0	26	121	0.2	4,060	5,460	0.7
Phy	13,500	13,100	1.0	8,600	7,440	1.2	7,100	7,010	1.0	22	101	0.2	3,260	3,950	0.8
BP(0)	185	364	0.5	348	521	0.7	231	361	0.6	0	17	b.d.	318	609	0.5
BP(1)	0	96	b.d.	53	179	0.3	107	161	0.7	0	3	b.d.	239	377	0.6
BP(2)	0	38	b.d.	0	78	b.d.	27	114	0.2	0	0	b.d.	245	462	0.5
BP(3)	0	4	b.d.	0	2	b.d.	0	5	b.d.	0	0	b.d.	0	62	b.d.

III.4.4.1. Bacterial lipids

Dual labeling incubations in the presence of methane at 37°C yield a $\text{prod}_{\text{lipid}}$ of total bacterial lipids of $24 \pm 2 \mu\text{g lipid g}_{\text{dm}}^{-1} \text{yr}^{-1}$ and an assim_{IC} of $16 \pm 1 \mu\text{g lipid g}_{\text{dm}}^{-1} \text{yr}^{-1}$, resulting in an $R_{\text{a/p}}$ value of 0.70 ± 0.01 for experiments of 10, 17 and 24 day duration. This result indicates a strong contribution of lipid production linked to autotrophy by the active seep bacterial community. Interestingly, the total bacterial $\text{prod}_{\text{lipid}}$ at 50°C decreased relative to 37°C ($18.0 \mu\text{g lipid g}_{\text{dm}}^{-1} \text{yr}^{-1}$) although higher sulfide production rates were determined for this temperature (Table III.1). Additionally, contribution of total assim_{IC} was also reduced ($10.2 \mu\text{g lipid per g}_{\text{dm}}^{-1} \text{yr}^{-1}$), which led to a $R_{\text{a/p}}$ value of 0.6 (Table III.3; Fig. III.3). These findings suggest that 50°C exceeded the optimal growth temperature of the present community. Furthermore, higher temperatures result in higher expenditures of maintenance energy for microbial cells, possibly reducing the energy channeled to biomass production (cf. Price and Sowers, 2004). In the absence of methane (37°C, 24 days), the $\text{prod}_{\text{lipid}}$ of total bacterial lipids was reduced to 3.8 (equivalent to 15% of the $\text{prod}_{\text{lipid}}$ rates in the presence of methane) and the assim_{IC} dropped to $0.9 \mu\text{g lipid g}_{\text{dm}}^{-1} \text{yr}^{-1}$, resulting in a total bacterial lipid pool carrying a clear heterotrophic signal with a $R_{\text{a/p}}$ value of 0.2 (Table III.3; Fig. III.3).

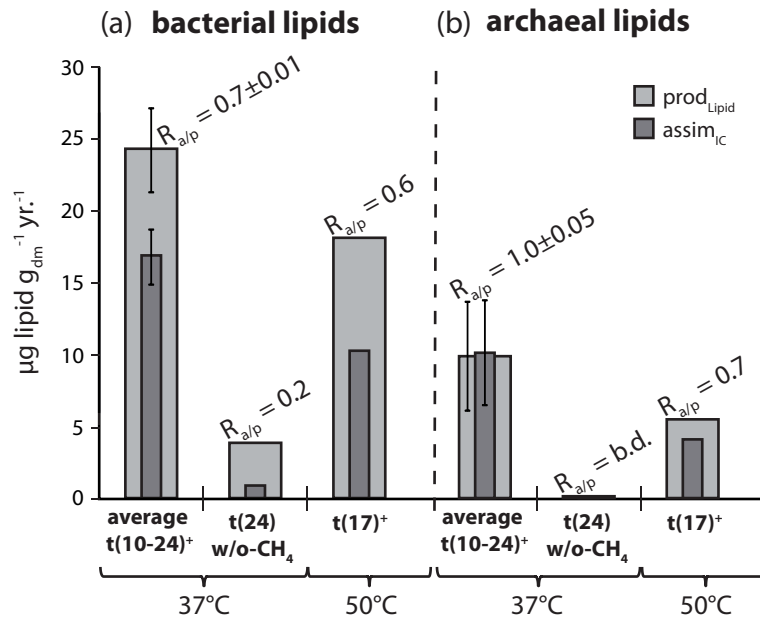


Fig. III.3. Production of lipids ($prod_{lipid}$; light gray bars) and assimilation of inorganic carbon ($assim_{IC}$; dark gray bars) into (a) bacterial and (b) archaeal lipids. Data for the 37°C experiment are average values (\emptyset) from the time series experiments. In the absence of methane, $R_{a/p}$ values are not presented because of low values detected for archaeal inorganic carbon lipid assimilation; (+) indicates incubations with unlabeled methane.

The bacterial lipids with the highest production in the presence of methane were $C_{18:1\omega7}$, $iC_{16:0}$, $C_{16:0}$, $iC_{16:1\omega6}$ and $iC_{18:1\omega6}$ (Fig. III.4a and Fig. III.5a; Table III.3). Some of these lipids, including $C_{18:1\omega7}$ and the two HotSeep-1 phylotype specific FAs $iC_{16:1\omega6}$ and $iC_{18:1\omega6}$ (cf. section III.4.2), show comparable $prod_{lipid}$ and $assim_{IC}$ and are thus indicating autotrophic pathways (Fig. III.4a and Table III.3). In the absence of methane, $C_{18:1\omega7}$, $iC_{16:1\omega6}$ and $iC_{18:1\omega6}$ experienced stronger reduction in both $prod_{lipid}$ and $assim_{IC}$, leaving lipids such as $C_{16:0}$, $iC_{16:0}$, $aiC_{15:0}$ and $C_{18:1\omega9}$ as the FAs with higher production rates. Those lipids have $R_{a/p}$ values of ≤ 0.5 , indicating predominantly heterotrophic sources (Fig. III.4b and Fig. III.5a; Table III.3). The continuously low $R_{a/p}$ values observed for some *i*- and *ai*-FAs, specifically $iC_{15:0}$ and $iC_{17:0}$ (Fig. III.4; Fig. III.5a; Table III.3 and Fig. III.S1) might be best explained by heterotrophic carbon fixation of non-*Deltaproteobacteria* phylotypes, such as *Chloroflexi* or members of the candidate division *OP8*, which are abundant in 16S rRNA gene sequence libraries from this thermophilic enrichment (Holler et al., 2011). Cultivation of heterotrophic organisms from marine sediments (e.g. *Chloroflexi*, *Methanosarcinales*, etc.) has been demonstrated before (Webster et al., 2011).

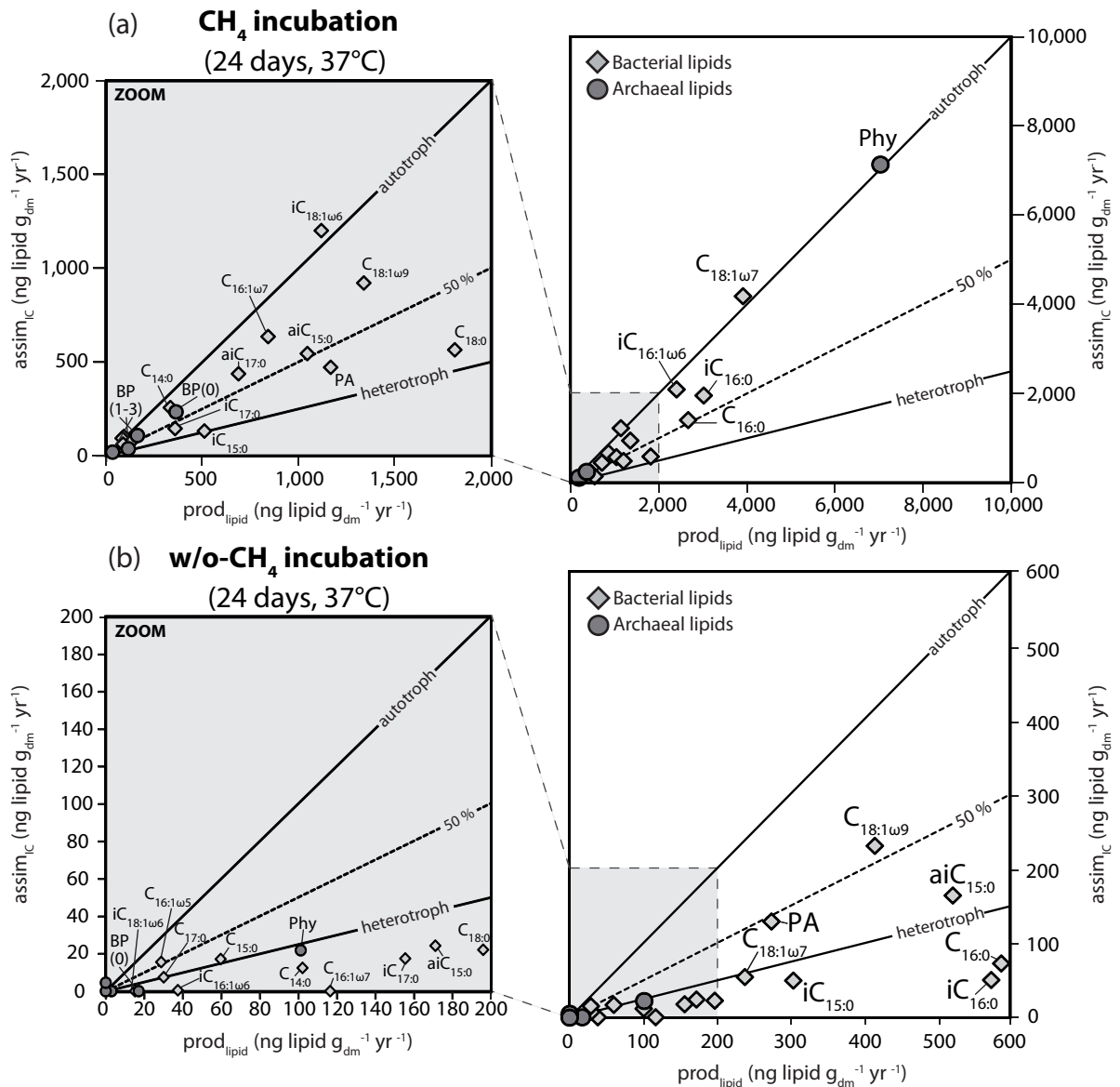


Fig. III.4. Two-dimensional plots of inorganic carbon assimilation rate ($assim_{IC}$) versus lipid production rate ($prod_{lipid}$) of individual bacterial fatty acids (diamonds) and archaeal isoprenoids (circles) in the (a) presence and (b) absence of methane at 37°C after 24 days of incubation.

Taken together, the methane-dependent production of bacterial lipids (particularly $iC_{16:1\omega6}$, $iC_{18:1\omega6}$ and $C_{18:1\omega7}$) with signals indicating autotrophic carbon fixation is possibly linked to the SRB HotSeep-1 phylotype (Holler et al., 2011). The observed production of these lipids is strongly elevated compared to their relative concentrations in the analyzed sediment (Fig. III.5b). This indicates that the bacterial lipid concentration pattern is a cumulative record affected by the varied production and decomposition rates of individual lipids, whereas the $prod_{lipid}$ rate most likely displays metabolic activity of the actual community pattern.

III.4.4.2. Archaeal lipids

Similar to bacterial lipids, production of archaeal lipids was highest at 37°C in incubations with methane. The $prod_{lipid}$ of total archaeal lipids, averaged over different time series experiments, was $10 \pm 3 \mu\text{g lipid g}_{dm}^{-1} \text{yr}^{-1}$ (Fig. III.3; Table III.3). The production rates of lipids

and assimilation rates of carbon assimilation were similar ($R_{a/p}$ values of 1.03 ± 0.05), implying a strictly autotrophic archaeal community (Fig. III.3). At 50°C, the $prod_{lipid}$ and $assim_{IC}$ (5.4 and $4.1 \mu g \text{ lipid } g_{dm}^{-1} \text{ yr}^{-1}$, respectively) of total archaeal lipids were both lower than those of the 37°C incubations and resulted in a lower $R_{a/p}$ value of 0.74 (Table III.3 ; Fig. III.S1). This suggests an increasing contribution of heterotrophy at the higher temperature range, possibly related to increased release of palatable substrates such as acetate from sedimentary organic matter at elevated temperatures (Wellsbury et al., 1997). In the absence of methane, the archaeal $prod_{lipid}$ and $assim_{IC}$ rates were marginal (0.1 and $0.03 \mu g \text{ lipid per } g_{dm}^{-1} \text{ yr}^{-1}$, respectively; Fig. III.3), demonstrating that the presence of methane is mandatory to sustain elevated growth of archaeal communities in hot seep sediments.

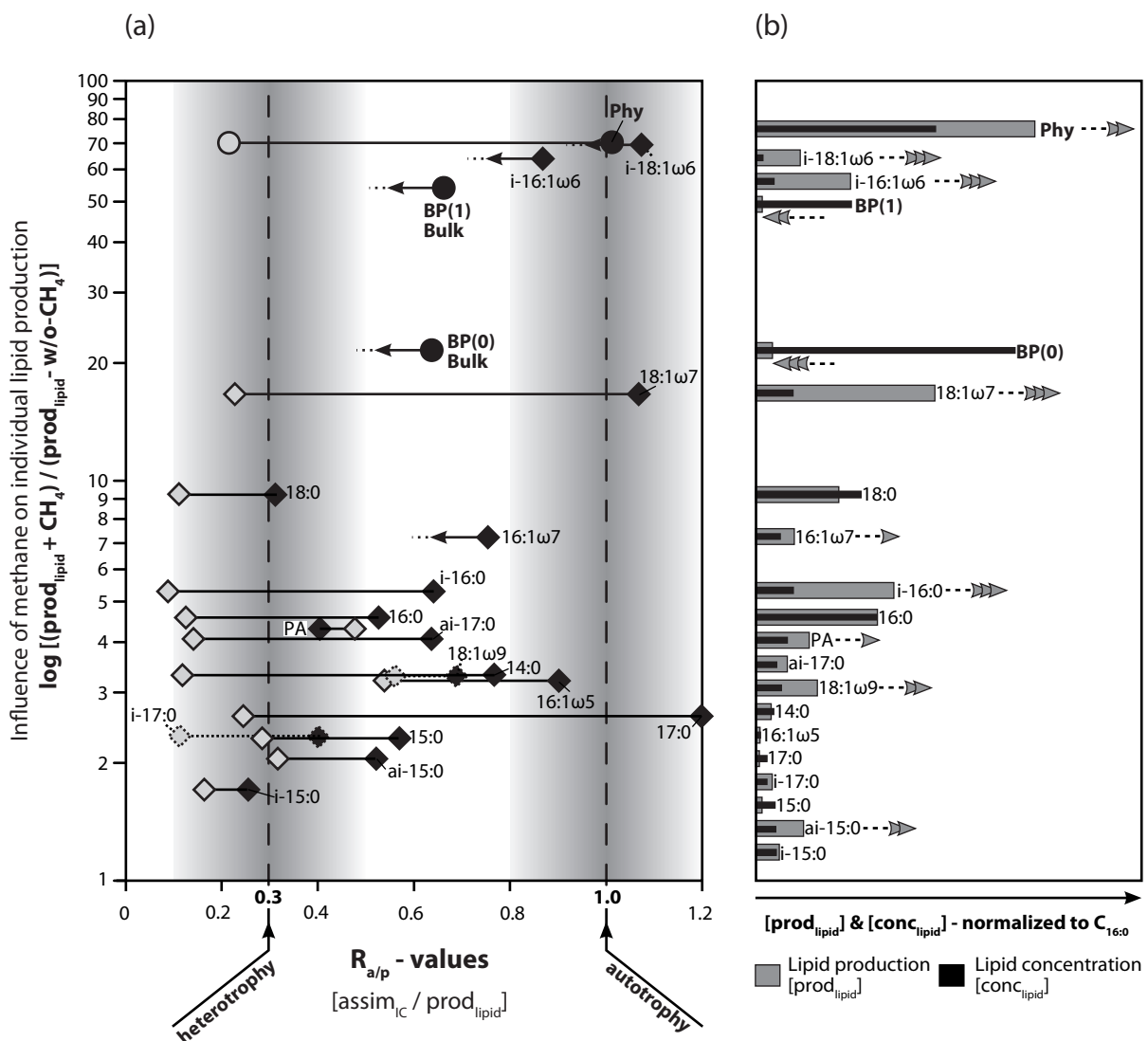


Fig. III.5. (a) Illustration showing the increase of individual $prod_{lipid}$ by methane addition compared to incubations without methane, plotted against the ratio of $assim_{IC} / prod_{lipid}$ ($R_{a/p}$). Archaeal (circles) and bacterial (diamonds) derived lipids were either produced in the presence (black) or absence of methane (gray). $R_{a/p}$ values could not be determined for $iC_{18:1\omega6}$; $iC_{16:1\omega6}$; $C_{16:1\omega7}$ and for BP(0) and BP(1) in the absence of methane due to $assim_{IC}$ values close to the detection limit. (b) Distribution of $C_{16:0}$ -normalized $prod_{lipid}$ and concentrations ($conc_{lipid}$) (experiment: 37°C, 24 days) of individual lipids. Gray arrows indicate the direction of changes in $prod_{lipid}$ values (enhancement or reduction) relative to $conc_{lipid}$. Gray bars indicate windows of significance for heterotrophy or autotrophy.

In all incubations with methane, the $\text{prod}_{\text{lipid}}$ of phytane was at least one order of magnitude higher than that of biphytanes (Fig. III.4a, Fig. III.S1). Comparable $\text{prod}_{\text{lipid}}$ and assim_{IC} during production of phytane with $R_{\text{a/p}}$ values of around 1 indicate its strict production via autotrophic carbon fixation. Detection of assim_{IC} in biphytanes, on the other hand, was overwhelmed by the large background of fossil core-GDGTs in the TLE, which reduces sensitivity and prevents the use of $R_{\text{a/p}}$ values as a gauge for distinguishing hetero- or autotrophic lipid production in the incubations (Fig. III.4a; Table III.3). To overcome this problem, we performed a similar isotopic assay on biphytanes from intact polar GDGTs of the TLE purified by preparative liquid chromatography (cf. section III.3.4; Kellermann et al., in preparation). Focusing on the intact polar lipid-derived biphytanes, we obtained significant and similar $\text{prod}_{\text{lipid}}$ and assim_{IC} values as for the phytane (e.g., 220 and 250 $\text{ng lipid g}_{\text{dm}}^{-1} \text{yr}^{-1}$, respectively, for the sample incubated at 37°C for 24 days). The $R_{\text{a/p}}$ values are comparable to the autotrophically produced phytane (average $R_{\text{a/p}}$ value = ~ 1.2 for the time series experiments at 37°C; Fig. III.6). Interestingly, the production of mono and bicyclic biphytanes was higher in incubations with methane at 50°C than at 37°C (Fig. III.S1), evidencing the preferential synthesis of cyclic over acyclic GDGTs at increased temperatures (Gliozzi et al., 1983; Schouten et al., 2003). In the absence of methane, the $\text{prod}_{\text{lipid}}$ and assim_{IC} of phytane were strongly reduced (0.1 and 0.02 $\mu\text{g lipid g}_{\text{dm}}^{-1} \text{yr}^{-1}$, respectively), resulting in a $R_{\text{a/p}}$ value = of 0.2 which thus indicates heterotrophic lipid production of the remaining active community (Fig. III.4b and Fig. III.5a; Table III.3).

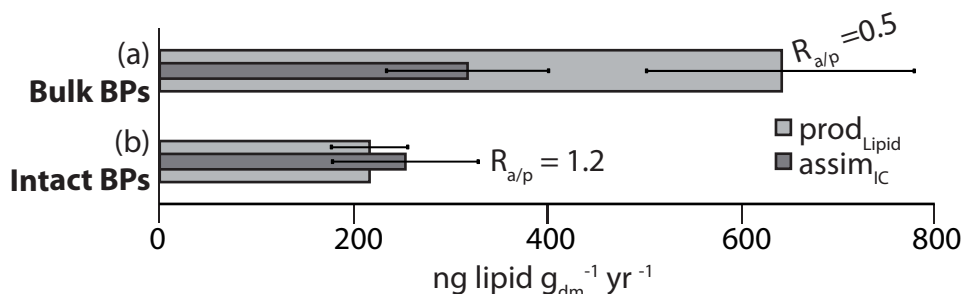


Fig. III.6. $\text{Prod}_{\text{lipid}}$ and assim_{IC} values for (a) bulk GDGT (in the total lipid extract) derived biphytanes and (b) total intact polar GDGT derived biphytanes both from the 37°C incubations with methane present. Error bars indicate the fluctuating $\text{prod}_{\text{lipid}}$ and assim_{IC} values over different time series experiments.

Taken together, our findings strongly suggest that these thermophilic ANME-1 archaea mediate autotrophic carbon fixation for lipid biomass whereas methane is mostly channeled to dissimilatory pathways. Interestingly, the archaeal $\text{prod}_{\text{lipid}}$ patterns do not match with the actual lipid concentrations (Fig. III.5b). Relative high phytane production is accompanied by low phytane pools, whereas biphytanes, which had low production rates, register the largest lipid fraction (Fig. III.1). The preferential production of archaeol –indicating phytane compared to GDGT–indicating biphytanes in ANME-1 is surprising, since lipid pools from ANME-1–dominated mats at cold seeps consist mainly of GDGTs as opposed to archaeols (Blumenberg et al., 2004; Rossel et al., 2008, 2011). We suggest that the elevated phytane production observed in this study is consistent with archaeol being an intermediate in lipid

synthesis of the thermophilic ANME-1 community (cf. Kellermann et al., in preparation). Our result also demonstrates that the persistent nature of core-GDGT derived biphytanes reduces the sensitivity of our isotopic assay (Fig. III.6). For future SIP experiments targeting archaeal membrane lipids, we advise to focus exclusively on the intact polar lipid pool of archaeol and GDGTs to minimize isotope dilution derived from the combination of already dead and living microbial biomass (Kellermann et al., in preparation).

III.5. Conclusions

We used stable isotope probing to examine the production rates of lipids of a novel thermophilic AOM enrichment originally retrieved from hydrothermally influenced sediments of the Guaymas Basin. The comparison of ^{13}C labeled methane- and DIC-associated uptake reveals that both bacteria and archaea perform autotrophic carbon fixation. Direct methane assimilation does not seem to be relevant for lipid biosynthesis of the thermophilic AOM community. This is further confirmed by dual stable isotope probing, demonstrating that inorganic carbon fixation rates (assim_{IC}) equals total lipid formation rates ($\text{prod}_{\text{lipid}}$). In the absence of methane, metabolic rates drop dramatically, suggesting the importance of methane as an energy source for sustaining the autotrophic methane-oxidizing communities. As an implication of our results, lipid isotopic composition in AOM systems should be revisited as the microbes are expected to fractionate carbon from DIC rather than from methane for building membrane lipids. We demonstrated that dual stable isotope probing provides novel insights into lipid formation, microbial activity and metabolism of microbial consortia mediating in marine sediments globally.

III.6. Acknowledgements

We are indebted to the shipboard, scientific crew and pilots of the R/V Atlantis and Research Submersible Alvin. We thank Jenny Wendt and Arne Leider for technical support and Jan Hoffmann for analyzing water isotopic compositions. This study was supported by the Deutsche Forschungsgemeinschaft (through the Research Center MARUM Center for Marine Environmental Sciences), the GLOMAR graduate school (MYK), the Gottfried Wilhelm Leibniz Prize awarded to Antje Boetius (to GW) and the Max Planck Society (to GW and TH). Additional funding was provided by the European Research Council Advanced Grant DARCLIFE to KUH.

III.7. Supporting information

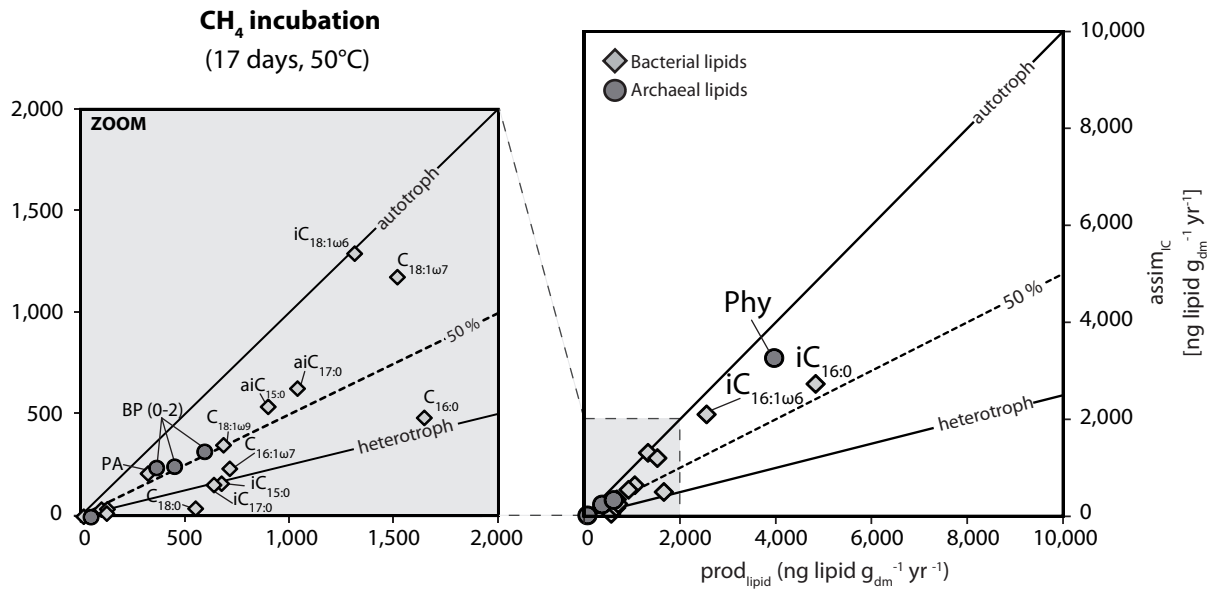


Fig. III.S1. Two-dimensional plots of inorganic carbon assimilation rate ($assim_{IC}$) versus lipid production rate ($prod_{lipid}$) of individual bacterial (diamonds) and archaeal (circles) lipids in the presence of methane at 50°C and after 17 days of incubation.

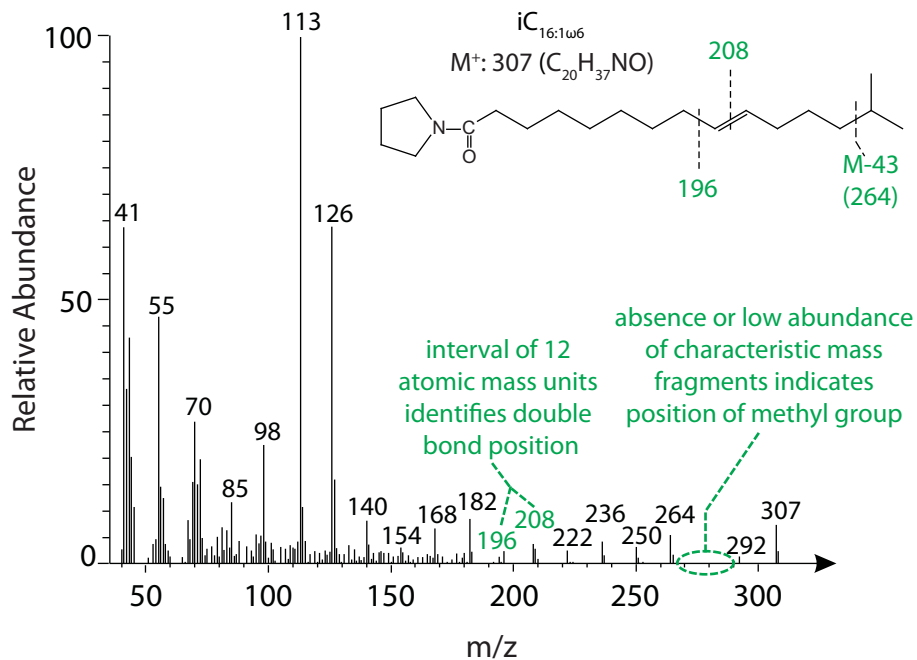


Fig. III.S2. Mass spectrum of the $iC_{16:1\omega6}$ pyrrolidine derivative enabling the determination of double bond and methyl group positions (Andersson and Holman, 1974).

Table III.S1. Absolute concentrations (averaged over all experiments) and isotopic composition ($\delta^{13}\text{C}$ and δD) of individual bacterial and archaeal lipids from each time point (T0, T10, T17, T24), temperatures (37 and 50°C) and substrate combinations (D_2O and $^{13}\text{C}_{\text{DIC}}$; $^{13}\text{C}_{\text{CH}_4}$) with and without methane headspace.

Name microbial lipids	absolute concentration (ng lipid $\text{g}_{\text{DM}}^{-1}$)	t(0)		t(10)		t(17)		t(24)		t(24) + $^{13}\text{C}_{\text{CH}_4}$		t(24) w/o- CH_4		t(17) + CH_4 (50 °C)	
		$\delta^{13}\text{C}$	δD	$\delta^{13}\text{C}$	δD	$\delta^{13}\text{C}$	δD	$\delta^{13}\text{C}$	δD	$\delta^{13}\text{C}$	δD	$\delta^{13}\text{C}$	δD	$\delta^{13}\text{C}$	δD
Bacteria:															
C_{140}	1100	-27	-89	37	1,700	75	3,100	110	3,900	-0.31	-110	-20	1,100	-28	77
3Me- C_{15}	410	-21	b.d.	-21	290	-21	550	-21	470	-22	b.d.	-22	370	-24	140
i- C_{150}	880	-49	b.d.	-8.4	3,700	8.1	6,500	37	76	-36	b.d.	-16	4,500	-52	76
ai C_{150}	850	-48	-120	151	8,400	220	12,000	320	16,000	25	-170	63	7,800	-51	-43
C_{150}	460	-29	b.d.	20	2,000	35	2,600	67	3,800	-20	b.d.	-8.0	1,700	-31	100
i- $\text{C}_{161/166}$	770	-39	-110	791	20,000	1,100	32,000	1,500	40,000	79	-190	-39	520	-42	30
i- C_{160}	1600	-48	-92	291	12,000	450	18,000	650	25,000	25	-150	-30	4,600	-50	150
$\text{C}_{161/167}$	1100	-37	-86	136	5,700	220	7,400	310	10,000	-9.8	-130	-39	1,400	-39	730
$\text{C}_{161/165}$	200	-46	b.d.	109	2,800	150	4,200	200	5,800	-26	b.d.	-0.11	1,700	-47	390
C_{160}	5200	-30	-150	33	3,200	86	4,000	120	6,500	-18	-180	-22	1,300	-31	-54
i- C_{170}	820	-38	-89	6.2	3,000	37	5,300	62	5,500	-32	-110	-26	2,400	-42	230
ai- C_{170}	900	-50	-100	107	5,000	160	8,100	230	9,900	-20	-140	-35	2,400	-52	89
C_{170}	470	-30	b.d.	7.4	1,500	22	1,700	82	2,100	-29	b.d.	-21	790	-37	31
i- $\text{C}_{181/186}$	300	-44	b.d.	1,300	31,000	1,500	56,000	2,300	49,000	130	b.d.	-43	620	-44	-78
PA	1400	-32	-180	61	6,800	170	11,000	170	11,000	-25	-200	23.0	2,400	-35	-92
$\text{C}_{181/169}$	770	-41	-190	330	14,000	640	24,000	650	22,000	7.4	-200	130	6,800	-43	-40
$\text{C}_{181/167}$	1600	-49	-230	780	20,000	1,200	27,000	1,500	32,000	55	-230	-29	1,700	-50	-300
C_{180}	4500	-27	-190	3.8	1,000	25	2,500	44	5,000	-21	-180	-25	370	-29	34
Archaea:															
Phy	7,700	-42	-150	377	9,100	412	8,800	490	12,000	100	-230	-40	24	-46	130
Bp(0)	11,000	-27	-290	-23	-110	-14	150	-14	140	-23	-290	-28	-270	-29	-260
Bp(1)	4,100	-47	-260	-49	-130	-42	150	-32	250	-41	-260	-48	-250	-50	-240
Bp(2)	7,800	-41	-270	-44	-240	-42	-180	-39	-77	-40	-280	-42	-270	-43	-260
Bp(3)	3,700	-18	-260	-18	-250	-18	-250	-18	-240	-18	-260	-17	-260	-17	-240

[CHAPTER IV] - FRAGMENTATION PATTERNS OF ARCHAEOAL IPLS**Systematic fragmentation patterns of archaeal intact polar lipids by high-performance liquid chromatography/electrospray ionization ion-trap mass spectrometry**

Marcos Y. Yoshinaga^{1,2*}, Matthias Y. Kellermann^{1,2}, Pamela E. Rossel^{1,2†}, Florence Schubotz^{1,2‡}, Julius S. Lipp^{1,2} and Kai-Uwe Hinrichs¹

Published in *Rapid Communication in Mass Spectrometry*

Vol: 25 (2011), page: 3563-3574, doi:0.1002/rcm.5251

© 2011 John Wiley & Sons, Ltd.

- ¹ MARUM – Center for Marine Environmental Sciences, University of Bremen. Leobener Str./MARUM, 28359 Bremen, Germany
- ² Department of Geosciences, University of Bremen. Leobener Str./MARUM, 28359 Bremen, Germany
- [†] Present address: Max Planck Research Group for Marine Geochemistry, Carl von Ossietzky University, ICBM, Carl von Ossietzky-Strasse 9–11, 26111 Oldenburg, Germany.
- [‡] Present address: Department of Earth and Planetary Sciences, Massachusetts Institute of Technology, 45 Carleton St, Cambridge, MA 02139, USA.
- * Corresponding author.
Tel.: +49 421 218 65744; Fax: + 49 421 218 65715
E-mail address: marcosyukio@gmail.com

Keywords:

archaeal lipids | HPLC/ESI-ITMSⁿ | intact polar lipids | MS/MS fragmentation patterns

IV.1. Abstract

Archaea are ubiquitous and abundant microorganisms on Earth that mediate key global biogeochemical cycles. The headgroup attached to the *sn*-1 position of the glycerol backbone and the ether-linked isoprenoid lipids are among the diagnostic traits that distinguish Archaea from Bacteria and Eukarya. Over the last 30 years, numerous archaeal lipids have been purified and described in pure cultures. Coupled high-performance liquid chromatography (HPLC) ion-trap mass spectrometry (ITMS) now enables the detection and rapid identification of intact polar lipids in relatively small and complex samples, revealing a wide range of archaeal lipids in natural environments. Although major structural groups have been identified, the lack of a systematic evaluation of MS/MS fragmentation patterns has hindered the characterization of several atypical components that are therefore considered as unknowns. Here, we examined mass spectra resulting from lipid analysis of natural microbial communities using HPLC/electrospray ionization (ESI)-ITMSⁿ, and depicted the systematics in MS² fragmentation of intact archaeal lipids. This report will be particularly useful for environmental scientists interested in a rapid and straightforward characterization of intact archaeal membrane lipids.

IV.2. Introduction

Archaea thrive in ecological niches where other organisms often fail to survive, such as hydrothermal systems, saline lakes, oligotrophic oceans and the seafloor biosphere (e.g., Cavicchioli, 2011 and references therein). More importantly, Archaea are key players mediating global microbial processes such as aerobic ammonium oxidation (Francis et al., 2005; Könneke et al., 2005), methane production and consumption and the ultraslow remineralization of recalcitrant organic matter (Cavicchioli, 2011; Hinrichs et al., 1999; Biddle et al., 2006). Membrane lipids are one of the most prominent features differentiating Archaea from Bacteria and Eukarya (Kates, 1978; Koga et al., 1993). Profound differences in the lipid stereochemistry of the glycerol backbone distinguish Archaea (headgroup attached to *sn*-1-glycerol) from Bacteria and Eukarya (headgroup attached to *sn*-3-glycerol; Kates, 1978). Furthermore, the synthesis of isoprenoidal side chains (C_{20'}, C₂₅ or C_{40'}, respectively, phytanyl, sesterterpanyl and biphytanyl) attached via di- or tetraether linkage to the glycerol backbone imparts the unique lipid characteristics of the Archaea (Kates, 1993; Koga et al., 1993). Examination of archaeal cultures, using techniques including thin layer chromatography, NMR and FAB-MS, revealed a multitude of archaeal lipids (Sprott et al., 1991; Kates, 1993; Koga et al., 1993; Morii et al., 1998; Corcelli et al., 2000; Sinningh  Damst  et al., 2002). However, these studies focused mostly on the major lipids found in the isolates.

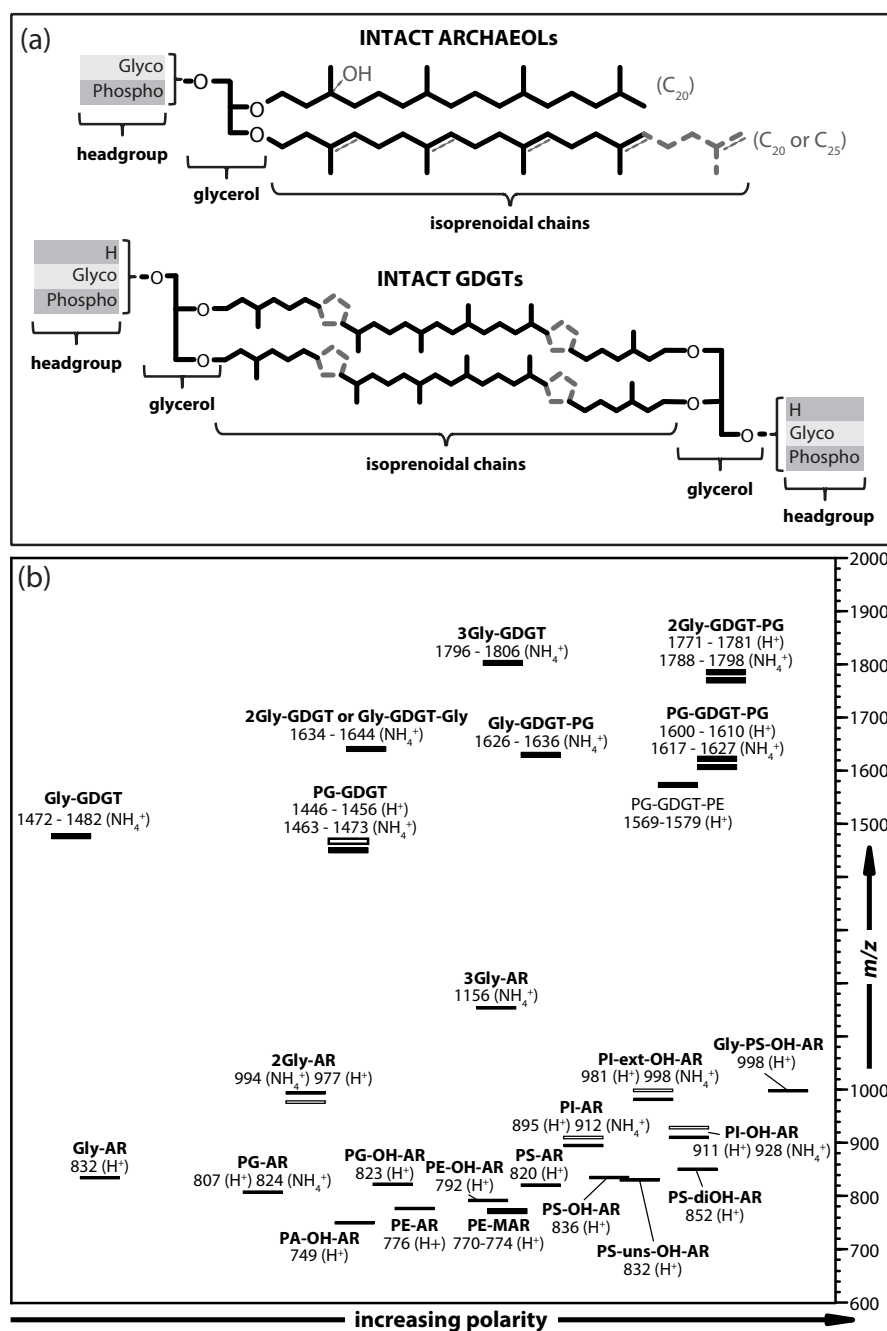


Fig. IV.1. (a) Schematic structures of archaeal IPLs, showing DGDs and GDGTs. Major structural differences influencing MS/MS fragmentation of IPLs are related to headgroups (glyco-, phospho- or glycopospho-based) and functionalization of isoprenoidal alkyl substituents. The latter can vary not only in length (C₂₀, C₂₅ and C₄₀), but also contain OH-groups, double bonds and cyclopentane and cyclohexane rings. (b) Schematic density map plot showing the major diagnostic ions of selected archaeal lipids in MS¹ mode, including the majority of headgroups found in this study, and their elution time during normal-phase/positive-mode HPLC/ESI-ITMSⁿ. Thin and thick bars represent molecular masses of intact archaeols ($m/z < 1200$) and intact GDGTs ($m/z > 1400$), respectively. For the latter, the range of [M H] is given because these compounds are often observed acyclic or containing one to five rings in their core lipids. Filled and open bars represent major and minor adduct formation, respectively. Note that glycolipids are commonly ionized as ammonium adducts, whereas phospho- and mixed phosphoglycolipids (e.g., Gly-PS-OH-AR) are often found in their protonated form. Compound abbreviations, GDGT: glycerol dibiphytanyl glycerol tetraether (C₄₀-C₄₀ isoprenoidal chains); DGD: glycerol dialkyl diether; AR: archaeol (C₂₀-C₂₀ isoprenoidal chains); Ext-AR: extended archaeol (C₂₀-C₂₅ isoprenoidal chains); OH-AR: monohydroxylated-archaeol; diOH-AR: dihydroxylated-archaeol; Uns-AR: unsaturated-archaeol; MAR: macrocyclic-archaeol; Gly: glycosyl (hexose); dGly: deoxy-glycosyl; PA: phosphatidic acid; PE: phosphatidylethanolamine; PME: phosphatidylmethylethanolamine; PG: phosphatidylglycerol; PGP: phosphatidylglycerol phosphate; PI: phosphatidylinositol; PS: phosphatidylserine.

Intact polar lipids (IPLs) from Archaea encompass a wide array of structures, in which both the polar headgroup (e.g., glyco-, phospho- and glycophospho-based headgroups) and several combinations of diether and tetraether core lipids result in a diverse range of IPLs (Fig. IV.1a). For instance, archaeal tetraether core lipids, the glycerol dibiphytanyl glycerol tetraethers (GDGTs), entail a variety of acyclic, ring-containing and H-shaped structures (Kates, 1978; Koga et al., 1993; Morii et al., 1998). Archaeal dialkyl glycerol diether (DGD) core lipids, also termed archaeols (ARs), may contain variations in length of isoprenoidal chain, degree of unsaturation and hydroxyl functional groups (Kates, 1993; Koga et al., 1993). In addition, diether macrocyclic core lipids and cardiolipin analogues are also reported for specific lineages of Archaea (Sprott et al., 1991; Corcelli et al., 2000). Thus analytical techniques need to be compatible with IPL complexity to comprehensively capture their structural diversity. High performance liquid chromatography coupled to electrospray ionization ion trap multistage mass spectrometry (HPLC/ESI-ITMSⁿ) allows detailed structural characterization of IPLs by combining information gained in positive and negative ionization modes (cf. Sturt et al., 2004). For instance, archaeal IPLs have been examined in cultures (Jahn et al., 2004; Strapoc et al., 2008) and natural environments, ranging from terrestrial (Liu et al., 2010) to marine (Sturt et al., 2004; Lipp et al., 2008; Rossel et al., 2008; 2011; Schubotz et al., 2009; 2011b) or lacustrine (Ertefai et al., 2008) realms.

Here we describe the systematics in MS² fragmentation of archaeal IPLs, emphasizing how structural features of diether and tetraether IPLs (e.g., type of headgroup, unsaturation and presence of functional groups in the isoprenoidal chains) affect the way molecules behave during HPLC/ESIITMSⁿ fragmentation (Fig. IV.1). The samples used in this study were exclusively collected in natural environments and mainly obtained from cold seep sediments, where archaeal IPLs are highly diverse. A good portion of the inferred compounds has not been observed in archaeal cultures and sufficient quantities for their rigorous identification by nuclear magnetic resonance (NMR) are not available. Archaeal IPLs are therefore tentatively identified based on mass spectral interpretation. This study provides extensive information for a rapid and straightforward characterization of archaeal membrane IPLs and may serve as a guide for researchers analyzing microbial lipids in natural samples.

IV.3. Experimental

IV.3.1. Samples

This study is a comprehensive interpretation of HPLC/ESIITMSⁿ mass spectra, which were analyzed and compared across several environmental samples (Table 1). Some of the compounds have been already published elsewhere (Rossel et al., 2008; 2011; Schubotz et al., 2011b) but the mass spectra were not examined in a systematic, comparative manner. The other samples are part of ongoing projects, with the majority coming from cold seep sediments that were taken at the Makran Accretionary Wedge off Pakistan margin during R/V Meteor

expedition M74/3 in 2007 (Bohrmann et al., 2008). In addition, we used sediment samples from the Northern Cascadia margin (Cruise 2008-007-PGC, U.S. Geological Survey, USGS) and push corers from Thermokarst Lakes at the Northern Alaskan Slope (USGS Gas Hydrates Project).

IV.3.2. Extraction of IPLs

Mussel IPLs were extracted from 10 to 20 g of freeze-dried sediments using a modified Bligh and Dyer method according to the protocol by Sturt et al. (2004). In brief, a mixture of dichloromethane/methanol/buffer (DCM/MeOH/buffer, 1:2:0.8; v/v/v) was added to the sediment and ultrasonicated for 10 min in four steps. For the first two extraction steps a phosphate buffer was used (pH 7.4), and, for the last two steps, a trichloroacetic acid buffer (50 g/L, pH 2.0). After each sonication step the mixture was centrifuged and the supernatant was collected in a separatory funnel. Equal amounts of DCM and deionized Milli-Q water were added to the combined supernatants to a final ratio of 1:1:0.8 (MeOH/DCM/buffer, v/v/v) and the organic phase was separated. The remaining aqueous phase was washed three times with DCM. Subsequently, the organic phase was washed three times with Milli-Q water, gently reduced to dryness under a stream of nitrogen at 37°C and stored as total lipid extract (TLE) at -20°C until HPLC/ESI-ITMSⁿ analysis.

IV.3.3. HPLC/MS

For analysis of IPLs utilized a ThermoFinnigan Surveyor HPLC system equipped with a LiChrosphere Diol-100 column (2.1 x 150 mm, 5 mm particle size; Alltech, Germany) coupled to a ThermoFinnigan LCQ Deca XP Plus ion trap mass spectrometer, equipped with an electrospray ionization (ESI) interface using settings previously described by Sturt et al. (2004). The mass spectrometer was set to data-dependent mode, where the base peak of each spectrum was automatically selected for fragmentation up to MS³. Collision-induced dissociation settings used for higher-order MS experiments were set to: isolation width 6 Da with normalized collision energy of 100%. The q-factor was lowered from the standard value of 0.25 to 0.2 in order to achieve a lower mass cut-off of 22% while still providing good MSⁿ spectra quality. Wideband activation was turned 'on' to facilitate the loss of water of hydroxylated compounds in the first stage of MSⁿ analysis and produce additional structurally useful information. Chromatographic conditions were as follows: flow rate of 0.2 mL/min, 100% A (79:20:0.12:0.04 of hexane/propan-2-ol/formic acid/14.8 M NH₃aq) to 35% A and 65% B (88:10:0.12:0.04 of propan-2-ol/water/formic acid/14.8 M NH₃aq) over 45 min, hold for 15 min, then back to 100% A for 15 min to re-equilibrate the column for the next run.

TLE purification was performed by preparative HPLC (cf. Lin et al., 2010 and Schubotz et al., 2011b) for selected samples with particularly high background signal in order to obtain a better signal-to-noise ratio and better MS/MS fragmentation patterns. A preparative LiChrosphere Diol-100 column (250 x 10 mm, 5 mm particle size; Alltech Associates, Inc., Deerfield, IL, USA) was connected to a ThermoFinnigan Surveyor HPLC system equipped with a FC204 fraction

collector (Gilson Inc., Middleton, WI, USA). The flow rate was set to 1.5 mL min⁻¹, and the eluent gradient was: 100% A to 100% B in 120 min, hold at 100% B for 30 min, then 30 min column re-equilibration with 100% A, where eluent A was n-hexane/propan-2-ol (79:20, v/v) and eluent B was propan-2-ol/Milli-Q water (90:10, v/v). Fractions were collected in time windows between 5 to 10 min and were subsequently analyzed by HPLC/ESI-ITMSⁿ. Identification of compounds was based on mass spectral information in MS² in positive ionization mode. Additional and complementary fragmentation patterns can be also obtained in negative ionization mode and in MS³ in positive and negative ionization modes (Sturt et al., 2004). The structures of archaeal IPLs presented in the paper are tentative. However, fragmentation patterns were confirmed with commercially available standards (e.g., PE-AR, Gly-GDGT-PG) and with complementary analysis of core lipids by GC/MS and HPLC/APCI (for DGDs and GDGTs, respectively).

IV.4. Results

We identified a systematic fragmentation of archaeal IPLs under MS/MS conditions that is related to the structural properties of headgroups and isoprenoidal chains. Stereoconfiguration of the glycerol backbone cannot be resolved by ESI-ITMSⁿ, so that the exact *sn*-2 or *sn*-3 positions for isoprenoidal chains and their functional groups (e.g., hydroxyl group) or double bonds cannot be predicted in DGDs. Likewise, the number of rings and their position in intact GDGTs cannot be determined.

Here we focused on fragmentation patterns observed in positive ionization mode (Fig. IV.1b), because it yields more detailed information on structural properties of isoprenoidal chains. Molecular ions of IPLs obtained in positive mode are observed either in their protonated form ([M H]) or as an ammonium adduct ([M NH₄]). Typically, glycolipids are present as ammonium adducts, while phospholipids tend to be protonated, but a few exceptions in adduct formation are observed and illustrated in Fig. IV.1b. Although MS² experiments are sufficient for compound elucidation, positive mode MS³ can be useful for further elucidation of core lipids, especially for glycopospholipids, and intact polar GDGTs.

Neutral losses of alkyl substituents in MS² experiments are generally associated with the transfer of an H-atom from the cleaved phytanyl substituent and two H-atoms from the biphytanyl substituent, as also observed by Knappy et al. (2009), resulting in a charged residual fragment of 1 and 2 Da higher mass, respectively. For example, in ARs, a saturated phytanyl substituent is lost as phytane (280.3 Da) and the biphytanyl substituent is presumably lost as a biphytadiene (558.6 Da). In order to distinguish losses of saturated vs. unsaturated alkyl substituents, we will therefore refer to the degree of unsaturation in the original compound and not the cleaved fragment (e.g., phytanyl for saturated ARs and phytenyl for (poly)-unsaturated ARs). Similarly, losses resulting from cleavage of hexoses or phosphoester-linked polar headgroups (e.g., ethanolamine from phosphatidylethanolamine (PE)) are associated with the transfer of an H-atom to the charged core fragment.

Table IV.1. Archaeal IPLs from environmental samples organized according to headgroups and core lipid characteristics. Molecular masses with types of adduct formation in positive ion mode MS1, neutral fragments and diagnostic ions in MS2 experiments are shown. For compound abbreviations see main text. Detailed interpretations of mass spectra are available in the main text and in the Appendices (see Supporting Information).

IPL ^a	<i>m/z</i>	Neutral losses ^b (Da)	Diagnostic ions ^c in MS ²	Sample location ^d
Phosphoarchaeols				
PA-AR	733.6 [M H]	phityanyl - 1 H = 280.3	453.3, 357.4	A
PA-OH-AR	749.6 [M H]	OH-phityanyl - 1 H = 296.3	453.3	A, B, D, E
PG-AR	807.7 [M H]	74.0 (loss of glycerol)	733.6, 653.7, 527.4, 373.4	A, B, D, E
PG-OH-AR	823.7 [M H]	OH-phityanyl - 1 H = 296.3	527.4	A, B, D, E
PG-diOH-AR	839.7 [M H]	Two times OH-phityanyl - 1 H = 296.3	247.1, 543.4 (525.4)	A
PG-Uns(2)-OH-AR	817.6 [M H]	phityadienyl - 1 H = 276.3, OH-phityanyl - 1 H = 296.3	541.3 (523.3), 247.1	A
PG-Uns(1)-Ext-OH-AR	891.7 [M H]	sesterterpenyl - 1 H = 348.3, OH-phityanyl - 1 H = 296.3	543.4 (525.4), 595.4, 247.1	A
PE-AR	776.7 [M H]	43.0 (loss of ethanolamine)	733.6, 453.3, 357.4	A, B, C, D, E
PE-OH-AR	792.7 [M H]	OH-phityanyl - 1 H = 296.3	496.4, 453.3	A, B, C, D, E
PME-AR	790.7 [M H]	57.0 (loss of methyl-ethanolamine)	733.6, 453.3, 357.4	A, C
PME-OH-AR	806.7 [M H]	OH-phityanyl - 1 H = 296.3	510.4, 453.3	C
PS-AR	820.7 [M H]	87.0 (loss of serine)	733.6, 453.3, 357.4	A, D
PS-OH-AR	836.7 [M H]	OH-phityanyl - 1 H = 296.3	540.4 (522.4), 453.3	A, D
PS-diOH-AR	852.7 [M H]	Two times OH-phityanyl - 1 H = 296.3	556.4 (538.4), 260.1	A, D, E
PS-Uns(2)-AR	816.6 [M H]	phityadienyl - 1 H = 276.3	540.4, 260.1	A
PS-Uns(5)-AR	810.6 [M H]	phityadienyl - 1 H = 276.3, phityatrienyl - 1 H = 274.3	534.3, 260.1	A
PS-Uns(2)-OH-AR	832.6 [M H]	phityadienyl - 1 H = 276.3, OH-phityanyl - 1 H = 296.3	556.4 (538.4), 260.1	A
PS-Uns(1)-diOH-AR	850.7 [M H]	OH-phityanyl - 1 H = 294.3, OH-phityanyl - 1 H = 296.3	554.3 (536.3), 556.4 (538.4), 260.1	A
PS-Ext-OH-AR	906.8 [M H]	OH-phityanyl - 1 H = 296.3	610.4 (592.4), 260.1	A
PI-AR	895.7 [M H]	162.1 (loss of inositol)	733.6, 653.7, 615.4	A, D
PI-OH-AR	911.7 [M H]	OH-phityanyl - 1 H = 296.3	615.4, 261.0	A, D, E
PI-diOH-AR	927.7 [M H]	Two times OH-phityanyl - 1 H = 296.3	631.4, 335.1, 261.0	A
PI-Uns(2)-OH-AR	907.7 [M H]	phityadienyl - 1 H = 276.3, OH-phityanyl - 1 H = 296.3	631.4, 335.1	A
PI-Ext-OH-AR	981.8 [M H]	OH-phityanyl - 1 H = 296.3	685.5, 261.0	A, D, E
PI-Ext-Uns(1)-OH-AR	979.8 [M H]	sesterterpenyl - 1 H = 348.3, OH-phityanyl - 1 H = 296.3	683.4, 631.4, 335.1	A
PI-Ext-Uns(5)-OH-AR	971.7 [M H]	340.3 (sesterterpenteptyl chain), OH-phityanyl - 1 H = 296.3	631.4 (613.4), 335.1	A
PI-Ext-Uns(4)-diOH-AR	989.7 [M H]	358.3 (OH-sesterterpenteptyl chain), OH-phityanyl - 1 H = 296.3	631.4 (613.4), 335.1	A
Glycoarchaeols				
Gly-AR	832.8 [M NH ₄]	179.1 (loss of hexose plus NH ₃)	653.7, 373.4	A
Gly-OH-AR	848.8 [M NH ₄]	179.1 (loss of hexose plus NH ₃), OH-phityanyl - 1 H = 296.3	669.7 (651.7), 373.4	A, D
2Gly-AR	994.8 [M NH ₄]	341.1 (loss of two hexoses plus NH ₃)	653.7, 373.4	A, B, D, E
2Gly-Uns-AR	992.8 [M NH ₄]	341.1 (loss of two hexoses plus NH ₃), phityenyl - 1 H = 278.3	813.7, 651.7, 535.4, 373.4	A, D
3Gly-AR	1156.9 [M NH ₄]	503.1 (loss of three hexoses plus NH ₃)	653.7, 373.4	A
3Gly-Uns-AR	1154.8 [M NH ₄]	503.1 (loss of three hexoses plus NH ₃), phityenyl - 1 H = 278.3	813.7, 651.7, 535.4, 373.4	A

Table IV.1. (continued)

Glyco-phospho-archaeol	Gly-PS-OH-AR	998.7 [M H]	162.1 (loss of one hexose), OH-phytanyl - 1 H = 296.3	836.7 (818.7), 540.4 (522.4)	A, D
	PE-MAR(2)	770.6 [M H]	43.0 (loss of ethanolamine from headgroup)	727.6, 629.6, 553.6	B
Macrocyclic-archaeol	Gly-GDGT(2)	1477.4 [M NH ₄]	179.1 (loss of one hexose plus NH ₃)	1298.3, 743.7	A, B, E
	2Gly-GDGT(1)	1641.4 [M NH ₄]	341.1 (loss of two hexoses plus NH ₃)	1462.4, 1300.3, 743.7	A, B, D, E
	3Gly-GDGT(2)	1801.5 [M NH ₄]	503.1 (loss of three hexoses plus NH ₃)	1460.4, 1298.3	A, D, E
	4Gly-GDGT(1)	1965.5 [M NH ₄]	665.1 (loss of three hexoses plus NH ₃)	1462.4, 1300.3, 743.7	A, D
	2Gly-GDGT(2)-dGly	1785.5 [M NH ₄]	341.1 (loss of two hexoses plus NH ₃), 146.1 (loss of deoxy sugar)	1444.3, 1298.3	A, D
Phospho-GDGTs	PG-GDGT(1)	1454.3 [M H]	74.0 (loss of glycerol), 80.0 (loss of PA)	1380.3, 1300.3 (1282.3), 897.7	A, B, D, E
	PG-GDGT(2)-PG	1606.3 [M H]	154.0 (loss of PG), 74.0 (loss of glycerol)	1452.3 (1434.3), 1378.3, 1298.3	A, B, D, E
Glyco-Phospho-GDGTs	PG-GDGT(2)-PGP	1686.3 [M H]	234.0 (loss of PGP)	1452.3	D
	PG-GDGT(1)-PE	1577.3 [M H]	154.0 (loss of PG), 43.0 (loss of ethanolamine)	1423.3, 1380.3	A, D, E
	Gly-GDGT(2)-PG	1631.4 [M NH ₄]	179.1 (loss of one hexose plus NH ₃)	1452.3	A, D
	2Gly-GDGT(2)-PG	1793.4 [M NH ₄]	342.1 (loss of two hexoses plus NH ₃)	1452.3, 897.7	A, D, E
	2Gly-GDGT(1)-PE	1747.4 [M H]	324.1 (loss of two hexoses), 43.0 (loss of ethanolamine)	1423.3, 1380.3	A, D
	2Gly-GDGT(1)-PME	1761.4 [M H]	324.1 (loss of two hexoses)	1437.3, 823.7	A

^aNumber in parentheses for archaeols denotes the number of unsaturations in isoprenoidal chains, and in MAR and GDGTs it denotes the number of cyclopentyl rings. ^bNote that neutral losses in MS/MS experiments are associated with transfer of one H-atom from the cleaved phytanyl substituent and two H-atoms from the biphytanyl substituent.

^cDiagnostic ions in bold indicate the major base peak observed in MS² spectra.

^dA = Makran cold seeps, B = Cascadia margin sediments, C = Alaskan lakes, D = Rossel *et al.*,^[17,20] E = Schubotz *et al.*^[21]

In the following section, we classify several archaeal IPLs according to their distinct structural characteristics, and demonstrate how these features influence fragmentation patterns during ESI-ITMSⁿ. A complete list of compounds is given in Table IV.1 and examples of mass spectral interpretations are given throughout the manuscript.

IV.4.1. C₂₀ - C₂₀ Saturated Intact polar DGDS

In MS² experiments, saturated intact archaeols give a base peak corresponding to the neutral loss of the headgroup (Fig. IV.2a and Fig. IV.2b). Glycosylated (Gly) ARs lose the sugar headgroup(s), yielding a core AR fragment ion of m/z 653.7 (Table IV.1). On the other hand, phospho-based (Phos) ARs partially lose their headgroup (e.g. glycerol from phosphatidylglycerol (PG), serine from phosphatidylserine (PS)), while retaining phosphatidic acid (PA), as shown by the major base peak at m/z 733.6. Minor fragment ions, particularly at m/z 373.4 (for Gly-AR, Fig. IV.2) and m/z 453.3 (for Phos-AR, Fig. 2(b)), result from the loss of one phytanyl group (as phytene, 280.3 Da loss) from major ions in MS² (Table IV.1). Consequently, the polar headgroup can be identified by subtraction of m/z 653.7 (AR) for Gly-ARs and m/z 733.6 (PA-AR) for Phos-ARs from the [M H] deduced in MS¹ experiments.

IV.4.2. Hydroxylated, saturated C₂₀ - C₂₀ intact polar DGDS

Fragmentation of Gly-mono-hydroxy (OH) AR in MS² is similar to saturated Gly-ARs, with the distinction that Gly-OH-AR shows a base peak at m/z 373.4 (Fig. IV.2c). This fragment ion derives from the concerted losses of the sugar headgroup (hexose plus 17 Da of NH₃, 179.1 Da loss) and the OH-phytanyl chain (lost as OH-phytene, 296.3 Da). Ions at m/z 669.7 and 651.7 arise from the exclusive loss of the sugar headgroup. The former fragment ion is equivalent to the OH-AR core lipid while the latter results from additional loss of water, presumably from the phytanyl moiety. The base peak of Phos-OH-ARs in MS² spectra results from the loss of the OH-phytanyl chain, i.e. a 296.3 Da loss (Table 1, Fig. IV.2d). Polar headgroup assignments can be obtained by subtraction of m/z 749.6 (PA-OH-AR) for Phos-OH-ARs from the [M H] deduced in MS¹ experiments.

Dihydroxy (diOH) ARs were characterized by single hydroxylation of each phytanyl substituent and were only observed in combination with Phos-based headgroups, exclusively the PG, PS and PI (Table IV.1). Fragmentation of this IPL class involves two losses of OH-phytanyl (296.3 Da) chains, thus a Phos-based headgroup attached to a glycerol backbone appears as the major fragment ion in MS² spectra (Fig. IV.2e). Minor fragment ions derived from the loss of one OH-phytanyl chain.

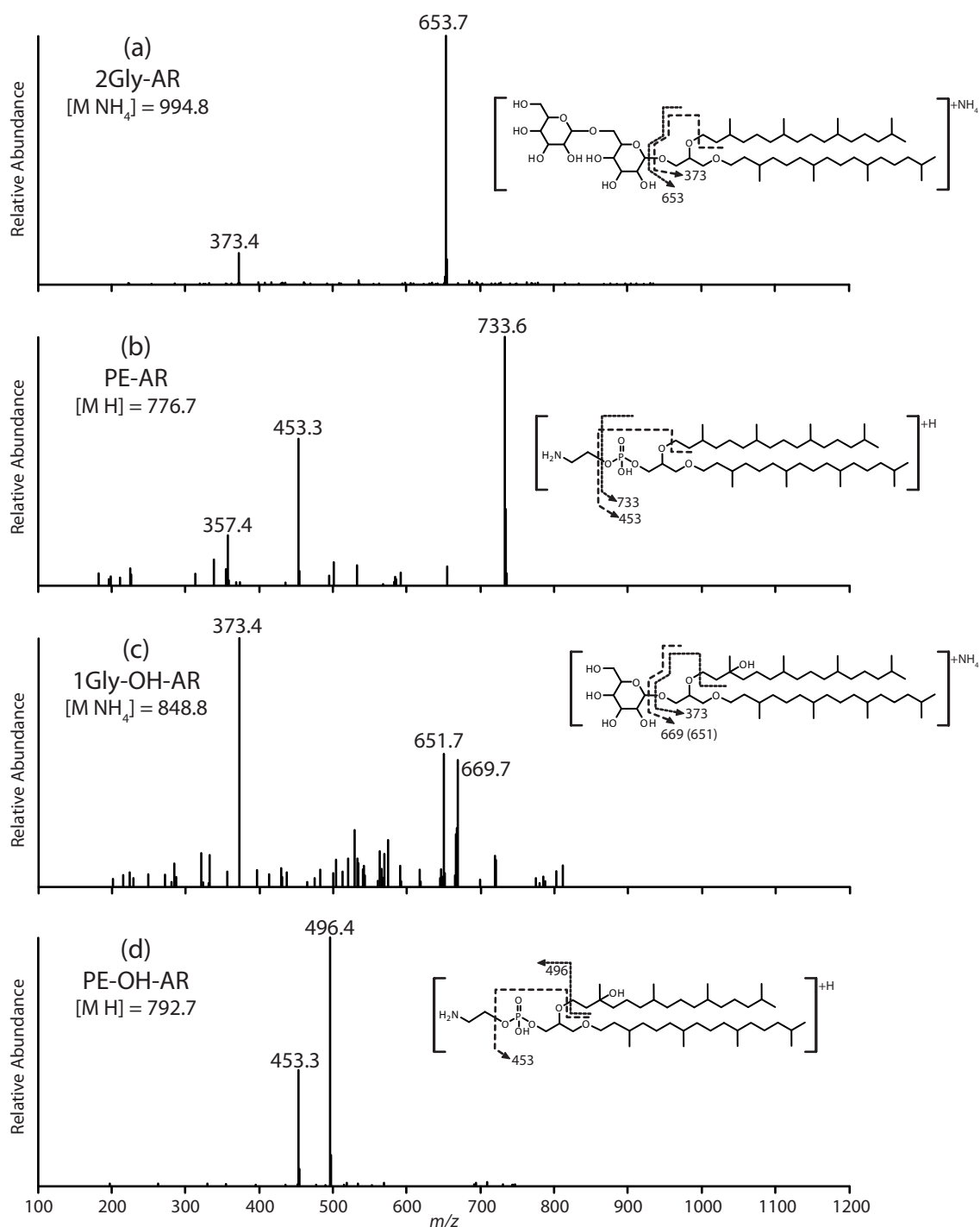


Fig. IV.2. Positive mode MS² spectra of selected archaeal lipids. (a–h) Gly- and Phos-based C₂₀–C₂₀ ARs with saturated, monohydroxylated (OH), dihydroxylated (diOH) and unsaturated (Uns) core lipids; (i, j) saturated and unsaturated phospho C₂₀–C₂₅ extended (Ext) OH-ARs; (k) PE macrocyclic archaeol (MAR) and (l) MS² and MS³ of a novel archaeal glycophospholipid. The *m/z* value in parentheses represents the base peak after loss of water. The reader is referred to the main text for detailed interpretation of mass spectra.

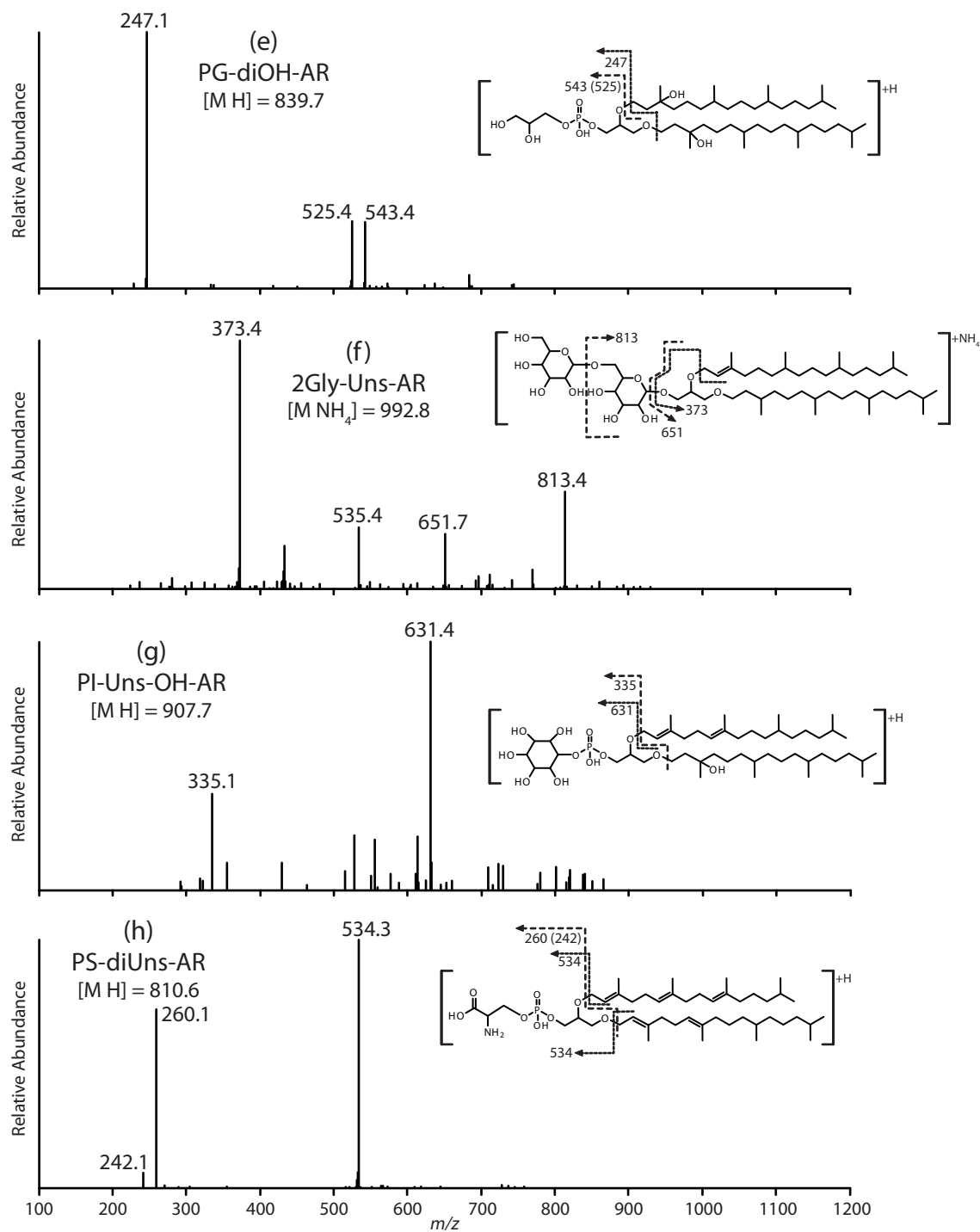


Fig. IV.2. (Continued)

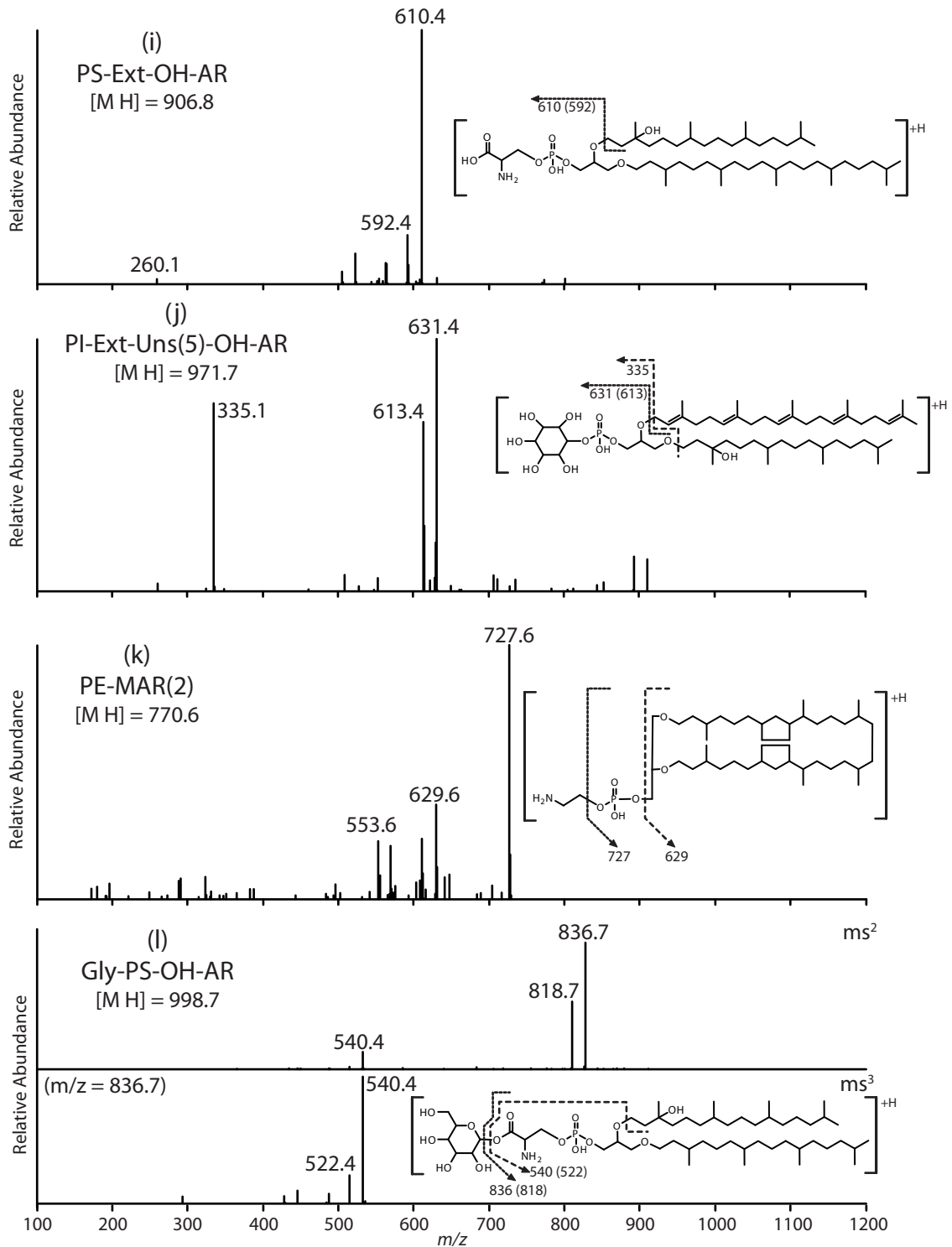


Fig. IV.2. (Continued)

IV.4.3. *Unsaturated C₂₀ - C₂₀ intact polar DGDS*

Unsaturated (Uns) phytanyl substituents were observed with one, two or three double bonds and associated with PG, PS, PI and Gly (Table IV.1). Unsaturation was present in either one or both side chains, with or without an additional OH-group. Given the general observation of an H-transfer from the cleaved alkyl substituents, neutral losses attributed to phytanyl chains with one to three double bonds are 278.3, 276.3 and 274.3 Da, respectively. In addition, a loss of 294.3 Da arising from the cleavage of the OH-phytenyl chain was also observed (Table IV.1).

Gly-Uns(1)-ARs, which are observed exclusively with one unsaturation, lose their sugar headgroup together with the phytenyl substituent, thus the major ion of m/z 373.4 in MS² spectra corresponds to the residual phytanyl group attached to the glycerol backbone (Fig. IV.2f). On the other hand, the fragmentation pattern of Phos-Uns-ARs is marked by the loss of the polyunsaturated phytenyl chain, which is favored over the headgroup and hydroxylated or saturated phytanyl chain (Fig. IV.2). Furthermore, among polyunsaturated phytenyl substituents we observed a tendency of preferential loss of species with lower number of double bonds, as shown in PS-Uns(5)-AR by the base peak at m/z 534.3 (Fig. IV.2h). Fragment ions in MS² spectra from Phos- Uns-ARs correspond to the headgroup attached to a glycerol backbone (Table IV.1).

IV.4.4. *Intact polar C₂₀ - C₂₅ DGDS*

C₂₀ - C₂₅ DGDS, hereafter called extended (Ext)-ARs, were in their intact polar form exclusively found as PS and PI derivatives (Table IV.1). The phytanyl substituent contains invariably an OH-group, whereas the sesterterpanyl moieties are saturated, mono- or pentaunsaturated, or hydroxylated. The fragmentation in MS² for the saturated Ext-OH-AR is defined by cleavage of the OH-phytanyl substituent (i.e. 296.3 Da, Fig. IV.2i). The MS² spectrum of the PI-Uns(5)-Ext-OH-AR shows the base peak at m/z 631.4 resulting from a neutral loss of 340.3 Da (Fig. IV.2j). In line with the fragmentation pattern for Phos-Uns-OH-ARs, this observation illustrates the order of reactions under MS² experiments, in which the loss of the penta-unsaturated sesterterpenyl chain as a hexa-unsaturated neutral fragment (340.3 Da) is followed by loss of the OH-phytanyl chain. Additional fragment ions at m/z 613.4 and 335.1 correspond to the loss of water from the major fragment ion and the PI headgroup attached to a glycerol backbone, respectively (Fig. IV.2i and Fig. IV.2j).

IV.4.5. *Intact macrocyclic archaeols*

Macrocyclic archaeols (MAR) are glycerol biphytanyl diether compounds originally detected in *Methanococcus janaschii* (Comita et al., 1084; Sprott et al., 1991; Sturt et al., 2004). The only Phos-MAR thus far detected in our survey of environmental samples contains a PE headgroup (Table IV.1). Variation in cyclopentane ring numbers from 0 to 2 in this IPL results in three major ions in MS² (base peaks at m/z 731.6, 729.6 and 727.6, respectively 0, 1 and 2 cyclopentyl rings), corresponding to the PA-MAR fragments after loss of ethanolamine (Fig. IV.2k). This fragmentation pattern resembles those of saturated C₂₀ - C₂₀ ARs, with the exception

that the macrocyclic structure remains integral after MS₂ experiments. This is reflected in minor fragment ions, arising from the loss of the entire headgroup, yielding a core MAR with a loss of water (m/z 633.6, 631.6 and 629.6), and a subsequent cleavage of the glycerol backbone from the core MAR (m/z 557.6, 555.6 and 553.6).

IV.4.6. Intact polar GDGTs with one or two headgroups

Membrane spanning GDGTs with one headgroup are present as either glycosylated or phospho derivatives (Table IV.1). Their fragmentation patterns in MS² resemble those of intact saturated C₂₀ - C₂₀ ARs. Sugar headgroup(s) from Gly-GDGTs are lost during MS² fragmentation, resulting in the base peak ion representing the core GDGT (m/z 1292.3-1302.3, ranging from 0 to 5 rings) (Fig. IV.3a). Minor fragment ions in MS², which are sometimes observed, are related to the loss of one biphytanyl chain from the core GDGT (e.g., m/z 743.7 in 4Gly-GDGT, Fig. IV.3a). The neutral loss of a biphytanyl chain during fragmentation is generally accompanied by transfer of two H-atoms from the biphytane to the charged fragment as indicated by a mass deficiency of 2 Da. The PG-GDGT was thus far the only single-headgroup phospho-GDGT detected in environmental samples (Fig. IV.3b). PG-GDGT loses the headgroup, giving a base peak corresponding to the core GDGT (m/z 1292.3-1302.3) and an ion resulting from the additional loss of water. Minor fragment ions correspond to a PA-GDGT (m/z 1372.3-1382.3) and the loss of one biphytanyl chain from PA-GDGT and PG-GDGT.

GDGTs with two headgroups are composed of glycopospholipids and phospholipids (Table IV.1). During MS² fragmentation, Gly-GDGT-Phos always loses the sugar headgroup(s), resulting in major fragment ions corresponding to a Phos-GDGT (Fig. IV.3c). As for Phos-GDGTs, the MS² fragmentation of Phos-GDGT-Phos results in complete loss of one phospho headgroup, yielding a Phos-GDGT ion as base peak in MS² spectra (Fig. IV.3d). Minor fragment ions for both classes of intact polar GDGTs with two headgroups mirror those of single headgroup Phos-GDGTs.

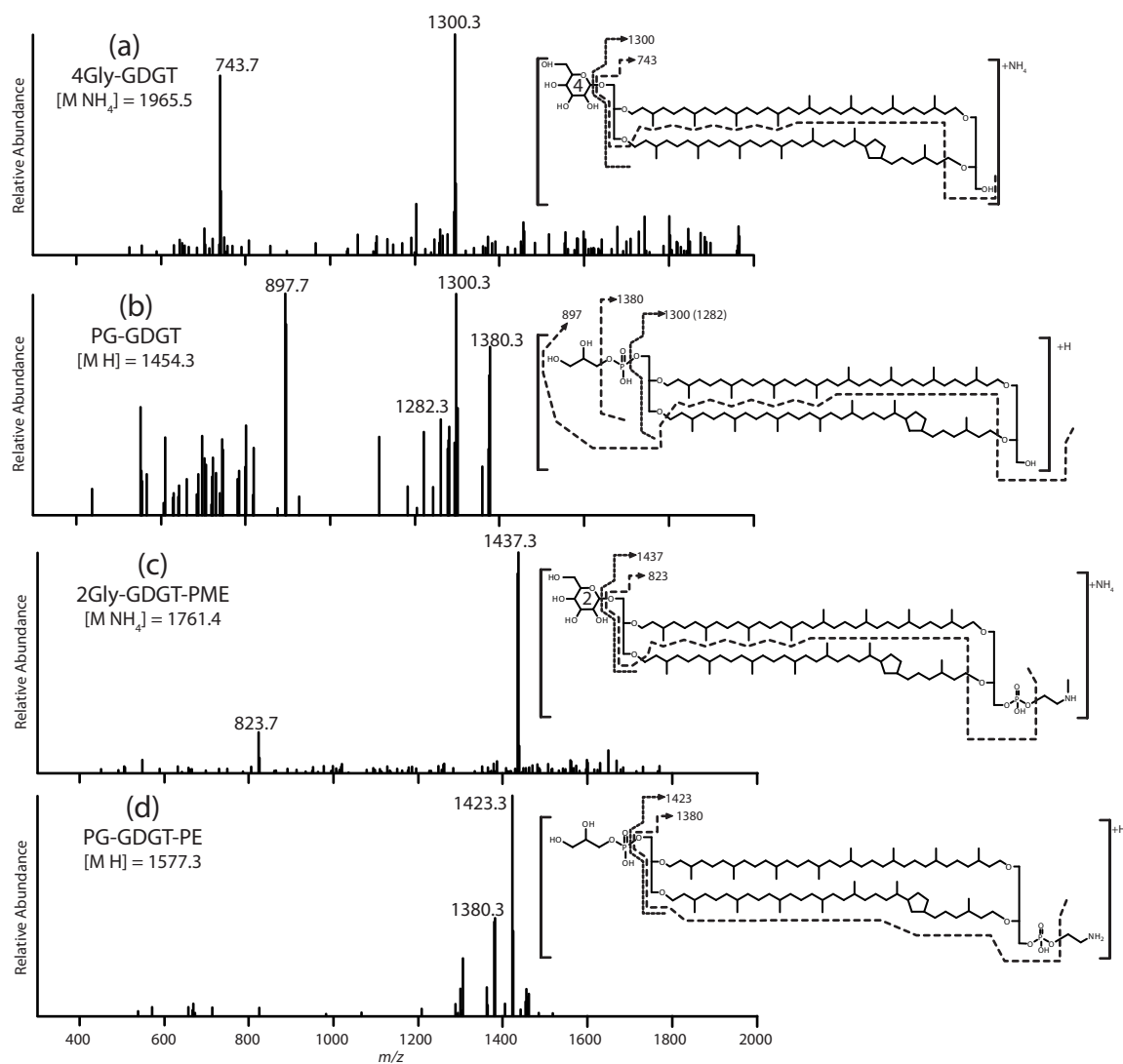


Fig. IV.3. Positive mode MS² spectra of intact polar GDGTs with one headgroup (a, b) and two mixed headgroups (c, d). Numbers inside the hexoses in (a) and (c) represent the number of sugar headgroups of the IPLs. The m/z value in parentheses represents loss of water from the base peak ion. The reader is referred to the main text for detailed interpretation of mass spectra.

IV.4.7. Negative ionization mode

In negative ionization mode, the major fragments of Phos-ARs are commonly formed by the headgroup (e.g., major fragment ion at m/z 241.1 for PI-AR (Jahn et al., 2004)). However, minor fragment ions from OH-AR, Uns-AR and Ext-OH-AR are not regularly related to the cleavage of the isoprenoidal chains from the molecular ion (data not shown). Thus, important information about the isoprenoidal chains, such as whether the compound possesses a combination of unsaturated, hydroxylated or saturated alkyl substituents, cannot be directly obtained. In case of unknown compounds, the complementary information provided by the negative ion mode can, however, be useful. For instance, headgroups can be differentiated based on types of adduct formation (Sturt et al., 2004).

IV.5. Discussion

Systematic order in fragmentation of archaeal IPLs during MS/MS experiments as a function of headgroups and isoprenoidal substituents

During MS² experiments, sugar headgroups are preferentially cleaved, regardless of the complexity of the archaeal core lipid (i.e. diether, tetraether, hydroxylated, unsaturated or saturated, Fig. IV.4). This fragmentation pattern is likely related to the stability of the neutral fragment obtained, but the exact mechanism is not examined in this study. The compound 2Gly-Uns-AR containing both a phytanyl and a phytenyl substituent is often observed in methane seep sediments (Rossel et al., 2011) and exemplifies this systematic fragmentation (Fig. IV.2f). The base peak at m/z 373.4 in the MS² spectrum results from the cleavage of sugar headgroups and the loss of a phytenyl chain (278.3 Da loss). Minor fragment ions at m/z 813.7 ([M NH⁴⁺] – Gly), 651.7 ([M NH⁴⁺] – 2Gly) and 535.4 (m/z 813.7 – 278.3 Da loss) demonstrate successive losses of sugar headgroups and an unsaturated isoprenoidal chain (Fig. IV.2f). Gly-based GDGTs with single or mixed phospho and glycosylated headgroups show invariably sugar loss(es) during fragmentation in MS² experiments, independent of the number of cyclopentane rings in the core GDGT and/or the associated type of phospho headgroup (Fig. IV.4).

Because isoprenoidal substituents are structurally more diverse in phospho than in glycosylated ARs, fragmentation patterns during MS² experiments are more complex. In phospho-DGDs, the preferential order of fragmentation is unsaturated C₂₀ and C₂₅ isoprenoidal substituents followed by other IPL components. The PI-Uns(2)-OH-AR and the PI-Uns(5)-Ext-OH-AR contain phytadienyl and sesterterpapytenyl chains, respectively, combined with an OH-phytanyl (Fig. IV.2g and Fig. IV.2j, respectively). These IPLs show the preferential loss of unsaturated over hydroxylated alkyl chains (Fig. IV.4). In turn, cleavage of OH-phytanyl in MS² experiments is favored over saturated alkyl substituents (phytanyl and sesterterpanyl) and phosphoester-linked polar headgroups (i.e. glycerol, ethanolamine, serine, etc.) (Fig. IV.2d and Fig. IV.2i). The major base peak in MS² spectra of saturated Phos-ARs corresponds to a PA-AR and indicates that the phosphoester-linked polar headgroups are cleaved preferentially over the saturated phytanyl chains (Fig. IV.2b).

In this study, the PG-GDGT-PE and PG-GDGT-PGP (PGP = phosphatidylglycerol phosphate) were the only GDGTs with two different phospho headgroups (Table IV.1). The former compound exhibits a preferential loss of PG over PE, ensuing PE-GDGT as the major fragment ion in the MS² spectrum (Fig. IV.2d). It is thus reasonable to infer that fragmentation of GDGTs with two distinct headgroups also follows a systematic order of neutral losses: hexoses followed by PG, which is preferentially lost over PE in MS² experiments (Fig. IV.4). Interestingly, losses observed in intact MARs are related to the headgroup, and these IPLs appear as the most stable core lipids during MS² fragmentation (Fig. IV.2k).

Having established the systematic patterns of fragmentation of archaeal IPLs under MS/MS conditions, in the following we describe a novel glycopospholipid AR that exemplifies the

benefits of the knowledge of fragmentation patterns established in this study. The putative Gly-PS-OH-AR is a minor archaeal IPL in seep sediments (Fig. IV.2I, this study). Its protonated mass at m/z 998.7 yields a base peak at m/z 836.7 and a related peak at m/z 818.7 in MS^2 , corresponding to the loss of a hexose ($[M H]^+ - 162.1$ Da) and a further loss of water from the major fragment ion in MS^2 . Minor fragment ions (better visualized in MS^3) at m/z 540.4 and 522.4 are related to a subsequent 296.3 Da loss (OH-phytanyl chain) from m/z 836.7, mirroring the fragmentation observed in PS-OH-AR (Table IV.1). The characteristics observed above are in line with the order of reactions during MS^2 experiments (Fig. IV.4), in which first hexoses are lost, followed by the OH-phytanyl chain.

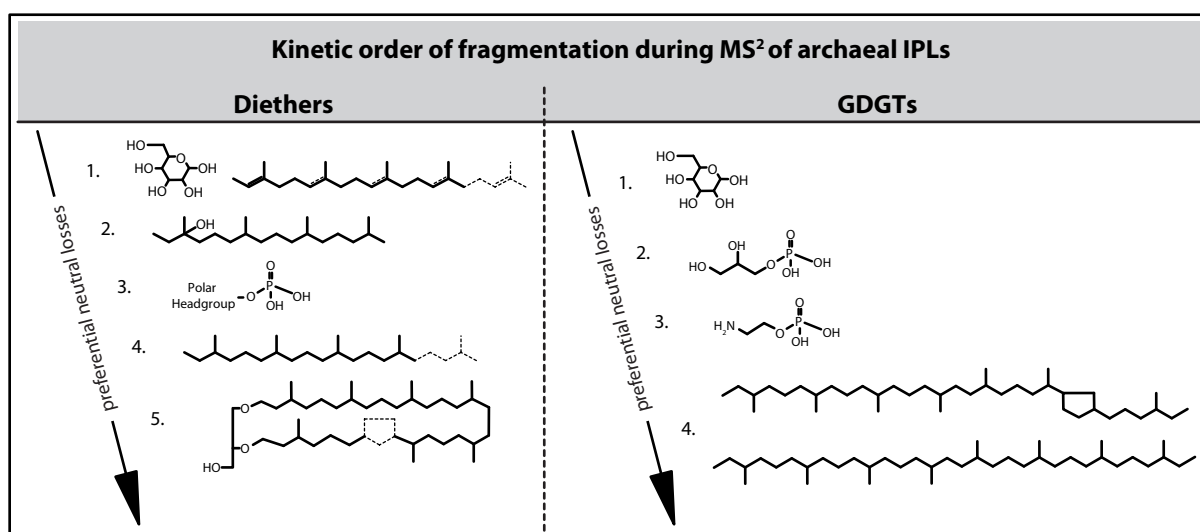


Fig. IV.4. Simplified overview of fragmentation patterns of archaeal di- and tetraether IPLs during HPLC/ESI-ITMSⁿ.

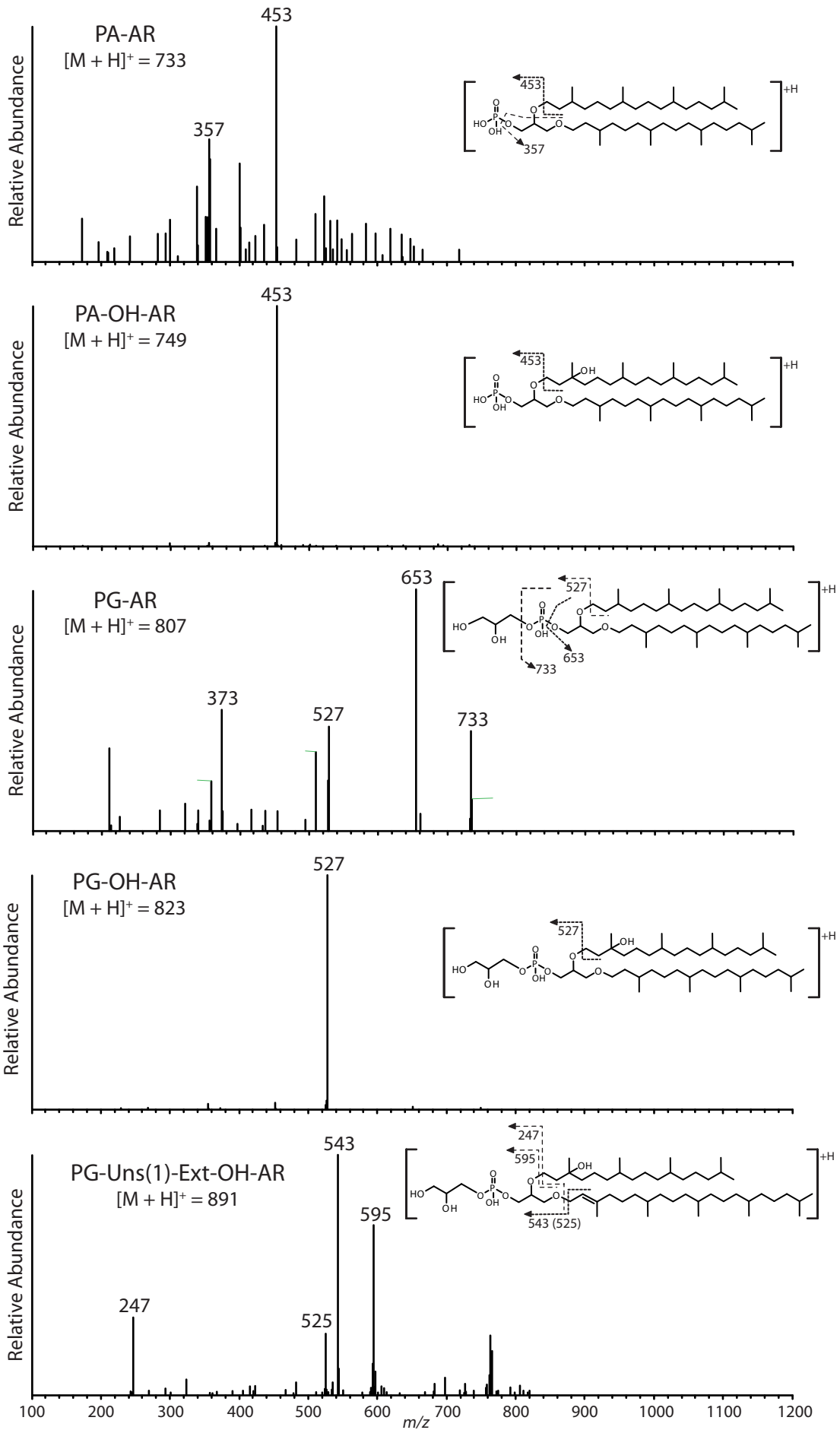
IV.6. Final considerations

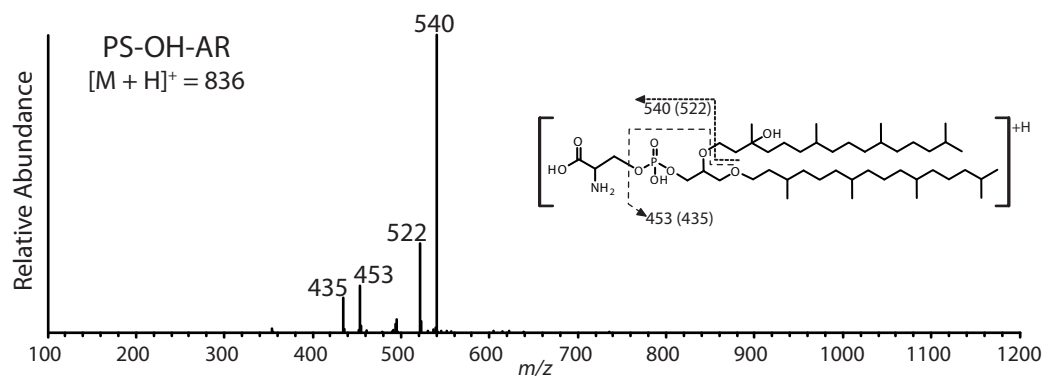
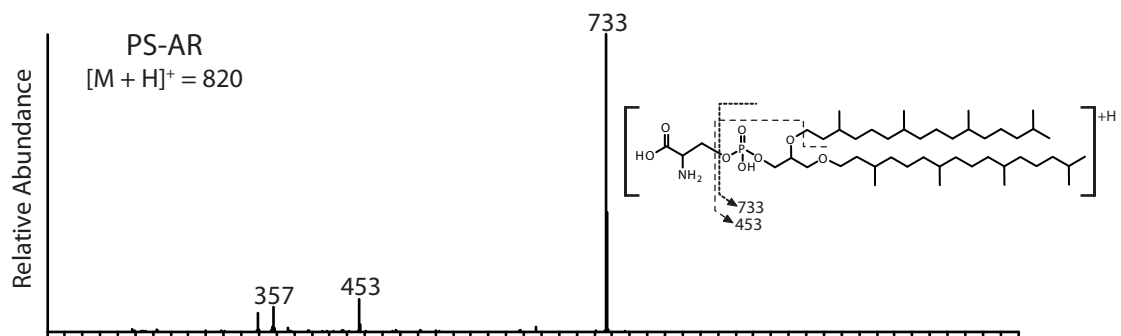
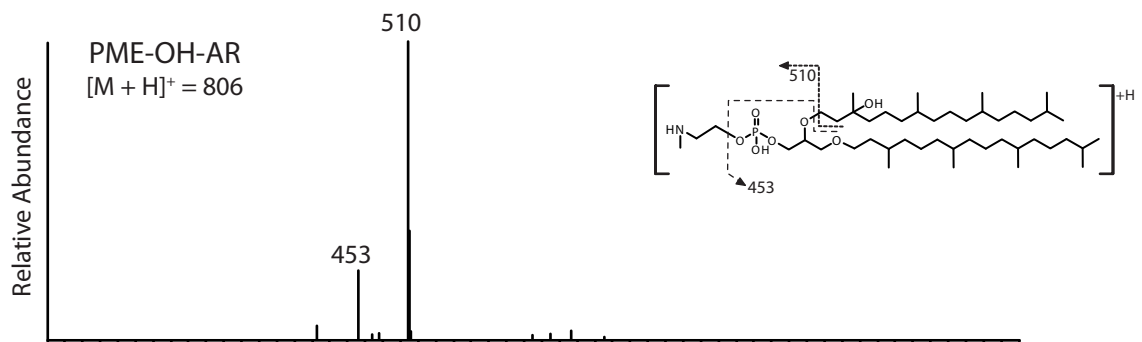
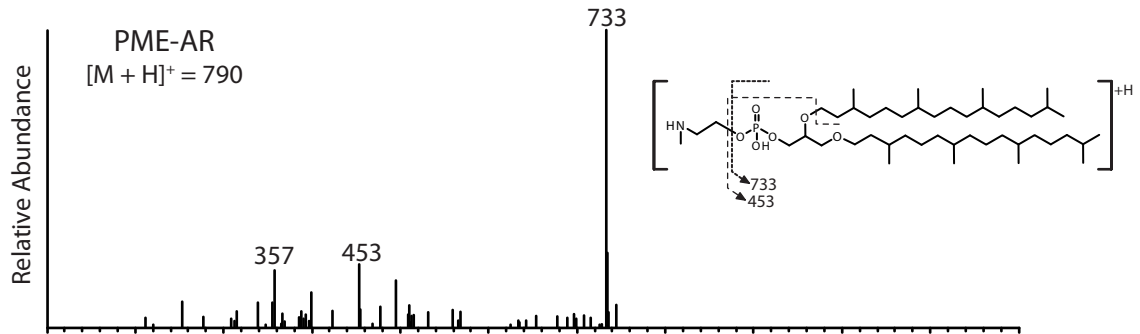
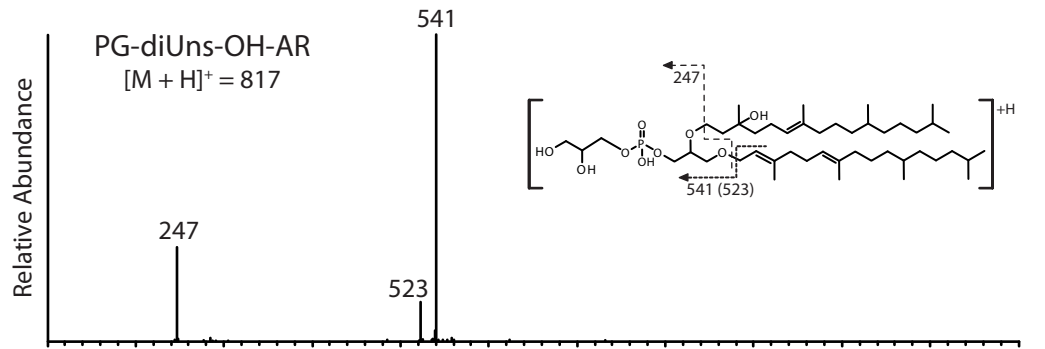
Previous publications using HPLC/ESI-ITMSⁿ focused on ecological microbial processes rather than compound elucidation. The present study is a detailed examination of 48 mass spectra of archaeal IPLs from several samples of natural environments (Table IV.1, Fig. IV.2 and Fig. IV.3, and Appendices, see Supporting Information), in which not only the fragmentation patterns of Gly- and Phos-based intact archaeal lipids were depicted, but also novel compounds were tentatively identified. The low concentrations of archaeal IPLs often found in environmental samples prevent the analysis of individual compounds by NMR, which is mandatory for strict structural identification. Improved characterization of previously unknown archaeal IPLs was facilitated by preparative HPLC, which attenuates the influence of the complex organic matrices from natural environments in MS^n experiments. Given the central importance of archaeal membrane lipids in ecological and evolutionary research, this report will be a useful guide for the mass spectral identification of IPLs in both natural environmental samples and microbial cultures.

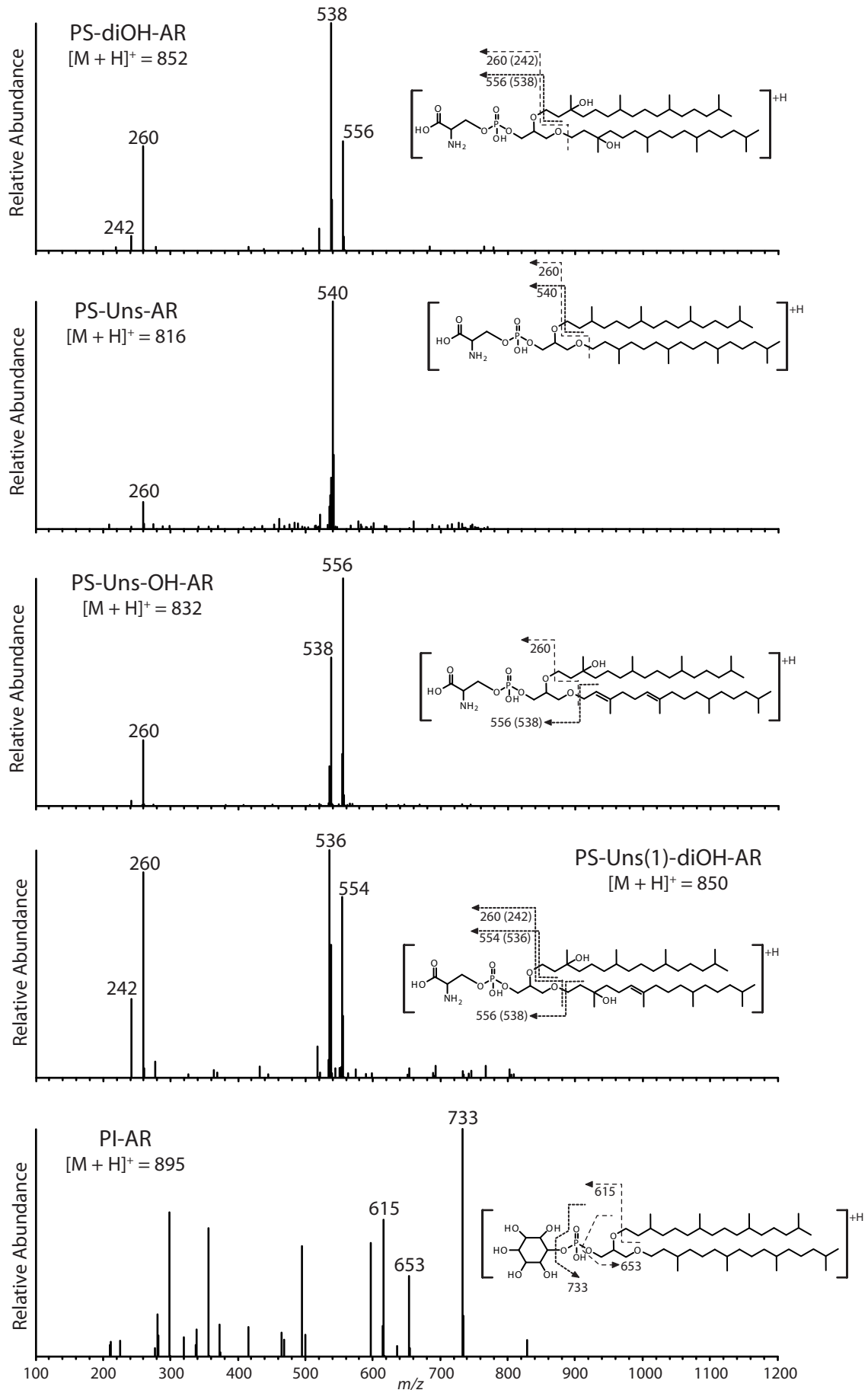
IV.7. Acknowledgements

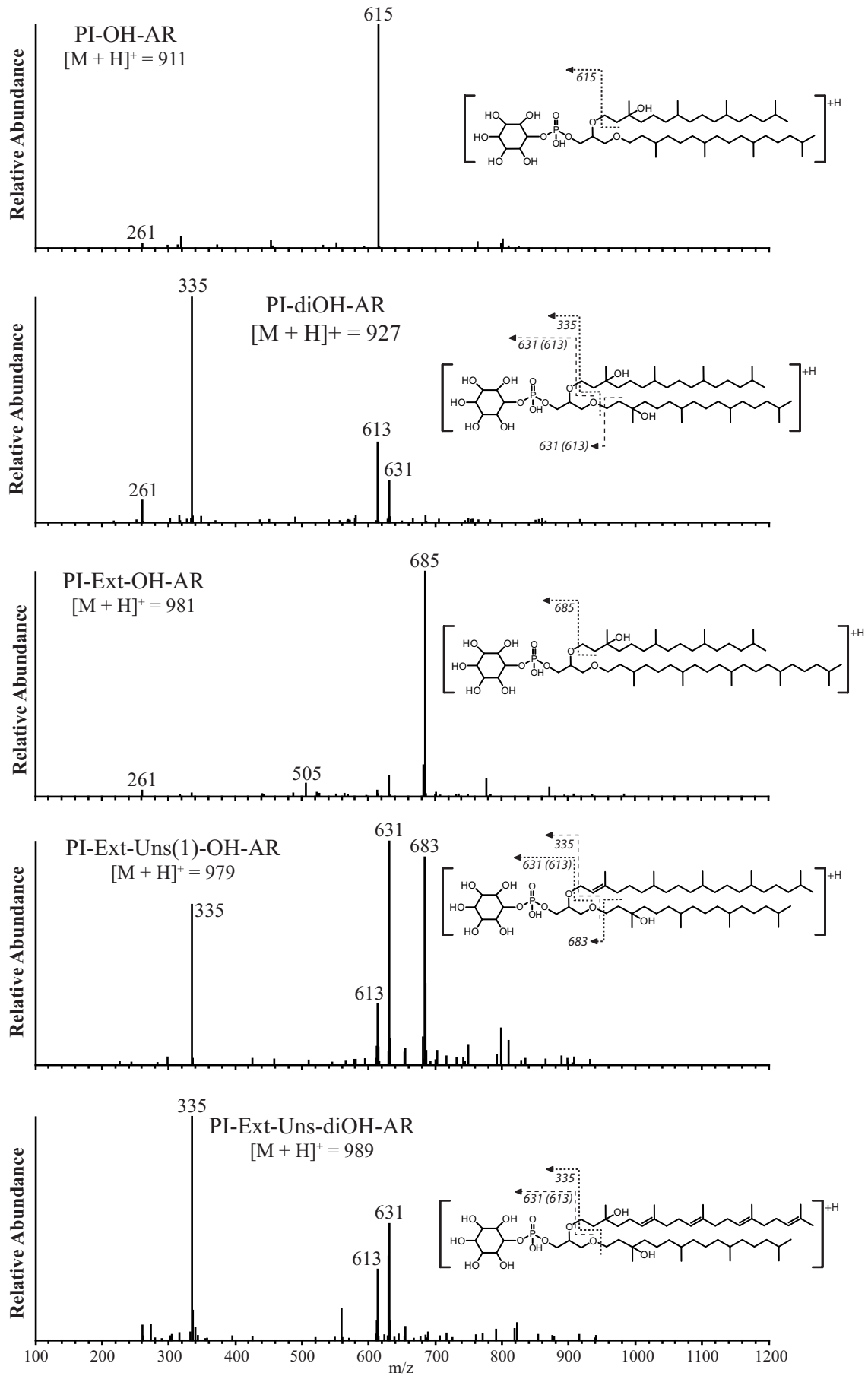
This work was funded by the Alexander von Humboldt Foundation (M.Y.Y.), the DFG-MARUM excellence cluster (M.Y.K., P.E.R., F.S. and J.S.L.) and the European Research Council (ERC advanced grant DARCLIFE to K.-U.H.). The crew and participants of the expedition M74/3 aboard R/V Meteor are acknowledged. The authors are grateful to John W. Pohlman (USGS), who has provided samples from the Cascadia margin and an Alaskan lake for this study.

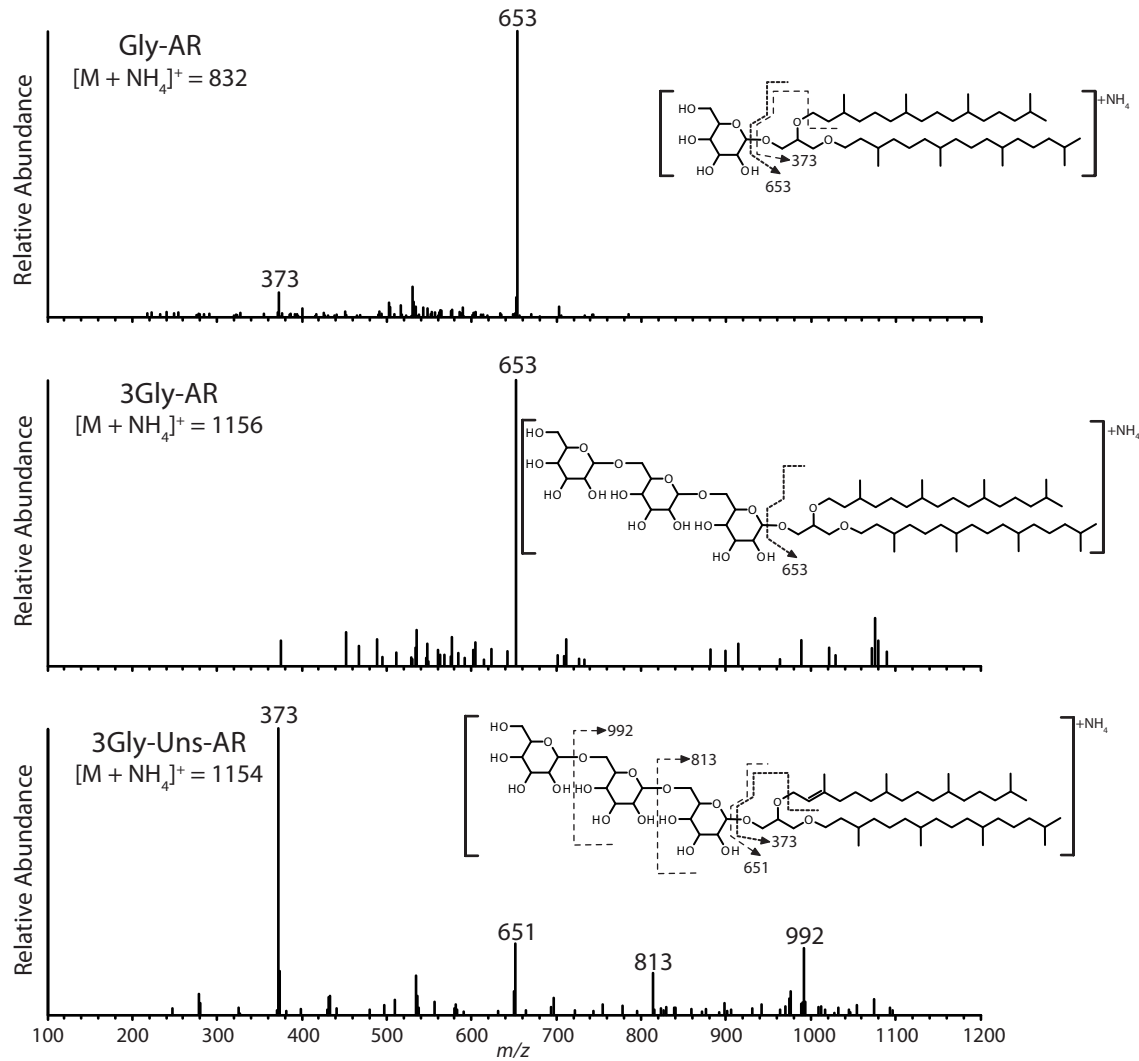
IV.8. Supporting information

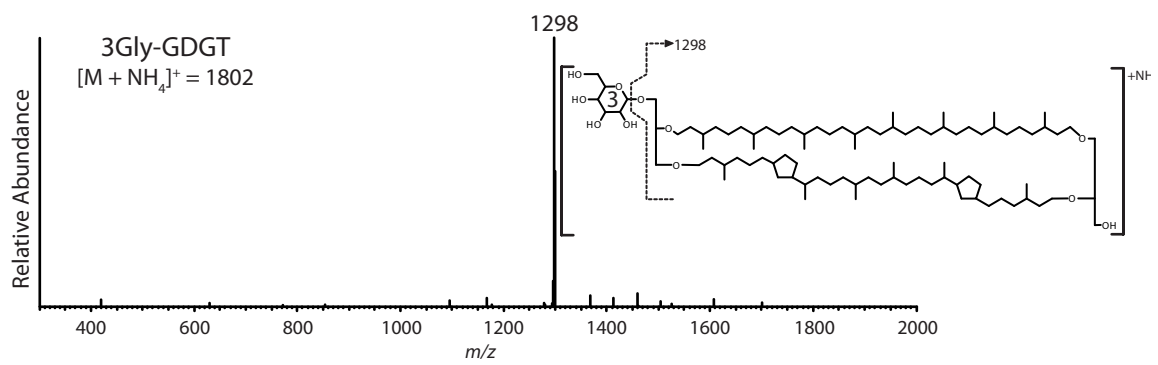
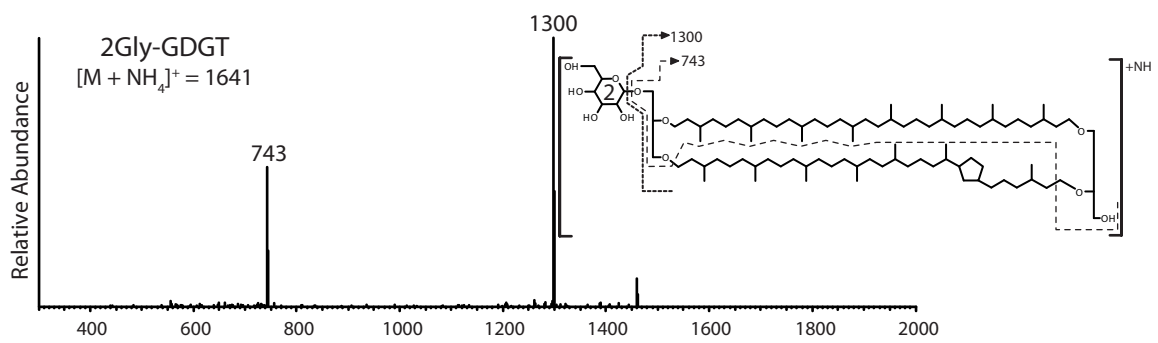
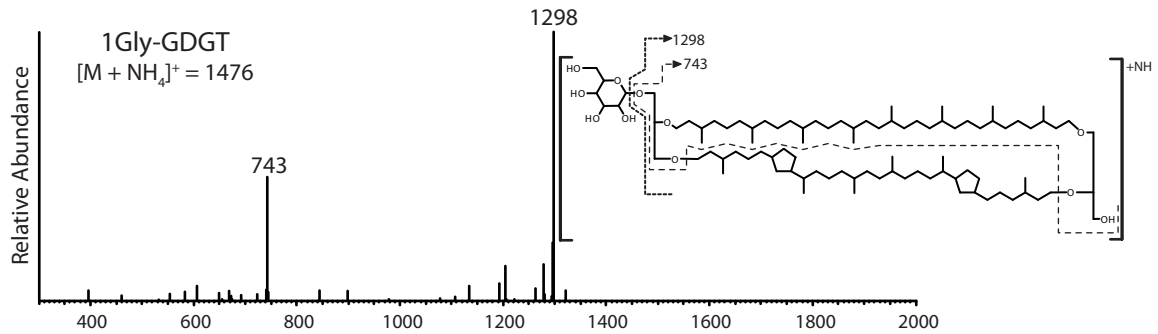


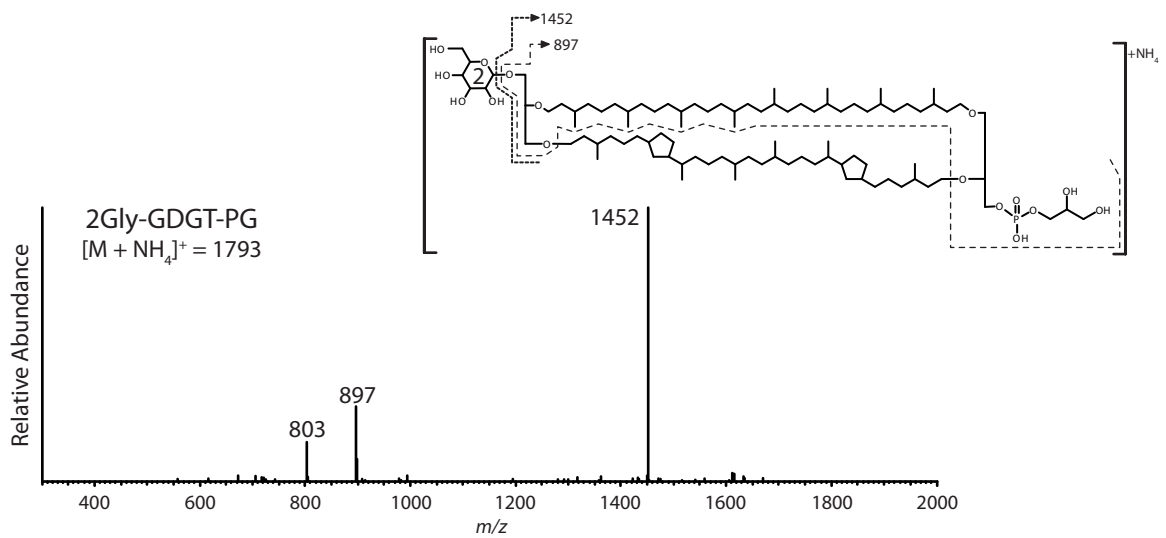
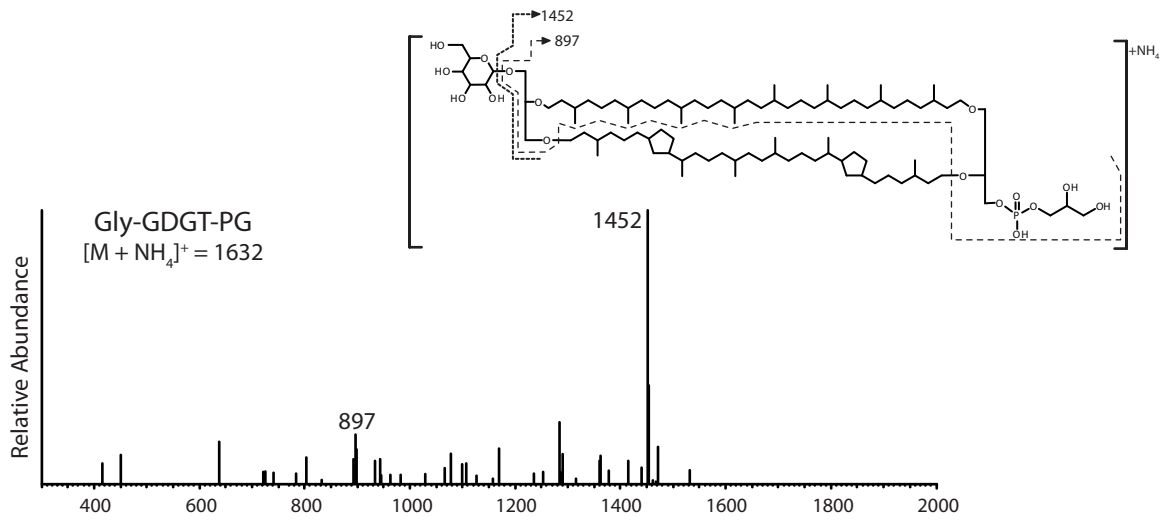
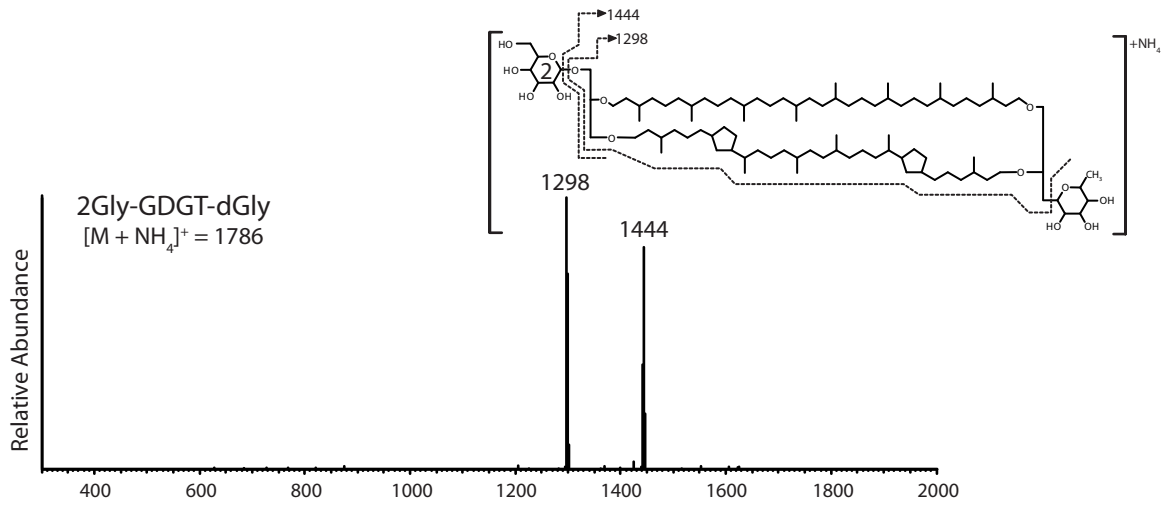


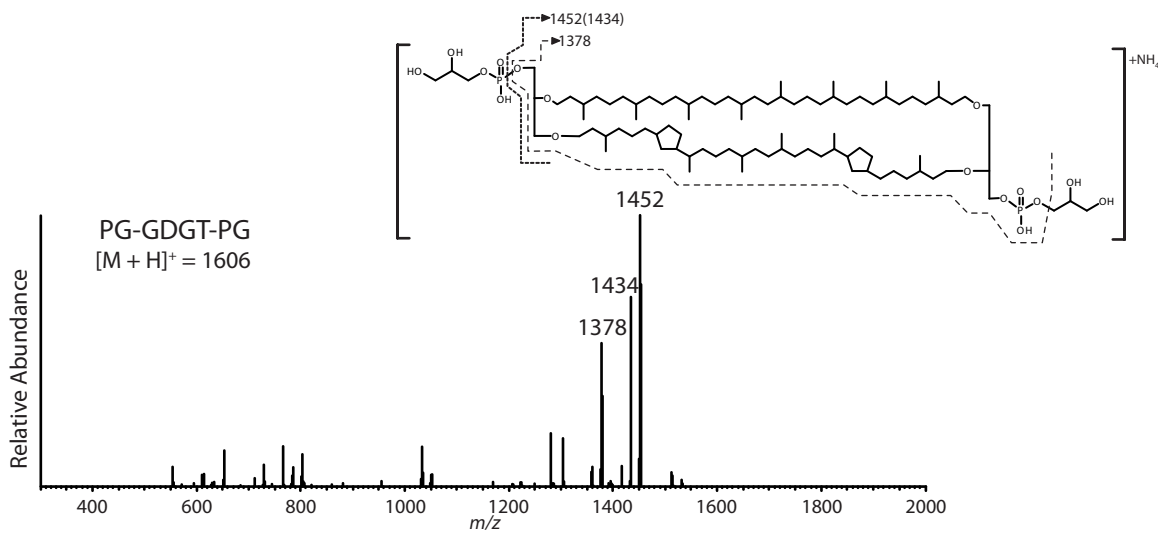
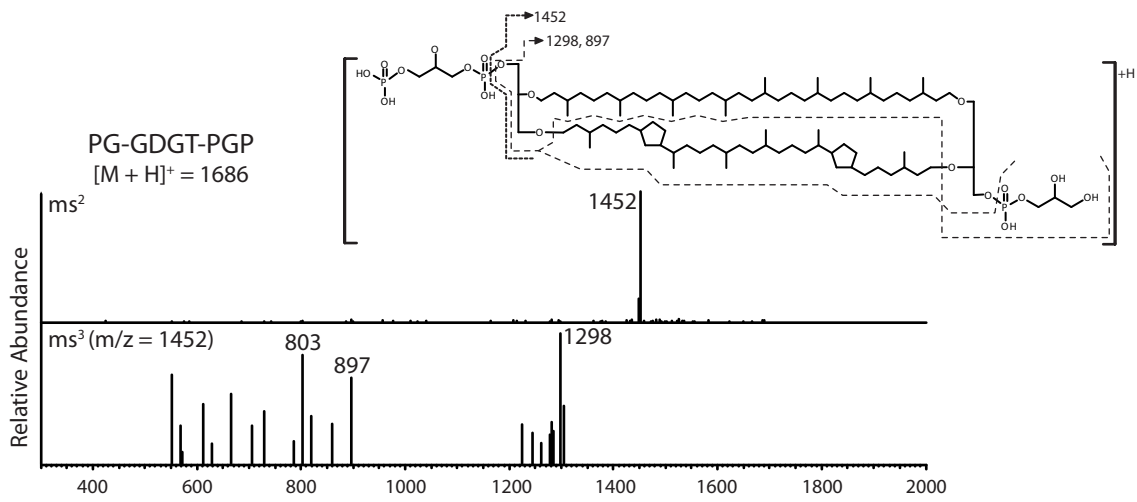
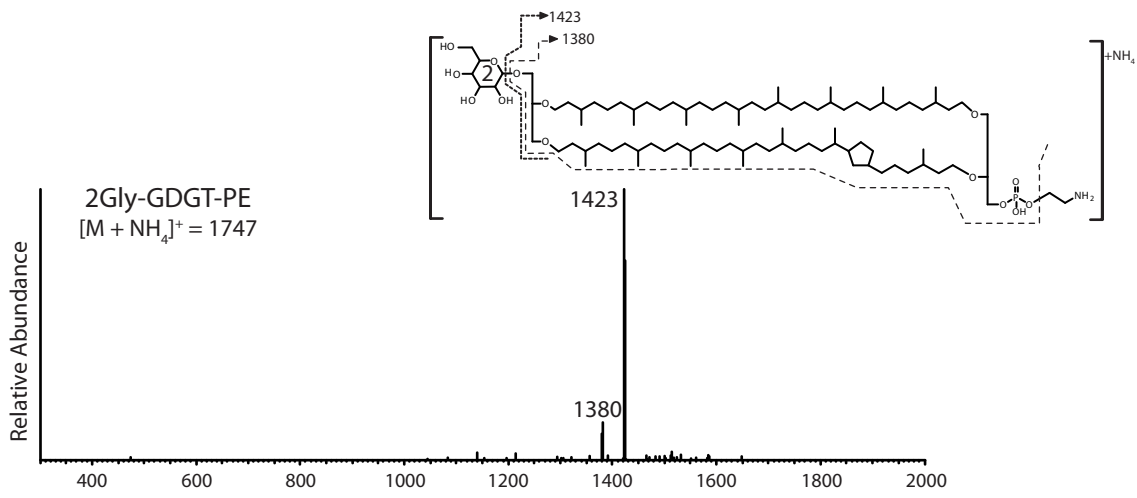












[CHAPTER V] - IPL-SIP / TETRAETHER BIOSYNTHESIS**Stable isotope probing of an anaerobic methane-oxidizing enrichment provides clues on archaeal tetraether lipid biosynthesis**

Matthias Y. Kellermann^{a*}, Marcos Y. Yoshinaga^a, Gunter Wegener^{a,b}, Yu-Shih Lin^a, Thomas Holler^b, Kai-Uwe Hinrichs^a

For submission to:

Geochimica et Cosmochimica Acta

- ^a Organic Geochemistry Group, MARUM Center for Marine Environmental Sciences & Department of Geosciences, University of Bremen, Leobener Strasse, D-28359 Bremen, Germany
^b Max Planck Institute for Marine Microbiology, Celsiusstr. 1, D-28359 Bremen, Germany

- * Corresponding author.
Tel.: +49 421 218 65742; Fax: + 49 421 218 65715
E-mail address: kellermann.matthias@gmail.com

Keywords:

¹³C assimilation | Archaea | diether | tetraether | ANME-1 enrichment | IPL-SIP | *de novo* lipid biosynthesis | tetraether biosynthesis | 2Gly-GDGTs

V.1. Abstract

This stable isotope probing (SIP) study aimed at evaluating the ^{13}C assimilation into individual archaeal intact polar lipids (IPLs). The SIP experiments were conducted in natural enrichment of thermophilic microbes performing the anaerobic oxidation of methane (AOM). Metabolic activity of the anaerobic methanotrophic (ANME) archaea was stimulated by amending the incubations with methane and ^{13}C -labeled bicarbonate in a time series (0, 10, 17 and 24 days) at 37°C. Archaeal lipids were chemically hydrolyzed for isoprenoids (phytanes and biphytanes), sugar moieties and glycerol backbone ^{13}C analysis. Intact compared to bulk archaeal lipids incorporated 5 and 35 times more label in archaeols (ARs) and glycerol dibiphytanyl glycerol tetraethers (GDGTs), respectively. Archaeal IPL distribution indicated a predominance of ANME-1 methanotrophs and additional membrane lipid characteristics (e.g., presence of macrocyclic AR and degree of cyclization in biphytanes) evidenced archaeal membrane adaptations to thrive under elevated temperatures. ^{13}C uptake demonstrated unambiguously *de novo* lipid synthesis, with generally higher incorporation in the isoprenoidal chains compared to sugar moieties and glycerol backbones. A progression in ^{13}C uptake for individual IPLs from this thermophilic ANME-1 enrichment revealed a possible precursor role of a diether phospholipid and glycosidic tetraethers as end-products lipid biosynthesis. Our findings have potential implications for understanding cell-membrane composition in environments under heat and/or energy stress.

V.2. Introduction

The anaerobic oxidation of methane (AOM) is considered as effective biofilter for methane fluxes from marine sediments to the water column, minimizing the oceans contribution to the atmospheric methane budget to only ~2% (Reeburgh, 2007). In marine cold seeps, the oxidation of methane is coupled to sulfate reduction and performed by a syntrophic association of anaerobic methanotrophic archaea and sulfate reducing bacteria (ANMEs and SRBs, respectively, Hinrichs et al., 1999; Hinrichs and Boetius, 2002; Knittel and Boetius, 2009). The stable carbon isotopic composition of whole cells and lipids from ANMEs and SRBs is generally characterized by strong ^{13}C depletion, ranging from -60‰ to -130‰, leading to the conclusion that AOM microbial communities directly assimilate ^{13}C -depleted methane (Elvert et al., 1999; Hinrichs et al., 1999; Pancost et al., 2001; Orphan et al., 2002; Blumenberg et al., 2004; Niemann and Elvert, 2008). Further insights into the activity and C-metabolism of AOM microbes were provided by stable isotope probing (SIP) experiments using ^{13}C -labelled methane and bicarbonate in "ex situ" AOM natural enrichments. These incubation experiments revealed that lipid biosynthesis occurred via bicarbonate uptake in SRBs, i.e. strict autotrophy, whereas a significant portion of carbon in archaeal lipids derived from methane assimilation (Wegener et al., 2008). However, the long incubation time employed (e.g. 176 to 316 days) and the analysis of total lipid extracts (TLE) could have potentially introduced biases in those AOM-SIP experiments. For instance,

cross-feeding of ^{13}C from the primary consumer to the rest of the community in long-term SIP incubations (Dumont and Murrell, 2005) and isotope dilution combining free and intact lipid pools, thereby mixing signals from fossil and living microbial biomass.

More compelling results were obtained with SIP experiments performed in a recently isolated thermophilic AOM enrichment from the Guaymas Basin sediments with apparent doubling time of 68 days (Kellermann et al., in preparation; cf. Holler et al., 2011). Kellermann and colleagues (in preparation) inoculated these AOM enrichments with unlabeled methane in combination with a dual labeling approach ($\text{D}_2\text{O}/^{13}\text{C}$ -bicarbonate; cf. Wegener et al., in revision) for only 24 days, and thus identified autotrophic carbon fixation as the dominant pathway for both archaeal and bacterial biomass build up. Furthermore, these authors detected, by examining the TLE, a significant discrepancy of low lipid production versus high concentration of archaeal tetraether lipids. This result was attributed to the presence of a large pool of fossil relative to intact glycerol dibiphytanyl glycerol tetraethers (GDGTs). Similarly, a dilution in label assimilation by the fossil archaeal lipid component could potentially explain the greater ^{13}C uptake into bacterial than into archaeal lipids found by Blumenberg et al. (2005) and Wegener et al. (2008). In conclusion, the previous lipid-SIP studies in AOM enrichments might have underestimated the actual archaeal activity in response to ^{13}C -labelled substrates by analyzing the TLE rather than the intact lipid pool.

In AOM environments, intact polar lipids (IPLs) from Archaea encompass a wide array of structures, in which both the polar headgroup (e.g., glyco-, phospho- and glycophospho-based headgroups) and several combinations of diether and tetraether core lipids result in a diverse range of IPLs, which can be readily analyzed using high performance liquid chromatography/mass spectrometry (HPLC/MS; Rossel et al., 2008; 2011; Schubotz et al., 2011; Yoshinaga et al., 2011). Because of the finite lifetime of IPLs after cell death (White et al., 1979; Harvey et al., 1986), IPLs are considered to concentrate signals of living biomass in environmental samples in comparison to analytical strategies that target total lipids. Benefitting from the recent developments in preparative HPLC (Biddle et al., 2006; Lin et al., 2010; Schubotz et al., 2011; Lin et al., in preparation), we aimed at examining the assimilation of ^{13}C -labelled bicarbonate into individual archaeal IPLs in thermophilic AOM enrichments. The present IPL-SIP study sought to: (1) compare the ^{13}C uptake into TLE and IPLs; (2) describe the sources of IPLs; (3) identify possible inter- and intramolecular differences in label assimilation; (4) evaluate the *de novo* synthesis of IPLs in Archaea.

V.3. Material and Methods

V.3.1. SIP experimental design

Sediments samples were taken by push-coring a gas-rich, *Beggiatoa* – covered hydrothermal site in the Guaymas Basin (Alvin dive 4570; 27°00.437 N, 111°24.548 W) during the R/V Atlantis cruise AT15–56 (cf. Holler et al., 2011). Retrieved samples were homogenized,

transferred into Duran bottles, diluted with artificial anaerobic seawater medium (Widdel and Bak, 1992) and stored with a methane headspace. A sediment batch of the same material incubated at 50°C for 90 days obtained archaeal 16S rRNA genes and transcribed *mcrA* genes clearly enriched in ANME-1, which represented 82 and 94% of total archaeal sequences, respectively (Holler et al., 2011). After 90 days of pre-incubation at 37°C, sediment enrichments were transferred into 256 mL culture vials. Previous results demonstrated pure autotrophic growth of archaea in this thermophilic AOM enrichment (Kellermann et al., in preparation). Sediment slurries (75 mL, ~4 g dry mass (gdm)) were diluted with 75 mL artificial anaerobic seawater medium and spiked with ¹³C-labeled bicarbonate. Samples were incubated at 37°C under methane atmosphere (200 kPa) for 0, 10, 17 and 24 days ((t(0), t(10), t(17), t(24)). Samples were stored on shaking tables and sulfide production constantly monitored spectrophotometrically during the experiment (Cord-Ruwisch, 1985).

At the end of each incubation period, aliquots of the medium were sampled, filtered through 0.2 µm nylon filters; (Rotilabo®, Karlsruhe, Germany) and stored headspace-free in 6 mL Exetainer® vials (Labco, Buckinghamshire, UK). To determine the ¹³C labeling strength of the media for all incubations, 3 mL of the medium was replaced with He, and the residual aquatic solution acidified using 100 µL of 4 N H₃PO₄. Subsequently, CO₂ released into the gaseous phase was analyzed for its isotopic composition using a gas chromatograph coupled to a continuous-flow isotope ratios mass spectrometer (VG Optima), resulting in δ¹³C values of ~8,300±300‰ (average value of all time points, Kellermann et al., in preparation).

V.3.2. IPL extraction

Sediment enrichments were extracted using a modified Bligh and Dyer protocol (Bligh and Dyer, 1959) with a mixture of dichloromethane (DCM) : methanol (MeOH) : buffer (1:2:0.8), twice neutrally buffered at pH 7 using phosphate buffer and twice buffered at pH 2 with trichloroacetic acid. Finally, all aqueous and organic phases were combined and washed against DCM and water, respectively, to obtain the TLE (cf. Sturt et al., 2004).

The TLEs were dissolved in 500 µL of 5:1 DCM:MeOH and the analysis of IPLs utilized using a ThermoFinnigan Surveyor high performance liquid chromatography (HPLC) system equipped with a LiChrosphere Diol-100 column (2.1 x 150 mm, 5 µm particle size; Alltech, Germany) coupled to a ThermoFinnigan LCQ Deca XP Plus ion trap mass spectrometer (MS), equipped with an electrospray ionization (ESI) interface using settings previously described (Sturt et al., 2004). Archaeal IPLs were identified according to their fragmentation patterns during MS/MS experiments (cf. Yoshinaga et al., 2011).

V.3.3. Preparative HPLC

For purification of individual IPL fraction, we applied a combination of normal- and reverse-phase preparative HPLC. Normal-phase separation was performed on a LiChrosphere Diol-100 column (250 x 10 mm, 5 µm particle size; Alltech Associates Inc.), connected to a guard column containing the same packing material, both operated at room temperature (Lin et al.,

2010; Kellermann et al., 2011). The flow rate was set to 1.5 mL min^{-1} , and the eluent gradient was: 100% A to 65% B in 120 min, hold at 65% B for 30 min, then 30 min column re-equilibration with 100% A; where eluent A was composed of *n*-hexane/2-propanol (8:2, v:v) and eluent B was 2-propanol/MilliQ water (9:1, v:v). The fraction collector (Gilson FC204) separated a total of 12 fractions over 120 min (Fig. V.1). Co-elution of diglycosidic (2Gly)-GDGT and 2Gly-AR in fraction 4 (F_N -4) was further separated by the reverse-phase preparative column Eclipse XDB-C₁₈, (250 x 9.4 mm, 5 μm particle size; Agilent, Böblingen, Germany) operated at 40°C and the flow rate was set to 2 mL min^{-1} with the following solvent gradient: from 100% A to 100% B in 50 min, then hold for 20 min at 100% B, and finally 30 min column re-equilibration with 100% A; where eluent A and B were, respectively, 100% methanol and 100% 2-propanol. The time-based fraction collector was programmed to retrieve 2 fractions containing the targeted compounds (Fig. V.1). Separation and purity of all fractions obtained from normal- and reverse-phase preparative HPLC was verified by repeated analysis by HPLC-MS as above.

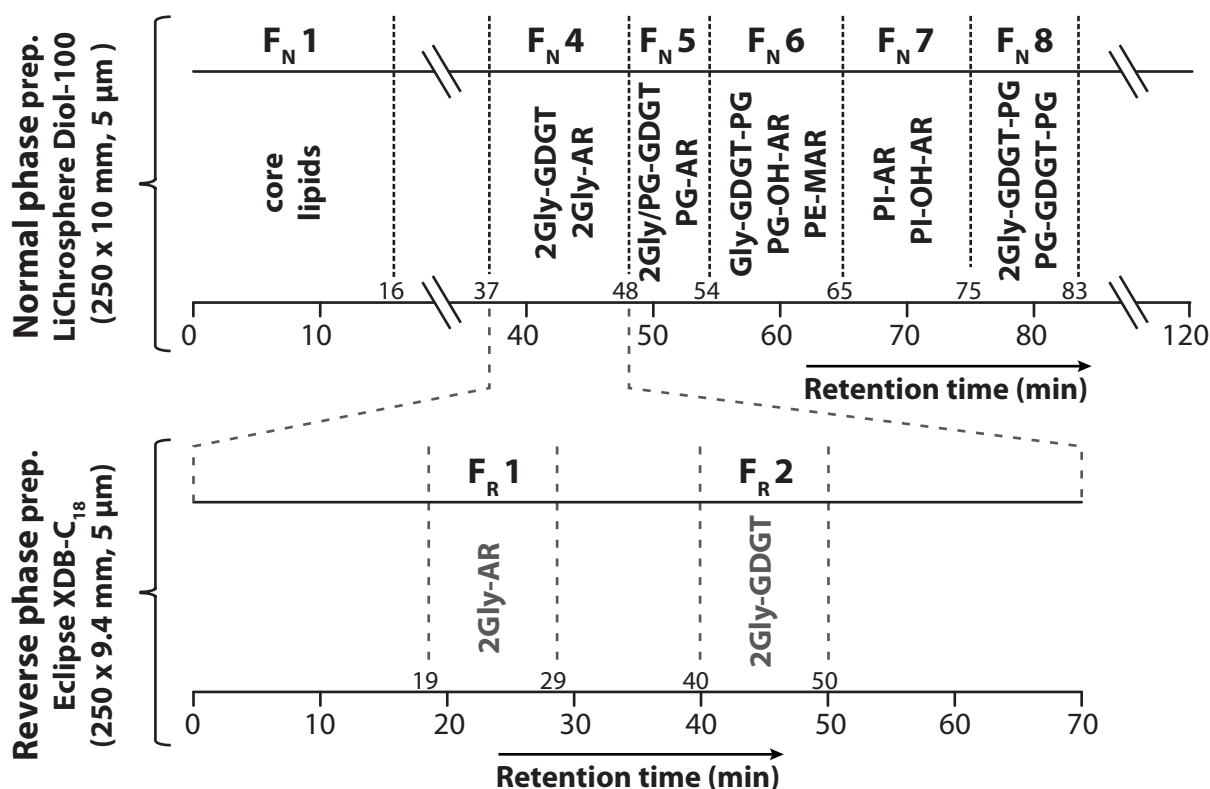


Fig. V.1. Schematic diagram showing all major archaeal IPLs separated by preparative HPLC operating in normal-phase (fractions: F_N 1– F_N 8) and reverse-phase (F_R 1– F_R 2). Compound abbreviations, GDGT: glycerol dibiphytanyl glycerol tetraether (C_{40} – C_{40} isoprenoidal chains); AR: archaeol (C_{20} – C_{20} isoprenoidal chains); OH-AR: monohydroxylated-archaeol; MAR: macrocyclic-archaeol; Gly: glycosyl (hexose); PE: phosphatidylethanolamine; PG: phosphatidylglycerol; PI: phosphatidylinositol.

V.3.4. Sugar analysis (acid hydrolysis)

The procedure to analyze sugar moieties from individual IPLs containing glycosidic headgroups has been described in Lin et al. (2010). In brief, the glycosidic containing IPL fractions

(F_R 1, 2Gly-AR; F_R 2, 2Gly-GDGT, F_N 7, PI-AR, PI-OH-AR; F_N 8, 2Gly-GDGT-PG) were treated with 50% trifluoroacetic acid at 70°C over night (at least 8 hrs). After hydrolysis, the remaining TFA solution was neutralized by complete evaporation using a gentle stream of N₂ while seated on a heating plate set to 50°C. To separate the released monosaccharides from the core lipids, we added DCM and Milli-Q water (each 1 mL) and performed a liquid-liquid extraction. The DCM phase was collected and the aqueous phase re-extracted five times with DCM. The combined DCM phases, containing core AR and GDGTs, were evaporated to dryness and stored at -20°C until further analysis. After addition of an internal standard (3-O-methyl-D-glucopyranose, 1 µg), the aqueous phase containing lipid-derived sugars was blown down mildly to < 100 µL at 50°C and finally freeze-dried overnight to ensure complete dehydration. For isotopic analysis of sugars, aldonitrile derivatives were prepared (according to Guerrant and Moss (1984). Prior to gas chromatography (GC) analysis, the derivatives were purified using a self-packed silica gel column (0.5 g of pre-activated silica, 0.06–0.2 mm; Carl Roth GmbH, Karlsruhe, Germany), using 8 mL of hexane/ethyl acetate (1:1, v/v) as eluent.

V.3.5. Isoprenoidal side chains (ether cleavage and subsequent reduction)

Archaeal isoprenoidal moieties were released and subsequently reduced to hydrocarbons using a modified protocol described by Summons et al. (1998). In brief, the prepped IPL fractions were treated with 200 µL boron tribromide (Aldrich, St. Louis, MO, USA) dissolved in dry DCM. After ether cleavage, the products were separated via liquid-liquid extraction into isoprenoidal hydrocarbons (DCM phase) and free glycerols (aqueous phase; Lin et al., in preparation). The aqueous was stored at 4°C until further analysis (see section V.3.6). The DCM phase was dried and the alkyl bromides subsequently reduced using 200 µL of 1 M solution of lithium triethylborohydrate in tetrahydrofuran (Aldrich, St. Louis, MO, USA). Finally, prior to GC analysis, products of ether cleavage were purified by passing through a short silica gel column (0.2 g of pre-activated silica, 0.06–0.2 mm) by elution with hexane.

V.3.6. Glycerol moieties

The preparation of the glycerol moieties has been described in more detail in Lin et al. (in preparation). Briefly, the remaining DCM within the aqueous phase left from the liquid-liquid extraction after ether cleavage (see section V.3.5), was evaporated on a heating plate (80°C). Subsequently, the DCM-free aqueous phase was then neutralized with silver carbonate (Aldrich, St. Louis, MO, USA), centrifuged and the supernatant filtered (PTFE, 0.45 µm, 13 mm diameter, Carl Roth GmbH, Karlsruhe, Germany) and collected. The silver carbonate precipitate was washed twice with additionally 500 µL Milli-Q, filtered and all supernatants were combined. The aqueous solution was dried completely overnight (at 80°C) and the residue re-dissolved in 500 µL cold ethanol, vortexed, centrifuged and the supernatant transferred to another vial. This washing step with ethanol was repeated two more times. The ethanol was blown down mildly to < 100 µL at 80°C, an internal standard was added (~1 µg of 1,2 cyclohexanediol) and finally

evaporated to complete dryness by heat only (at 80°C). For derivatization 200 µL of pyridine and 100 µL N,O-bis(trimethylsilyl)trifluoroacetamide (BSTFA) were added and kept at 70°C for 1 h. Finally, prior to GC analysis, the derivatives were purified using a self-packed silica gel column (0.4 g of pre-activated silica, 0.06–0.2 mm; Carl Roth GmbH, Karlsruhe, Germany), using 5 mL of hexane/ethyl acetate (1:1, v/v) as eluent.

V.3.7. Gas chromatography

Isoprenoidal hydrocarbons, sugar headgroups and glycerol moieties derived from individual intact di- and tetraether fractions were quantified by GC coupled to a flame ionization detector (FID; ThermoFinnigan, San Jose, CA). For quantification of phytane and biphytanes, squalane (20 ng) was used as injection standard. The GC was equipped with a Rxi-5ms capillary column (Restek GmbH, Bad Homburg, Germany; L=30 m; ID=0.25 mm; 0.25 µm film thickness; carrier gas: He, flow rate 1 mL min⁻¹). All samples were injected into the GC at 300°C in splitless mode. For hydrocarbons, the GC was programmed from 60°C (hold for 1 min), followed by heating at 10°C min⁻¹ to 150°C, then at 4°C min⁻¹ to 320°C and hold for 27.5 min. GC operation modes for the analysis of sugars and glycerol can be found respectively in Lin et al. (2010; in preparation)

Stable carbon isotopic compositions of isoprenoids, sugar headgroups and glycerol moieties were determined using a GC-isotope ratio-MS (Trace GC Ultra coupled to a GC-IsoLink, ConFlow IV interface and a DeltaV Plus isotope ratio mass spectrometer, all from Thermo Scientific GmbH). GC conditions were the same utilized for the GC-FID. Compounds were oxidized in a combustion interface at 940°C. Stable carbon isotopic compositions are expressed as δ¹³C values in the per mil (‰) notation relative to VPDB standards. The analytical error was <0.5‰ for non-labeled δ¹³C values, respectively. δ¹³C values were corrected for additional carbon introduced during derivatization.

V.4. Results and Discussion

V.4.1. Increased sensitivity of IPL-SIP over TLE-SIP

Both archaeal lipids from the TLE and IPL pools were quantified, after ether cleavage, as phytane (derived from diether lipids or archaeols, ARs) and biphytanes (from tetraether lipids or GDGTs) for comparison. The majority of the total archaeal lipid pool was composed of non-IPLs (~97%), i.e., compounds with a presumed high fraction of lipids from dead biomass, with the major compounds being GDGTs (biphytanes, BP 0–3; 75.8±3.2%) and to a lesser extent from AR (phytane, Phy; 21.2±2.3%; Fig. 2a). These fractions of IPLs are somewhat lower but generally consistent with previously reported ranges in marine sediments (Lipp and Hinrichs, 2009; Liu et al., 2011). By contrast, the intact ARs and GDGTs (quantified as Phy and BP, respectively) accounted for only 3.0±0.2% of the total archaeal lipid pool, contributing 1.2±0.1% and 1.8±0.1, respectively (Fig. V.2a). In our study, intact ARs represented 5.3±0.5% of the total AR pool,

whereas intact GDGTs contributed only $2.3 \pm 0.1\%$ relative to the total GDGT pool (Fig. V.2a).

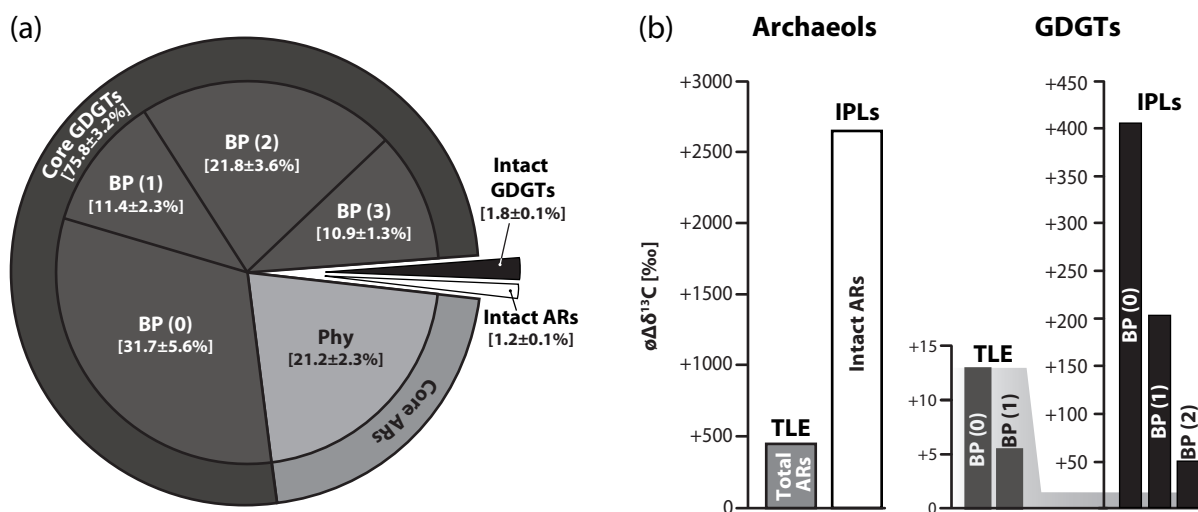


Fig. V.2. (a) Relative archaeal lipid composition: core and intact di- and tetraether lipids determined after ether cleavage, as phytane (derived from diether lipids or ARs) and biphytanes (from tetraether lipids or GDGTs) relative to an injection standard (squalane) by GC-FID. (b) Total ^{13}C -bicarbonate uptake, $t(24)$ relative to $t(0)$ [$\Delta\delta^{13}\text{C}$], in bulk (TLE) versus IPL derived phytanes and biphytanes. Intact polar di- and tetraether lipids are displayed as weighted average alteration (Δ), taking into account the concentrations and $\delta^{13}\text{C}$ values of IPLs. Compound abbreviations, BP: biphytane; (0 to 3): cyclic rings; Phy: phytane.

The ^{13}C assimilation into intact ARs was more than 5 times greater compared to the total ARs pool, while the intact GDGT indicated an even stronger increase of >35 times relative to total GDGTs (Fig. V.2b). We were able to demonstrate that the ^{13}C -uptake was highest in intact acyclic followed by mono- and bicyclic biphytanes, a fact underscored by TLE based analysis (Fig. V.2c; Table V.1; cf. Blumenberg et al., 2005). In addition, the apolar fraction of the preparative HPLC (i.e. total fossil pool, $F_N 1$; Fig. V.1) showed a total alteration of 10 and 2‰ in ^{13}C uptake for phytane (phy) and acyclic biphytane, respectively (Table V.1). This result likely reflects turnover of recently produced IPLs. Taken together, our results clearly show an increase in SIP sensitivity by focusing on the intact archaeal lipid pool, and thus demonstrate that the label uptake of archaeal communities was largely underestimated by previous TLE-SIP in in vitro AOM studies (e.g. Blumenberg et al., 2005, Wegener et al., 2008, Kellermann et al., in preparation).

Table V.1. Absolute concentrations, stable carbon isotopic composition ($\delta^{13}\text{C}$) and ^{13}C -incorporation of archaeal bulk (TLE), apolar ($F_{\text{N}-1}$) and intact di- and tetraether lipid fractions. All lipids were quantified, after ether cleavage, as phytane (derived from diether lipids or ARs) and biphytanes (from tetraether lipids or GDGTs) relative to an injection standard (squalane) by GC-FID. Averaged lipid concentrations and standard deviations for all incubation periods ($t = 0$ to 24 days) are provided. $\delta^{13}\text{C}$ is given for $t(0)$ and total label uptake relative to $t(0)$ [$\Delta\delta^{13}\text{C}$] are expressed for days of incubations $t(10)$, $t(17)$ and $t(24)$. All isotopic values are given in per mil (‰). For compound abbreviations the reader is referred to Fig. V.1 and Fig. V.2.

	Absolute concentrations and [$\delta^{13}\text{C}$ or $\Delta\delta^{13}\text{C}$] (ng isoprenoids $\text{g}_{\text{dm}}^{-1}$) and [‰]				
	t(0) conc. / [$\delta^{13}\text{C}$]	t(10) conc. / [$\Delta\delta^{13}\text{C}$]	t(17) conc. / [$\Delta\delta^{13}\text{C}$]	t(24) conc. / [$\Delta\delta^{13}\text{C}$]	averaged (ng $\text{g}_{\text{dm}}^{-1}$)
-TLE-					
Phy	6800 [-42]	6500 [+420]	8200 [+454]	7800 [+530]	7300±700
BP(0)	10000 [-27]	9300 [+4]	12000 [+13]	11000 [+12]	11000±1100
BP(1)	3800 [-42]	3300 [±0]	4500 [+5]	4100 [+15]	3900±440
BP(2)	7200 [-41]	5800 [±0]	8400 [±0]	7700 [+2]	7300±940
BP(3)	3500 [-18]	3000 [±0]	4100 [±0]	3700 [±0]	3600±410
-Apolar fraction ($F_{\text{N}-1}$)-					
Phy	6000 [-35]	6900 [+5]	6700 [+7]	6600 [+10]	6500±320
BP(0)	7200 [-26]	8000 [±0]	7400 [+1]	7600 [+2]	7500±300
BP(1)	2500 [-43]	2800 [±0]	2700 [±0]	2900 [±0]	2700±130
BP(2)	5100 [-39]	5700 [±0]	5500 [±0]	5600 [±0]	5500±220
BP(3)	2900 [-19]	3200 [±0]	3000 [±0]	3100 [±0]	3100±100
-Intact ARs [Phy]-					
2Gly-AR ($F_{\text{R}-1}$)	100 [-78]	120 [+390]	70 [+780]	130 [+880]	100±21
PG-AR ($F_{\text{N}-5}$)	88 [-71]	310 [+4300]	110 [+4600]	260 [+5200]	190±94
PG-OH-AR ($F_{\text{N}-6}$)	87 [-61]	85 [+450]	90 [+700]	n.a. [+1100*]	87±2
PI-OH-AR ($F_{\text{N}-7}$)	37 [-64]	17 [+240]	29 [+630]	n.a. [+480]	28±8
PE-MAR ($F_{\text{N}-6}$)	n.a.	n.a.	n.a.	n.a. [+1100*]	n.a.
-Intact GDGTs [BP]-					
SUM-2Gly-GDGT ($F_{\text{R}-2}$)	340 [-65]	440 [+1]	270 [±0]	370 [+16]	350±63
BP(0)	89 [-56]	110 [+1]	67 [+1]	110 [+32]	93±17
BP(1)	120 [-66]	150 [+4]	92 [±0]	120 [+8]	120±20
BP(2)	130 [-69]	180 [±0]	110 [±0]	150 [+12]	140±27
SUM-PG(2Gly)-GDGT ($F_{\text{N}-5}$)	110 [-60]	140 [+77]	63 [+150]	95 [+230]	100±28
BP(0)	35 [-52]	43 [+130]	27 [+190]	39 [+330]	36±6
BP(1)	29 [-60]	36 [+91]	19 [+210]	25 [+230]	27±6
BP(2)	43 [-67]	63 [+23]	17 [+63]	31 [+130]	39±17
SUM-Gly-GDGT-PG ($F_{\text{N}-6}$)	90 [-57]	67 [+59]	94 [+140]	n.a.	84±12
BP(0)	41 [-49]	33 [+86]	35 [+160]	n.a.	36±3
BP(1)	16 [-62]	11 [+67]	15 [+210]	n.a.	14±2
BP(2)	33 [-64]	23 [+25]	43 [+87]	n.a.	33±8
SUM-PG(2Gly)-GDGT-PG ($F_{\text{N}-8}$)	98 [-65]	70 [+380]	94 [+930]	n.a. [+730]	87±12
BP(0)	39 [-60]	32 [+710]	42 [+1500]	n.a. [+920]	38±4
BP(1)	29 [-66]	19 [+270]	27 [+890]	n.a. [+940]	25±4
BP(2)	30 [-70]	19 [+47]	25 [+200]	n.a. [+260]	24±5

(*) $\delta^{13}\text{C}$ values of PG-OH-AR and PE-MAR at $t(24)$ analyzed as core lipid OH-AR and MAR as TMS derivate, respectively, after saponification (e.g., Elvert et al., 2003).
n.a. not analyzed.

V.4.2. Chemotaxonomy of archaeal IPLs

From the total archaeal IPLs, intact GDGTs represented 60% (Fig. V.3a), and were primarily composed of diglycosidic (2Gly)–GDGT, followed by compounds with either phosphatidylglycerol (PG; PG–GDGT, PG–GDGT–PG) or mixed PG and Gly (2Gly–GDGT–PG, Gly–GDGT–PG) as headgroups. In AOM settings, the predominance of intact GDGTs relative to ARs is indicative of seep communities dominated by ANME–1 (Rossel et al., 2008; 2011). Additional chemotaxonomic information can be gained from the sugar headgroups of 2Gly–GDGT and 2Gly–GDGT–PG, which were mainly composed of galactose (Fig. V.3b), the major hexose from ANME–1 dominated seep off the Pakistan margin (Lin et al., 2010). Among the archaeal diethers (40% of total archaeal IPLs; Fig. V.3a), a relatively higher abundance of non–hydroxylated (PG– and 2Gly–ARs) relative to mono–hydroxylated (OH)–ARs (PG and phosphatidylinositol as headgroups) was observed (Fig. V.3a). Differences in proportion of these core lipids are often used to estimate the predominance of ANME–1 or –2 methanotrophic archaea (Blumenberg et al., 2004; Niemann and Elvert, 2008; see also Rossel et al., 2008; 2011 for intact ARs). The low amount of intact OH–ARs and the high abundance and composition of intact GDGTs further support the predominance of ANME–1 over ANME–2 observed in 16S rRNA and *mcrA* gene libraries from this enrichment (Holler et al., 2011).

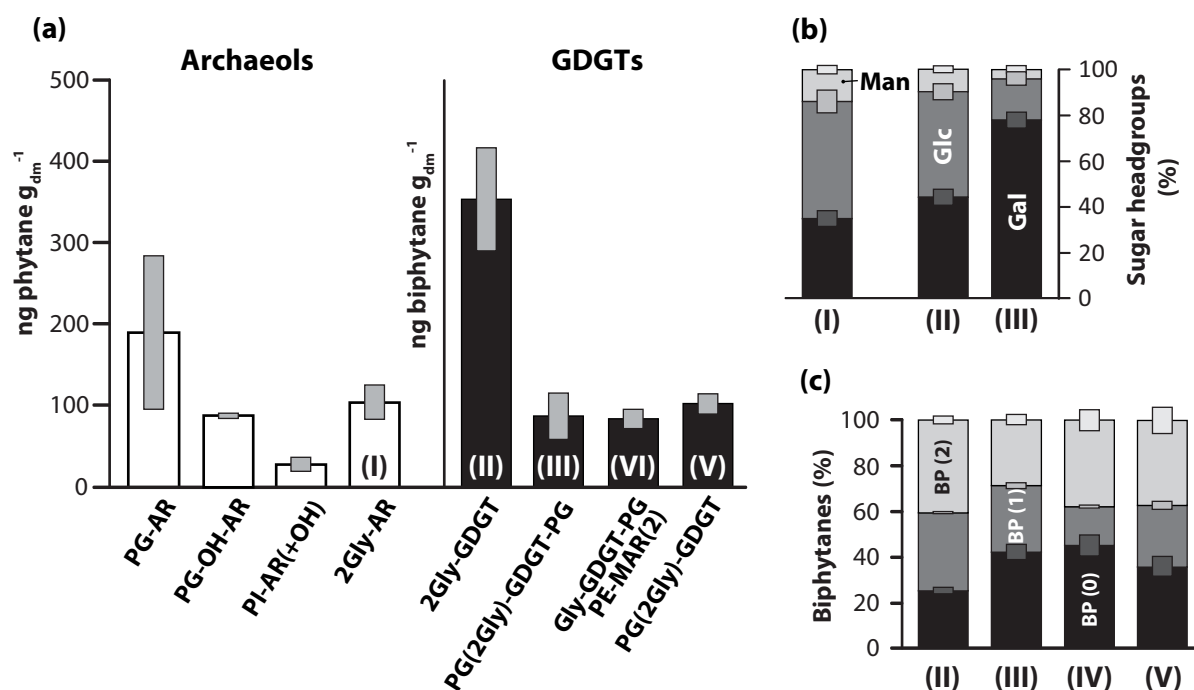


Fig. V.3. (a) Averaged ($t=0$ to 24 days) archaeal IPL absolute concentrations given in ng phytane/biphytane per g_{dm} and their standard deviation (gray bars) (Table 1). (b) Relative sugar headgroup composition in 2Gly–AR (I), 2Gly–GDGT (II) and 2Gly–GDGT–PG (III). (c) Relative distribution of acyclic, one and two cyclopentane rings in biphytanes (BP 0 to 2) from individual tetraether fractions.

Another interesting feature of the archaeal IPL composition from this enrichment was the distribution of pentacyclic rings among intact GDGTs and the presence of an intact

macrocyclic AR (MAR) with phosphatidylethanolamine as headgroup (Fig. V.1, Table V.S1). In cold seep sediments a strong dominance of acyclic relative to cyclic compounds is generally observed for archaeal biphytanes (e.g. Blumenberg et al., 2004, Niemann and Elvert, 2008; Lin et al., 2010). By contrast, the higher contribution of bicyclic relative to acyclic biphytanes detected in this thermophilic enrichment (especially in 2Gly–GDGT, see Fig. V.2c) likely reflects a response of archaeal membranes to increased temperatures from the Guaymas Basin sediments (Gliozzi et al., 1983; Langworthy and Pond, 1986; De Rosa and Gambacorta, 1988; Schouten et al., 2003). MARs are found in the cultured methanogen *Methanococcus jannaschii* (e.g. Comita and Gagosian, 1983; Sprott et al., 1991) and *Methanococcus igneus* (Trincon et al., 1992), but they have also been detected in hydrothermal systems (Blumenberg et al., 2007) and AOM-related settings (Stadnitskaia et al., 2003; Birgel and Peckmann 2008; Yoshinaga et al., 2011). MARs are exclusively lipids of cultured thermophilic methanogens, and their unique structural characteristics have been associated with evolutionary adaptations (e.g. decreased proton permeability of the lipid membrane, Mathai et al., 2001; and resistance to heat stress, Sprott et al., 1991).

Archaeal 16S rRNA and *mcrA* gene libraries from this enrichment point to the predominance of ANME-1, subclusters Guaymas I and II, with relatively minor contribution of *Thermoplasmatales*, *Halobacteriales* and ANME-2 sequences (Holler et al., 2011). The observed unconventional thermophilic aspects of the archaeal lipid membranes (i.e. high contribution of cyclopentane rings in major intact GDGTs and the presence of MAR) seem to be consistent with the phylogenetic separation of the Guaymas subclusters among the widespread ANME-1.

V.4.3. Inter- and intramolecular label uptake into individual IPLs

Both di- and tetraether archaeal IPLs were characterized by ^{13}C -depleted stable carbon isotope values at the beginning of the experiment. For intact ARs $\delta^{13}\text{C}$ values of phytanes ranged from -61 to -78‰ and for intact GDGTs a range from -49 to -70‰ was observed in biphytanes, the latter being more ^{13}C -depleted according to the increase in the number of cyclopentane rings (Table V.1). Those $\delta^{13}\text{C}$ values of lipids have been consistently reported in cold seep sediments and related to archaeal AOM activity (e.g., Elvert et al., 1999; Hinrichs et al., 1999; Blumenberg et al., 2004; Elvert et al., 2005; Niemann and Elvert, 2008).

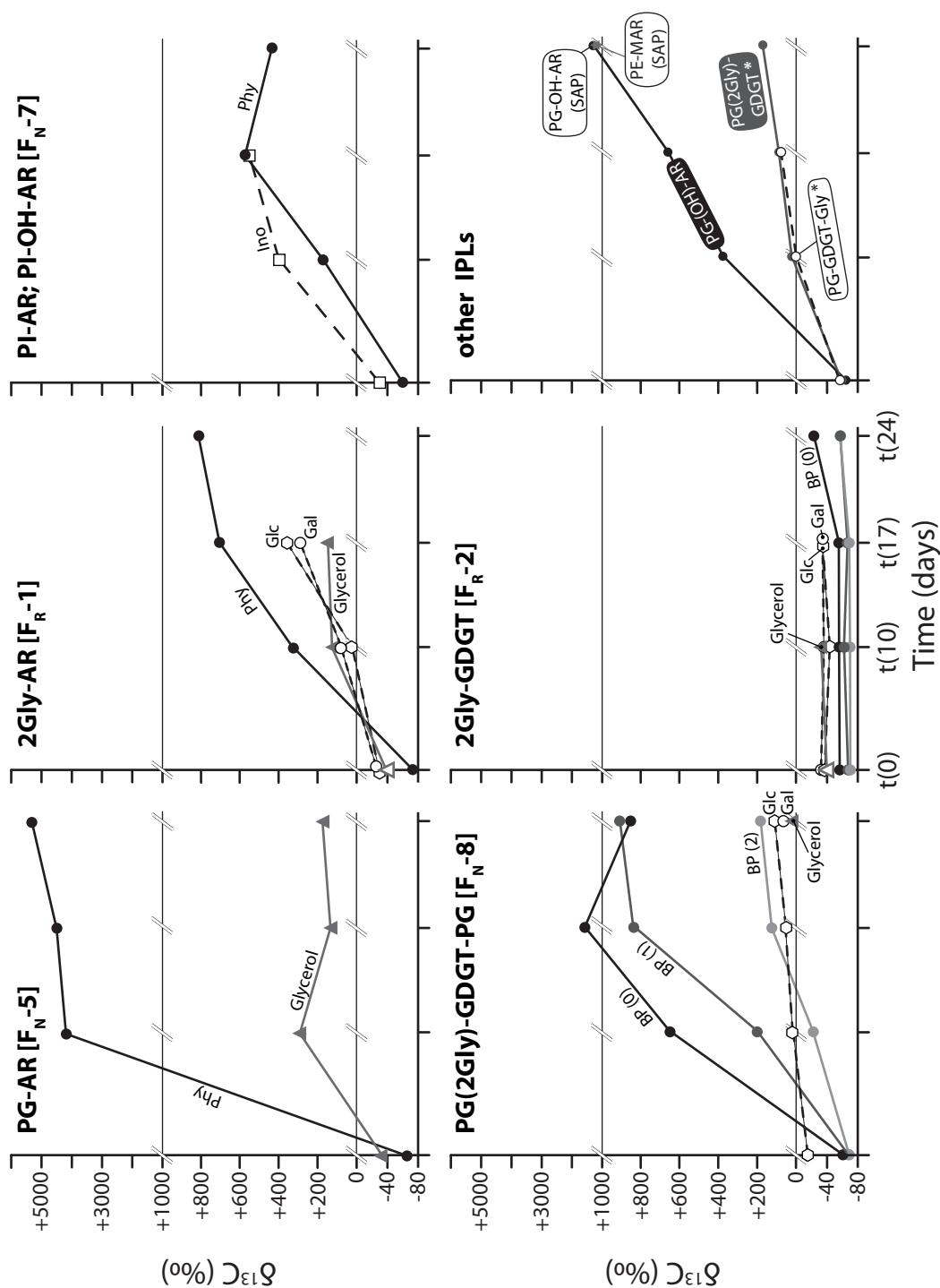


Fig. V.4. Inter- and intramolecular analysis of intact di- and tetraether lipids for 0, 10, 17 and 24 days of incubation with ^{13}C -labeled bicarbonate. $\delta^{13}\text{C}$ (‰) values are shown for hexose headgroups (Glc: glucose, Gal: galactose, Ino: myo-inositol), glycerol backbone and the isoprenoidal side chains (Phy, BP 0–2). PE-MAR and PG-OH-AR at T(24) were measured as core lipid after saponification (SAP). (*) displayed as averaged weight-balanced alteration for biphytanes.

Incubations with ^{13}C -labeled bicarbonate in the presence of methane led to variable alteration of δ values in individual archaeal lipids (Fig. V.4). Although the incubation period was almost 1/3 of the doubling time for the enrichment (Holler et al., 2011), the archaeal lipid concentration has not been significantly altered throughout the incubation periods (Fig. V.3a; Table 1). After 24 days of incubation, the ^{13}C assimilation into intact diether lipids (Fig. V.4; Table V.1) was highest in PG-AR (+5200‰), followed by PG-OH-AR (+1100‰), 2Gly-AR (+880‰) and the mixed fraction of PI-AR and PI-OH-AR (+480‰). PG-AR showed by far the highest ^{13}C uptake, exhibiting an asymptotic curve over time, whereas a linear uptake of ^{13}C was observed

for the other archaeal IPLs (Fig. V.4). Given a label strength of $\delta^{13}\text{C}$ -bicarbonate $\sim 8300\text{‰}$, the uptake of ^{13}C into PG-AR after 10 days represents more than half of total added substrate (ca. 4300‰), indicating that this IPL was approaching equilibrium with the medium, most likely before 10 days (see Fig. V.4). Among the intact GDGTs, higher label assimilation was observed into biphytanes containing acyclic and monocyclic over bicyclic biphytanes, indicating initial synthesis of acyclic and monocyclic relative to bicyclic biphytanes. Averaged weight-balanced alteration (Δ) for biphytanes (0–2 rings) was highest in the fraction PG(2Gly)-GDGT-PG (930‰), followed by PG(2Gly)-GDGT (230‰), Gly-GDGT-PG (140‰; Fig. V.4; Table V.1). Surprisingly low label assimilation was observed into biphytanes from 2Gly-GDGTs (+16‰ at 24 days; Fig. V.4; Table V.1).

With the exception of 2Gly-GDGT, all other archaeal IPLs clearly assimilated ^{13}C in isoprenoids, glycerol moieties and sugar headgroups (Fig. V.4; Table V.1). The co-elution of PI-(OH)-AR with PI-based bacterial IPLs in F_N-7 could explain the higher ^{13}C incorporation of myo-inositol headgroup compared to phytanyl chain. However, in general, the ^{13}C label uptake into glycerol and sugars is lower than into isoprenoidal chains (Fig. V.4; Table V.1; Table V.S1). For instance, 2Gly-AR showed after 17 days differential ^{13}C assimilation in phytane (780‰), sugars (glucose 350‰ and galactose 270‰) and glycerol moiety (150‰). Our findings contrast with the *in situ* ^{13}C -glucose SIP study performed with benthic archaea, which detected pronounced *de novo* production of the glycerol backbone of core GDGTs, while the isoprenoidal chains were suggested to be recycled from relic archaeal membranes (Takano et al., 2010). These contrasting results could be attributed to the study design and the targeted organisms: benthic archaeal communities under starving conditions (Takano et al., 2010) and methanotrophic archaea from highly active AOM enrichments (Holler et al., 2011). In our study, distinct intramolecular ^{13}C assimilation is likely related to efficiencies in label uptake and biosynthetic pathways during biomass formation, i.e. glycogenesis, isoprenoid and glycerol backbone formation, in Archaea (e.g. Kates et al., 1970; Nemoto et al., 2003; Morii et al., 2007; Koga, 2010). Likewise, in environmental samples, stable carbon isotopic differences between sugar headgroups and isoprenoids in glycosidic archaeal IPLs (Lin et al., 2010) can be also attributed to differential fractionation of carbon substrates during biosynthesis.

By applying IPL-SIP in AOM sediments under optimum growth conditions and using short-time incubations, our results unambiguously demonstrate *de novo* synthesis of IPLs. However, although 2Gly-GDGTs represented the major archaeal IPL in this thermophilic AOM enrichment (Fig. V.2a; Table V.1), these compounds displayed the lowest ^{13}C assimilation (Fig. V.4; Table V.1), raising questions regarding their role in ANME-1 dominated cold seep sediments and microbial mats, where they often dominate (Thiel et al., 2007; Rossel et al., 2008; 2011) and their role as presumably most abundant archaeal IPL in worldwide marine sediments (e.g. Lipp and Hinrichs 2009; Liu et al., 2011). By carefully examining the differential intermolecular label assimilation, this study provides a unique opportunity to characterize the tetraether biosynthesis in Archaea.

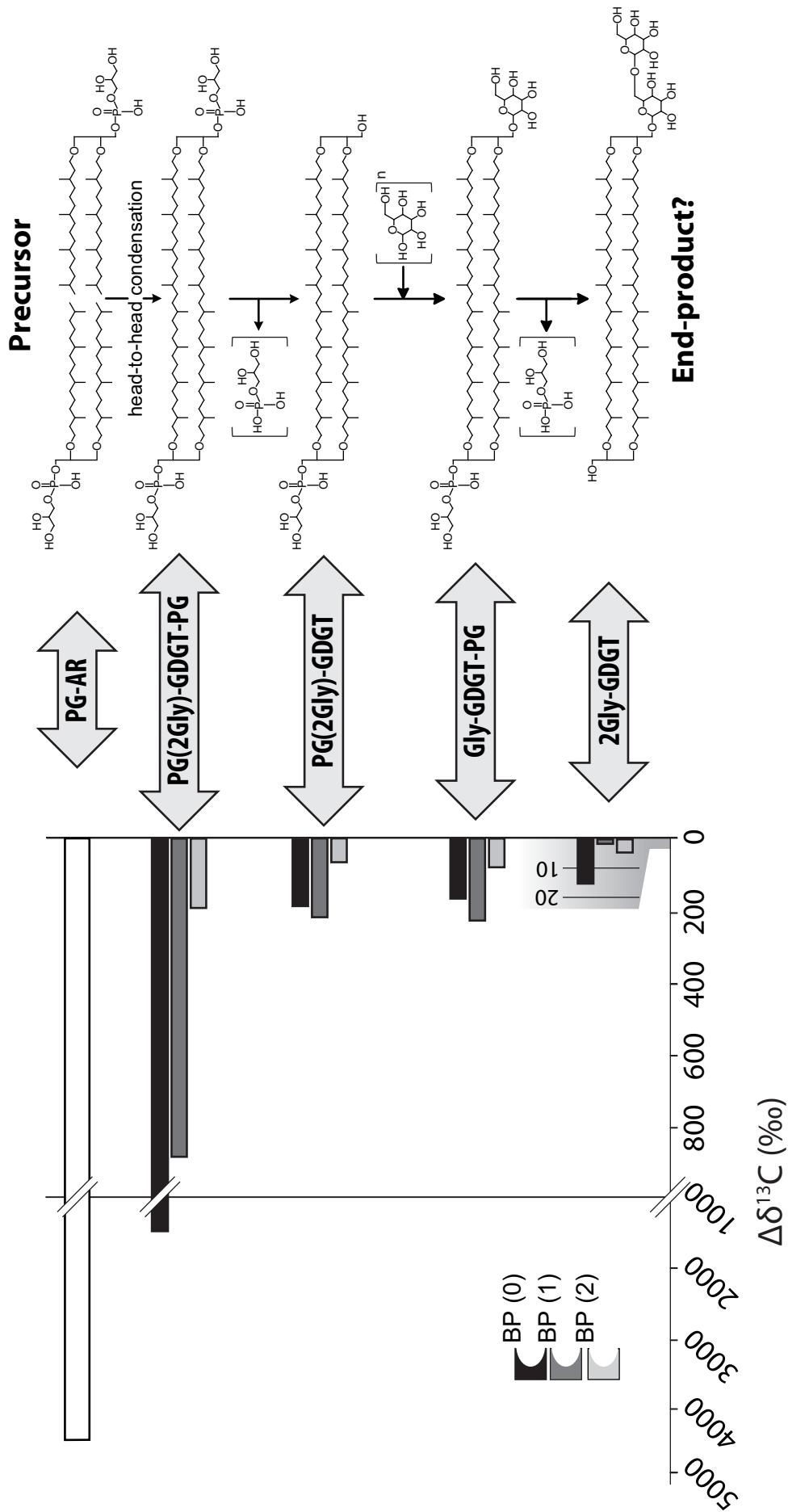


Fig. V.5. Left panel: total label uptake [Δδ¹³C] after 24 days of incubation relative to t(0) for PG-AR and intact tetraether lipids. Note that for 2Gly-GDGT a different scale was used. Right panel: A possible pathway for tetraether biosynthesis in thermophilic ANME-1 revealed by stable isotope probing of archaeal intact polar lipids (modified from Nemoto et al., 2003).

V.4.4. 2Gly-GDGT as possible end-product of ANME-1 membrane lipid biosynthesis

The pathway of archaeal IPLs biosynthesis has been only partially elucidated (Koga and Morii, 2007). For instance, archaeal isoprenoidal synthesis proceeds via the classical mevalonate pathway (Ekiel et al., 1983; De Rosa and Gambacorta, 1986) and the enzymes involved in glycerol backbone formation have been well characterized (e.g. Nishihara and Koga, 1995). The mechanism of polar headgroup attachment to the core lipid has been demonstrated to be similar in both archaeal diether phospho- and glycolipids (e.g. Koga and Morii, 2007; Morii et al., 2007), which theoretically imply that the label uptake should be comparable among the intact ARs from our experiments. With the exception of PG-AR, which stands out in terms of label uptake, diether lipids showed similar ^{13}C assimilation (2Gly-AR, PI(-OH)-AR and PG-OH-AR; Fig. V.4) corroborating the theoretical steps in intact AR synthesis. By contrast to the diethers, the formation of tetraether lipids is still to be elucidated and is considered the most challenging problem in archaeal lipid biochemistry, because it involves a C-C bond formation between two terminal methyl groups of phytanyl chains (Koga and Morii, 2007). In general, ^{13}C assimilation into tetraethers was lower than into diethers (Fig. V.4), indicating a possible role of intact ARs as precursors for tetraether synthesis.

Head-to-head condensation of diether lipids has been proposed as the main pathway of tetraether formation in Archaea (e.g. De Rosa et al., 1980, Nishihara et al., 1989; Nemoto et al., 2003). These observations derived from growth experiments in cultured archaeal strains, which usually display a significant increase in amount of tetraether lipids from the exponential phase towards the stationary phase (e.g. Nishihara et al., 1989; Morii and Koga, 1993; Matsuno et al., 2009). This aspect is explained as a response to cell division efficiency, which is increased by cell membranes composed of diether lipids due to higher flexibility and fluidity relative to membrane-spanning tetraethers (Matsuno et al., 2009). Similarly, the highest ^{13}C assimilation into archaeal IPLs was observed for the diethers, especially the PG-AR, which within 10 days rapidly approached the isotopic composition of the medium (Fig. V.4; Table V.1). Although to a lesser extent, the highest ^{13}C uptake among the intact GDGTs was detected in the mixed fraction containing PG and (2Gly)-GDGT-PG, and a sequential decrease in label assimilation into tetraethers was observed as follows: PG-(2Gly)-GDGT, Gly-GDGT-PG and 2Gly-GDGT (Fig. V.5).

The molecular composition of and the differential label assimilation into IPLs from our enrichment are consistent with the pathway of tetraether lipid biosynthesis proposed by Nemoto et al. (2003) (Fig. V.5). Studying the thermoacidophilic *Thermoplasma acidophilum*, Nemoto et al. (2003) asserted the synthesis of PG-GDGT-PG by head-to-head condensation reaction of two molecules of PG-AR (cf. De Rosa et al., 1980), with subsequent loss of one PG headgroup (yielding PG-GDGTs) and the addition of a sugar headgroup resulting in Gly-GDGT-PG, which was the main IPL in *T. acidophilum*. In line with their results, we hypothesize that PG-AR is the possible precursor of tetraether biosynthesis in our ANME-1 enrichment. PG-AR represented not only the most dynamic lipid within the archaeal IPL pool, given its

fluctuations in terms of absolute concentration, but also displayed by far the highest ^{13}C uptake and prevailed among the diether lipids throughout the incubation periods (Table V.1; Fig. V.3a and Fig. V.4). By contrast, although 2Gly-GDGTs represent the main IPL in our enrichments, they are positioned at the bottom of the ^{13}C assimilation cascade (Table V.1). Our results suggest 2Gly-GDGTs as possible end-products of the tetraether biosynthetic pathway in thermophilic ANME-1.

Alternatively, low label uptake into 2Gly-GDGTs could be interpreted as signals from a metabolically inactive cell pool, dead biomass or even extracellular material. However, circumstantial lines of evidence that argue against this possibility can be drawn from our experiments. First, according to the doubling time of this AOM enrichment (Holler et al., 2011), our incubations investigated only a third of a cell cycle. Still we obtained strong indications of microbial growth by the assimilation of label into the whole series of intact tetraether lipids (Fig. V.5). Second, the prevalence of 2Gly-GDGTs among archaeal IPLs is inherent to adaptations of the lipid membrane to proton permeability and membrane fluidity at elevated temperatures from Guaymas Basin sediments. By increasing cyclization of the biphytanes (Fig. V.2c) and substituting phospho-based by glycosylated headgroups (e.g. Shimada et al., 2008), both well-known archaeal strategies to reduce proton permeability, cytoplasmic membranes can be packed more tightly. Thus, we hypothesize that the low ^{13}C label assimilation into 2Gly-GDGTs reflects their position as end-products of archaeal lipid biosynthesis in thermophilic AOM enrichments.

In mesophilic environments, such as marine sediments, the intrinsic structural aspects of these ubiquitous intact tetraether lipids (i.e., membrane-spanning configuration and glycosylated headgroups) could potentially represent an archaeal strategy for cell maintenance under energy limitation. Conversely, high ^{13}C label assimilation into diether and/or phospho-based IPLs suggests replication of cellular material (Fig. V.4 and Fig. V.5), which in high microbial biomass environments such as methane seeps or hydrogen-rich hydrothermal settings could indicate exponential growth of the archaeal community.

V.5. Conclusion

Separation of core (fossil) from intact lipids by extensive preparative HPLC allowed the evaluation of SIP in archaeal IPLs. Results have shown an increase of up to 35 times in sensitivity of SIP by focusing on intact membrane lipids rather than bulk archaeal lipids (TLE). The chemotaxonomic analysis of archaeal IPLs indicates a predominance of ANME-1 over ANME-2 archaea. Moreover, the occurrence of PE-MAR and the high contribution of cyclopentane rings in intact GDGTs evidenced archaeal membrane adaptations to thrive under heat stress. This distinctive membrane lipid composition is suggested to reflect the phylogenetic affiliation of thermophilic ANME-1 from this AOM enrichment. Finally, we hypothesized that the PG-AR is the precursor of ANME-1 tetraether biosynthesis and 2Gly-GDGTs are the possible end-products. The presence of glycosidic headgroups attached to membrane-spanning tetraether

lipids confers reduced proton-permeability and thus integrity of cells at elevated temperatures from the Guaymas Basin sediments. Accordingly, the ubiquity of 2Gly-GDGTs in mesophilic environments might be an indicator of cell-wall adaptation to cope with energy stress.

V.6. Acknowledgements

We thank the shipboard, scientific crew and pilots of the R/V Atlantis and DSV Alvin. Xavier Prieto-Mollar, Jenny Wendt, Julius Lipp and Lars Wörmer are thanked for technical support. This study was supported by the Deutsche Forschungsgemeinschaft (through the Research Center MARUM Center for Marine Environmental Sciences), the European Research Council Advanced Grant DARCLIFE (awarded to KUH), the GLOMAR graduate school (MYK), Alexander von Humboldt Foundation (MYY) and the Gottfried Wilhelm Leibniz Price awarded to Antje Boetius (to GW).

V.7. Supporting information

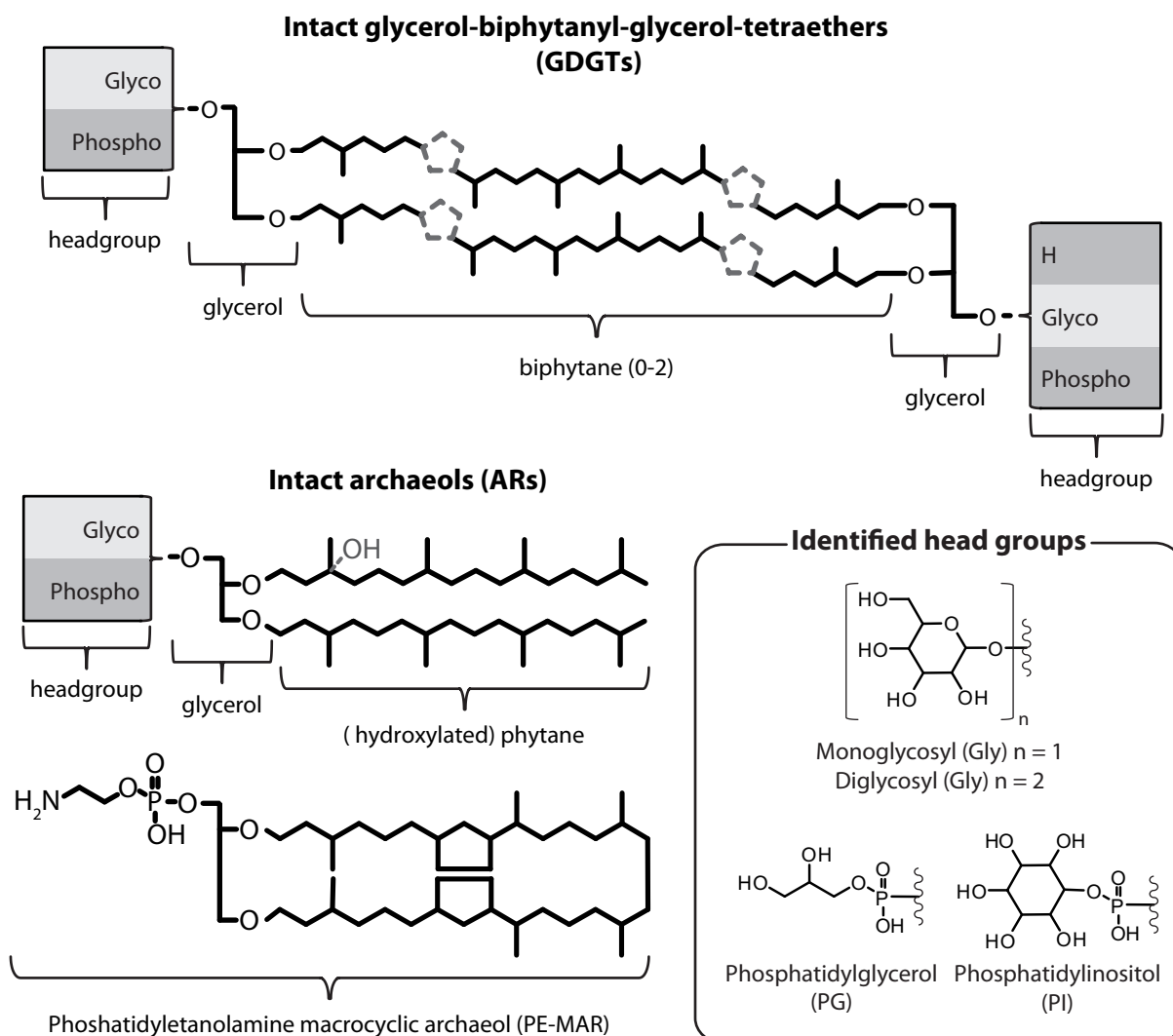


Fig. V.S1. Schematic structures of archaeal IPLs identified in this study. Major structural differences are related to headgroup (glyco-, phospho-, or glycophospho-based) and core lipid (GDGTs, ARs, MAR) composition. Additional structural characteristics are the presence of hydroxyl group in ARs and cyclopentane rings among GDGTs and PE-MAR. For IPL abbreviations the reader is referred to Fig. V.1.

Table V.S1. ^{13}C stable isotopic composition of hexose containing headgroups and glycerol backbone of IPLs. All isotopic values are given in per mil (‰). For IPL abbreviations the reader is referred to Fig. V.1 and Fig. V.3.

IPL fraction		t(0)	t(1)	t(2)	t(3)
		$\delta^{13}\text{C}$ [‰]	$\delta^{13}\text{C}$ [‰]	$\delta^{13}\text{C}$ [‰]	$\delta^{13}\text{C}$ [‰]
Hexose containing headgroups					
2Gly-AR [F _R -1]	Glc	-30	+23	+350	n.a.
	Gal	-26	+76	+270	n.a.
2Gly-GDGT [F _R -2]	Glc	-36	-42	-35	n.a.
	Gal	-34	-36	-35	n.a.
2Gly-AR/2Gly-GDGT [F _N -4]	Glc	n.a.	n.a.	n.a.	+140
	Gal	n.a.	n.a.	n.a.	+90
2Gly-GDGT-PG [F _N -8]	Glc	-21	+23	+52	+110
	Gal	(*)	(*)	(*)	+63
PI-AR (OH) [F _N -7]	Ino	-37	+360	+540	n.d.
Glycerol backbone					
PG-AR [F _N -5]		-30	+300	+150	+190
2Gly-AR [F _R -1]		n.a.	+110	+150	n.a.
2Gly-GDGT [F _R -2]		n.a.	-32	b.d.	n.a.
2Gly-AR; 2Gly-GDGT [F _N -4]		-39	n.a.	n.a.	+51
PG-GDGT-PG; 2Gly-GDGT-PG [F _N -8]		b.d.	b.d.	b.d.	+42

(*) – co-elution with contaminant

n.a. – not analyzed

b.d. – below detection

[CHAPTER VI] - CONCLUDING REMARKS & FUTURE PERSPECTIVES

Summary and Conclusion

This dissertation focused on microbial presence and metabolic activity in two types of oceanic extreme environments (Fig. VI.1): cold seeps and hot vents. Those two habitats are characterized by the dominance of microorganisms with chemoautotrophic metabolism. At these extreme environments microorganisms rely exclusively on reduced compounds (e.g., H_2S and CH_4). The active microbial community was examined in field [Chapters II and IV] and laboratory [Chapters III and V] studies by analyzing the presence and isotopic composition of lipid biomarkers, particularly of the intact polar lipids (IPLs), which are thought to reflect the live/active biomass (White et al., 1979; Harvey et al., 1986; Moodley et al., 2000). The taxonomic information encoded in the IPL molecules in conjunction with its isotopic compositions (e.g., carbon and hydrogen) enabled to reveal the function of the microorganisms in these settings. Symbiotic relations between mussels and aerobic bacteria in hot and cold seeps were successfully investigated [Chapter II]. Lipid analysis in combination with stable isotope probing experiments (SIP) allowed to identify the major metabolic processes and dominant microorganisms involved in thermophilic AOM. Here, the dominant carbon fixation pathway of the AOM methanotrophic consortia was identified [Chapter III] and archaeal strategies to adapt to chronic energy stress were hypothesized [Chapter V].

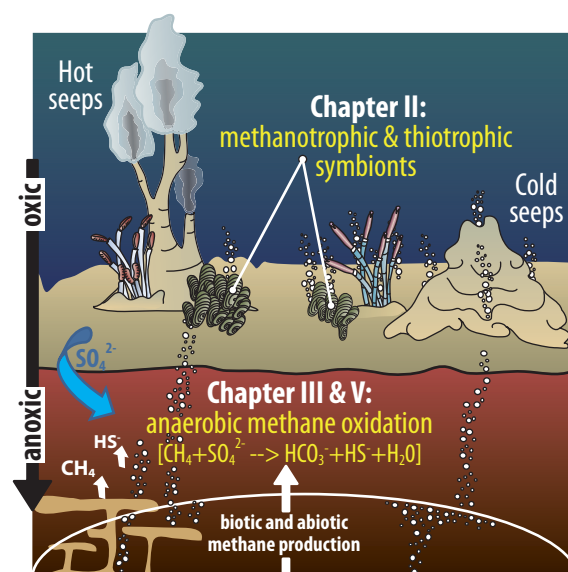


Fig. VI.1. Aerobic and anaerobic zones fueled by reduced chemicals at extreme deep-ocean environments. The production of CH_4 in subsurface sediments occurs by either biologically- (by methanogens) or abiologically-mediated (thermogenesis; Lollar et al., 2002) breakdown of organic matter. Through advection and/or diffusion reduced compounds (here CH_4) are transported to the overlying sediment layers where archaea anaerobically oxidize a vast fraction of the CH_4 . Finally, excessive CH_4 , escaping AOM, is oxidized aerobically and excess H_2S is utilized by methanotrophic and thiotrophic bacteria, respectively, both of which sustain diverse benthic communities (e.g., tubeworms and mussels) at hot and cold seeps.

In the first research manuscript of this thesis [**Chapter II**] symbiont–host interactions were studied using a comprehensive lipid biomarker approach. Three different types of symbiotic associations were chosen: one host species contained methanotrophic symbionts (*Bathymodiolus childressi* from the Gulf of Mexico (GOM); Duperron et al., 2007), a second contained thiotrophic symbionts (*B. cf. thermophilus* from the Pacific Antarctic Ridge; Petersen and Dubilier, unpublished data) and a third with both methanotrophic and thiotrophic symbionts (*B. brooksi* from the GoM; Duperron et al., 2007). In their gills, *Bathymodiolus* mussels host abundant symbiotic bacteria, which are powered by reducing compounds (e.g., CH₄ and H₂S) emerging from the interior of sediments (Fig. VI.1; Van Dover, 2000). Prior lipid-based studies of symbiont–host relations focused on derivatives of intact polar lipids (IPL) such as fatty acids and/or hopanols (e.g., Gillan et al., 1988; Fang et al., 1993; Abrajano et al., 1994; Jahnke et al., 1995; Pond et al., 1998). Progress in analytical techniques allowed us to target the abundance of intact bacterial and host IPLs, which significantly improves the quantification and assignment of bacterial and eukaryotic biomass inside the gill and foot tissue of the mussels. We were able to distinguish thiotrophic from methanotrophic bacteria based on their IPL composition, demonstrating the potential of this lipid class as a powerful tool in symbiont research. The IPL fingerprinting enabled the estimation of the abundance of bacterial symbionts in the host tissues. In addition, fatty acids (FA), bacteriohopanepolyols (BHP) and selected methyl sterols were targeted, since they encode specific information about the metabolic function of the bacteria. In particular we studied their compound-specific stable carbon isotopic composition, which can be used to determine dominant symbiotic lifestyle of the bacteria living within the mussel's tissue. Furthermore, the distribution and $\delta^{13}\text{C}$ values of individual FAs, 4-methyl sterols, monoalkylglycerolethers (MAGE) and BHPs were indicative of the presence of methanotrophic or thiotrophic symbionts in the host mussels. Lipids of symbionts which utilized methane showed a stronger ^{13}C –depletion compared to sulfide-consuming bacteria. Moreover, the lipid $\delta^{13}\text{C}$ imprints of the gills and foot tissues highlighted the importance of chemosynthetic carbon supply for all three bivalves.

In [**Chapter III**], we conducted a lipid–based SIP experiment, aiming to investigate hetero– and autotrophic carbon fixation for anaerobic methanotrophic archaea (ANME) and sulfate reducing bacteria (SRB). The combination of SIP with gas chromatography–amenable compounds (e.g., lipids) is a well–established method which requires the lowest ^{13}C incorporation for detection. Due to very low carbon assimilation rates during AOM in cold seep settings (Girguis et al., 2003, 2005; Niemann et al., 2006), previous AOM-SIP experiments performed in microbial mats using $^{13}\text{CH}_4$ (Blumenberg et al., 2005) and sediments inoculated with $^{13}\text{CH}_4$ and $^{13}\text{CO}_2$ (Wegener et al., 2008) required a long period of incubation in order to detect significant ^{13}C –uptake in bacterial and archaeal lipids. However, long–term incubations might cause bias due to cross-feeding of ^{13}C –label from primary consumers to other community members (Dumont and Murrell, 2005). In our study, we performed short–term incubations of a maximum of 24 days in a hot seep natural enrichment dominated by ANME–1 and SRBs from

the HotSeep-1 SRB cluster from the Guaymas Basin (Holler et al., 2011). In addition, multiple carbon sources ($^{13}\text{C}_{\text{DIC}}$ and $^{13}\text{CH}_4$) and deuterated water (D_2O) in the presence and absence of unlabeled CH_4 have been used to study the thermophilic AOM carbon fixation. Introduced by Wegener et al., (in revision), the dual-SIP involves the assimilation of deuterated protons from water (i.e., total lipid production) in combination with carbon assimilation from DIC (i.e., autotrophic production) in lipid biosynthesis, thereby allowing an estimation of auto- and heterotrophic microbial carbon fixation. Dual-SIP experiments unambiguously showed that ANMEs and SRBs are pure autotrophs, assimilating almost exclusively inorganic carbon. Furthermore, this thermophilic enrichment revealed a higher lipid production for the Archaea than for the Bacteria, highlighting their importance in terms of both biomass production and activity. Thus, direct methane assimilation does not seem to be relevant for lipid biosynthesis. This result contrasts from previous studies (SIP-studies) with cold seep sediments (Wegener et al., 2008), in which methane contributed up to 50% to the archaeal lipid carbon assimilation (Fig. VI.2). In the absence of methane, metabolic rates dropped dramatically, suggesting that methane is the crucial energy source to sustain the anaerobic communities in the studied sediments. As a direct implication of our results, the interpretation of lipid stable carbon isotopic compositions in AOM systems should be revisited as the microbes are expected to fractionate carbon from DIC rather than from methane for biomass built up. The application of dual-SIP provided novel insights to lipid formation and metabolism of microbial consortia mediating the thermophilic AOM (Fig. VI.2).

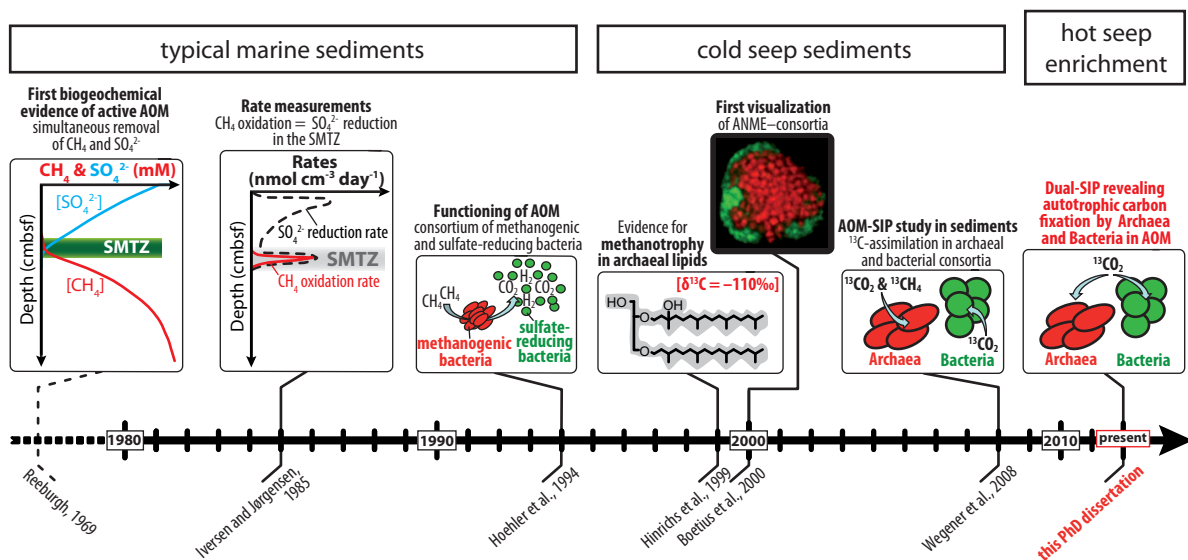


Fig. VI.2. History of AOM research. Timeline illustrates the key scientific discoveries in the past three decades and the significant contribution presented in this thesis.

In the third research project we focused on the identification of diverse intact archaeal IPLs from environmental samples. [Chapter IV] demonstrated the systematic fragmentation patterns of archaeal IPLs providing extensive information for a rapid and straightforward characterization of archaeal IPLs, which can be readily assessed using high performance liquid chromatography (HPLC) electrospray ionization mass spectrometry. This archaeal lipid identification guide enabled us to reveal the archaeal lipid composition in environmental samples such as the complex archaeal IPL diversity of the thermophilic ANME-1 enrichment (Holler et al., 2011; [Chapters III and V]).

The last research chapter [Chapter V] utilized the identical short-term incubations described earlier. However, this SIP experiment only focused on the assimilation of ^{13}C -labeled bicarbonate, since [Chapter III] already identified the archaeal community as pure autotrophs. This stable isotope probing (SIP) study aimed at evaluating ^{13}C assimilation into archaeal intact polar lipids (IPLs) relative to total lipid extracts (TLE). Thus, in theory, IPL-SIP should reduce the requirement of ^{13}C lipid uptake, allowing either a shorter labelling time and/or a reduction of the label strength. After TLE extraction, extensive preparative HPLC (normal- and reversed-phase) was used to successively separate the core from the individual intact archaeal lipids. A substantial increase in sensitivity of SIP was observed with IPLs compared to TLEs. While diethers experienced a five-fold increase in sensitivity, the strongest increase in label uptake of archaeal IPLs has been observed in the tetraether fraction (>35 times). These results are in accordance to recent studies on archaeal tetraether lipid distribution in marine sediments (Lipp and Hinrichs, 2009; Liu et al., 2010, 2011) showing a range from 84 to 96% of fossil relative to the total glyceroldialkylglyceroltetraether (GDGT) pool (Lipp and Hinrichs, 2009; Liu et al., 2010; 2011). Thus, our results clearly demonstrate that previous TLE-SIP in *in vitro* AOM studies (e.g., Blumenberg et al., 2005, Wegener et al., 2008; Chapter III) largely underestimated the actual label uptake of archaeal communities. The chemotaxonomic analysis of this ANME-1 dominated enrichment resulted in an IPL composition clearly affected by elevated temperatures. In particular, the occurrence of macrocyclic archaeol with phosphatidylethanolamine headgroup (PE-MAR) and the high contribution of cyclopentane rings in intact GDGTs evidenced archaeal membrane adaption in order to thrive under heat stress. Furthermore, differences in ^{13}C -label assimilation of individual archaeal IPLs provided multiple lines of evidence for phosphatidylglycerolarchaeol (PG-AR) as the precursor of tetraether biosynthesis and diglycosidic GDGTs (2Gly-GDGT) are the possible end-products in thermophilic ANME-1 (Fig. VI.3). Here we also postulated that the formation of membrane-spanning tetraether lipids with glycosidic headgroups reduces proton-permeability and thus protects the integrity of cells at elevated temperatures. Finally, we hypothesized that the worldwide ubiquity of 2Gly-GDGTs in mesophilic environments may likely represent an expression of cell-wall adaptation to cope with energy stress.

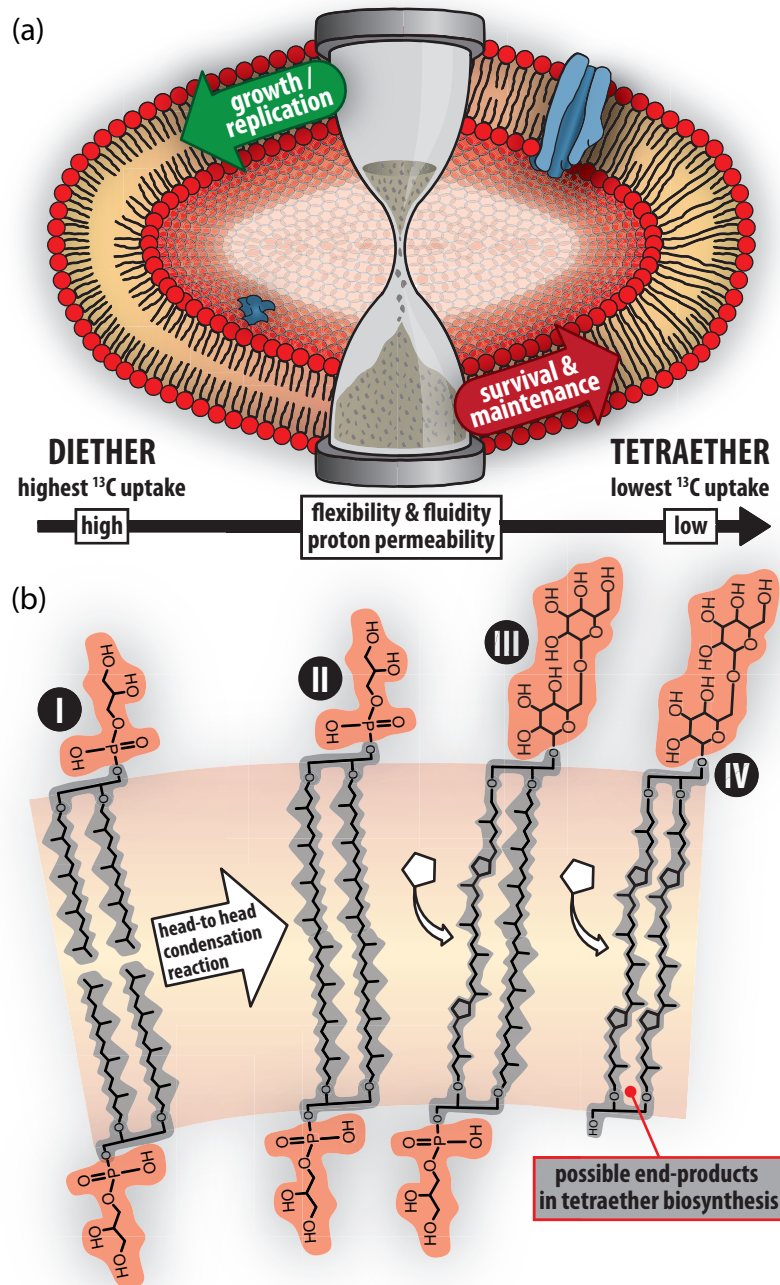


Fig. VI.3. (a) Archaeal intact polar membrane lipid composition and its physiological implications in thermophilic ANME-1. (b) A possible pathway of tetraether biosynthesis revealed by IPL-SIP. A characteristic ^{13}C assimilation pattern provided evidence for the synthesis of diphosphatidylglycerol-GDGT (PG-GDGT-PG) (II) by head-to-head condensation reaction of two molecules of PG-AR (I). Lowest label uptake into 2Gly-GDGT (IV) suggested this IPL as a possible end-product of the tetraether biosynthesis. Furthermore, increasing cyclization of intact GDGTs and the substitution of phospho-based by glycosylated headgroups, e.g., diglycosidic phosphatidylglycerol GDGT (2Gly-GDGT-PG, (III)) and 2Gly-GDGT, are both well-known archaeal strategies to pack the cytoplasmic membranes more tightly.

Future perspective

This thesis contributed with novel and valuable scientific information that expands our current knowledge in organic geochemistry. Nevertheless, new insights into symbiont–host interaction, autotrophic carbon fixation in thermophilic AOM, and tetraether biosynthetic pathways have also raised interesting questions for future research:

- **Towards precise biomass estimation of symbionts within a eukaryotic host:** Quantifying the proportion of symbionts within a host tissue by IPLs is a promising new method. However this new technique still needs to be validated to test the robustness of the IPL-based quantification, preferably in tandem with cell-specific quantification protocols.
- **Putative autotrophy in AOM environments:** The autotrophic nature of AOM microbial communities should also be investigated in cold seep sediments and/or microbial mats inhabited by different ANME and SRB clades, using the same dual SIP approach described in [Chapter III]. Although previous AOM-SIP experiments have shown to be challenging due to limited microbial growth (Blumenberg et al., 2005; Wegener et al., 2008), the next attempts should exclusively focus on individual IPLs [Chapter V], thus reducing the requirement of ^{13}C uptake for detection.
- **IPL-SIP in combination with microbial ecology:** Future SIP experiments should examine both IPL-SIP and RNA-SIP in order to combine advantages of both methods (sensitivity and quantification versus specificity). Although attempted by Webster et al. (2006) and Singh and Tate (2007), the traditional chromatographic separation of lipids as PLFAs should be replaced by more extensive preparative HPLC separation of lipids as shown in [Chapter V].
- **SIP experiments in situ:** SIP experiments have been mostly performed *ex situ* in bottle incubations which are limited to mimic *in situ* temperatures. Experimental data has shown that pressure as well as CH_4 concentration impacts rates and pathways of metabolism (de Angelis et al., 1991; Girguis et al., 2003; Kallmeyer and Boetius, 2004). Future SIP experiments should consider the possibility performing incubation studies *in situ* (cf. Takano et al., 2010) in order to exclude biases caused by changing environmental conditions.

[CHAPTER VII] - REFERENCES

A

- Abrajano, T.A., Murphy, D.E., Fang, J., Comet, P. and Brooks, J.M. (1994) $^{13}\text{C}/^{12}\text{C}$ ratios in individual fatty acids of marine mytilids with and without bacterial symbionts. *Org. Geochem.* **21**, 611–617.
- Allen, C.E., Tyler, P.A. and Van Dover, C.L. (2001) Lipid composition of the hydrothermal vent clam *Calyptogena pacifica* (Mollusca: Bivalvia) as a trophic indicator. *J. Mar. Biol. Assoc. UK* **81**, 817–821.
- Allen, D.E. and Seyfried, W.E. (2003) Compositional controls on vent fluids from ultramafic-hosted hydrothermal systems at mid-ocean ridges: An experimental study at 400 degrees C, 500 bars. *Geochim. Cosmochim. Acta* **67**, 1531–1542.
- Alperin, M.J. and Hoehler, T.M. (2009a) Anaerobic methane oxidation by archaea/sulfate-reducing bacteria aggregates: 1. Thermodynamic and physical constraints. *Am. J. Sci.* **309**, 869–957.
- Alperin, M.J. and Hoehler, T.M. (2009b) Anaerobic methane oxidation by archaea/sulfate-reducing bacteria aggregates: 2. Isotopic constraints. *Am. J. Sci.* **309**, 958–984.
- Amend, J.P. and Teske, A. (2005) Expanding frontiers in deep subsurface microbiology. *Palaogeogr. Paleoclimatol. Paleoecol.* **219**, 131–155.
- Anderson, A.L., Abegg, F., Hawkins, J.A., Duncan, M.E. and Lyons, A.P. (1998) Bubble populations and acoustic interaction with the gassy floor of Eckernförde Bay. *Continental Shelf Res.* **18**, 1807–1838.
- Andersson B. and Holman R. (1974) Pyrrolidides for mass spectrometric determination of the position of the double bond in monounsaturated fatty acids. *Lipids* **9**, 185–190.

B

- Bach, W., Edwards, K.J., Hayes, J.M., Huber, J.A., Sievert, S.M. and Sogin, M.L. (2006) Energy in the dark: Fuel for life in the deep ocean and beyond. *EOS* **87**, 73–75.
- Barnes, R.O. and Goldberg, E.D. (1976) Methane production and consumption in anoxic marine sediments. *Geology* **4**, 297–300.
- Bazylinksi, D. A., Farrington, J.W. and Jannasch, H.W. (1988) Hydrocarbons in surface sediments from a Guaymas Basin hydrothermal vent site. *Org. Geochem.* **12**, 547–559.
- Becker, E.L., Lee, R.W., Macko, S.A., Faure, B.M. and Fisher, C.R. (2010) Stable carbon and nitrogen isotope compositions of hydrocarbon-seep bivalves on the Gulf of Mexico lower continental slope. *Deep-Sea Res. Pt. II* **57**, 1957–1964.
- Bian L.Q., Hinrichs K.-U., Xie T.M., Brassell S.C., Beck J.P., Iversen N., Fossing H., Jørgensen B. B. and Hayes J.M. (2001) Algal and archaeal isoprenoids in a recent marine sediment: Molecular–isotopic evidence for anaerobic oxidation of methane. *Geochem. Geophys. Geosy.* **2**, 1525–2027.
- Biddle, J.F., Cardman, Z., Mendlovitz, H., Albert, D.B., Lloyd, K.G., Boetius, A. and Teske, A., Anaerobic oxidation of methane at different temperature regimes in Guaymas Basin hydrothermal sediments. *ISME J.* (2011), doi:10.1038/ismej.2011.164
- Biddle, J.F., Fitz-Gibbon, S., Schuster, S.C., Brenchley, J.E. and House, C.H. (2008) Metagenomic signatures of the Peru Margin seafloor biosphere show a genetically distinct environment. *Proc. Nat. Acad. Sci. USA* **105**, 10583–10588.
- Biddle, J.F., Lipp, J.S., Lever, M.A., Lloyd, K.G., Sorensen, K.B., Anderson, R., Fredricks, H.F., Elvert, M., Kelly, T.J., Schrag, D.P., Sogin, M.L., Brenchley, J.E., Teske, A., House, C.H. and Hinrichs, K.-U. (2006) Heterotrophic archaea dominate sedimentary subsurface ecosystems off Peru. *Proc. Natl. Acad. Sci. USA* **103**, 3846–3851.
- Birgel, D. and Peckmann, J. (2008) Aerobic methanotrophy at ancient marine methane seeps: A synthesis. *Org. Geochem.* **39**, 1659–1667.
- Birgel, D., Feng, D., Roberts, H.H. and Peckmann, J. (2011) Changing redox conditions at coldseeps as revealed by authigenic carbonates from Alaminos Canyon, northern Gulf of Mexico. *Chem. Geol.* **285**, 82–96.
- Bligh, E.G. and Dyer, W.J. (1959) A rapid method of total lipid extraction and purification. *Can. J. Biochem. Phys.* **37**, 911–917.
- Blumenberg, M. and Kiel, S. (2010) Microbial chemofossils in specific marine hydrothermal and methane cold seep settings: The Vent and Seep Biota. Springer Netherlands.
- Blumenberg, M., Seifert, R., Nauhaus, K., Paper, T. and Michaelis, W. (2005) *In vitro* study of lipid biosynthesis

- in an anaerobically methane-oxidizing microbial mat. *Appl. Environ. Microbiol.* **71**, 4345-4351.
- Blumenberg, M., Seifert, R., Petersen, S. and Michaelis, W. (2007) Biosignatures present in a hydrothermal massive sulfide from the Mid-Atlantic Ridge. *Geobiology* **5**, 435-450.
- Blumenberg, M., Seifert, R., Reitner, J., Pape, T. and Michaelis, W. (2004) Membrane lipid patterns typify distinct anaerobic methanotrophic consortia. *Proc. Nat. Acad. Sci. USA* **101**, 11111-11116.
- Boetius, A. and Suess, E. (2004) Hydrate Ridge: A natural laboratory for the study of microbial life fueled by methane from near-surface gas hydrates. *Chemical Geology* **205**, 291-310.
- Boetius, A., Ravenschlag, K., Schubert, C.J., Rickert, D., Widdel, F., Gieseke, A., Amann, R., Jørgensen, B.B., Witte, E.G. and Pfannkuche, O. (2000) A marine microbial consortium apparently mediating anaerobic oxidation of methane. *Nature* **407**, 623-626.
- Bohrmann, G. and cruise participants. Report and preliminary results of *R/V Meteor* Cruise M74/3. Berichte, Fachbereich Geowissenschaften, Universität Bremen, Bremen, 2008, 266.
- Bohrmann, G. and Torres, M.E. (2006) Gas hydrates in marine sediments. In: Schulz, H. D. and Zabel, M. (Eds.), *Marine Geochemistry*. Springer.
- Boschker, H.T.S., Nold, S.C., Wellsbury, P., Bos, D., de Graaf, W., Pel, R., Parkes, R.J. and Cappenberg, T.E. (1998) Direct linking of microbial populations to specific biogeochemical processes by ¹³C-labelling of biomarkers. *Nature* **392**, 801-805.
- Bouvier, P., Rhomer, M., Benveniste, P. and Ourisson, G. (1976) $\Delta^8(14)$ -Steroids in the bacterium *Methylococcus capsulatus*. *Biochem. J.* **159**, 267-271.
- Bowman, J.P., Skerrat, J.H., Nichols, P.D. and Sly, L.I. (1991) Phospholipid fatty acid and lipopolysaccharide fatty acid signature lipids in methane-utilizing bacteria. *FEMS Microb. Lett.* **85**, 15-21.
- Brenna, J.T., Corso, T.N., Tobias, H.J. and Caimi, R.J. (1997) High-precision continuous-flow isotope ratio mass spectrometry. *Mass Spectrom. Rev.* **16**, 227-258.
- Brett, M.T. and Müller-Navarra, D.C. (1997) The role of highly unsaturated fatty acids in aquatic foodweb processes. *Freshw. Biol.* **38**, 483-499.
- Brites, P., Waterham, H.R. and Wanders, R.J.A. (2004) Functions and biosynthesis of plasmalogens in health and disease. *Biochim. Biophys. Acta* **1636**, 219-231.
- Brocks, J.J. and Summons, R.E. (2003) Sedimentary hydrocarbons, biomarkers for early life. *Treatise on Geochem.* **8**, 63-115.
- Bühning, S.I., Lampadariou, N., Moodley, L., Tselepides, A. and Witte, U. (2006) Benthic microbial and whole-community responses to different amounts of ¹³C-enriched algae: *In situ* experiments in the deep Cretan Sea (Eastern Mediterranean). *Limnol. Oceanogr.* **51**, 157-165.
- ## C
- Calvert, S.E. (1966) Accumulation of diatomaceous silica in the sediments of the Gulf of California. *Geol. Soc. Amer. Bull.* **77**, 569-596.
- Campbell, K.A. (2006) Hydrocarbon seep and hydrothermal vent paleoenvironments and paleontology: Past developments and future research directions. *Palaogeogr. Paleoclimatol. Paleoecol.* **232**, 362-407.
- Canfield, D.E. and Thamdrup, B. (2009) Towards a consistent classification scheme for geochemical environments, or, why we wish the term 'suboxic' would go away. *Geobiology* **7**, 385-392.
- Carracedo, J.C., Day, S., Guillou, H., Rodríguez-Badiola, E., Canas, J.A. and Pérez Torrado, F.J. (1998) Hotspot volcanism close to a passive continental margin: The Canary Islands. *Geol. Mag.* **135**, 591-604.
- Cavanaugh, C.M. (1983) Symbiotic chemoautotrophic bacteria in marine invertebrates from sulfide-rich habitats. *Nature* **302**, 58-61.
- Cavanaugh, C.M., McKiness, Z.P., Newton, I.L.G. and Stewart, F.J. (2006) in *The Prokaryotes* (Eds Dworkin, M., Falkow, S.I., Rosenberg, E., Schleifer, K.H. and Stackebrandt, E.) 475-507 (Springer, New York).
- Cavicchioli, R. (2011) Archaea-timeline of the third domain. *Nat. Rev. Micro.* **9**, 51-61.
- Childress, J.J., Fisher, C.R., Brooks, J.M., Kennicutt II, M.C., Bidigare, R. and Anderson, A.E. (1986) A methanotrophic marine molluscan (*Bivalvia*, *Mytilidae*) symbiosis: Mussels fueled by gas. *Science* **233**, 1306-1308.
- Claypool, G.E. and Kvenvolden, K.A. (1983) Methane and other hydrocarbon gases in marine sediment.

- Annu. Rev. Earth Planet. Sci.* **11**, 299-327.
- Colaço, A., Martins, I., Laranjo, M., Pires, L., Leal, C., Prieto, C., Costa, V., Lopes, H., Rosa, D., Dando, P.R. and Serrão-Santos, R. (2006) Annual spawning of the hydrothermal vent mussel, *Bathymodiolus azoricus*, under controlled aquarium conditions at atmospheric pressure. *J. Exp. Mar. Biol. Ecol.* **333**, 166–171.
- Colaço, A., Prieto, C., Martins, A., Figueiredo, M., Lafon, V., Monteiro, M. and Bandarra, N.M. (2009) Seasonal variations in lipid composition of the hydrothermal vent mussel *Bathymodiolus azoricus* from the Menez Gwen vent field. *Mar. Environ. Res.* **67**, 146–152.
- Collister, J.W., Summons, R.E., Lichtfouse, E. and Hayes, J.M. (1992) An isotopic biogeochemical study on the Green River oil shale. *Org. Geochem.* **19**, 265–276.
- Comita, P.B. and Gagosian, R.B. (1983) Membrane lipid from deep-sea hydrothermal vent methanogen: A new macrocyclic glycerol diether. *Science* **222**, 1329-1331.
- Comita, P.B., Gagosian, R.B., Pang, H. and Costello, C.E. (1984) Structural elucidation of a unique macrocyclic membrane lipid from a new, extremely thermophilic, deep-sea hydrothermal vent Archaeobacterium, *Methanococcus jannaschii*. *J. Biol. Chem.* **259**, 5234-5241.
- Conway, N. and McDowell-Capuzzo, J. (1991) Incorporation and utilization of bacterial lipids in the Solemya velum symbiosis. *Mar. Biol.* **108**, 277–291.
- Corcelli, A., Colella, M., Mascolo, G., Fanizzi, F.P. and Kates, M. (2000) A novel glycolipid and phospholipid in the purple membrane. *Biochemistry* **39**, 3318-3326.
- Cordes, E.E., Arthur, M.A., Shea, K., Arvidson, R.S. and Fisher, C.R. (2005) Modeling the mutualistic interactions between tubeworms and microbial consortia. *PLoS Biol.* **3**, 497-506.
- Cord-Ruwisch R. (1985) A quick method for the determination of dissolved and precipitated sulfides in cultures of sulfate-reducing bacteria. *J. Microbiol. Meth.* **4**, 33–36.
- Corliss, J.B., Dymond, J., Gordon, L.I., Edmond, J.M., von Herzen, R.P., Ballard, R.D., Green, K., Williams, D., Bainbridge, A., Crane, K. and van Andel, T.H. (1979) Submarine thermal springs on the Galapagos Rift. *Science* **203**, 1073-1083.
- Cronan, J.E. Jr. and Gelmann, E.P. (1975) Physical properties of membrane lipids: Biological relevance and regulation. *Bacteriol. Rev.* **39**, 232–256.

D

- De Rosa, M. and Gambacorta, A. (1988) The lipids of archaeobacteria. *Prog. Lipid Res.* **27**, 153-175.
- De Rosa, M., Gambacorta, A. and Gliozzi, A. (1986) Structure, biosynthesis and physicochemical properties of archaeobacterial lipids. *Microbiol. Rev.* **50**, 70-80.
- De Rosa, M., Gambacorta, A. and Nicolaus, B. (1980) Regularity of isoprenoid biosynthesis in the ether lipids of archaeobacteria. *Phytochemistry* **19**, 791-793.
- DeLong, E.F. and Yayanos, A.A. (1986) Biochemical function and ecological significance of novel bacterial lipids in deep-sea prokaryotes. *Appl. Environ. Microbiol.* **51**, 730-737.
- Dembitsky, V.M. (1996) Betaine ether-linked glycerolipids: Chemistry and biology. *Prog. Lipid Res.* **35**, 1-51.
- Deming, J.W. and Baross, J.A. (1993) Deep-sea smokers: Windows to a subsurface biosphere? *Geochim. Cosmochim. Acta* **57**, 3219–3230.
- DeNiro, M.J. and Epstein, S. (1976) You are what you eat (plus a few ‰): The carbon isotope cycle in food chains. *Geol. Soc. Am. Abs. Prog.* **8**, 834-835.
- Dhillon, A., Lever, M., Lloyd, K., Albert, D.B., Sogin, M. L. and Teske, A. (2005) Methanogen diversity evidenced by molecular characterization of methyl coenzyme M reductase A (mcrA) genes (mcrA) in hydrothermal sediments of the Guaymas Basin. *Appl. Environ. Microbiol.* **71**, 4592-4601.
- Dhillon, A., Teske, A., Dillon, J., Stahl, D. and Sogin, M.L. (2003) Molecular characterization of sulfate reducing bacteria in the Guaymas Basin. *Appl. Environ. Microbiol.* **69**, 2765-2772.
- D'Hondt, S., Jørgensen, B.B., Miller, D.J., Batzke, A., Blake, R., Cragg, B.A., Cypionka, H., Dickens, G.R., Ferdelman, T., Hinrichs, K.-U., Holm, N.G., Mitterer, R., Spivack, A., Wang, G., Bekins, B., Engelen, B., Ford, K., Gettemy, G., Rutherford, S.D., Sass, H., Skilbeck, C.G., Aiello, I.W., Guerin, G., House, C.H., Inagaki, F., Meister, P., Naehr, T., Niitsuma, S., Parkes, R.J., Schippers, A., Smith, D.C., Teske, A., Wiegel, J., Padilla, C.N. and Acosta, J.L.S. (2004) Distributions of microbial activities in deep seafloor sediments. *Science* **306**, 2216-2221.

- D'Hondt, S., Rutherford, S. and Spivack, A.J. (2002) Metabolic activity of subsurface life in deep-sea sediments. *Science* **295**, 2067-2070.
- Didyk, B.M. and Simoneit, B.R. (1989) Hydrothermal oil of Guaymas Basin and implications for petroleum formation mechanisms. *Nature* **342**, 65-69.
- Dimitrov, L.I. (2002) Mud volcanoes-the most important pathway for degassing deeply buried sediments. *Earth-Sci. Rev.* **59**, 49-76.
- Distel, D., Lane, D., Olsen, G., Giovannoni, S., Pace, B., Pace, N., Stahl, D.A. and Felbeck, H. (1988) Sulfur-oxidizing bacterial endosymbionts – analysis of phylogeny and specificity by 16S ribosomal RNA sequences. *J. Bacteriol.* **170**, 2506– 2510.
- Distel, D.L., Lee, H.K.W. and Cavanaugh, C.M. (1995) Intracellular coexistence of methano- and thioautotrophic bacteria in a hydrothermal vent mussel. *Proc. Natl Acad. Sci. USA* **92**, 9598–9602.
- Dowhan, W. (1997) Molecular basis for membrane phospholipid diversity: Why are there so many lipids? *Annu. Rev. Biochem.* **66**, 199–232.
- Dowhan, W. and Bogdanov, M. (2002) Chapter 1– Functional roles of lipids in membranes. In: D.E. Vance and J.E. Vance (Eds) *Biochemistry of Lipids, Lipoproteins and Membranes* (4th Edition) Elsevier Science, 2002, pp. 1-35.
- Dubilier, N., Bergin, C. and Lott, C., (2008) Symbiotic diversity in marine animals: The art of harnessing chemosynthesis. *Nat. Rev. Micro.* **6**, 725-740.
- Dumont, M.G. and Murrell, J.C. (2005) Stable isotope probing – linking microbial identity to function. *Nat. Rev. Micro.* **3**, 499-504.
- Duperron, S., Lorion, J., Lopez, P., Samadi, S., Gros, O. and Gail F. (2009) Symbioses between deep-sea mussels (*Mytilidae: Bathymodiolinae*) and chemosynthetic bacteria: Diversity, function and evolution. *C. R. Biol.* **332**, 298–310.
- Duperron, S., Nadalig, T., Caprais, J.C., Sibuet, M., Fiala-Médioni, A., Amann, R. and Dubilier, N. (2005) Dual symbiosis in a *Bathymodiolus* mussel from a methane seep on the Gabon continental margin (South East Atlantic): 16S rRNA phylogeny and distribution of the symbionts in the gills. *Appl. Environ. Microb.* **71**, 1694–1700.
- Duperron, S., Sibuet, M., MacGregor, B.J., Kuypers, M.M.M., Fisher, C.R. and Dubilier, N. (2007) Diversity, relative abundance and metabolic potential of bacterial endosymbionts in three *Bathymodiolus* mussel species from cold seeps in the Gulf of Mexico. *Environ. Microb.* **9**, 1423–1438.

E

- Edgcomb, V., Kysela, D., Teske, A., de Vera Gomez, A. and Sogin, M.L. (2002) Benthic eukaryotic diversity in the Guaymas Basin, a hydrothermal vent environment. *Proc. Nat. Acad. Sci. USA* **99**, 7658-7662.
- Eglinton, G. and Calvin, M. (1967) Chemical Fossils. *Sci. Am.* **261**, 32-43.
- Eglinton, G., Scott, P.M., Besky, T., Burlingame, A.L. and Calvin, M. (1964) Hydrocarbons of biological origin from a one-billion-year-old sediment. *Science* **145**, 263–264.
- Einsele, G., Gieskes, J.M., Curray, J., Moore, D.M., Aguayo, E., Aubry, M.P., Fornari, D., Guerrero, J., Kastner, M., Kelts, K., Lyle, M., Matoba, Y., Molina-Cruz, A., Niemitz, L., Rueda, J., Saunders, A., Schrader, H., Simoneit, B. and Vacquier, V. (1980) Intrusion of basaltic sills into highly porous sediments, and resulting hydrothermal activity. *Nature* **283**, 441–445.
- Eisen, J.A., Smith, S.W. and Cavanaugh, C.M. (1992) Phylogenetic relationship of chemoautotrophic bacterial symbionts of *Solemya velum* say (*Mollusca: Bivalvia*) determined by 16S rRNA gene sequence analysis. *J. Bacteriol.* **174**, 3416–3421.
- Ekiel, I.I., Smith, C.P., Sprott, G.D. (1983) Biosynthetic pathway in *Methanospirillum hungatei* as determined by ¹³C nuclear magnetic resonance. *J. Bacteriol.* **156**, 316–326.
- Elderfield, H. and Schultz, A. (1996) Mid-ocean ridge hydrothermal fluxes and the chemical composition of the ocean. *Annu. Rev. Earth Planet. Sci.* **24**, 191–224.
- Elferink, M.G.L., de Wit, J.G., Driessen, A.J.M. and Konings, W.N. (1994) Stability and proton-permeability of liposomes composed of archaeal tetraether lipids. *Biochim. Biophys. Acta* **1193**, 247-254.
- Elsgaard, L., Isaksen, M.F., Jørgensen, B.B., Alayse, A.-M. and Jannasch, H.W. (1994) Microbial sulfate reduction in deep-sea sediments at the Guaymas Basin hydrothermal vent area: Influence of temperature and

- substrates. *Geochim. Cosmochim. Acta* **58**, 3335-3343.
- Elvert, M. and Niemann, H. (2008) Occurrence of unusual steroids and hopanoids derived from aerobic methanotrophs at an active marine mud volcano. *Org. Geochem.* **39**, 167-177.
- Elvert, M., Boetius, A., Knittel, K. and Jørgensen, B.B. (2003) Characterization of specific membrane fatty acids as chemotaxonomic markers for sulfate-reducing bacteria involved in anaerobic oxidation of methane. *Geomicrobiol. J.* **20**, 403-419.
- Elvert, M., Hopmans, E.C., Treude, T., Boetius, A. and Suess, E. (2005) Spatial variations of methanotrophic consortia at cold methane seeps: Implications from a high-resolution molecular and isotopic approach. *Geobiology* **3**, 195-209.
- Elvert, M., Suess, E. and Whiticar, M.J. (1999) Anaerobic methane oxidation associated with marine gas hydrates: Superlight C-isotopes from saturated and unsaturated C₂₀ and C₂₅ irregular isoprenoids. *Naturwissenschaften* **86**, 295-300.
- Ertefai, T.F., Fisher, M.C., Fredricks, H.F., Lipp, J.S., Pearson, A., Birgel, D., Udert, K.M., Cavanaugh, C.M., Gschwend, P.M. and Hinrichs, K.-U. (2008) Vertical distribution of microbial lipids and functional genes in chemically distinct layers of a highly polluted meromictic lake. *Org. Geochem.* **39**, 1572-1588.
- Estep, M.F. and Hoering, T.C. (1980) Biogeochemistry of the stable hydrogen isotopes. *Geochim. Cosmochim. Acta* **44**, 1197-1206.
- Eyster, K.M. (2007) The membrane and lipids as integral participants in signal transduction: Lipid signal transduction for the non-lipid biochemist. *Adv. Physiol. Educ.* **31**, 5-16.

F

- Fang, J. and Barcelona, M.J. (1998) Structural determination and quantitative analysis of bacterial phospholipids using liquid chromatography/ electrospray ionization/ mass spectrometry. *J. Microbiol. Methods* **33**, 23-35.
- Fang, J., Abrajano, T.A., Comet, P.A., Brooks, L.M., Sassen, R. and MacDonald, I.R. (1993) Gulf of Mexico hydrocarbon seep communities XI. Carbon isotopic fractionation during fatty acid biosynthesis of seep organisms and its implication for chemosynthetic processes. *Chem. Geol.* **109**, 271-279.
- Fang, J., Barcelona, M.J. and Semrau, J.D. (2000) Characterization of methanotrophic bacteria on the basis of intact phospholipid profiles. *FEMS Microbiol. Lett.* **189**, 67-72.
- Fang, J., Comet, P.A., Wade, T.L. and Brooks, J.M. (1992) Gulf of Mexico hydrocarbon seep communities XI. Sterol biosynthesis of seep mussels and its implications for host-symbiont association. *Org. Geochem.* **18**, 861-867.
- Fang, J.S., Barcelona, M.J. and Alvarez, P.J.J. (2000b). A direct comparison between fatty acid analysis and intact phospholipid profiling for microbial identification. *Org. Geochem.* **31**, 881-887.
- Fisher, C. R. (1990) Chemoautotrophic and methanotrophic symbioses in marine invertebrates. *Rev. Aquat. Sci.* **2**, 399-436.
- Fisher, C.R. and Childress, J.J. (1992) Organic carbon transfer from methanotrophic symbionts to the host hydrocarbon-seep mussel. *Symbiosis* **12**, 221-235.
- Fisher, C.R., Brooks, J.M., Vodenichar, J.S., Zande, J.M., Childress, J.J. and Burke Jr., R.A. (1993) The co-occurrence of methanotrophic and chemoautotrophic sulfur oxidizing bacterial symbionts in a deep-sea mussel. *Mar. Ecol.* **14**, 277-289.
- Fisher, C.R., Childress, J.J., Oremland, R.S. and Bidigare, R.R. (1987) The importance of methane and thiosulphate in the metabolism of the bacterial symbionts of two deep-sea mussels. *Mar. Biol.* **96**, 59-71.
- Fisher, C.R., Takai, K. and Le Bris, N. (2007) Hydrothermal vent ecosystems. *Oceanography* **20**, 14-23.
- Fossing, H., Ferdelman, T.G. and Berg, P. (2000) Sulfate reduction and methane oxidation in continental margin sediments influenced by irrigation (South-East Atlantic off Namibia). *Geochim. Cosmochim. Acta* **64**, 897-910.
- Foustoukos, D.I. and Seyfried, W.E., Jr. (2004) Hydrocarbons in hydrothermal vent fluids: The role of chromium-bearing catalysts. *Science* **304**, 1002-1005.
- Francis, C.A., Roberts, K.J., Beman, J.M., Santoro, A.E. and Oakley, B.B. (2005) Ubiquity and diversity of

ammonia-oxidizing archaea in water columns and sediments of the ocean, *Proc. Natl. Acad. Sci.* **102**, 14683-14688.

Froelich, P.N., Klinkhammer, G.P., Bender, M.L., Luedtke, N.A., Heath, G.R., Cullen, D., Dauphin, P., Hammond, D., Hartman, B. and Maynard, V. (1979) Early oxidation of organic matter in pelagic sediments of the eastern equatorial Atlantic: Suboxic diagenesis. *Geochim. Cosmochim. Acta* **43**, 1075-1090.

Fullarton, J.G., Wood, A.P. and Sargent, J.R. (1995) Fatty acid composition of lipids from sulphur-oxidizing and methylophilic bacteria from thyastrid and lucinid bivalves. *J. Mar. Biol. Assoc. UK* **75**, 445-454.

G

Gallagher, E., McGuinness, L., Phelps, C., Young L. Y. and Kerkhof, L. J. (2005) ¹³C-varrier DNA shortens the incubation time needed to detect benzoate-utilizing denitrifying bacteria by stable-isotope probing. *Appl. Environ. Microbiol.* **71**, 5192-5196.

German, C. R. and von Damm, K. L. (2003) Hydrothermal processes, p. 625. In H. Elderfield (ed.), *Treatise on geochemistry*, vol. 6. Elsevier, Oxford, United Kingdom.

Gillan, F.T., Stoilov, I.L., Thompson, J.E., Hogg, R.W., Wilkinson, C.R. and Djerassi, C. (1988) Fatty acids as biological markers for bacterial symbionts in sponges. *Lipids* **23**, 1139-1145.

Girguis, P.R., Cozen, A.E. and DeLong, E.F. (2005) Growth and population dynamics of anaerobic methane-oxidizing archaea and sulfate-reducing bacteria in a continuous-flow bioreactor. *Appl. Environ. Microb.* **71**, 3725-3733.

Girguis, P.R., Orphan, V., Hallam, S. and DeLong, E.F. (2003) Growth and methane oxidation rates of anaerobic methanotrophic archaea in a continuous-flow bioreactor. *Appl. Environ. Microb.* **69**, 5472-5482.

Giozzi, A., Paoli, G., De Rosa, M. and Gambacorta, A. (1983) Effect of isoprenoid cyclization on the transition temperature of lipids in thermophilic archaeobacteria. *Biochim. Biophys.* **735**, 234-242.

Godet, L., Zelnio, K.A. and Van Dover, C.L. (2011) Scientists as stakeholders in conservation of hydrothermal vents. *Conserv. Biol.* **25**, 214-222.

Goetz, F.E. and Jannasch, H.W. (1993) Aromatic hydrocarbon-degrading bacteria in the petroleum-rich sediments of the Guaymas Basin hydrothermal vent site: Preference for aromatic carboxylic acids. *Geomicrobiol. J.* **11**, 1-18.

Goldfine, H. (1984) Bacterial membranes and lipid packing theory. *J. Lipid Res.* **25**, 1501-1507.

Greinert, J., Artemov, Y., Egorov, V., De Batist, M. and McGinnis, D. (2006) 1300-m-high rising bubbles from mud volcanoes at 2080m in the Black Sea: Hydroacoustic characteristics and temporal variability. *Earth Planet. Sci. Lett.* **244**, 1-15.

Guckert, J.B., Antworth, C.P., Nichols, P.D. and White, D.C. (1985) Phospholipid, ester linked fatty-acid profiles as reproducible assays for changes in prokaryotic community structure of estuarine sediments. *FEMS Microbiol. Ecol.* **31**, 147-158.

Guerrant, G.O. and Moss, C.W. (1984) Determination of monosaccharides as aldonitrile, O-methyloxime, alditol, and cyclitol acetate derivatives by gas chromatography. *Anal. Chem.* **56**, 633-638.

Guezennec, J. and Fiala-Medioni, A. (1996) Bacterial abundance and diversity in the Barbados Trench determined by phospholipid analysis. *FEMS Microb. Ecol.* **19**, 83-93.

Guezennec, J.G., Dussauze, J., Bian, M., Rocchiccioli, F., Ringelberg, D., Hedrick, D.B. and White, D.C. (1996) Bacterial community structure from Guaymas Basin, Gulf of California, as determined by analysis of phospholipid ester-linked fatty acids. *J. Mar. Biotechnol.* **4**, 165-175.

Gundersen, J.K., Jørgensen, B.B., Larsen, E. and Jannasch, H.W. (1992) Mats of giant sulfur bacteria on deep-sea sediments due to fluctuation hydrothermal flow. *Nature* **360**, 454-455.

H

Haase, K.M., Petersen, S., Koschinsky, A., Seifert, R., Devey, C.W., Keir, R., Lackschewitz, K.S., Melchert, B., Perner, M., Schmale, O., Süling, J., Dubilier, N., Zielinski, F., Fretzdorff, S., Garbe-Schönberg, D., Westernströer, U., German, C.R., Shank, T.M., Yoerger, D., Giere, O., Kuever, J., Marbler, H., Mawick, J., Mertens, C., Stöber, U., Walter, M., Ostertag-Henning, C., Paulick, H., Peters, M., Strauss, H., Sander, S., Stecher, J., Warmuth, M. and Weber, S. (2007) Young volcanism and related hydrothermal activity at 5 °S on the slow-spreading southern Mid-Atlantic Ridge. *Geochem. Geophys. Geosyst* **8**, 1-17.

- Hanson, R.S., Hanson, T.E. (1996) Methanotrophic bacteria. *Microbiol. Rev.* **60**, 439–471.
- Harvey, H.R., Fallon, R.D. and Patton, J.S. (1986) The effect of organic matter and oxygen on the degradation of bacterial membrane lipids in marine sediments. *Geochim. Cosmochim. Acta* **50**, 795–804.
- Hasegawa, Y., Kawada, N. and Nosoh, Y. (1980) Change in chemical composition of membrane of *Bacillus caldotenax*: After shifting the growth temperature. *Arch. Microbiol.* **126**, 103–108.
- Haucke, V. and Di Paolo, G. (2007) Lipids and lipid modifications in the regulation of membrane traffic. *Curr. Opin. Cell Biol.* **19**, 426–435.
- Hayes, J.M. (1993) Factors controlling ^{13}C contents of sedimentary organic compounds: Principles and evidence. *Marine Geol.* **113**, 111–125.
- Hayes, J.M. (2001) Fractionation of carbon and hydrogen isotopes in biosynthetic processes. In *Stable Isotope Geochemistry*, vol 43. pp. 225–277.
- Hayes, J.M., Freeman, K.H., Popp, B.N. and Hoham, C.H. (1990) Compound-specific isotopic analyses - a novel tool for reconstruction of ancient biogeochemical processes. *Org. Geochem.* **16**, 1115–1128.
- Hazel, J.R. (1995) Thermal adaption in biological membranes: Is homeoviscous adaption the explanation? *Annu. Rev. Physiol.* **57**, 19–42.
- Hazel, J.R. and Williams, E.E. (1990) The role of alterations in membrane lipid composition in enabling physiological adaptation of organisms to their physical environment. *Prog. Lipid Res.* **29**, 167–227.
- Heuer, V.B., Pohlman, J.W., Torres, M.E., Elvert, M., Hinrichs, K.-U. (2009) The stable carbon isotope biogeochemistry of acetate and other dissolved carbon species in deep seafloor sediments at the northern Cascadia Margin. *Geochim. Cosmochim. Acta* **73**, 3323–3336.
- Hinrichs, K., Hmelo, L.R. and Sylva, S.P. (2003) Molecular fossil record of elevated methane levels in Late Pleistocene coastal waters. *Science* **299**, 1214–1217.
- Hinrichs, K.-U. (2002) Microbial fixation of methane carbon at 2.7 Ga: Was an anaerobic mechanism possible? *Geochem. Geophys. Geosyst.* **3**, 1042–1050.
- Hinrichs, K.-U. and Boetius, A. (2002) The anaerobic oxidation of methane: New insights in microbial ecology and biogeochemistry. In: Wefer, G., Billet, D., Hebbeln, D., Jørgensen, B.B., Schlüter, M., and Weering, T. v. Eds.), *Ocean Margin Systems*. Springer-Verlag, Berlin-Heidelberg.
- Hinrichs, K.-U., Hayes, J.M., Sylva, S.P., Brewer, P.G. and DeLong, E.F. (1999) Methane-consuming archaeobacteria in marine sediments. *Nature* **398**, 802–805.
- Hinrichs, K.-U., Summons, R.E., Orphan, V.J., Sylva, S.P. and Hayes, J.M. (2000) Molecular and isotopic analyses of anaerobic methane-oxidizing communities in marine sediments. *Org. Geochem.* **31**, 1685–1701.
- Hoehler, T. M., Amend, J.P. and Shock, E.L. (2007) Introduction – a “follow the energy” approach for astrobiology. *Astrobiology* **7**, 819–823.
- Hoehler, T.M., Alperin, M.J., Albert, D.B. and Martens, C.S. (1994) Field and laboratory studies of methane oxidation in an anoxic marine sediment: Evidence for a methanogen-sulfate reducer consortium. *Global Biogeochem Cy.* **8**, 451–463.
- Hoering, T.C. (1974) The isotopic composition of the carbon and hydrogen in organic matter of recent sediments. *Carnegie Inst. Washington Yearb.* **73**, 590–595.
- Holler, T., Wegener, G., Knittel, K., Boetius, A., Brunner, B., Kuypers, M.M.M. and Widdel, F. (2009). Substantial $^{13}\text{C}/^{12}\text{C}$ and D/H fractionation during anaerobic oxidation of methane by marine consortia enriched *in vitro*. *Environ. Microbiol. Rep.* **1**, 370–376.
- Holler, T., Wegener, G., Niemann, H., Deusner, C., Ferdelman, T. G., Boetius, A., Brunner, B. and Widdel, F. Carbon and sulfur back flux during anaerobic microbial oxidation of methane and coupled sulfate reduction. *Proc. Natl. Acad. Sci.* (2011b), doi: 10.1073/pnas.1106032108
- Holler, T., Widdel, F., Knittel, K., Amann, R., Kellermann, M.Y., Hinrichs, K.-U., Teske, A., Boetius, A. and Wegener, G. (2011a) Thermophilic anaerobic oxidation of methane by marine microbial consortia. *ISME J.* **5**, 1946–1956.
- Hölzl, G. and Dörmann, P. (2007) Structure and function of glyco-glycerolipids in plants and bacteria. *Prog. Lipid Res.* **46**, 225–243.
- House, C.H., Schopf, J.W. and Stetter, K.O. (2003) Carbon isotopic fractionation by Archaeans and other thermophilic prokaryotes. *Org. Geochem.* **34**, 345–356.

Hovland, M. (1992) Hydrocarbon seeps in northern marine waters-their occurrence and effects. *Palaios* **7**, 376-382.

Hutnak, M., Fisher, A. T., Harris, R., Stein, C., Wang, K., Spinelli, G., Schindler, M., Villinger, H. and Silver, E. (2008) Large heat and fluid fluxes driven through mid-plate outcrops on ocean crust. *Nature Geosci.* **1**, 611-614.

I

Inagaki, F., Kuypers, M.M.M., Tsunogai, U., Ishibashi, J.-I., Nakamura, K.-I., Treude, T., Ohkubo, S., Nakaseama, M., Gena, K., Chiba, H., Hirayama, H., Nunoura, T., Takai, K., Jørgensen, B.B., Horikoshi, K. and Boetius, A. (2006) Microbial community in a sediment-hosted CO₂ lake of the southern Okinawa Trough hydrothermal system. *Proc. Natl. Acad. Sci.* **103**, 14164-14169.

Innes, H.E., Bishop, A.N., Head, I.M. and Farrimond, P. (1997) Preservation and diagenesis of hopanoids in recent lacustrine sediments of Priest Pot, England. *Org. Geochem.* **26**, 565-576.

Itoh, Y.H., Sugai, A., Uda, I. and Itoh, T. (2001) The evolution of lipids. *Adv. Space Res.* **28**, 719-724.

Iversen, N. and Blackburn, T.H. (1981). Seasonal rates of methane oxidation in anoxic marine sediments. *Appl. Environ. Microbiol.* **41**, 1295-1300.

Iversen, N. and Jørgensen, B.B. (1985) Anaerobic methane oxidation rates at the sulfate-methane transition in marine sediments from Kattegat and Skagerrak (Denmark). *Limnol. Oceanogr.* **30**, 944-955.

J

Jahn, U., Summons, R., Sturt, H., Grosjean, E., and Huber, H., 2004. Composition of the lipids of Nanoarchaeum equitans and their origin from its host Ignicoccus sp. strain KIN4/I. *Arch. Microb.* **182**, 404-413.

Jahnke, L.L., Summons, R.E., Dowling, L.M. and Zahiralis, K.D. (1995) Identification of methanotrophic lipid biomarkers in cold seep mussel gills: Chemical and isotopic analysis. *Appl. Environ. Microbiol.* **61**, 576-582.

Jahnke, L.L., Summons, R.E., Hope, J.M. and Des Marais, D.J. (1999) Carbon isotopic fractionation in lipids from methanotrophic bacteria II: The effects of physiology and environmental parameters on the biosynthesis and isotopic signatures of biomarkers. *Geochim. Cosmochim. Acta* **63**, 79-93.

Jannasch, H. W. and Mottl, M.J. (1985) Geomicrobiology of deep-sea hydrothermal vents. *Science* **229**, 717-725.

Jannasch, H.W., Nelson, D.C. and Wirsén, C.O. (1989) Massive natural occurrence of unusually large bacteria (*Beggiatoa* spp.) at a hydrothermal deep-sea vent site. *Nature* **342**, 834-836.

Jehmlich, N., Schmidt, F., von Bergen, M., Richnow H. and Vogt C. (2008) Protein-based stable isotope probing (protein-SIP) reveals active species within anoxic mixed cultures. *ISME J.* **2**, 1122-1133.

Jones, A.A., Sessions A.L., Campbell, B.J., Li, C. and Valentine, D.L. (2008) D/H ratios of fatty acids from marine particulate organic matter in the California Borderland Basins. *Org. Geochem.* **39**, 485-500.

Jørgensen, B. B. and Boetius, A. (2007) Feast and famine-microbial life in the deep-sea bed. *Nat. Rev. Microbiol.* **5**, 770-781.

Jørgensen, B.B. (1982) Mineralization of organic-matter in the sea bed-the role of sulfate reduction. *Nature* **296**, 643-645.

Jørgensen, B.B., Isaksen, M.F. and Jannasch, H.W. (1992) Bacterial sulfate reduction above 100°C in deep-sea hydrothermal vent systems. *Science* **258**, 1756-1757.

Jørgensen, B.B., Zawacki, L.X. and Jannasch, H.W. (1990) Thermophilic bacterial sulfate reduction in deep-sea sediments at the Guaymas Basin hydrothermal vents (Gulf of California). *Deep-Sea Res. I* **37**, 695-710.

Joye, S.B., Boetius, A., Orcutt, B.N., Montoya, J.P., Schulz, H.N., Erickson, M.J. and Lugo, S. K. (2004) The anaerobic oxidation of methane and sulfate reduction in sediments from Gulf of Mexico cold seeps. *Chem. Geol.* **205**, 219-238.

Judd, A.G., Hovland, M., Dimitrov, L.I., Garcia Gil, S. and Jukes V. (2002) The geological methane budget at Continental Margins and its influence on climate change. *Geofluids* **2**, 109-126.

K

Kádár, E., Bettencourt, R., Costa, V., Serrão Santos, R., Lododa-Cunha, A. and Dando, P.R. (2005) Experimentally

- induced endosymbiont loss and re-acquirement in the hydrothermal vent bivalve *Bathymodiolus azoricus*. *J. Exp. Mar. Biol. Ecol.* **318**, 99–110.
- Kallmeyer, J. and Boetius, A. (2004) Effects of temperature and pressure on sulfate reduction and anaerobic oxidation of methane in hydrothermal sediments of Guaymas Basin. *Appl. Environ. Microbiol.* **70**, 1231–1233.
- Kallmeyer, J., Ferdelman, T.G. Jansen, K.-H. and Jørgensen, B.B. (2003) A high pressure thermal gradient block for investigating microbial activity in multiple deep-sea samples. *J. Microbiol. Methods* **55**, 165–172.
- Kaneda, T. (1991) Iso- and anteiso-fatty acids in bacteria: Biosynthesis, function, and taxonomic significance. *Microbiol. Rev.* **55**, 288–302.
- Karig, D.E., R.N. Anderson, and L.D. Bibee. (1978) Characteristics of back arc spreading in the Mariana trough. *J. Geophys. Res.* **83**, 213–226.
- Karl, D.M., McMurtry, G.M., Malahoff, A. and Garcia, M.O. (1988) Loihi Seamount, Hawaii: A mid-plate volcano with a distinctive hydrothermal system. *Nature* **335**, 532–535.
- Kashefi, K. and Lovley, D.R. (2003) Extending the upper temperature limit for life. *Science* **301**, 934.
- Kates, M. (1978) The phytanyl ether-linked polar lipids and isoprenoid neutral lipids of extremely halophilic bacteria. *Prog. Chem. Fats Other Lipids* **15**, 301–342.
- Kates, M. (1993) In: The biochemistry of archaea (Archaeobacteria), (Eds: M. Kates, D. J. Kushner, A. T. Matheson), Elsevier, Amsterdam, pp. 261–295.
- Kates, M., Wassef, M.K. and Pugh, E.L. (1970) Origin of the glycerol moieties in the glycerol diether lipids of *Halobacterium cutirubrum*. *Biochim. Biophys. Acta* **202**, 206–208.
- Kellermann, M.Y., Schubotz, F., Elvert, M., Lipp, J.S., Birgel, D., Prieto-Mollar, X., Dubilier, N., Hinrichs, K.-U. (2011) Symbiont-host relationships in chemosynthetic mussels: A comprehensive lipid biomarker study. *Org. Geochem.* **43**, 112–124.
- Kelley, D.S., Karson, J.A., Blackman, D.K., Früh-Green, G.L., Butterfield, D.A., Lilley, M.D., Olson, E.J., Schrenk, M.O., Roe, K.K., Lebon, G.T., Rivizzigno, P. and the A.T.S.P. (2001) An off-axis hydrothermal vent field near the Mid-Atlantic Ridge at 30° N. *Nature* **412**, 145–149.
- Kelley, D.S., Karson, J.A., Früh-Green, G.L., Yoerger, D.R., Shank, T.M., Butterfield, D.A., Hayes, J.M., Schrenk, M.O., Olson, E.J., Proskurowski, G., Jakuba, M., Bradley, A., Larson, B., Ludwig, K., Glickson, D., Buckman, K., Bradley, A.S., Brazelton, W.J., Roe, K., Elend, M.J., Delacour, A.I., Bernasconi, S.M., Lilley, M.D., Baross, J.A., Summons, R.E. and Sylva, S.P. (2005) A Serpentinite-Hosted Ecosystem: The Lost City Hydrothermal Field. *Science* **307**, 1428–1434.
- Kennicutt, M. C., Brooks, J. M., Bidigare, R. R., Fay, R. R., Wade, T. L. and McDonald, T. J. (1985) Vent-type taxa in a hydrocarbon seep region on the Louisiana slope. *Nature* **317**, 351–353.
- Knab, N.J., Dale, A.W., Lettmann, K., Fossing, H. and Jørgensen, B.B. (2008) Thermodynamic and kinetic control on anaerobic oxidation of methane in marine sediments. *Geochim. Cosmochim. Acta* **72**, 3746–3757.
- Knappy, C.S. Chong, J.P.J. and Keely, B.J. (2009) Rapid discrimination of archaeal tetraether lipid cores by liquid chromatography tandem mass spectrometry. *J. Am. Soc. Mass Spectrom.* **20**, 51–59.
- Knittel, K. and Boetius, A. (2009) Anaerobic Oxidation of Methane: Progress with an unknown process. *Annu. Rev. Microbiol.* **63**, 311–334.
- Knittel, K., Boetius, A., Lemke, A., Eilers, H. and Lochte, K. (2003) Activity, distribution, and diversity of sulfate reducers and other bacteria in sediments above gas hydrate (Cascadia margin, Oregon). *Geomicrobiol. J.* **20**, 269–294.
- Knittel, K., Lösekann, T., Boetius, A., Kort, R. and Amann, R. (2005) Diversity and distribution of methanotrophic archaea at cold seeps. *Appl. Environ. Microbiol.* **71**, 467–479.
- Kobayashi, K., Ashi, J., Boulegue, J., Cambray, H., Chamot-Rooke, N., Fujimoto, H., Furuta, T., Iiyama, J.T., Koizumi, T., Mitsuzawa, K., Monma, H., Murayama, M., Naka, J., Nakanishi, M., Ogawa, Y., Otsuka, K., Okada, M., Oshida, A., Shima, N., Soh, W., Takeuchi, A., Watanabe, M. and Yamagata, T. (1992) Deep-tow survey in the KAIKO-Nankai cold seepage areas. *Earth Planet. Sci. Lett.* **109**, 347–354.
- Koga, Y. (2010) The biosynthesis and evolution of archaeal membranes and ether phospholipids. K. N. Timmis (Ed.), *Handbook of Hydrocarbon and Lipid Microbiology*, Springer-Verlag Berlin Heidelberg,

pp. 452-456.

- Koga, Y. and Morii, H. (2005) Recent advances in structural research on ether lipids from Archaea including comparative and physiological aspects. *Biosci. Biotech. Bioch.* **69**, 2019-2034.
- Koga, Y. and Morii, H. (2007) Biosynthesis of ether-type polar lipids in Archaea and evolutionary considerations. *Microbiol. Mol. Biol. Rev.* **71**, 97-120.
- Koga, Y. and Nakano, M. (2008) A dendrogram of archaea based on lipid component parts composition and its relationship to rRNA phylogeny. *Syst. Appl. Microbiol.* **31**, 169-182.
- Koga, Y., Morii, H., Akagawa-Matsushita, M. and Ohga, I. (1998) Correlation of polar lipid composition with 16S rRNA phylogeny in methanogens. Further analysis of lipid component parts. *Biosci. Biotech. Bioch.* **62**, 230-236.
- Koga, Y., Nishihara, M., Morii, H. and Akagawa-Matsushita M. (1993) Ether polar lipids of methanogenic bacteria: Structures, comparative aspects, and biosynthesis. *Microbiol. Rev.* **57**, 164-182.
- Kohring, L.L., Ringelberg, D.B., Devereux, R., Stahl, D.A., Mittelman, M.W. and White, D.C. (1994) Comparison of phylogenetic relationships based on phospholipid fatty acid profiles and ribosomal RNA sequence similarities among dissimilatory sulfate-reducing bacteria. *FEMS Microbiol. Lett.* **119**, 303-308.
- Könneke, M., Bernhard, A.E., de la Torre, J.R., Walker, C.B., Waterbury, J.B. and Stahl, D.A. (2005) Isolation of an autotrophic ammoniaoxidizing marine archaeon. *Nature* **437**, 543-546.
- Kopf, A. J. (2002) Significance of mud volcanism. *Rev. Geophys.* **40**, 1-52.
- Kostetsky, E.Y. and Velansky, P.V. (2009) Phospholipids of sea worms, mollusks, and arthropods. *Russ. J. Mar. Biol.* **35**, 187-199.
- Kraffe, E., Saudant, P. and Marty, Y. (2004) Fatty acids of serine, ethanolamine, and choline plasmalogens in some marine bivalves. *Lipids* **39**, 59-66.
- Kulm, L.D. and Suess, E. (1990) Relationship between carbonate deposits and fluid venting: Oregon accretionary prism. *J. Geophys. Res.* **95**, 8899-8915.
- Kvenvolden, K.A. (1993) Gas hydrates - geological perspective and global change. *Rev. Geophys.* **31**, 173-187.
- ## L
- Lahiri, S. and Futerman, A.H. (2007) The metabolism and function of sphingolipids and glycosphingolipids. *Cell. Mol. Life Sci.* **64**, 2270-2284.
- Lallemand, S.E., Glaçon, G., Lauriat-Rage, A., Fiala-Médioni, A., Cadet, J-P, Beck, C., Sibuet, M., Iiyama, J.T., Sakai, H. and Taira, A. (1992) Seafloor manifestations of fluid seepage at the top of a 2000-meter deep ridge in the eastern Nankai accretionary wedge: Long-lived venting and tectonic implications. *Earth Planet. Sc.Lett.* **109**, 333-346.
- Langworthy, T.A. (1982) Lipids of bacteria in extreme environments. In: Current Topics in Membranes and Transport, Membrane lipids of prokaryotes 17 (Eds. Razin, S., Rottem, S.), 45-77. Academic press.
- Langworthy, T.A. and Pond, J.L. (1986) Archaeobacterial ether lipids and chemotaxonomy. *System. Appl. Microbiol.* **7**, 253-257.
- Langworthy, T.A., Holzer, G., Zeikus, J. and Tornabene, T.G. (1983) Iso- and anteiso-branched glycerol diethers of the thermophilic anaerobe *Thermodesulfotobacterium commune*. *Syst. Appl. Microbiol.* **4**, 1-17.
- Lanoil, B.D., Sassen, R., La Duc, M.T., Sweet, S.T. and Nealson, K.H. (2001) Bacteria and Archaea physically associated with Gulf of Mexico gas hydrates. *Appl. Environ. Microbiol.* **67**, 5143-5153.
- Larowe, D.E., Dale, A.W. and Regnier, P. (2008) A thermodynamic analysis of the anaerobic oxidation of methane in marine sediments. *Geobiology* **6**, 436-449.
- Lechevalier, H. and Lechevalier, M.P. (1988) Chemotaxonomic use of lipids - an overview. In: Ratledge and Wilkinson, S. G. Eds., Microbial Lipids Volume 1. Academic Press Limited.
- Lelieveld, J., Crutzen, P. J. and Brühl, C. (1993) Climate effects of atmospheric methane. *Chemosphere* **26**, 739-768.
- Lelieveld, J.O.S., Crutzen, P.J. and Dentener, F.J. (1998) Changing concentration, lifetime and climate forcing of atmospheric methane. *Tellus B* **50**, 128-150.
- Li, C., Sessions, A.L., Kinnaman, F.S. and Valentine, D.L. (2009) Hydrogen-isotopic variability in lipids from Santa Barbara Basin sediments. *Geochim. Cosmochim. Acta* **73**, 4803-4823.

- Liefkens, W., Boon, J.J., De Leeuw, J.W. (1979) On the occurrence of alkyl- and alk-1-enyl-diacylglycerides in the lugworm *Arenicola marina*. *Neth. J. Sea Res.* **13**, 479–486.
- Lin, Y.S., Kellermann, M.Y., Lipp, J.S., Elvert, M., Wegener, G., Holler, T. and Hinrichs, K.-U. Intramolecular stable carbon isotope probing of archaeal diglycosyl tetraether lipids, a dominant group of intact polar lipid in marine sediment. (In preparation).
- Lin, Y.-S., Lipp, J.S., Yoshinaga, M.Y., Lin, S.-H., Elvert, M. and Hinrichs, K.-U. (2010) Intramolecular stable carbon isotopic analysis of archaeal glycosyl tetraether lipids. *Rapid Commun. Mass Spectrom.* **24**, 2817–2826.
- Lipp, J.S. and Hinrichs, K.-U. (2009) Structural diversity and fate of intact polar lipids in marine sediments. *Geochim. Cosmochim. Acta* **73**, 6816–6833.
- Lipp, J.S., Morono, Y., Inagaki, F. and Hinrichs, K.-U. (2008) Significant contribution of Archaea to extant biomass in marine subsurface sediments. *Nature* **454**, 991–994.
- Liu, X.-L., Leider, A., Gillespie, A., Gröger, J., Versteegh, G. J. M. and Hinrichs, K.-U. (2010) Identification of polar lipid precursors of the ubiquitous branched GDGT orphan lipids in a peat bog in Northern Germany. *Org. Geochem.* **41**, 653–660.
- Liu, X.-L., Lipp, J.S. and Hinrichs, K.-U. (2011) Distribution of intact and core GDGTs in marine sediments. *Org. Geochem.* **42**, 368–375.
- Lollar, B.S., Westgate, T.D., Ward, J.A., Slater, G.F. and Lacrampe-Couloume, G. (2002) Abiogenic formation of alkanes in the Earth's crust as a minor source for global hydrocarbon reservoirs. *Nature* **416**, 522–524.
- Lonsdale, P. (1977) Clustering of suspension-feeding macrobenthos near abyssal hydrothermal vents at oceanic spreading centers. *Deep-Sea Res.* **24**, 857–863.
- Lonsdale, P. and Becker, K. (1985) Hydrothermal plumes, hot springs, and conductive heat flow in the southern trough of the Guaymas Basin. *Earth Planet. Sci.* **73**, 211–225.
- Lonsdale, P. and Lawver, L.A. (1980) Immature plate boundary zones studied with a submersible in the Gulf of California. *Geol. Soc. Amer. Bull.* **91**, 555–569.
- Lösekan, T., Robador, A., Niemann, H., Knittel, K., Boetius, A. and Dubilier, N. (2008) Endosymbioses between bacteria and deep-sea siboglinid tubeworms from an Arctic Cold Seep (Haakon Mosby Mud Volcano, Barents Sea). *Environ. Microbiol.* **10**, 3237–3254.

M

- Macalady, J.L., Vestling, M.M., Baumler, D., Boekelheide, N., Kaspar, C.W. and Banfield, J.F. (2004) Tetraether-linked membrane monolayers in *Ferroplasma* spp: A key to survival in acid. *Extremophiles* **8**, 411–419.
- MacDonald, I.R., Bohrmann, G., Escobar, E., Abegg, F., Blanchon, P., Blinova, V., Brückmann, W., Drews, M., Eisenhauer, A., Han, X., Heeschen, K., Meier, F., Mortera, C., Naehr, T., Orcutt, B., Bernard, B., Brooks, J. and de Farago, M. (2004) Asphalt volcanism and chemosynthetic life in the Campeche Knolls, Gulf of Mexico. *Science* **304**, 999–1002.
- MacDonald, I.R., Boland, G.S., Baker, J.S., Brooks, J.M., Kennicutt, M.C. and Bidigare, R.R. (1989) Gulf of Mexico hydrocarbon seep communities. *Mar. Biol.* **101**, 235–247.
- MacDonald, I.R., Guinasso Jr., N.L., Sassen, R., Brooks, J.M., Lee, L. and Scott, K.T. (1994) Gas hydrate that breaches the sea floor on the continental slope of the Gulf of Mexico. *Geology* **22**, 699–702.
- Makula, R.A. (1978) Phospholipid composition of methane-utilizing bacteria. *J. Bacteriol.* **134**, 771–777.
- Männistö, M. and Puhakka, J. (2001) Temperature- and growth-phase-regulated changes in lipid fatty acid structures of psychrotolerant groundwater Proteobacteria. *Arch. Microbiol.* **177**, 41–46.
- Martens, C.S. (1990) Generation of short chain organic acid anions in hydrothermally altered sediments of the Guaymas Basin, Gulf of California. *Appl. Geochem.* **5**, 71–76.
- Martens, C.S. and Berner, R.A. (1974) Methane production in the interstitial waters of sulfate-depleted marine sediments. *Science* **185**, 1167–1169.
- Martens, C.S. and Val Klump, J. (1980) Biogeochemical cycling in an organic-rich coastal marine basin-I. Methane sediment-water exchange processes. *Geochim. Cosmochim. Acta* **44**, 471–490.
- Mathai, J.C., Sprott, G.D. and Zeidel, M.L. (2001) Molecular mechanisms of water and solute transport across archaeobacterial lipid membranes. *J. Biol. Chem.* **276**, 27266–27271.
- Matsubara, T., Morita, M. and Hayashi, A. (1990) Determination of the presence of ceramide

- aminoethylphosphonate and ceramide N-methylaminoethylphosphonate in marine animals by fast atom bombardment mass spectrometry. *Biochim. Biophys. Acta* **1042**, 280–286.
- Matsuno, Y., Sugai, A., Higashibata, H., Fukuda, W., Ueda, K., Uda, I., Sato, I., Itoh, T., Imanaka, T. and Fujiwara, S. (2009) Effect of growth temperature and growth phase on the lipid composition of the archaeal membrane from *Thermococcus kodakaraensis*. *Biosci. Biotechnol. Biochem.* **73**, 104–108.
- McCaffrey, M.A., Farrington, J.W. and Repeta, D.J. (1989) Geochemical implications of the lipid composition of *Thioploca* spp. from the Peru upwelling region 15 S. *Org. Geochem.* **14**, 61–68.
- Michael W., F. (2006) Stable-isotope probing of DNA: Insights into the function of uncultivated microorganisms from isotopically labeled metagenomes. *Curr. Opin. Biotech.* **17**, 59–66.
- Michaelis, W., Seifert, R., Nauhaus, K., Treude, T. and Thiel, V. (2002) Microbial reefs in the Black Sea fueled by anaerobic oxidation of methane. *Science* **297**, 1013–1015.
- Miyatake, T., MacGregor, B.J. and Boschker, T.S. (2009) Linking microbial community function to phylogeny of sulfate-reducing Deltaproteobacteria in marine sediments by combining stable isotope probing with magnetic-bead capture hybridization of 16S rRNA. *Appl. Environ. Microbiol.* **75**, 4927–4935.
- Moodley, L., Boschker, H.T.S., Middelburg, J.J., Pel, R., Herman P.M.J., de Deckere, E. and Heip, C.H.R. (2000) Ecological significance of benthic foraminifera: C-13 labelling experiments. *Mar. Ecol. Progr. Ser.* **202**, 289–295.
- Morand, O.H., Zoeller, R.A. and Raetz, C.R.H. (1988) Disappearance of plasmalogens from membranes of animal cells subjected to photosensitized oxidation. *J. Biol. Chem.* **263**, 11597–11606.
- Morii, H., Eguchi, T. and Koga, Y. (2007) *In vitro* biosynthesis of ether-type glycolipids in the methanoarchaeon *Methanothermobacter thermautotrophicus*. *J. Bacteriol.* **189**, 4053–4061.
- Morii, H., Eguchi, T., Nishihara, M., Kakinuma, K., König, H. and Koga, Y. (1998) A novel ether core lipid with H-shaped C₈₀-isoprenoid hydrocarbon chain from the hyperthermophilic methanogen *Methanothermus fervidus*. *Biochim. Biophys. Acta* **1390**, 339–345.
- Mukhamedova, K.S. and Glushenkova, A.I. (2000) Neutral phosphonolipids. *Chem. Nat. Comp.* **36**, 329–341.
- ## N
- Nagan, N. And Zoeller, R.A. (2001) Plasmalogens: Biosynthesis and functions. *Prog. Lipid Res.* **40**, 199–229.
- Nauhaus, K., Albrecht, M., Elvert, M., Boetius, A. and Widdel, F. (2007) *In vitro* cell growth of marine archaeal–bacterial consortia during anaerobic oxidation of methane with sulfate. *Environ. Microbiol.* **9**, 187–196.
- Nauhaus, K., Boetius, A., Krüger, M. and Widdel, F. (2002) *In vitro* demonstration of anaerobic oxidation of methane coupled to sulphate reduction in sediment from a marine gas hydrate area. *Environ. Microbiol.* **4**, 296–305.
- Nauhaus, K., Treude, T., Boetius, A. and Krüger, M. (2005) Environmental regulation of the anaerobic oxidation of methane: A comparison of ANME–I and ANME–II communities. *Environ. Microbiol.* **7**, 98–106.
- Nelson, D.C., Wirsén, C.O. and Jannasch, H.W. (1989) Characterization of large autotrophic *Beggiatoa* abundant at hydrothermal vents of the Guaymas Basin. *Appl. Environ. Microbiol.* **55**, 2909–2917.
- Nemoto, N., Shida, Y., Shimada, H., Oshima, T. and Yamagishi, A. (2003) Characterization of the precursor of tetraether lipid biosynthesis in the thermoacidophilic archaeon *Thermoplasma acidophilum*. *Extremophiles* **7**, 235–243.
- Nichols, D.S., Nichols, P.D., Russell, N.J., Davies, N.W. and McMeekin, T.A. (1997) Polyunsaturated fatty acids in the psychrophilic bacterium *Shewanella gelidimarina* ACAM 456T: Molecular species analysis of major phospholipids and biosynthesis of eicosapentaenoic acid. *Biochim. Biophys. Acta* **1347**, 164–176.
- Nichols, P.D., Guckert, J.B. and White, D.C. (1986) Determination of monounsaturated fatty acid double-bond position and geometry for microbial monocultures and complex consortia by capillary GC–MS of their dimethyl disulphide adducts. *J. Microbiol. Methods* **5**, 49–55.
- Nichols, P.D., Smith, G.A., Antworth, C.P., Hanson, R.S. and White, D.C. (1985) Phospholipid and lipopolysaccharide normal and hydroxy fatty acids as potential signatures for methane-oxidizing bacteria. *FEMS Microb. Ecol.* **31**, 327–335.
- Nicolaus, B., Manca, M.C., Lama, L., Esposito, E. and Gambacorta, A. (2001) Lipid modulation by environmental

- stresses in two models of extremophiles isolated from Antarctica. *Polar Biol.* **24**, 1-8.
- Niemann, H. and Elvert, M. (2008) Diagnostic lipid biomarker and stable carbon isotope signatures of microbial communities mediating the anaerobic oxidation of methane with sulphate. *Org. Geochem.* **39**, 1668–1677.
- Niemann, H., Elvert, M., Hovland, M., Orcutt, B., Judd, A. G., Suck, I., Gutt, J., Joye, S.B., Damm, E., Finster, K. and Boetius, A. (2005) Methane emission and consumption at a North Sea gas seep (Tommeliten area). *Biogeosciences* **2**, 335–351.
- Niemann, H., Lösekann, T., de Beer, D., Elvert, M., Nadalig, T., Knittel, K., Amann, R., Sauter, E.J., Schluter, M., Klages, M., Foucher, J.P. and Boetius, A. (2006) Novel microbial communities of the Haakon Mosby mud volcano and their role as a methane sink. *Nature* **443**, 854-858.
- Nishihara, M., Morii, H. and Koga, Y. (1989) Heptads of polar ether lipids of an archaeobacterium, *Methanobacterium thermoautotrophicum*: Structure and biosynthetic relationship. *Biochemistry* **28**, 95-102.
- O**
- Oba, M., Sakata, S. and Tsunogai, U. (2006) Polar and neutral isopranyl glycerol ether lipids as biomarkers of archaea in near-surface sediments from the Nankai Trough. *Org. Geochem.* **37**, 1643-1654.
- Orcutt, B., Boetius, A., Elvert, M., Samarking, V. and Joye, S.B. (2005) Molecular biogeochemistry of sulfate reduction, methanogenesis and the anaerobic oxidation of methane at Gulf of Mexico cold seeps. *Geochim. Cosmochim. Acta* **69**, 4267-4281.
- Orcutt, B.N., Sylvan, J.B., Knab, N.J. and Edwards, K.J. (2011) Microbial Ecology of the Dark Ocean above, at, and below the Seafloor. *Microbiol. Mol. Bio. R.* **75**, 361-422.
- Orphan, V.J. and Hoehler, T.M. (2011) Microbiology: Hydrogen for dinner. *Nature* **476**, 154-155.
- Orphan, V.J., House, C.H., Hinrichs, K.-U., McKeegan, K.D. and DeLong, E.F. (2002) Multiple archaeal groups mediate methane oxidation in anoxic cold seep sediments. *Proc. Natl. Acad. Sci. USA* **99**, 7663–7668.
- Ourisson, G. and Rohmer, M. (1982) Prokaryotic polyterpenes: Phylogenetic precursors of sterols. In: Bronner, F., Kleinzeller, A. (Eds.), *Current Topics in Membranes and Transport, Membrane Lipids of Prokaryotes*, vol. 17. Academic Press, New York, pp. 153–182.
- Ourisson, G., Rhomer, M. and Poralla, K. (1987) Prokaryotic hopanoids and other polyterpenoid sterol surrogates. *Annu. Rev. Microbiol.* **41**, 301-333.
- P**
- Page, H.M., Fisher, C.R. and Childress, J.J. (1990) Role of filter-feeding in the nutritional biology of a deep-sea mussel with methanotrophic symbionts. *Mar. Biol.* **104**, 251–257.
- Pancost R.D., Sinninghe Damste J.S., de Lint S., van der Maarel M.J.E.C., Gottschal J.C. and the medinaut shipboard scientific party (2000) Biomarker evidence for widespread anaerobic methane oxidation in mediterranean sediments by a consortium of methanogenic archaea and bacteria. *Appl. Environ. Microbiol.* **66**, 1126–1132.
- Pancost, R.D., Hopmans, E.C. and Damste, J.S.S. (2001) Archaeal lipids in Mediterranean cold seeps: Molecular proxies for anaerobic methane oxidation. *Geochim. Cosmochim. Acta* **65**, 1611-1627.
- Parkes, J.R. and Calder, G.A. (1985) The cellular fatty acids of three strains of *Desulfobulbus*, a propionate-utilising sulphate-reducing bacterium. *FEMS Microbiol. Let.* **31**, 361-363.
- Parkes, R.J., Webster, G., Cragg, B.A., Weightman, A.J., Newberry, C.J., Ferdeman, T.G., Kallmeyer, J., Jørgensen, B.B., Aiello, I.W. and Fry, J.C. (2005) Deep sub-seafloor prokaryotes stimulated at interfaces over geological time. *Nature* **436**, 390-394.
- Paull, C.K., Hecker, B., Commeau, R., Freeman-Lynde, R.P., Neumann, C., Corso, W.P., Golubic, S., Hook, J.E., Sikes, E. and Curray, J. (1984) Biological Communities at the Florida Escarpment Resemble Hydrothermal Vent Taxa. *Science* **226**, 965-967.
- Pearson, A. (2010) Pathways of carbon assimilation and their impact on organic matter values $\delta^{13}\text{C}$. In: Timmis, K.N. (Ed.), *Handbook of Hydrocarbon and Lipid Microbiology*. Springer-Verlag, Berlin-Heidelberg.
- Pearson, A., Seewald, J.S. and Eglinton, T.I. (2005) Bacterial incorporation of relict carbon in the hydrothermal

- environment of Guaymas Basin. *Geochim. Cosmochim. Acta* **69**, 5477-5486.
- Petersen, J.M., Dubilier, N., 2010. Symbiotic methane oxidizers. In: Timmis, K.N. (Ed.), Handbook of Hydrocarbon and Lipid Microbiology. Springer-Verlag, Berlin and Heidelberg, pp. 1978–1992.
- Petersen, J.M., Zielinski, F.U., Pape, T., Seifert, R., Moraru, C., Amann, R., Hourdez, S., Girguis, P.R., Wankel, S.D., Barbe, V., Pelletier, E., Fink, D., Borowski, C., Bach, W. and Dubilier, N. (2011) Hydrogen is an energy source for hydrothermal vent symbioses. *Nature* **476**, 176-180.
- Pitcher A., Hopmans E.C., Schouten S. and Sinninghe Damsté J.S. (2009) Separation of core and intact polar archaeal tetraether lipids using silica columns: Insights into living and fossil biomass contributions. *Org. Geochem.* **40**, 12-19.
- Pohlman, J.W., Ruppel, C., Hutchinson, D.R., Downer, R. and Coffin, R.B. (2008) Assessing sulfate reduction and methane cycling in a high salinity pore water system in the northern Gulf of Mexico. *Mar. Petrol. Geol.* **25**, 942-951.
- Pond, D.W., Bell, M.V., Dixon, D.R., Fallick, A.E., Segonzac, M. and Sargent, J.R. (1998) Stable-carbon-isotope composition of fatty acids in hydrothermal vent mussels containing methanotrophic and thiotrophic bacterial endosymbionts. *Appl. Environ. Microbiol.* **64**, 370–375.
- Popendorf, K.J., Lomas, M.W. and Van Mooy, B.A.S. (2011) Microbial sources of intact polar diacylglycerolipids in the Western North Atlantic Ocean. *Org. Geochem.* **42**, 803-811.
- Pranal, V., Fiala-Medioni, A. and Guezennec, J. (1997) Fatty acid characteristics in two symbiont-bearing mussels from deep-sea hydrothermal vents of the southwestern Pacific. *J. Mar. Biol. Assoc. UK* **77**, 473–492.
- Pranal, V., Guezennec, J. and Fiala-Medioni, A. (1996) Fatty acid characteristics in two symbiotic gastropods from a deep hydrothermal vent of the West Pacific. *Mar. Ecol. Prog. Series* **142**, 175–184.
- Price, P.B. and Sowers, T. (2004) Temperature dependence of metabolic rates for microbial growth, maintenance, and survival. *Proc. Natl. Acad. Sci. USA* **101**, 4631–4636.

R

- Radajewski, S., Ineson, P., Parekh, N. R. and Murrell, J. C. (2000) Stable-isotope probing as a tool in microbial ecology. *Nature* **402**, 646-649.
- Rao, V.P., Ramachandran, S. and Cornwell, D.G. (1967) Synthesis of fatty aldehydes and their cyclic acetals (new derivatives for the analysis of plasmalogens). *J. Lipid Res.* **8**, 380–390.
- Rau, G.H. and Hedges, J.I. (1979) Carbon-13 depletion in a hydrothermal vent mussel: Suggestion of a chemosynthetic food source. *Science* **203**, 648–649.
- Raulfs, E.C., Macko, S.A. Van Dover, C.L. (2004) Tissue and symbionts condition of mussels (*Bathymodiolus thermophilus*) exposed to varying levels of hydrothermal activity. *J. Mar. Biol. Assoc.* **84**, 229–234.
- Reeburgh, W.S. (1969) Observations of gases in Chesapeake Bay sediments. *Limnol. Oceanogr.* **14**, 368-375.
- Reeburgh, W.S. (1976) Methane consumption in Cariaco Trench waters and sediments. *Earth Planet. Sci. Lett.* **28**, 337-344.
- Reeburgh, W.S. (1980) Anaerobic methane oxidation: Rate depth distributions in Skan Bay sediments. *Earth Planet. Sci. Lett.* **47**, 345-352.
- Reeburgh, W.S. (2007) Oceanic methane biogeochemistry. *Chem. Rev.* **107**, 1-28.
- Reeves, E.P., Seewald, J.S., Saccocia, P., Bach, W., Craddock, P.R., Shanks, W.C., Sylva, S.P., Walsh, E., Pichler, T., Rosner, M. (2011) Geochemistry of hydrothermal fluids from the PACMANUS, Northeast Pual and Vienna Woods hydrothermal fields, Manus Basin, Papua New Guinea. *Geochem. Cosmochim. Acta* **75**, 1088-1123.
- Reitner, J., Peckmann, J., Blumenberg, M., Michaelis, W., Reimer, A. and Thiel, V. (2005) Concretionary methane-seep carbonates and associated microbial communities in Black Sea sediments. *Palaogeogr. Paleoclimatol. Paleoecol.* **227**, 18–30.
- Riou, V., Bouillon, S., Serrão Santos, R., Dehairs, F. and Colaco, A. (2010) Tracing carbon assimilation in endosymbiotic deep-sea hydrothermal vent Mytilid fatty acids by ¹³C-fingerprinting. *Biogeosci. Disc.* **7**, 3453–3475.
- Riou, V., Halary, S., Duperron, S., Bouillon, S., Elskens, M., Bettencourt, R., Santos, R.S., Dehairs, F. and Colaço, A. (2008) Influence of CH₄ and H₂S availability on symbiont distribution, carbon assimilation and

- transfer in the dual symbiotic vent mussel *Bathymodiolus azoricus*. *Biogeoscience* **5**, 1681–1691.
- Rohmer, M. (1993) The biosynthesis of triterpenoids of the hopane series in the Eubacteria: A mine of new enzyme reactions. *Pure Appl. Chem.* **65**, 1293–1298.
- Rohmer, M., Bouvier-Nave, P. and Ourisson, G. (1984) Distribution of hopanoid triterpenes in prokaryotes. *J. Gen. Microbiol.* **130**, 1137–1150.
- Rona, P.A., Bougault, H., Charlou, J.L., Appriou, P., Nelsen, T.A., Trefry, J.H. Eberhart, G.L., Barone, A. and Needham, H.D. (1992) Hydrothermal circulation, serpentinization, and degassing at a rift valley-fracture zone intersection; Mid-Atlantic Ridge near 15°N, 45°W. *Geology* **20**, 783–786.
- Rossel, P.E., Elvert, M., Ramette, A., Boetius, A. and Hinrichs, K.-U. (2011) Factors controlling the distribution of anaerobic methanotrophic communities in marine environments: Evidence from intact polar membrane lipids. *Geochim. Cosmochim. Acta* **75**, 164–184.
- Rossel, P.E., Lipp, J.S., Fredricks, H.F., Arnds, J., Boetius, A., Elvert, M. and Hinrichs, K.-U. (2008) Intact polar lipids of anaerobic methanotrophic archaea and associated bacteria. *Org. Geochem.* **39**, 992–999.
- Rothschild, L. J. and Mancinelli, R.L. (2001) Life in extreme environments. *Nature* **409**, 1092–1101.
- Roussel, E.G., Bonavita, M.-A.C., Querellou, J., Cragg, B.A., Webster, G., Prieur, D. and Parkes, R.J. (2008) Extending the subsea-floor biosphere. *Science* **320**, 1046–1056.
- Ruby, E.G., Jannasch, H.W. and Deuser, W.G. (1987) Fractionation of stable carbon isotopes during chemoautotrophic growth of sulfur-oxidizing bacteria. *Appl. Environ. Microbiol.* **53**, 1940–1943.
- Russell, N.J., Evans, R. I., ter Steeg, P.F., Hellemons, J., Verheul, A. and Abee, T. (1995) Membranes as a target for stress adaptation. *Int. J. Food Microbiol.* **28**, 255–261.
- Rütters, H., Sass, H., Cypionka, H. and Rullkötter, J. J. (2002a) Phospholipid analysis as a tool to study microbial communities. *J. Microbiolog. Meth.* **48**, 149–160.
- Rütters, H., Sass, H., Cypionka, H. and Rullkötter J. J. (2002b) Microbial communities in a Wadden Sea sediment core—clues from analyses of intact glyceride lipids, and released fatty acids. *Org. Geochem.* **33**, 803–816.
- Rütters, H., Sass, H., Cypionka, H., Rullkötter, J. (2001) Monoalkylether phospholipids in the sulfate-reducing bacteria *Desulfosarcina variabilis* and *Desulforhabdus amnigenus*. *Arch. Microbiol.* **176**, 435–442.

S

- Sander, S.G. and Koschinsky, A. (2011) Metal flux from hydrothermal vents increased by organic complexation. *Nature Geosci.* **4**, 145–150.
- Sassen, R., Roberts, H.H., Aharon, P., Larkin, J., Chinn, E.W. and Carney, R. (1993) Chemosynthetic bacterial mats at cold hydrocarbon seeps, Gulf of Mexico continental slope. *Org. Geochem.* **20**, 77–89.
- Sauter, E.J., Muyakshin, S.I., Charlou, J.L., Schlüter, M., Boetius, A., Jerosch, K., Damm, E., Foucher, J-P. and Klages, M. (2006) Methane discharge from a deep-sea submarine mud volcano into the upper water column by gas hydrate-coated methane bubbles. *Earth Planet. Sci. Lett.* **243**, 354–365.
- Schink, B. (1997). Energetics of syntrophic cooperation in methanogenic degradation. *Microbiol. Mol. Biol. Rev.* **61**, 262–280.
- Schmidt G.A., Bigg G.R. and Rohling E.J. (1999) Global seawater oxygen-18 database. Available from: <http://www.giss.nasa.gov/data/o18data/>
- Schouten, S., Bowman, J.P., Irene, W., Rijpstra, C. and Sinninghe-Damsté, J.S. (2000) Sterols in a psychrophilic methanotroph, *Methylosphaera hansonii*. *FEMS Microbiol. Lett.* **186**, 193–195.
- Schouten, S., Middelburg, J.J., Hopmans, E.C. and Sinninghe Damsté, J.S. (2010) Fossilization and degradation of intact polar lipids in deep subsurface sediments: A theoretical approach. *Geochim. Cosmochim. Acta* **74**, 3806–3814.
- Schouten, S., Ossebaar, J., Schreiber, K., Kienhuis, M.V.M., Langer, G., Benthien, A. and Bijma, J. (2006) The effect of temperature, salinity and growth rate on the stable hydrogen isotopic composition of long chain alkenones produced by *Emiliania huxleyi* and *Gephyrocapsa oceanica*. *Biogeoscience* **3**, 113–119.
- Schouten, S., Wakeham, S.G. Hopmans, E.C. and Sinninghe Damsté, J.S. (2003) Biogeochemical evidence that thermophilic archaea mediate the anaerobic oxidation of methane. *Appl. Environ. Microbiol.* **69**, 1680–1686.

- Schreiber, L., Holler, T., Knittel, K., Meyerdierks, A. and Amann, R. (2010) Identification of the dominant sulfate-reducing bacterial partner of anaerobic methanotrophs of the ANME-2 clade. *Environ. Microbiol.* **12**, 2327–2340.
- Schrenk, M.O., Kelley, D.S., Bolton, S.A. and Baross, J.A. (2004) Low archaeal diversity linked to seafloor geochemical processes at the Lost City Hydrothermal Field, Mid-Atlantic Ridge. *Environ. Microbiol.* **6**, 1086–1095.
- Schrenk, M.O., Kelley, D.S., Delaney, J.R. and Baross, J.A. (2003) Incidence and diversity of microorganisms within the walls of an active deep-sea sulfide chimney. *Appl. Environ. Microbiol.* **69**, 3580–3592.
- Schubotz F., Wakeham S.G., Lipp, J.S., Fredricks, H.F. and Hinrichs, K.-U. (2009) Detection of microbial biomass by intact polar membrane lipid analysis in the water column and surface sediments of the Black Sea. *Environ. Microbiol.* **11**, 2720–2734.
- Schubotz, F., Lipp, J., Elvert, M., Kasten, S., Zabel, M., Prieto-Mollar, X., Bohrmann, G. and Hinrichs, K.-U. (2011a) Petroleum degradation and associated microbial signatures at the Chapopote asphalt volcano, Southern Gulf of Mexico. *Geochim. Cosmochim. Acta* **75**, 4377–4398.
- Schubotz, F., Lipp, J.S., Elvert, M. and Hinrichs, K.-U. (2011b) Stable carbon isotopic compositions of intact polar lipids reveal complex carbon flow patterns among hydrocarbon degrading microbial communities at the Chapopote asphalt volcano. *Geochim. Cosmochim. Acta* **75**, 4399–4415.
- Scott, K.M. and Cavanaugh, C.M. (2007) CO₂ uptake and fixation by endosymbiotic chemoautotrophs from the bivalve *Solemya velum*. *Appl. Environ. Microbiol.* **73**, 1174–1179.
- Seewald, J.S., Cruse, A.M., Lilley, M.D. and Olsen, E.J. (1998) Hot-spring fluid chemistry at Guaymas Basin, Gulf of California: Temporal variations and volatile content. *EOS* **79**, 46–52.
- Seno, T. and Maruyama, S. (1984) Paleogeographic reconstruction and origin of the Philippine Sea. *Tectonophysics* **102**, 53–84.
- Sessions, A.L., Burgoyne, T.W., Schimmelmann, A. and Hayes, J.M. (1999) Fractionation of hydrogen isotopes in lipid biosynthesis. *Org. Geochem.* **30**, 1193–1200.
- Sherwood Lollar, B., Westgate, T.D., Ward, J.A., Slater, G.F. and Lacrampe-Couloume, G. (2002) Abiogenic formation of alkanes in the Earth's crust as a minor source for global hydrocarbon reservoirs. *Nature* **416**, 522–524.
- Shimada, H., Nemoto, N., Shida, Y., Oshima, T. and Yamagishi, A. (2008) Effects of pH and temperature on the composition of polar lipids in *Thermoplasma acidophilum* HO-62. *J. Bacteriol.* **190**, 5404–5411.
- Simoneit, B.R.T. and Lonsdale, P.F. (1982) Hydrothermal petroleum in mineralized mounds at the seabed of Guaymas Basin. *Nature* **295**, 198–202.
- Sinninghe Damsté, J.S., Schouten, S., Hopmans, E.C., van Duin, A.C.T. and Geenevasen, J.A.J. (2002) Crenarchaeol: The characteristic core glycerol dibiphytanyl glycerol tetraether membrane lipid of cosmopolitan pelagic crenarchaeota. *J. Lipid Res.* **43**, 1641–1651.
- Solomon, E.A., Kastner, M., MacDonald, I.R. and Leifer, I. (2009) Considerable methane fluxes to the atmosphere from hydrocarbon seeps in the Gulf of Mexico. *Nature Geosci.* **2**, 561–565.
- Sommer, S., Linke, P., Pfannkuche, O., Niemann, H., Treude, T. and Haeckel, M. (2009) Benthic respiration and energy transfer in cold seep habitats. *Geochim. Cosmochim. Acta* **73**, 1249–1249.
- Sprott, G.D., Meloche, M. and Richards, J.C. (1991) Proportions of diether, macrocyclic diether, and tetraether lipids in *Methanococcus jannaschii* grown at different temperatures. *J. Bacteriol.* **173**, 3907–3910.
- Stadnitskaia, A., Baas, M., Ivanov, M.K., Weering, T.C.E.v. and Sinninghe Damsté, J.S. (2003) Novel archaeal macrocyclic diether core membrane lipids in a methane-derived carbonate crust from a mud volcano in the Sorokin Trough, NE Black Sea. *Archaea* **1**, 165–173.
- Stecher, J., Türkay, M. and Borowski, C. (2002) Faunal assemblages on the Pacific–Antarctic ridge near the foundation seamount chain (37°30' S, 110°30' W). *Cah. Biol. Mar.* **43**, 271–274.
- Stetter, K. O. (1996) Hyperthermophilic prokaryotes. *FEMS Microbiol. Rev.* **18**, 149–158.
- Strapoć, D., Picardal, F.W., Turich, C., Schaperdoth, I., Macalady, J.L., Lipp, J.S., Lin, Y.-S., Ertefai, T.F., Schubotz, F., Hinrichs, K.-U., Mastalerz, M. and Schimmelmann, A. (2008) Methane-producing microbial community in a coal bed of the Illinois Basin. *Appl. Environ. Microbiol.* **74**, 2424–2432.
- Sturt, H., Summons, R., Smith, K., Elvert, M. and Hinrichs, K.-U. (2004) Intact polar membrane lipids in

- prokaryotes and sediments deciphered by high-performance liquid chromatography/electrospray ionization multistage mass spectrometry – new biomarkers for biogeochemistry and microbial ecology. *Rapid Commun. Mass Spectrom.* **18**, 617–628.
- Suess, E., Torres, M.E., Bohrmann, G., Collier, R.W., Greinert, J., Linke, P., Rehder, G., Trehu, A., Wallmann, K., Winckler, G. and Zuleger, E. (1999) Gas hydrate destabilization: Enhanced dewatering, benthic material turnover and large methane plumes at the Cascadia convergent margin. *Earth Planet. Sci. Lett.* **170**, 1–15.
- Summons, R.E., Albrecht, P., McDonald, G. and Moldowan, J. (2008) Molecular biosignatures. *Space Sci. Rev.* **135**, 133–159.
- Summons, R.E., Franzmann, P.D. and Nichols, P.D. (1998) Carbon isotopic fractionation associated with methylotrophic methanogenesis. *Org. Geochem.* **28**, 465–475.
- Summons, R.E., Jahnke, L.L. and Rocsandic, T. (1994) Carbon isotopic fractionation in lipids from methanotrophic bacteria: Relevance for interpretation of the geochemical record of biomarkers. *Geochim. Cosmochim. Acta* **58**, 2853–2863.
- Summons, R.E., Jahnke, L.L., Hope, J.M. and Logan, G.A. (1999) 2-Methylhopanoids as biomarkers for cyanobacterial oxygenic photosynthesis. *Nature* **400**, 554–557.
- Suzuki, D., Ueki, A., Amaishi, A. and Ueki, K. (2009) *Desulfovibrio portus* sp. nov., a novel sulfate-reducing bacterium in the class Deltaproteobacteria isolated from an estuarine sediment. *J. Gen. Appl. Microbiol.* **55**, 125–133.
- ## T
- Takai, K., Nakagawa, S., Reysenbach, A.L. and Hoek, J. (2006) Microbial ecology of mid-ocean ridges and back-arc basins. *Geophys. Monogr. Ser.* **166**, 185–213.
- Takai, K., Nakamura, K., Toki, T., Tsunogai, U., Miyazaki, M., Miyazaki, J., Hirayama, H., Nakagawa, S., Nunoura, T. and Horikoshi, K. (2008) Cell proliferation at 122°C and isotopically heavy CH₄ production by a hyperthermophilic methanogen under high-pressure cultivation. *Proc. Natl. Acad. Sci. U.S.A.* **105**, 10949–10954.
- Takano, Y., Chikaraishi, Y., Ogawa, N.O., Nomaki, H., Morono, Y., Inagaki, F., Kitazato, H., Hinrichs, K.-U. and Ohkouchi, N. (2010) Sedimentary membrane lipids recycled by deep-sea benthic archaea. *Nature Geosci.* **3**, 858–861.
- Talbot, H.M., Watson, D.F., Colin Murrell, J., Carter, J.F. and Farrimond, P. (2001) Analysis of intact bacteriohopanepolyols from methanotrophic bacteria by reversed phase high-performance liquid chromatography–atmospheric pressure chemical ionization mass spectrometry. *J. Chromatogr. A* **921**, 175–185.
- Teske, A., Dhillon, A. and Sogin, M.L. (2003) Genomic markers of ancient anaerobic microbial pathways: Sulfate reduction, methanogenesis, and methane oxidation. *The Biological Bulletin* **204**, 186–191.
- Teske, A., Hinrichs, K.-U., Edgcomb, V., de Vera Gomez, A., Kysela, D., Sylva, S.P., Sogin, M.L. and Jannasch, H.W. (2002) Microbial diversity of hydrothermal sediments in the Guaymas Basin: Evidence for anaerobic methanotrophic communities. *Appl. Environ. Microbiol.* **68**, 1994–2007.
- Thiel, V., Heim, C., Arp, G., Hahmann, U., Sjövall, P., Lausmaa, J. (2007) Biomarkers at the microscopic range: ToF-SIMS molecular imaging of Archaea-derived lipids in a microbial mat. *Geobiology* **5**, 413–421.
- Tivey, M.K. (2007) Generation of seafloor hydrothermal vent fluids and associated mineral deposits. *Oceanography* **20**, 50–65.
- Treude, T., Boetius, A., Knittel, K., Wallmann, K. and Jørgensen, B.B. (2003) Anaerobic oxidation of methane above gas hydrates at Hydrate Ridge, NE Pacific Ocean. *Mar. Ecol. Prog. Ser.* **264**, 1–14.
- Treude, T., Knittel, K., Blumenberg, M., Seifert, R. and Boetius, A. (2005) Subsurface microbial methanotrophic mats in the Black Sea. *Appl. Environ. Microbiol.* **71**, 6375–6378.
- Treude, T., Orphan, V.J., Knittel, K., Gieseke, A., House, C. and Boetius, A. (2007) Consumption of methane and CO₂ by methanotrophic microbial mats from gas seeps of the anoxic Black Sea. *Appl. Environ. Microbiol.* **73**, 2271–2283.
- Trincone, A., Nicolaus, B., Palmieri, G., De Rosa, M., Huber, R., Stetter, K.O. and Gambacorta (1992) Distribution of complex and core lipids within new hyperthermophilic members of the Archaea domain. *Syst.*

Appl. Microbiol. **15**, 11–17.

V

- Valentine, D.L. (2007) Adaptations to energy stress dictate the ecology and evolution of the Archaea. *Nat. Rev. Micro.* **5**, 316–323.
- Valentine, D.L. and Reeburgh, W.S. (2000) New perspectives on anaerobic methane oxidation. *Environ. Microbiol.* **2**, 477–484.
- Valentine, D.L., Blanton, D.C. and Reeburgh, W.S. (2000) Hydrogen production by methanogens under low-hydrogen conditions. *Arch. Microbiol.* **174**, 415–421.
- Valentine, R.C. and Valentine, D.L. (2004) Omega-3 fatty acids in cellular membranes: A unified concept. *Prog. Lipid Res.* **43**, 383–402.
- Van der Meer, M.T.J., Baas, M., Rijpstra, W.I.C., Marino, G., Rohling, E.J., Sinninghe Damsté, J.S. and Schouten, S. (2007) Hydrogen isotopic compositions of long-chain alkenones record freshwater flooding of the Eastern Mediterranean at the onset of sapropel deposition. *Earth Planet. Sci. Lett.* **262**, 594–600.
- Van der Meer, M.T.J., Sangiorgi, F., Baas, M., Brinkhuis, H., Sinninghe Damsté, J.S. and Schouten, S. (2008) Molecular isotopic and dinoflagellate evidence for Late Holocene freshening of the Black Sea. *Earth Planet. Sci. Lett.* **267**, 426–434.
- Van Dover, C.L. (2000) *The Ecology of Deep-Sea Hydrothermal Vents*. Princeton, N.J.: Princeton University Press.
- Van Dover, C.L., German, C.R., Speer, K.G., Parson, L.M. and Vrijenhoek, R.C. (2002) Marine biology - evolution and biogeography of deep-sea vent and seep invertebrates, *Science* **295**, 1253–1257.
- Van Meer, G., Voelker, D.R., Feigenson, G.W. (2008) Membrane lipids: Where they are and how they behave. *Nat. Rev. Mol. Cell. Biol.* **9**, 112–124.
- Van Mooy, B.A.S., Roca, G., Fredricks, H.F., Evans, C.T. and Devol, A.H. (2006) Sulfolipids dramatically decrease phosphorus demand by picocyanobacteria in oligotrophic marine environments. *Proc. Nat. Ac. Sci. USA* **103**, 8607–8612.
- Van Mooy, B.A.S. and Fredricks, H.F. (2010) Bacterial and eukaryotic intact polar lipids in the eastern subtropical South Pacific: Water-column distribution, planktonic sources, and fatty acid composition. *Geochim. Cosmochim. Acta* **74**, 6499–6516.
- Vossenberg, J.L.C.M. v.d., Driessen, A.J.M. and Konings, W. N. (1998) The essence of being extremophilic: The role of the unique archaeal membrane lipids. *Extremophiles* **2**, 163–170.
- Vossenberg, J.L.C.M. v.d., Ubbink-Kok, T., Elferink, M.G.L., Driessen, A.J.M. and Konings, W.N. (1995) Ion permeability of the cytoplasmic membrane limits the maximum growth temperature of bacteria and archaea. *Mol. Microbiol.* **18**, 925–932.

W

- Wakeham, S.G., Amann, R., Freeman, K.H., Hopmans, E.C., Jørgensen, B.B., Putnam, I.F., Schouten, S., Sinninghe Damsté, J.S., Talbot, H.M. and Woebken, D. (2007) Microbial ecology of the stratified water column of the Black Sea as revealed by a comprehensive biomarker study. *Org. Geochem.* **38**, 2070–2097.
- Weber, A. and Jørgensen, B.B. (2002). Bacterial sulfate reduction in hydrothermal sediments of the Guaymas Basin, Gulf of California, Mexico. *Deep-Sea Research I* **149**, 827–841.
- Webster, G., Sass, H., Cragg, B.A., Gorra, R., Knab, N.J., Green, C.J., Mathes, F., Fry, J.C., Weightman, A.J. and Parke, R.J. (2011) Enrichment and cultivation of prokaryotes associated with the sulphate–methane transition zone of diffusion–controlled sediments of Aarhus Bay, Denmark, under heterotrophic conditions. *FEMS Microbiol. Ecol.* **77**, 248–263.
- Webster, G., Watt, L. C., Rinna, J., Fry, J.C., Evershed, R.P., Parkes, R.J. and Weightman, A.J. (2006) A comparison of stable-isotope probing of DNA and phospholipid fatty acids to study prokaryotic functional diversity in sulfate-reducing marine sediment enrichment slurries. *Environ. Microbiol.* **8**, 1575–1589.
- Wegener, G., Bausch, M., Holler, T., Thang, N.M., Mollar, X.P., Kellermann, M.Y., Hinrichs, K.–U. and Boetius, A. Assessing sub-seafloor microbial activity by combined stable isotope probing with deuterated water and ¹³C-bicarbonate (In revision).

- Wegener, G., Niemann, H., Elvert, M., Hinrichs, K.-U. and Boetius, A. (2008) Assimilation of methane and inorganic carbon by microbial communities mediating the anaerobic oxidation of methane. *Environ. Microbiol.* **10**, 2287–2298.
- Welhan, J.A. (1988) Origins of methane in hydrothermal systems. *Chem. Geol.* **71**, 183–198.
- Wellsbury, P., Goodman, K., Barth, T., Cragg, B.A., Barnes, S.P. and Parkes, R.J. (1997) Deep marine biosphere fuelled by increasing organic matter availability during burial and heating. *Nature* **388**, 573–576.
- Wheat, C.G., Jannasch, H.W., Kastner, M., Plant, J. N. and DeCarlo, E. H. (2003) Seawater transport and reaction in upper oceanic basaltic basement: Chemical data from continuous monitoring of sealed boreholes in a ridge flank environment. *Earth Planet. Sci. Lett.* **216**, 549–564.
- Whelan, J.K., Simoneit, B.R.T. and Tarafa, M. E. (1988) C1-C8 hydrocarbons in sediments from Guaymas Basin, Gulf of California – Comparison to Peru Margin, Japan Trench, and California Borderlands. *Org. Geochem.* **12**, 171–194.
- White, D.C. and Ringelberg, D.B. (1998). Signature Lipid Biomarker Analysis. In: Burlage, R. S., Atlas, R., Stahl, D., Geesey, G., and Sayler, G. Eds., *Techniques in Microbial Ecology*. Oxford University Press, New York.
- White, D.C., Davis, W.M., Nickels, J.S., King, J.D. and Bobbie, R.J. (1979) Determination of the sedimentary microbial biomass by extractable lipid phosphate. *Oecologia* **40**, 51–62.
- Whiticar, M.J., Faber, E. and Schoell, M. (1986) Biogenic methane formation in marine and fresh-water environments - CO₂ reduction vs acetate fermentation isotope evidence. *Geochim. Cosmochim. Acta* **50**, 693–709.
- Whitman, W.B., Coleman, D.C. and Wiebe, W.J. (1998) Prokaryotes: The Unseen Majority. *Proc. Natl. Acad. Sci. USA* **95**, 6578–6583.
- Widdel, F. and Bak, F. (1992) Gram-negative mesophilic sulfate-reducing bacteria. In: *The Prokaryotes*. Balows, A., Trüper, H.G., Dworkin, M., Harder, W., and Schleifer K.H. (eds.). Berlin Heidelberg: Germany; New York, USA: Springer, pp. 3352–3378.
- Woese, C.R., Kandler, O. and Wheelos, M.L. (1990) Towards a natural system of organisms: Proposal for the domains, Archaea, Bacteria and Eukarya. *Proc. Natl. Acad. Sci. USA* **87**, 4576–4569.

Y

- Yoshinaga, M.Y., Kellermann, M.Y., Rossel, P.E., Schubotz, F., Lipp, J.S. and Hinrichs, K.-U. (2011) Systematic fragmentation patterns of archaeal intact polar lipids by high-performance liquid chromatography/electrospray ionization ion-trap mass spectrometry. *Rapid Commun. Mass Spectrom.* **25**, 3563–3574.

Z

- Zemski Berry, K.A. and Murphy, R.C. (2004) Electrospray ionization tandem mass spectrometry of glycerophosphoethanolamine plasmalogen phospholipids. *J. Am. Soc. Mass Spectr.* **15**, 1499–1508.
- Zhang, Y.-M. and Rock, C.O. (2008) Membrane lipid homeostasis in bacteria. *Nat. Rev. Microbiol.* **6**, 222–233.
- Zink, K., Wilkes, H., Disko, U., Elvert, M. and Horsfield, B. (2003) Intact phospholipids – microbial “life markers” in marine deep subsurface sediments. *Org. Geochem.* **34**, 755–769.
- Zink, K.-G., Mangelsdorf, K., Granina, L. and Horsfield, B. (2008) Estimation of bacterial biomass in subsurface sediments by quantifying intact membrane phospholipids. *Anal. Bioanal. Chem.* **390**, 885–896.
- Zink, K.-G. and Mangelsdorf, K. (2004) Efficient and rapid method for extraction of intact phospholipids from sediments combined with molecular structure elucidation using LC-ESI-MS-MS analysis. *Anal. Bioanalyti. Chem.* **380**, 798–812.

[CHAPTER VIII] - APPENDIX

In preparation for *Rapid Communication in Mass Spectrometry*

Compound-specific carbon isotope analysis of intact polar lipids after chemical oxidation of aqueous emulsions

Matthias Y. Kellermann*, Marcus Elvert, Kai-Uwe Hinrichs

^a Organic Geochemistry Group, MARUM Center for Marine Environmental Sciences & Department of Geosciences, University of Bremen, Leobener Strasse, D-28359 Bremen, Germany

* Corresponding author.
Tel.: +49 421 218 65742; Fax: + 49 421 218 65715
E-mail address: kellermann.matthias@gmail.com

Keywords:

Intact polar lipids | liposome preparation | LC IsoLink®

Abstract

The isotopic analysis of intact polar lipids (IPLs) is attractive since these are taxonomically more specific than their apolar derivatives that are commonly subject to isotopic analysis. Previously, carbon isotope analysis of IPLs was performed after labor-intensive chemical degradation, a procedure often associated with notoriously low yields. This study adapted the Finnigan LC IsoLink[®] interface for the development of a protocol for the determination of carbon isotopic compositions at natural abundance in IPLs from environmental samples. Using flow injection analysis of the Finnigan LC IsoLink[®], we explored the capability of direct carbon isotopic measurements of IPL standards (e.g., phospholipids such as phosphatidylethanolamine (PE), phosphatidylcholine (PC), phosphatidylglycerol (PG) as well the ether lipid-PC (O-PC)). In order to prepare these compounds for oxidation in the aqueous state, several preparation steps have been performed to produce small, unilamellar vesicles via dissolution in organic solvent, subsequent evaporation of the solvent and addition of aqueous medium. Emulsions of IPL standards with C equivalents of 60 to 130 ng were analyzed, resulting in reproducible peaks and precise and mostly accurate determinations of $\delta^{13}\text{C}$. For the IPLs PC, PG, ether lipid-PC and PG, δ -values determined from ng-quantities via chemical oxidation closely matched those from off line EA-analyses. However, PE and MGDG (data not shown) exhibited comparatively smaller peak areas and δ -values differed from those determined by EA by 2 to 4‰. Future work will extend this approach to a wider range of IPL classes including e.g. archaeal membrane lipids. Furthermore, additional steps and procedures of liposome preparation will be tested and evaluated (e.g., variation of temperature, pH, etc.). This new method will help to guide a way to natural-abundance carbon isotopic determination of IPLs at the ng-scale in combination with preparative HPLC separation from a wide variety of environmental samples.

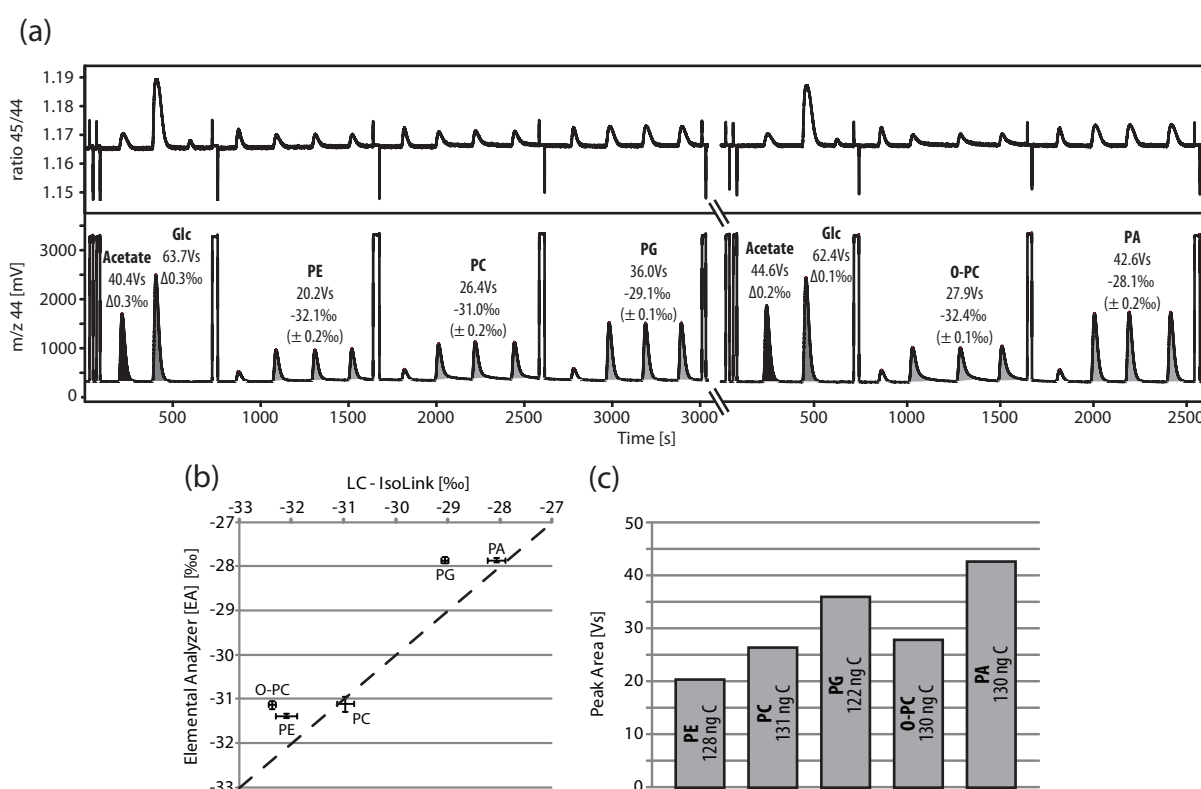


Fig. App.1. (a) Illustration of carbon isotopic analysis of different IPLs using flow injection analysis. 200 ng of IPLs (equivalent to ~ 120 ng C) were injected in triplicate, resulting in precise and accurate $\delta^{13}\text{C}$ values. The water soluble acetate and β -D-glucopyranose (Glc) are used as control; Δ indicates the deviation from the EA value. Rectangular peaks show the reference gas (CO_2). (b) Cross correlation of EA vs LC-IsoLink IPL measurements. (c) Peak areas of different IPLs after injection of 122–131 ng of C.

Thermophilic anaerobic oxidation of methane by marine microbial consortia

Thomas Holler ^a, Friedrich Widdel ^a, Katrin Knittel ^a, Rudolf Amann ^a,
Matthias Y. Kellermann ^b, Kai-Uwe Hinrichs ^b, Andreas Teske ^c,
Antje Boetius ^{a,b,d} and Gunter Wegener ^{a,b,*}

Published in *ISME Journal*

Vol: 5 (2011), page: 1946–1956, doi:10.1038/ismej.2011.77.

© 2011 International Society for Microbial Ecology. All rights reserved.

- ^a Max Planck Institute for Marine Microbiology, Celsiusstr. 1, D-28359 Bremen, Germany
- ^b Organic Geochemistry Group, MARUM Center for Marine Environmental Sciences & Department of Geosciences, University of Bremen, Leobener Strasse, D-28359 Bremen, Germany
- ^c Department of Marine Sciences, The University of North Carolina at Chapel Hill, Chapel Hill, NC, USA
- ^d Alfred Wegener Institute for Polar and Marine Research, Bremerhaven, Germany

* Corresponding author. gwegener@mpi-bremen.de

Keywords:

anaerobic methanotrophy | ANME | syntrophy | thermophilic microorganisms

Abstract

The anaerobic oxidation of methane (AOM) with sulfate controls the emission of the greenhouse gas methane from the ocean floor. AOM is performed by microbial consortia of archaea (ANME) associated with partners related to sulfate-reducing bacteria. In vitro enrichments of AOM were so far only successful at temperatures ≤ 25 °C; however, energy gain for growth by AOM with sulfate is in principle also possible at higher temperatures. Sequences of 16S rRNA genes and core lipids characteristic for ANME as well as hints of in situ AOM activity were indeed reported for geothermally heated marine environments, yet no direct evidence for thermophilic growth of marine ANME consortia was obtained to date. To study possible thermophilic AOM, we investigated hydrothermally influenced sediment from the Guaymas Basin. In vitro incubations showed activity of sulfate-dependent methane oxidation between 5 and 70 °C with an apparent optimum between 45 and 60 °C. AOM was absent at temperatures ≥ 75 °C. Long-term enrichment of AOM was fastest at 50 °C, yielding a 13-fold increase of methane-dependent sulfate reduction within 250 days, equivalent to an apparent doubling time of 68 days. The enrichments were dominated by novel ANME-1 consortia, mostly associated with bacterial partners of the deltaproteobacterial HotSeep-1 cluster, a deeply branching phylogenetic group previously found in a butane-amended 60 °C-enrichment culture of Guaymas sediments. The closest relatives (*Desulfurella* spp.; *Hippea maritima*) are moderately thermophilic sulfur reducers. Results indicate that AOM and ANME archaea could be of biogeochemical relevance not only in cold to moderate but also in hot marine habitats.

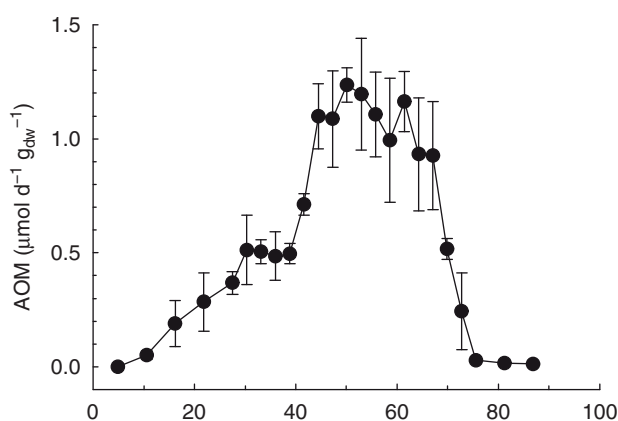


Fig. App.2. Rates of AOM in Guaymas Basin sediment at different temperatures measured as $^{14}\text{CH}_4$ conversion to $^{14}\text{CO}_2$. Homogenous samples (2–45cm Sediment depth, in situ temperature, 4–85°C) were pre-incubated for 5 days at designated temperatures followed by incubation with labeled methane for 48 h. Error bars indicate s.d. from triplicates.

Table App.1. Concentrations of archaeal glycerol dialkyl glycerol tetraether (GDGT) in the enrichment culture (top) and stable carbon isotopic compositions of GDGT-derived biphytane derivatives obtained by ether cleavage (bottom)

Tetraethers	Concentration $\mu\text{g g}_{\text{dw}}^{-1}$	Rel. abundance (%)
GDGT-0	1.90	25
GDGT-1	0.49	6
GDGT-2	0.70	9
GDGT-3	0.47	6
GDGT-4	1.78	23
GDGT-cr.	2.24	29
GDGT-cr. (iso)	0.07	1

Isoprenoids	Isotopic composition ($\delta^{13}\text{C}$ vs. PDB)	Rel. abundance (%)
Acyclic biphytane	-25.2‰	40
Monocyclic biphytane	-49.1‰	13
Bicyclic biphytane	-41.6‰	29
Tricyclic biphytane	-20.0‰	18

Structures of the GDGTs are shown in Schouten *et al.* (2003).

Assessing sub-seafloor microbial activity by combined stable isotope probing with deuterated water and ^{13}C -bicarbonate

Gunter Wegener ^{a,b,*}, Marlene Bausch ^{a,1}, Thomas Holler ^c, Nguyen Manh Thang ^c, Xavier Prieto Mollar ^b, Matthias Y. Kellermann ^b, Kai-Uwe Hinrichs ^b and Antje Boetius ^{a,d}

Manuscript in revision at *Environmental Microbiology*

- ^a HGF-MPG Group for Deep Sea Ecology and Technology, Alfred Wegener Institute for Polar and Marine Research, Am Handelshafen 12, D-27570 Bremerhaven, Germany ; and Max Planck Institute for Marine Microbiology, Celsiusstrasse 1, D-28359 Bremen, Germany.
 - ^b Organic Geochemistry Group, MARUM Center for Marine Environmental Sciences & Department of Geosciences, University of Bremen, Leobener Strasse, D-28359 Bremen, Germany.
 - ^c Max Planck Institute for Marine Microbiology, Celsiusstrasse 1, D-28359, Germany.
 - ^d Department of Geosciences, University of Bremen, Bremen, D-28359 Germany.
- * Corresponding author. gwegener@mpi-bremen.de

Keywords:

Dual-SIP | D_2O | $^{13}\text{C}_{\text{DIC}}$ | microbial metabolic activity | growth rates | carbon assimilation | microbial lipid production | auto- and heterotrophy

Abstract

Sub-seafloor sediments are populated by large numbers of microbial cells but not much is known about their metabolic activities, growth rates and carbon assimilation pathways. Here we introduce a new method enabling the sensitive detection of microbial lipid production and the distinction of auto- and heterotrophic carbon assimilation. Application of this approach to anoxic sediments from a Swedish fjord allowed to compare the activity of different functional groups, the growth and turnover times of the bacterial and archaeal communities. The assay involves dual stable isotope probing (SIP) with deuterated water (D_2O) and $^{13}C_{DIC}$ (DIC = dissolved inorganic carbon). Culture experiments confirmed that the D content in newly synthesized lipids is in equilibrium with the D content in labeled water, independent of whether the culture grew hetero- or autotrophically. The ratio of $^{13}C_{DIC}$ to D_2O -incorporation enables distinction between these two carbon pathways in studies of microbial cultures and in environmental communities. Furthermore, D_2O -SIP is sufficiently sensitive to detect the formation of few hundred cells per day in a gram of sediment. In anoxic sediments from a Swedish fjord, we found that >99% of newly formed lipids were attributed to predominantly heterotrophic bacteria. The production rate of bacterial lipids was highest in the top 5 cm and decreased 60-fold below this depth while the production rate of archaeal lipids was rather low throughout the top meter of seabed. The contrasting patterns in the rates of archaeal and bacterial lipid formation indicate that the factors controlling the growth of these two groups must differ fundamentally.

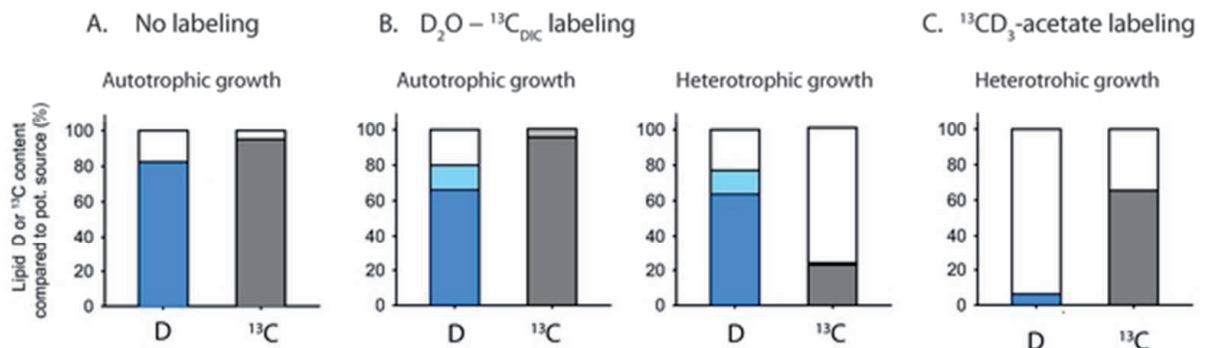


Fig. App.3. D and ^{13}C assimilation into lipids of *Desulfosarcina variabilis* grown on different substrates. A. Isotope discrimination ($H_2O/Lipid$) during growth of *Ds.variabilis* on H_2 , without addition of labeled substances. B. D_2O and $^{13}C_{DIC}$ recovery of in *Ds.variabilis* grown on hydrogen and acetate as sole energy substrate (light bars include correction by isotope fractionation factors derived from experiment (A)). C. Recovery of D and ^{13}C in *Ds.variabilis* grown on $^{13}CD_3$ -acetate.

Towards constraining H₂ concentration in subseafloor sediment: A proposal for combined analysis by two distinct approaches

Yu-Shih Lin ^{a,b,*}, Verena B. Heuer ^{a,b}, Tobias Goldhammer ^b,
Matthias Y. Kellermann ^{a,b}, Matthias Zabel ^b, Kai-Uwe Hinrichs ^{a,b}

Published in *Geochimica et Cosmochimica Acta*
Vol: 77 (2012), page: 186–201, doi:10.1016/j.gca.2011.11.008
© 2011 Elsevier Ltd. All rights reserved.

^a Organic Geochemistry Group, MARUM Center for Marine Environmental Sciences & Department of Geosciences, University of Bremen, Leobener Strasse, D-28359 Bremen, Germany

^b MARUM Center for Marine Environmental Sciences, University of Bremen, D-28359 Bremen, Germany

* Corresponding author. yushih@uni-bremen.de

Keywords:

hydrogen | H₂-extraction method | H₂-headspace equilibration method | microbial metabolic activity

Abstract

Molecular hydrogen (H_2) is a central metabolite that couples organic matter degradation and terminal electron-accepting processes. H_2 levels in natural environments are often regulated by microbial syntrophy; therefore, pore-water H_2 concentration is a useful parameter for studying biogeochemical processes in sediments. However, little is known about H_2 concentrations in marine subsurface sediments. Previous studies applying either a headspace equilibration technique or an extraction method for the analysis of pore-water H_2 in deeply buried sediments have generated results that sometimes contradict the principles established based on studies of microbial culture and surface sediments. In this study, we first evaluated and optimized an extraction method, which was then applied in combination with a headspace equilibration method to determine concentrations of pore-water H_2 in subseafloor sediments along a transect of five sites of different water depths and geochemical regimes at the continental margin off Namibia, SE Atlantic. The two methods generated depth profiles with some similarities in curve shape, but the extraction method yielded higher H_2 values than the headspace equilibration technique. By comparing the two data sets with thermodynamic calculations of potential terminal electron-accepting processes, we were able to provide a first evaluation of syntrophic conditions in subseafloor sediment from the perspective of H_2 biogeochemistry. We observed that in the sulfate reduction zone, the H_2 concentrations are higher than the H_2 threshold allowed for the next most favorable terminal metabolism (methanogenesis), suggesting relaxation of coupling between H_2 -producing and H_2 -consuming activities at these depths. In contrast, the H_2 concentrations in the upper methanogenic zone are low enough for methanogens to outcompete CO_2 -reducing acetogens. Our findings suggest the existence of varied extents of syntrophic H_2 coupling in subseafloor sediment.

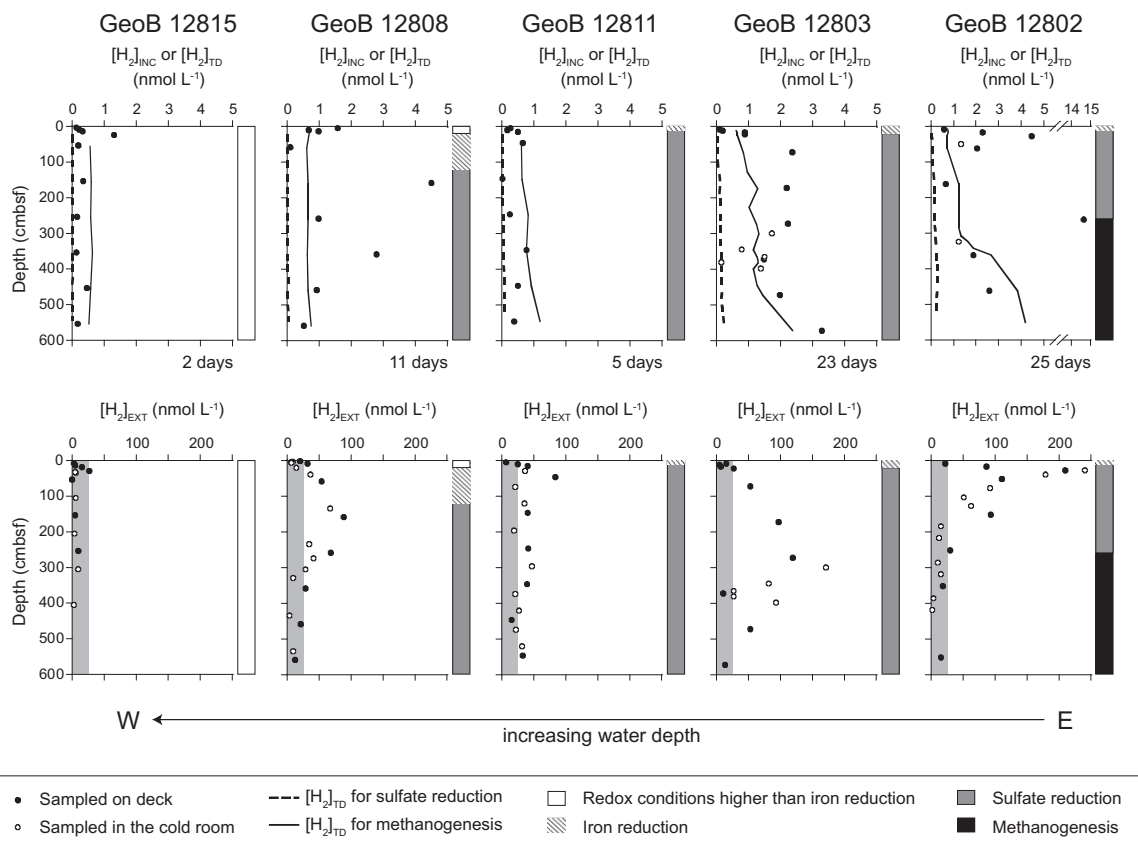


Fig. App.4. Depth profiles of $[H_2]_{INC}$ and $[H_2]_{EXT}$ in sediment interstitial waters at five stations, offshore Namibia. The distribution of $[H_2]_{TD}$ for sulfate reduction and methanogenesis is also plotted for comparison. The duration of sediment incubation was listed for individual stations. The shaded areas mark the methodological limit of detection of the extraction approach.

Methane in shallow cold seeps at Mocha Island off central Chile

Gerdhard L. Jessen ^a, Silvio Pantoja ^{b,c,*}, Marcelo A. Gutiérrez ^a, Renato A. Quiñones ^{b,c}, Rodrigo R. González ^c, Javier Sellanes ^{c,d}, Matthias Y. Kellermann ^e and Kai-Uwe Hinrichs ^e

Published in *Continental Shelf Research*

Vol: 31 (2011), page: 574–581, doi:10.1016/j.csr.2010.12.012

© 2011 Elsevier Ltd. All rights reserved.

- ^a Graduate Program in Oceanography, Department of Oceanography, University of Concepción, Chile
- ^b Department of Oceanography, University of Concepción, Chile
- ^c Center for Oceanographic Research in the eastern South Pacific (COPAS), School of Natural Sciences and Oceanography, University of Concepción, Chile
- ^d Department of Marine Biology, Universidad Católica del Norte, Chile
- ^e Organic Geochemistry Group, MARUM Center for Marine Environmental Sciences & Department of Geosciences, University of Bremen, Leobener Strasse, D-28359 Bremen, Germany

* Corresponding author. spantoja@udec.cl

Keywords:

methane | gas seepage | Chile | Mocha Island | stable isotope | methane flux

Abstract

We studied for the first time the intertidal and subtidal gas seepage system in Mocha Island off Central Chile. Four main seepage sites were investigated (of which one site included about 150 bubbling points) that release from 150 to 240 tonnes CH_4 into the atmosphere per year. The total amount of methane emitted into the atmosphere is estimated in the order of 800 tonnes per year. The gases emanated from the seeps contain 70% methane, and the stable carbon isotopic composition of methane, $\delta^{13}\text{C}\text{-CH}_4$ averaged $-44.4 \pm 1.4\text{‰}$ which indicates a major contribution of thermogenic gas. Adjacent to one of the subtidal seeps, rocky substrates support a diverse community of microbial filaments, macroalgae, and benthic organisms. While stable carbon isotopic compositions of marine benthic organisms indicate a dominant photosynthesis-based food web, those of some hard-substrate invertebrates were in the range -48.8‰ to -36.8‰ , suggesting assimilation of methane-derived carbon by some selected taxa. This work highlights the potential subsidy of the trophic web by $\text{CH}_4\text{-C}$, and that its emission to the atmosphere justifies the need of evaluating the use of methane to support the energy requirements of the local community.

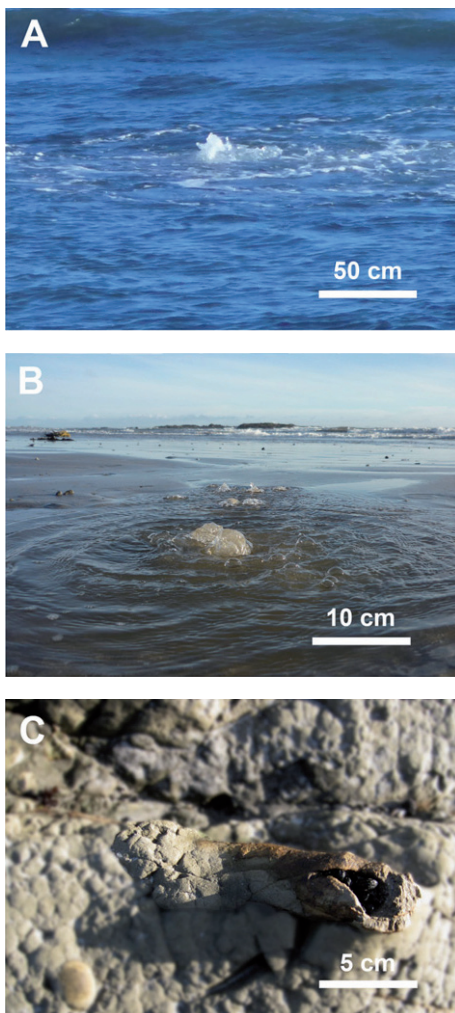


Fig. App.5. Subtidal Site C (A), intertidal gas seepage Site A (B), and relict chimney-like structure (C) at Mocha Island.

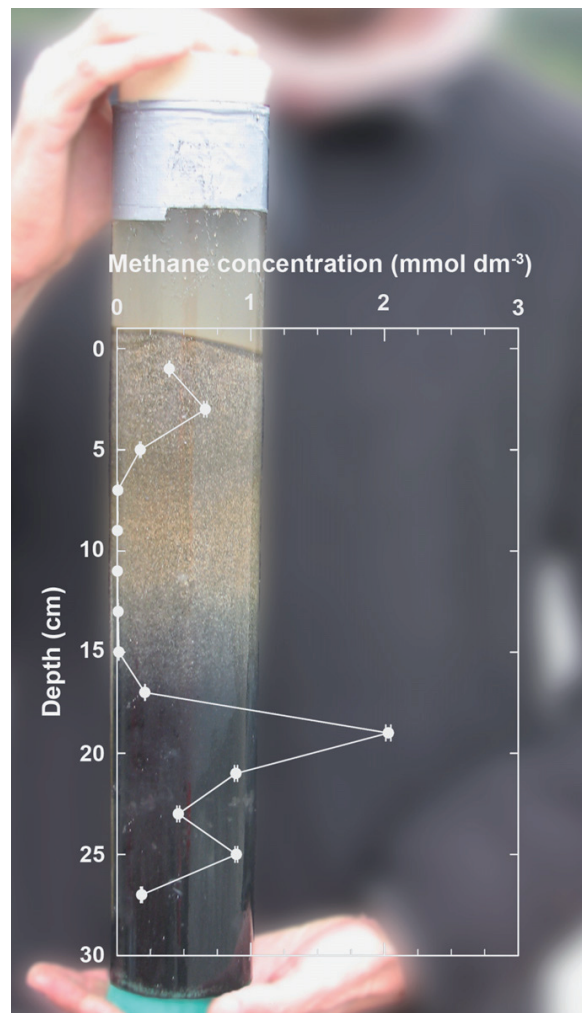


Fig. App.6. Photograph of a sediment core collected from sampling Site A showing the stratification pattern, and its sediment porewater methane concentration.

Curriculum vitae

Curriculum Vitae

Matthias Kellermann, M.Sc.



PERSONAL INFORMATION

Dept. of Geosciences
University of Bremen
PO Box 330 440
D-28334 Bremen

Phone: +49-421-218-65742
Fax: +49-421-218-65715
E-mail: kellermann.matthias@gmail.de
Web: www.marum.de/Matthias_Kellermann.html

Born: January 10th, 1982 in Bremen (Germany)
Gender: male
Family Status: single

EDUCATION

Mai 2008 – March 2012 **PhD** in the Organic Geochemistry Group, MARUM, Germany
External PhD student of the GLOMAR graduate school
("Global Change in the Marine Realm")

Dec. 2007 **Joint Master's Degree** in the Earth Science from the University of Waikato, New Zealand & University of Bremen, Germany

Nov. 2006 – Dec. 2007 **2nd** year of the German Master program "Geowissenschaften"
University of Bremen, Germany

Feb. 2005 – Oct. 2006 **1st** year of the German Master program "Geowissenschaften"
University of Waikato, New Zealand

Sep. 2005 **Bachelor of Science Degree** "Geowissenschaften", University of Bremen, Germany

Oct. 2002 – Sep. 2005 **Undergraduate studies** of the German Bachelor "Geowissenschaften"
University of Bremen, Germany

Oct. 2001 – Oct. 2002 **Undergraduate studies** of Mechanical/Electrical Engineering,
University of Applied Science, Bremen, Germany

June 2001 **Abitur** (high school diploma), KGS Weyhe-Leeste, Germany

AWARDS

Jan. 2009 **2008 MARUM research prize** for best Master thesis:
"Polar lipids as marker for the symbiosis between bacteria and mussels"

INTERNATIONAL EXPERIENCE

Sep. 2005 – Oct. 2006 **University of Waikato**, Department of Earth & Ocean Sciences, Hamilton, New Zealand

July – Sep. 2002 **Escola Oficial d'Idiomes**, Barcelona-Drassanes, Spain

April – July 2002 **Temporary employment** abroad, London & Staffordshire, England

Curriculum Vitae

Matthias Y. Kellermann, M.Sc.

FIELD EXPERIENCE

- Nov. - Dec. 2009 **R/V Atlantis Guaymas (Mexico) - Guaymas (Mexico)**
Investigation of hydrothermal vent sites at Guaymas Basin
- Feb. - March 2009 **R/V Maria S. Merian Martinique (Caribbean Sea) - Dakar (Senegal)**
Mid-Atlantic ridge site survey of sediments and basement in North Pond area
- Nov. - Dec. 2008 **R/V Atlantis Guaymas (Mexico) - Guaymas (Mexico)**
Investigation of hydrothermal vent sites at Guaymas Basin
- Mar. 2004 **FS Heinke 204/1 → Baltic Sea ("Mecklenburger Bucht")**
Introduction of geophysical techniques

STUDENT SUPERVISION

- July – Sep. 2009 **Co-supervision B.Sc. thesis of Tim Kahs:**
"Biphytanic diacids: An oxidative degradation product of GDGTs or directly biosynthesized by Archaea"
- June – Oct. 2009 **Co-supervision of Anja Cording (Summer Student Fellowship 2009; MARUM):**
"Water-based solid phase extraction of sediments – potential for evaluating sources and sinks of volatile fatty acids in the deep biosphere"

PRESENTATION LIST

- Sep. 2011 (Oral) **International Meeting on Organic Geochemistry (IMOG), Interlaken, Switzerland**
"Stable isotope probing of intact polar lipids indicates precursor role of archaeol in the biosynthesis of tetraether lipids"
- Sep. 2011 (Oral) **International Symposium of Subsurface Microbiology (ISSM), Garmisch-Partenkirchen, Germany**
"Dual isotopic probing reveals dominant autotrophic carbon fixation in methane-rich sediments from the Guaymas Basin"
- June 2011 (Oral) **North German Meeting on Organic Geochemistry (NGMOG), Bremen, Germany**
"Tracing ¹³C-labeled inorganic carbon into IPLs of thermophilic anaerobic methanotrophs (ANME-1) provides new insights into pathways of archaeal lipid biosynthesis"
- Sep. 2009 (Poster) **International Meeting on Organic Geochemistry (IMOG), Bremen, Germany**
"Compound- specific isotope analysis of intact polar lipids after chemical oxidation of aqueous emulsions"
- Sep. 2008 (Oral) **ECORD Summer School "The Deep Seafloor Biosphere", Bremen, Germany**
"Direct ^δ¹³C isotopic measurements of complex intact polar lipids (IPLs) determined via coupled LC/irMS"
- Aug. 2008 (Poster) **Gordon Research Conference on Organic Geochemistry, Holderness, NH, USA**
"Polar lipids as marker for the symbiosis between bacteria and mussels"

N a m e : **Datum**

Anschrift :

Erklärung

Hiermit versichere ich, dass ich

1. die Arbeit ohne unerlaubte fremde Hilfe angefertigt habe,
2. keine anderen als die von mir angegebenen Quellen und Hilfsmittel benutzt habe und
3. die den benutzten Werken wörtlich oder inhaltlich entnommenen Stellen als solche kenntlich gemacht habe.

_____, den

(Unterschrift)

